Analysis of Sampling and Multi-Vehicle Separation for BWIM Systems

Mathew A.C. Grabau

A thesis submitted to
The Faculty of Graduate Studies of
The University of Manitoba
in partial fulfillment of the requirements
of the degree of

Master of Science

Department of Electrical and Computer Engineering
The University of Manitoba
Winnipeg, Manitoba, Canada
August 2015

Thesis advisor
Dr. Dean McNeill, P. Eng

Author
Mathew A.C. Grabau, EIT

Analysis of Sampling and Multi-Vehicle Separation for BWIM Systems

Abstract

Structural Health Monitoring provides ample opportunity for deep analysis of our infrastructure, including using the bridge as a scale through a process called (Bridge) Weigh in Motion (BWIM). Many variables impact the BWIM's capabilities, accuracy, and by extension, overall usefulness. The overall goal of the research conducted was to identify methods of improving the accuracy and performance of BWIM. That goal was narrowed down to two specific objectives: 1) assess if a higher sampling rate leads to increased BWIM performance as postulated by some sources [1]; and 2) attempt to develop a means of analyzing complex multi-vehicle events where the distributed strain profile cannot be processed by the standard BWIM algorithms.

The first objective was accomplished using a Matlab simulation to generate sampled strain signals, with different sampling nonidealities such as offsets in the start of captured events. The testing demonstrated that the sampling rate is sufficient at 100 Hz, with minute peak detection errors manifesting only when running at unreasonable levels of accuracy for the Matlab analysis. Given that information, there is potentially room for reducing the sampling rate which benefits BWIM installations by saving on data storage requirements. Beyond that, no further testing is recommended in the area of sampling rate.

The second objective was accomplished by using higher-order signal processing techniques such as Independent Component Analysis (ICA). These techniques aim to, at a minimum, ensure that heavy-vehicle events are detected and recorded. A total of four tests were performed on Independent Component Analysis —two on simulated strain mixtures and two on signal samples collected from bridge data. The results of the tests demonstrate ICA may potentially be introduced into a BWIM implementation pending further refinements. The most likely targets for improvement are through analyzing the independence of truck signals using correlation, taking measures to decorrelate the mixtures, and also testing whether post-separation filtering of the strain readings impacts the result. Notwithstanding those areas of improvement, the overall verdict is that a clear recommendation for using ICA in active BWIM analysis is not currently feasible.

Contents

List of Figures

List of Tables

Acknowledgements

I would like to begin by thanking all the people who have supported me along the way:

- My advisor Dr. Dean McNeill for his patience, guidance and support throughout the years of graduate studies.
- The examining committee who have gave their time to review this work.
- The ISIS Canada team, especially Dr. Karim Helmi, Dr. Basheer Algohi and Mr. Geoff Cao for providing guidance in using the databases and BWIM algorithms.
- MIT (Manitoba Infrastructure and Transport) for granting their permission to use the South Perimeter Bridge data and the photographs used in this document.
- The employers who allowed me the time and flexibility to pursue this work - JCA Electronics, Magellan Aerospace Corporation, and Securris Inc.
- My friends who have supported, empathized, and provided much needed breaks at times.
- My sister Stephanie who ran errands, drove, and listened in spite of her own workload.
- My parents Susan and Claudio who are owed many thanks that extend beyond their support of my work. Thank you for putting me on a good path, supporting the pursuit of my many dreams, and providing quintessential motivation to continue even when the road was bumpy.
- My wife Katie, thank you for graciously surrendering large portions of our first year of married life. Thank you for being so willing to take on so much around the house and surrender large portions of our time together so that I could get this work completed.

This thesis is dedicated to everyone that had a hand in making this possible — no matter how near or far you are today, you shall not be forgotten.

Chapter 1

Introduction

The research project described in this document is focused on learning, verifying, validating and improving upon *Bridge Weight In Motion* (BWIM) techniques. BWIM is an analytical process made possible through the integration of *Structural Health Monitoring* (SHM) equipment into infrastructure (bridges). In new construction, the requisite strain gauges may be included, while existing structures may be augmented when performing upgrades or rehabilitation. In essence, BWIM uses the sensors installed in the bridge to utilize the bridge as a scale as vehicles traverse it.

A honed BWIM implementation enhances public safety by detecting the passage, and weight, of large vehicles. By detecting the vehicles that are overweight, monitoring parties can take action sooner to prevent structural fatigue and failure, and their potential for tragic outcomes including loss of expensive capital infrastructure and human injury or deaths. Therefore, in the long-term, the public ultimately benefits from the efforts undertaken.

The incumbent system in the weighing of larger vehicles is a station alongside a highway containing the apparatus (a scale) for weighing the trucks. Motorists may be familiar with these weighing stations positioned along various highways, allowing agencies to track the presence of large vehicles. The system has inefficiencies, including equipment that might not pass through the weighing station, or the station begin closed when a large truck is passing through. By measuring directly at the bridge, a more precise and accurate sample collection is available.

Within the last decade, Winnipeg, Manitoba, has seen BWIM introduced and developed through the collaboration of Manitoba Infrastructure and Transportation (MTI) and the ISIS Canada Resource Centre, which is headquartered at the Univeristy of Manitoba. The Resource Centre also provided guidance for this project —Drs Karim Helmi and Basheer Algohi supported by discussing the BWIM algorithms employeed on the South Perimeter Bridge data, while Mr. Geoff Cao, who's responsibilities include the database management, was instrumental in leveraging the available strain data.

1.1 Goals and Objectives

The ultimate goal of the research and this project is to contribute to enabling BWIM deployment as a regular component of weighing vehicles and monitoring the infrastucture. To that extent, the goal is accomplished by identifying, analyzing, and recommending methods for improving the accuracy of BWIM systems. Amongst the entire problem space, the following two areas are targeted:

1. Determine if an increased sampling rate provides a significant impact on BWIM's ability to process data.
2. Multi-vehicle processing, which is not handled by the present procedures owing to the nature of the signals for these scenarios.

One of the above goals is considered successfully accomplished if a useful result is found to pass onto the ISIS Canada researchers, who in turn incorporate it into their ongoing operations. In the case of the first goal, the sampling rate, a recommendation of whether additional sampling is necessary is sufficient. For the second goal, a tractable and reliable means of extracting individual load signals is a mark of accomplishment.

1.2 Outline

The research and work discussed in this document was performed with the aim of improving the accuracy of BWIM and spanned a longer than anticipated duration. As a result, the research was performed in two separate areas of BWIM. Both areas focus on the source signals, specifically the measurement and multi-vehicle signal processing. Therefore, the remainder of this document is divided into the following sections:

- Chapter 2 introduces the SHM/BWIM system setup and the algorithms that are used to process the data.
- Chapter 3 discusses an analysis performed to determine the impact of strain sampling rate on the accuracy of the BWIM input data.
- Chapter 4 discusses the Independent Component Analysis (ICA) separation process and series of experiments undertaken to determine the applicability of ICA to the area of BWIM.
- Chapter 5 provides conclusions and recommendations for follow-up work based on the work performed.

The following appendices have also been included to document information that was either too verbose or that did not fit within the scope of the discussion:

- Appendix A presents the detailed results of the simulation using a simulated semi-truck/garbage truck signal mixture.
- Appendix B presents the detailed results of the simulation using the same simulated semi-truck/garbage truck signals but including a noise model.
- Appendix C presents the detailed results of an attempt to separate two (2) independent components from a multi-vehicle event sample taken from an actual BWIM system.
- Appendix D presents the results of attempting to separate three (3) independent components from the same event.

Chapter 2

Bridge Weigh-in-Motion

Bridge Weigh-in-Motion (BWIM) is a natural extension of Structural Health Monitoring (SHM) efforts, transforming the bridge into a scale that measures the vehicles traversing it. Using the bridge as a scale is a complex process, which begins with obtaining a measurement of strain as trucks cross a bridge and concludes with post-processing of the collected data to extract various vehicle parameters such as length, speed and weight.

2.1 History and Background

BWIM has been discussed formally since the 1970's when Moses [3] introduced a system for weighing-in-motion (WIM) using magnetic tapes and other equipment. As early as 1989 [4] BWIM was considered for determining spot speed and axle spacing along with the vehicle weights. However, in that particular case, the accuracy of the weight calculation was insufficient under operating conditions (highway speeds) to utilize the methods for vehicle weight enforcement. However, the authors noted better accuracy in the spot speed and axle spacing measurements. Since then, the accuracy has been advanced to the point of being suitable for use in the envisioned weighing application [5].

While several algorithms have been developed to perform the processing of the signals, the specific algorithms are not the subject of the project.

2.2 BWIM Process

The BWIM process is two-fold: first, a bridge span is instrumented with strain gauges; second, the measurements collected while a vehicle is traversing the instrumented span are analyzed using a combination of algorithms that extract speed, vehicle length and, ultimately, weight parameters [6]. The first step is generally classified as an SHM procedure, and the BWIM procedure leverages the data collected in the SHM process. The following paragraphs decompose the BWIM process further and discuss some of the algorithms employed to process the data.

Chapter 3 and Chapter 4, which highlight the attempts to improve the BWIM process in two areas, discuss theory that is applicable in their respective domains.

2.2.1 Measurement and Signal Characteristics

A truck passing over an instrumented span naturally imparts a load on the bridge deck. Through structural mechanics the truck's weight can be decomposed into a series of point loads corresponding to the axle locations [7, 1, 6]. As each of these loads moves over an instrumented point (gauge location), a peak in the strain occurs. The BWIM process involves extracting the characteristics of the truck, the target being the weight, using the recorded strain profile and sometimes the locations of the peaks. Additional characteristics required are the event's start and end points; the speed of the vehicle may also be required to perform the calculation depending on the selected algorithm.

Using the data and derived or known characteristics, processing is performed to derive the weight using various algorithms such as the *Asymmetry coefficient method*, *Area method*, *Two stations method*, and *Beta method*. A full discussion of each of the algorithms is not in the scope of this discussion, but Bahkt et al [6] provide descriptions of all the aforementioned algorithms.

Overall, it can be concluded that the success of the BWIM process is contingent on:

1. Determining the proper start and end of the truck's signal, and;

2. Identifying the peak strains to use as the point loads of the truck.

2.2.2 Start/End Determination

The first point, determining the signal's time span is critical, though also difficult. It is obvious when examining a signal that a peak has occurred, but less obvious where the event's endpoints occurred. Without knowing the proper endpoints, the proper weight of the vehicles cannot be determined.

When first entering the instrumented section, the strain is relatively small compared to the peaks and may not be enough to escape the noise floor. A technique for overcoming the challenges of end-point recovery is to use a heuristic with a mean strain reading selected as a floor —the capture is made when the strain is above a certain threshold value. In the case of the bridge studied for this thesis, a two (2) percent threshold of the average strain reading for recent samples is used as an event collection trigger. In other words, the database archives a sample once the strain has exceeded two percent of the average reading. A time buffer is included in the sampling collection and storage components to save the data surrounding the actual vehicle event. The additional information is useful in performing analysis, especially in cases where the algorithms are under-performing due to abnormalities in the signals.

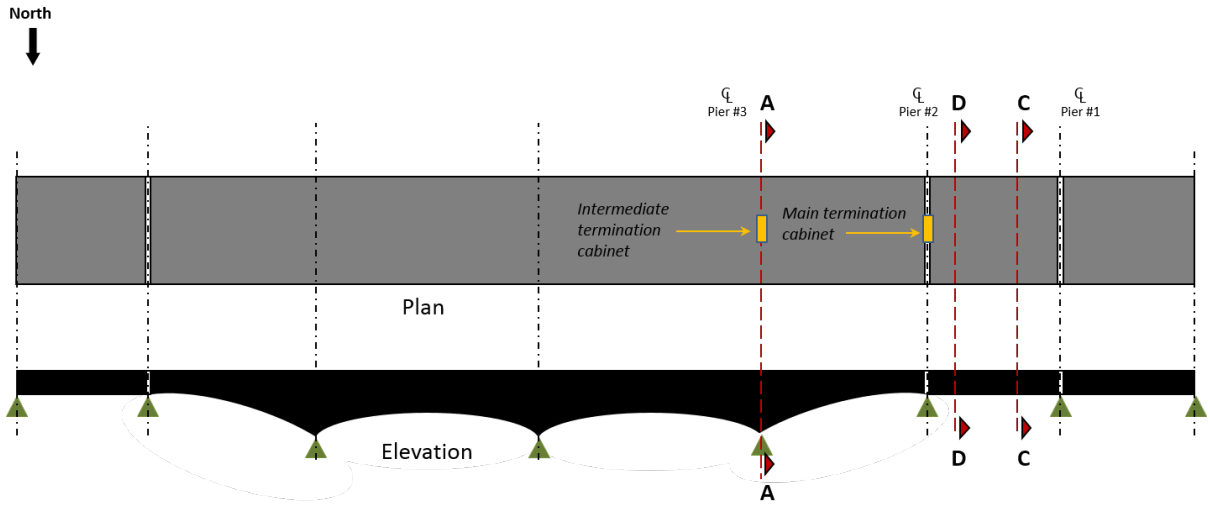

Figure 2.1: South Perimeter Bridge Instrumented Span [2]

2.2.3 Peak Strains

The peak strain is required to derive the weight. Not knowing the peak strain will result in some inaccuracy in the calculated weights. One possible mitigation is ensuring a sufficient sampling rate that allows the peaks to be properly captured.

Identifying the peak strains is a local maxima problem. The number of peaks that manifest in a sample is determined by the number of axles (or axle groupings when multiple axles are in close proximity). The peaks are leveraged to work back to the weight of the vehicle.

2.3 A Sample BWIM System

SHM was introduced on the South Perimeter Bridge in Winnipeg, Canada during recent renovation projects undertaken to replace the bridge deck. During the course of reworking the bridge, metal-foil strain gauges were installed to facilitate ongoing measurement collection and monitoring. The bridge has two instrumented spans, as illustrated in Figure 2.1. Each of the sections AA, CC, and DD contains a number of strain gauges (32, 23, 9, respectively) situated at multiple locations on each girder as shown in Figure 2.2 and Figure 2.3.

The positioning of the gauge determines the label applied to that particular gauge. Specifically, as demonstrated in Figure 2.4 and Figure 2.5 a gauge is classified as one of a girder (G_{nn}), strap (S_{nn}), or dummy gauge (D_{nn}). The gauges located on girders were used to perform the analysis in this work. The strap and dummy gauges were not used in the work reported in this document.

The measurements are taken by a digital aquisition unit (DAQ) at a configurable rate. The unit allows for each sample in the section to be recorded simultaneously, providing an accurate snapshot of the strain. After the DAQ collection occurs, a program stores the strain measurements into a database. The database is periodically backed up to an offsite storage location where is is

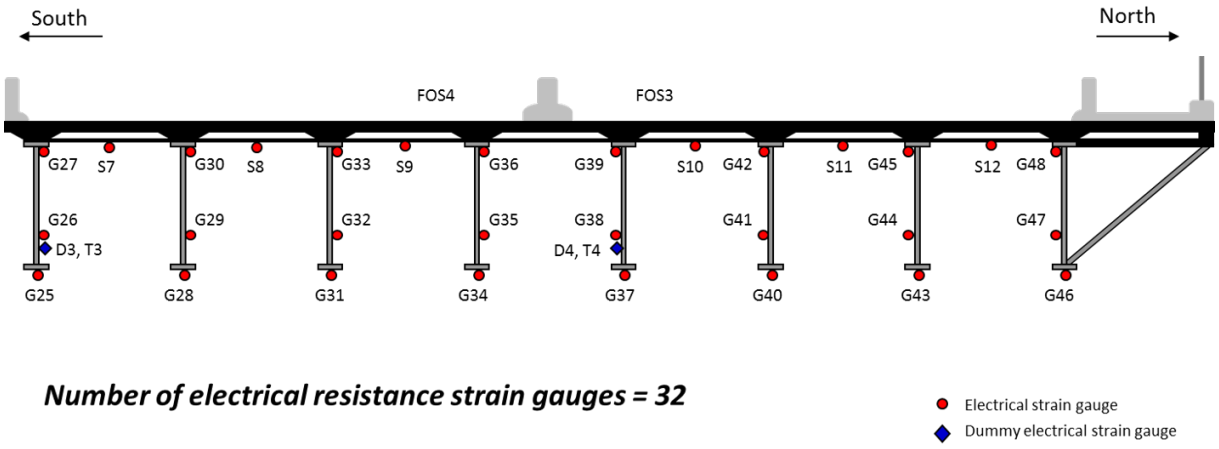

Figure 2.2: Gauge Locations - Section AA, South Perimeter Bridge [2]

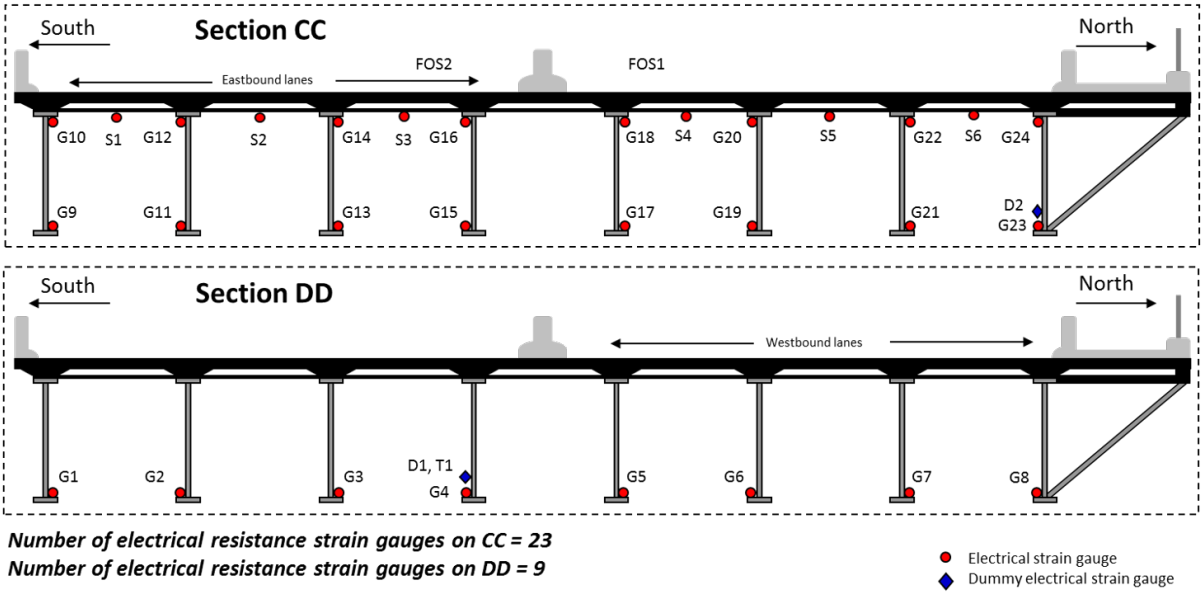

Figure 2.3: Guage Locations - Section CC and DD, South Perimeter Bridge [2]

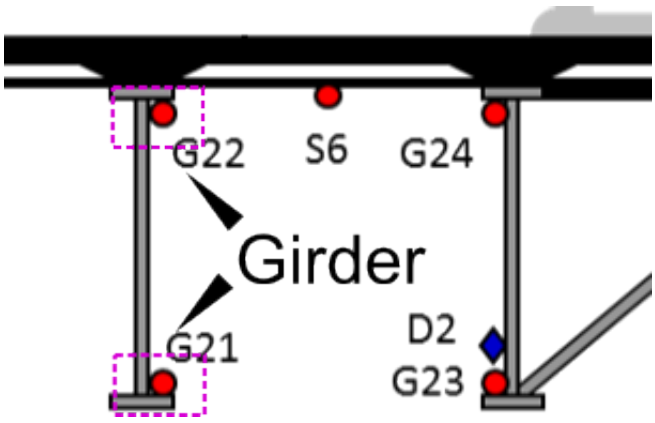

Figure 2.4: Girder-mounted strain gauges [2]

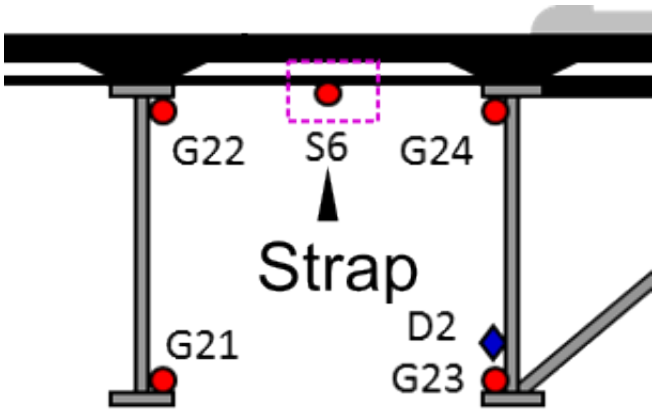

Figure 2.5: Strap-mounted strain gauges [2]

processed on a monthly basis.

2.4 Present and Future Developments

Deesomsuk and Pinkaew [5] concludes that with sufficient sampling, high accuracy is possible. The BWIM implementation on the South Perimeter Bridge represents significant advancement in Manitoba's infrastructure, but there are great possibilities for continued improvement and addition of more useful components. As of 2012, Oklahoma was undertaking the process of introducing BWIM-based weighing stations [8],

Ideally, Manitoba's highways will be augmented in the future to exploit BWIM technology. The linchpin is ensuring that the accuracy of the extracted signals is sufficient to provide an accurate measure of the weight of the trucks that traverse the bridge each day. Another problem area is multiple-vehicle scenarios, where more than one truck is captured in the event window. When this situation occurs, a potentially unrecoverable event is generated if the trucks pass side-by-side. The case where the trucks are following is simpler and the present algorithms are capable of recovering the signals. However, the case where two trucks pass side-by-side produces a breakdown in performance of the BWIM algorithms. The algorithms are not capable of directly processing the resulting signal mixture that is measured and recorded by the strain gauges.

Chapter 3

Sampling Analysis

Some sources [1] indicate a higher sampling rate may result in a more accuracte determination of parameters such as axle spacing. The authors are not alone in that assertion, and to that extent, an analysis was performed to quantify whether the strain is more accurately captured.

3.1 Theory and Background

3.1.1 Sampling

The Bridge Weigh-in-Motion (BWIM) algorithm uses a set of strain measurements sampled at 100Hz to infer the load (weight) of a vehicle traversing a span of the North Perimeter Bridge. As the algorithm relies on seeking local strain maxima, failing to sample (capture) the "true" maximum strain inevitably reduces the BWIM accuracy.

To demonstrate the concept and problem of missing the peak strain, consider the signal $x(t)$ shown in Figure 3.1. If $x(t)$ is then sampled using the sampling frequency $f_s = 10Hz$, the discrete time (sampled) signal $x[t]$ is as shown in Figure 3.2. The range has been constrained to $9 <= x[t] < 10.1$ to emphasize the peak.

Increased Sampling Rate

Figure 3.3 shows the same source signal sampled at double the frequency. The points joined by blue dots are connected to highlight the original sampled signal – no inference of signal reconstruction is intended.

As demonstrated in Figure 3.3, doubling the sampling rate results in obtaining twice the information. The goal of sampling is to capture sufficient information to process or reconstruct the signal. System design imposes constraints on the quality of sampling.

In terms of limitations, the capabilities of the sampling equipment play a major role. The equipment has an operational sampling range that will ultimately dictate the sampling. Additionally, increasing the sampling rate correspondingly increases the storage space required for

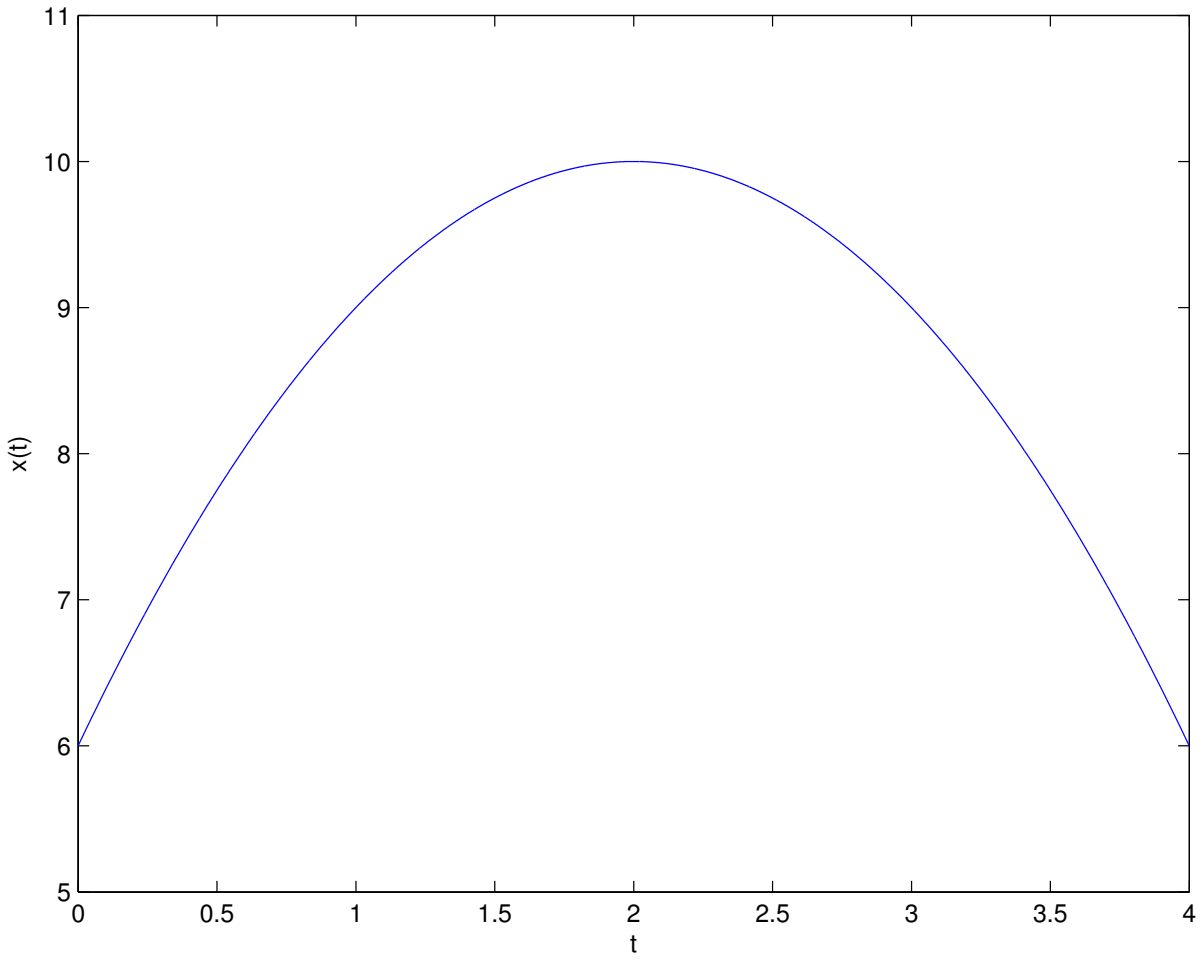

Figure 3.1: Example Continuous Time Signal

the data. For the Manitoba BWIM system, storage volume is a concern because the system is intended to run continuously and has been in operation for several years.

Missed/Off-Peak Sampling

The BWIM algorithm works by detecting strain peaks. Consequently, the algorithmic result – vehicle weight – is dependent upon capturing the peaks in the strain curves. A nomenclature of "off-peak" sampling is appropriate for the scenarios where the local maxima are not accurately captured. Figure 3.4 shows the previously used example signal sampled twice – once sampled ideally (no initial/peak offset), and again with $0.25T_s$ offset. Based on that figure, the relative error of the sampled value to the peak (desired) value is:

$$\Delta_\epsilon = \frac{x_{peak} - x_{sampled}}{x_{peak}} \tag{3.1}$$

3.1.2 Reverse Strain Calculation

The strain at a point is measured by:

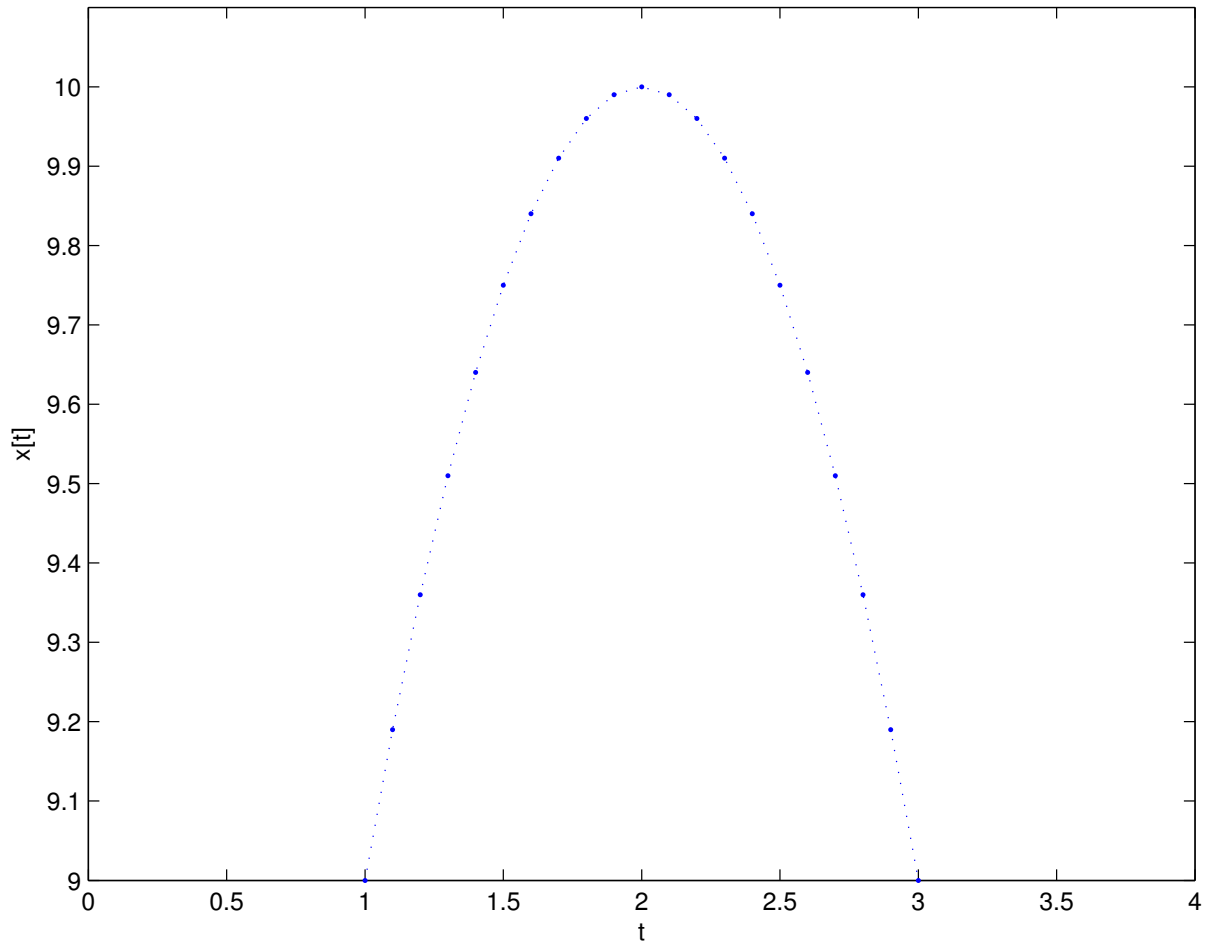

Figure 3.2: Example Signal Sampled with $f_s = 10Hz$

$$\epsilon = \frac{y}{EI}M \tag{3.2}$$

Where I and E are the bridge parameters – known values taken from [9] – and y is the strain gauge's distance to the neutral axis. Note that E and y are constants and can be neglected, leaving the following expression for pseudo-strain "pseudo-strain" [9]:

$$\epsilon = \frac{M}{I} \tag{3.3}$$

3.1.3 Moment

The moment of a point load (axle group) at a given snapshot in time during the truck's traversal is determined by:

$$M = \frac{x(L-x)}{L}P \tag{3.4}$$

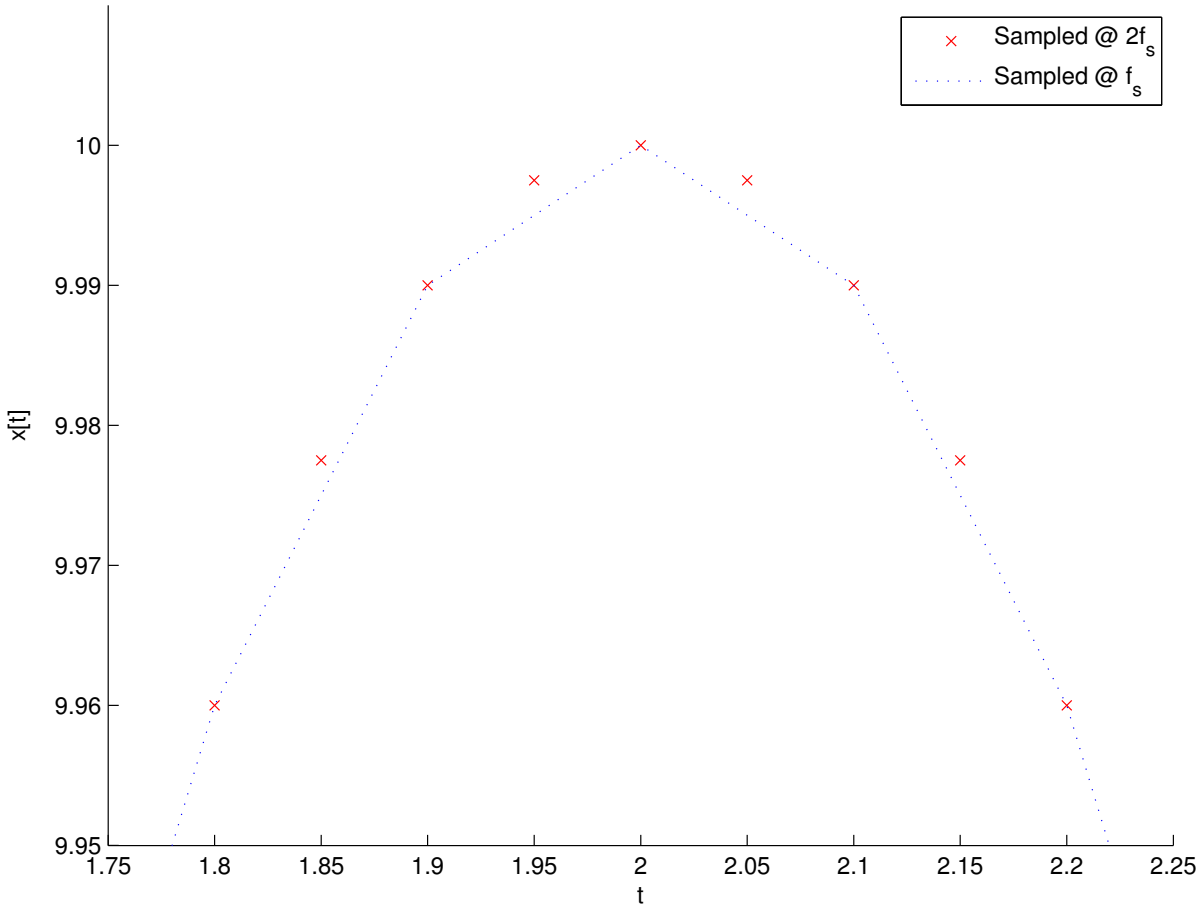

Figure 3.3: Example Signal, with Double-Sampled Overlay

Where P is a point load and L is the length of the instrumented span, as per the simply supported beam model. The moment at a specific point x due to two or more point loads is the superposition of the individual loads.

3.1.4 Truck Movement

Assuming constant velocity v, the displacement of a given axle group (point load) after t seconds is given by:

$$x_{P_i} = v * t - x_{di} \tag{3.5}$$

Where x_{di} is the displacement from the front of the truck for the axle grouping (for the first axle, $x_{d0} = 0$).

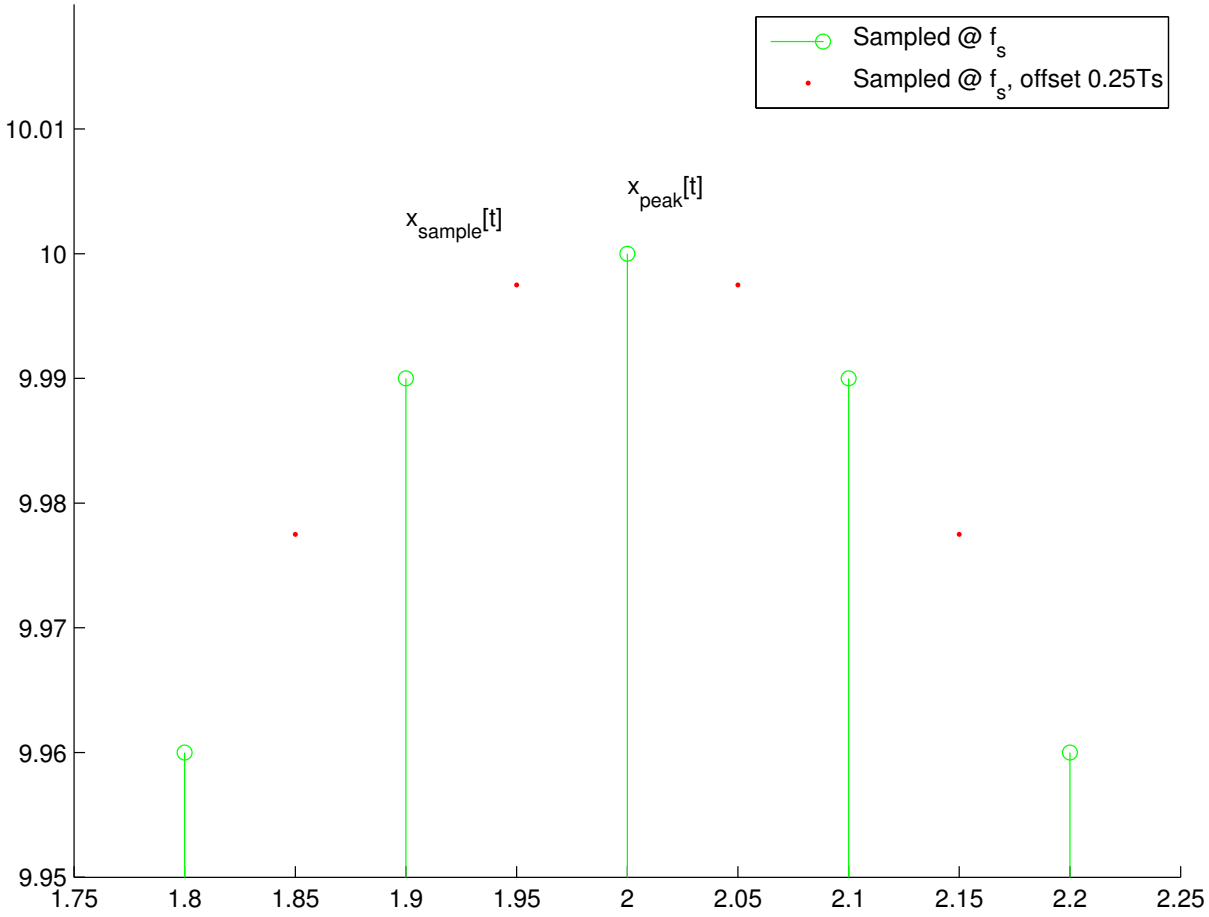

Figure 3.4: Off-Peak Sampled Signal

3.2 Simulation Description

3.2.1 Description

The simulation scenario is replicating the movement of the truck across the bridge from east to west. The truck is assumed to be traveling at 100 km/h in the curb lane. The strain measured on the first girder at $x = 3$ metres is modeled. A vehicle axle moves approximately 28 cm during one sampling period when using these parameters.

3.2.2 Outcomes

The expected outcome of the analysis is to provide a quantification of the relative amount of error in the strain when the truck's strain is sampled "off-peak". To do so, the sampling is performed at the nominal rate of 100 Hz, and at double that rate. The lower of the frequencies, 100 Hz, was selected as the baseline frequency for the South Perimeter Bridge's gauges. The higher of the frequencies, 200 Hz, was selected because it reflects the increased sampling rate supported by the strain gauge components on the South Perimeter Bridge —the primary reference for this project.

Table 3.1: Truck Load Parameters

Load ID	Axle Group Description	Load Amount (kN)	Displacement, x_{di} (m)
$P1$	Front wheels	55	0
$P2$	Back of cab	170	5.0
$P3$	Wheels of trailer 1	170	12.07
$P4$	Wheels of trailer 2	170	21.29

3.2.3 Simulation Parameters

The bridge parameters required for the E, I values were [9]:

- $x_A = 3m$ – location of the strain gauge;
- $E = 2e8$ – E of the girder material;
- $I = 0.03767352$ – the moment of inertia.

As previously described, y is unknown but removed since is is carried as a constant throughout the calculations. The truck values used to configure the simulation are listed in Table 3.1. The axle groupings' load magnitude and displacements, cumulative from the front of the truck, were derived from Figure 6 of [7].

3.3 Results

3.3.1 Load Movement

The movement of the loads across the bridge is shown in Figure 3.5. As expected, each of the four groups enters the instrumented section and imparts a positive moment at a time delay corresponding to the axle position. The dashed line at $x = 24$ metres emphasizes where each load is removed from the simulation – ie. out of the testing range. Note that under ordinary/real circumstances, the load would be expected to have a diminishing effect on the strain measurements as it travels away from $x = 24$ and off the bridge. The load modelling should suffice for these simulation runs.

3.3.2 Individual Loads

For the truck previously described, the moment of each load (axle group) is shown in Figures 3.6, 3.7, 3.8, and 3.9. The loads were considered only in the range $0 <= x <= L$, the test range that was used in actual testing of BWIM on the North Perimeter bridge.

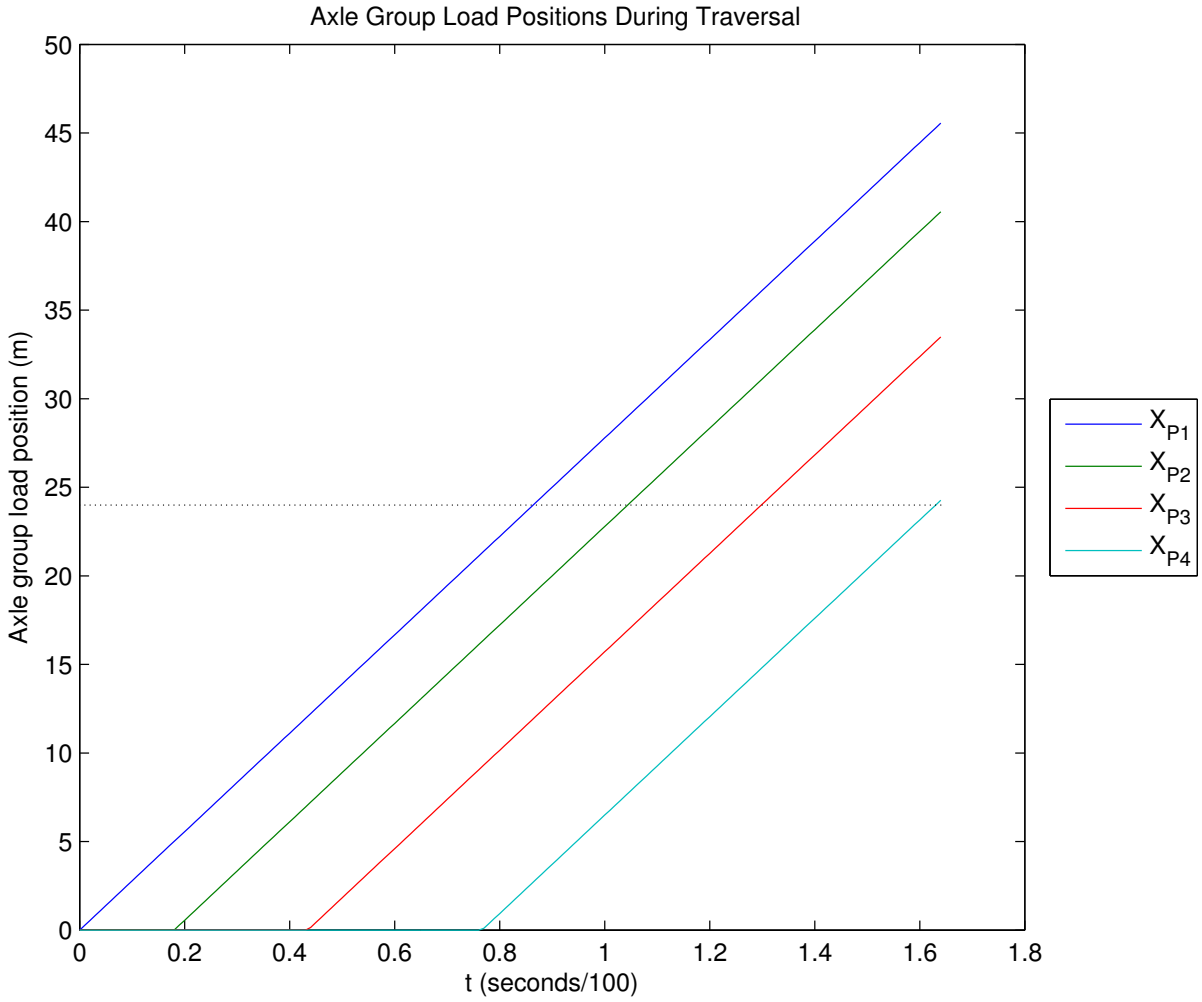

Figure 3.5: Movement of Axle Groups Across the Bridge

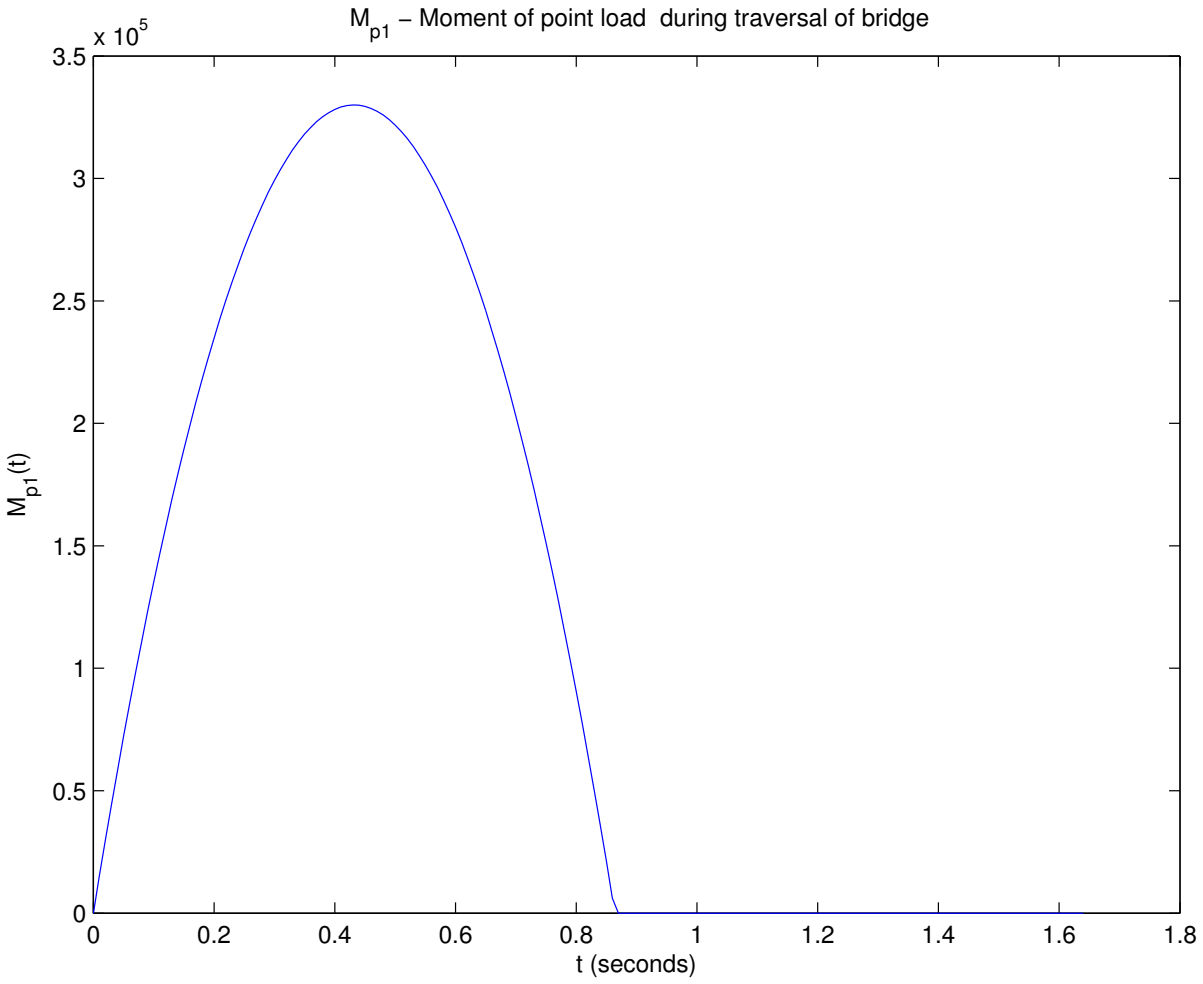

Figure 3.6: Moment of Axle Group (Point Load) 1 - Front Axle

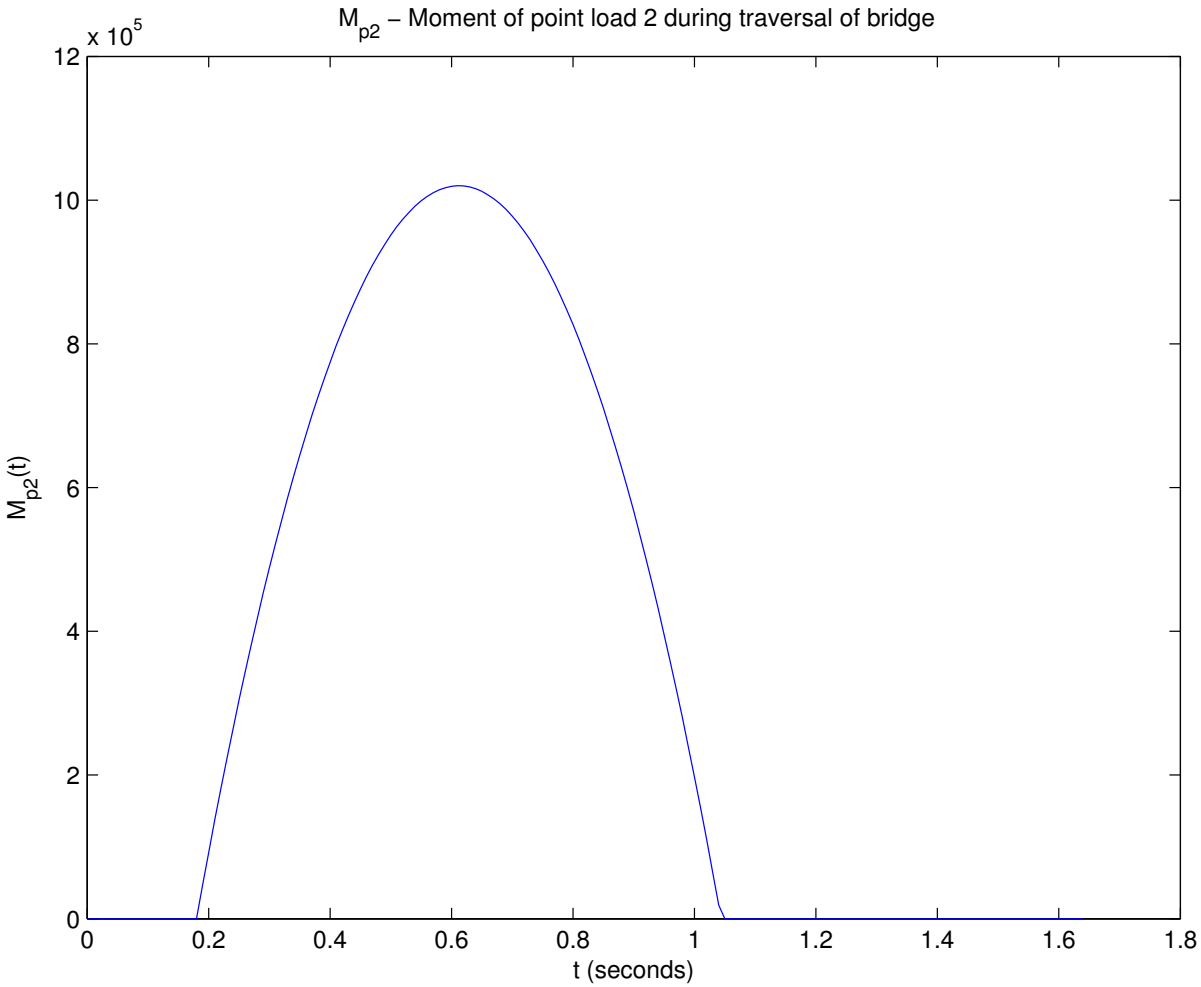

Figure 3.7: Moment of Axle Group (Point Load) 2

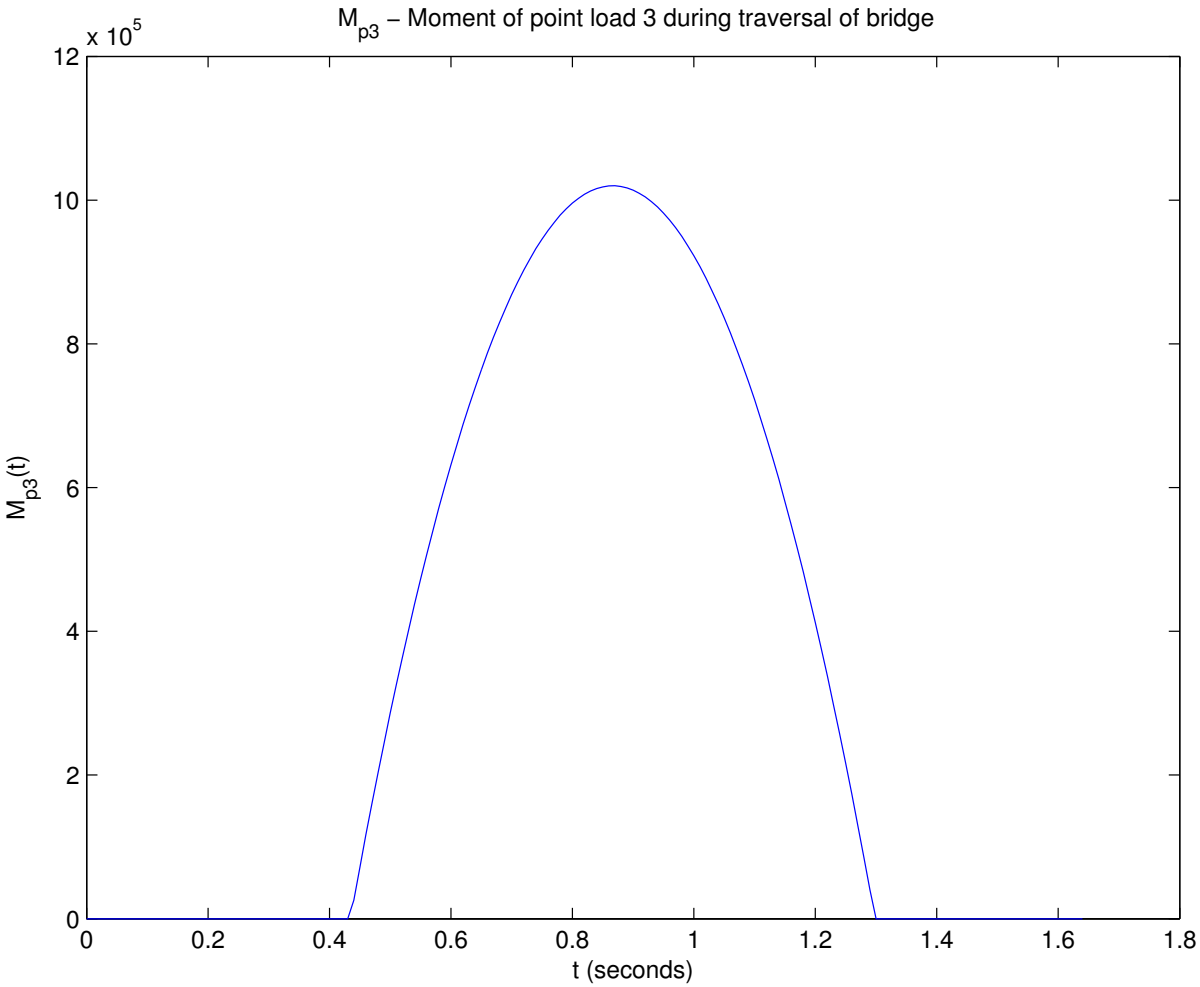

Figure 3.8: Moment of Axle Group (Point Load 3)

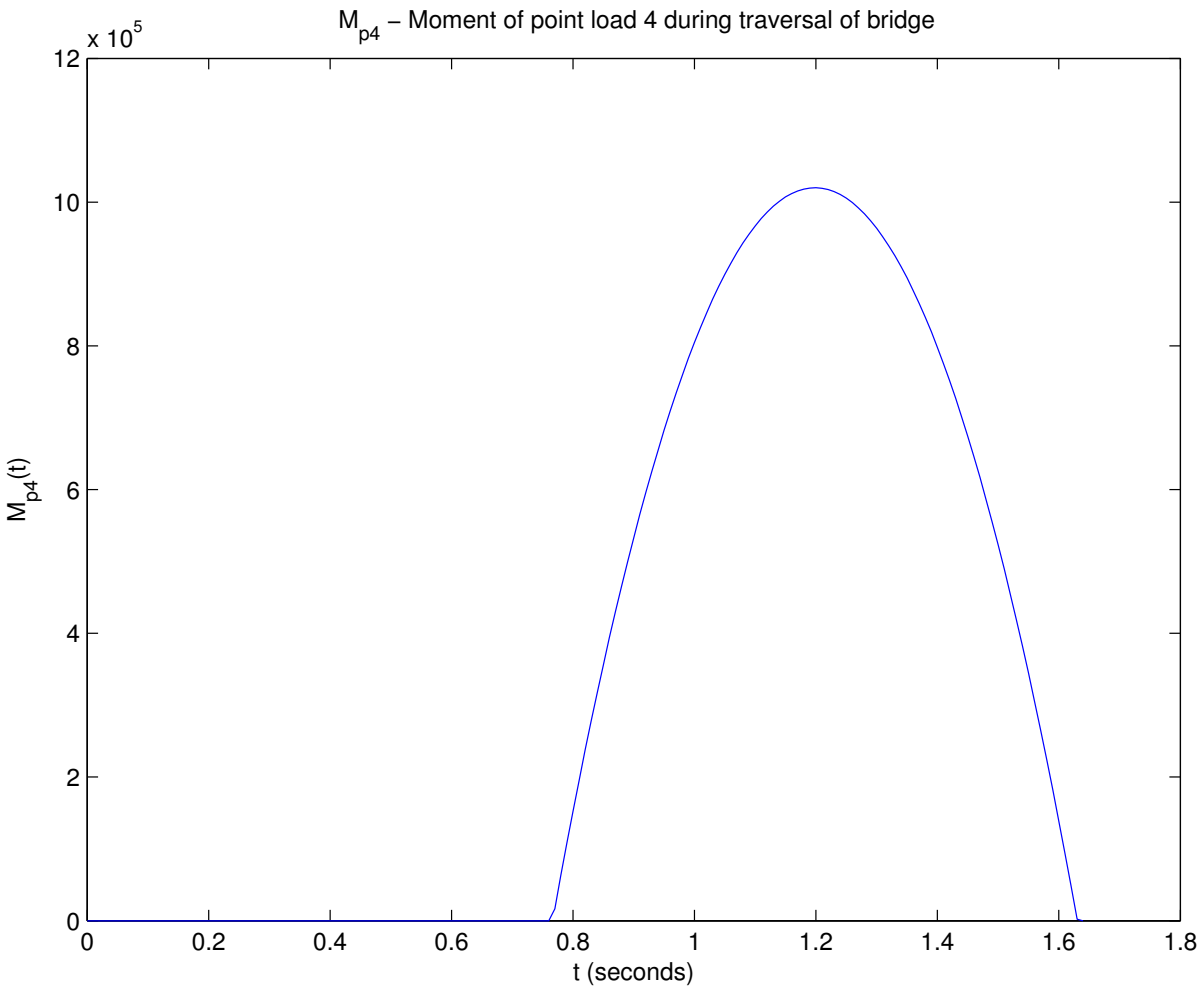

Figure 3.9: Moment of Axle Group (Point Load 4)

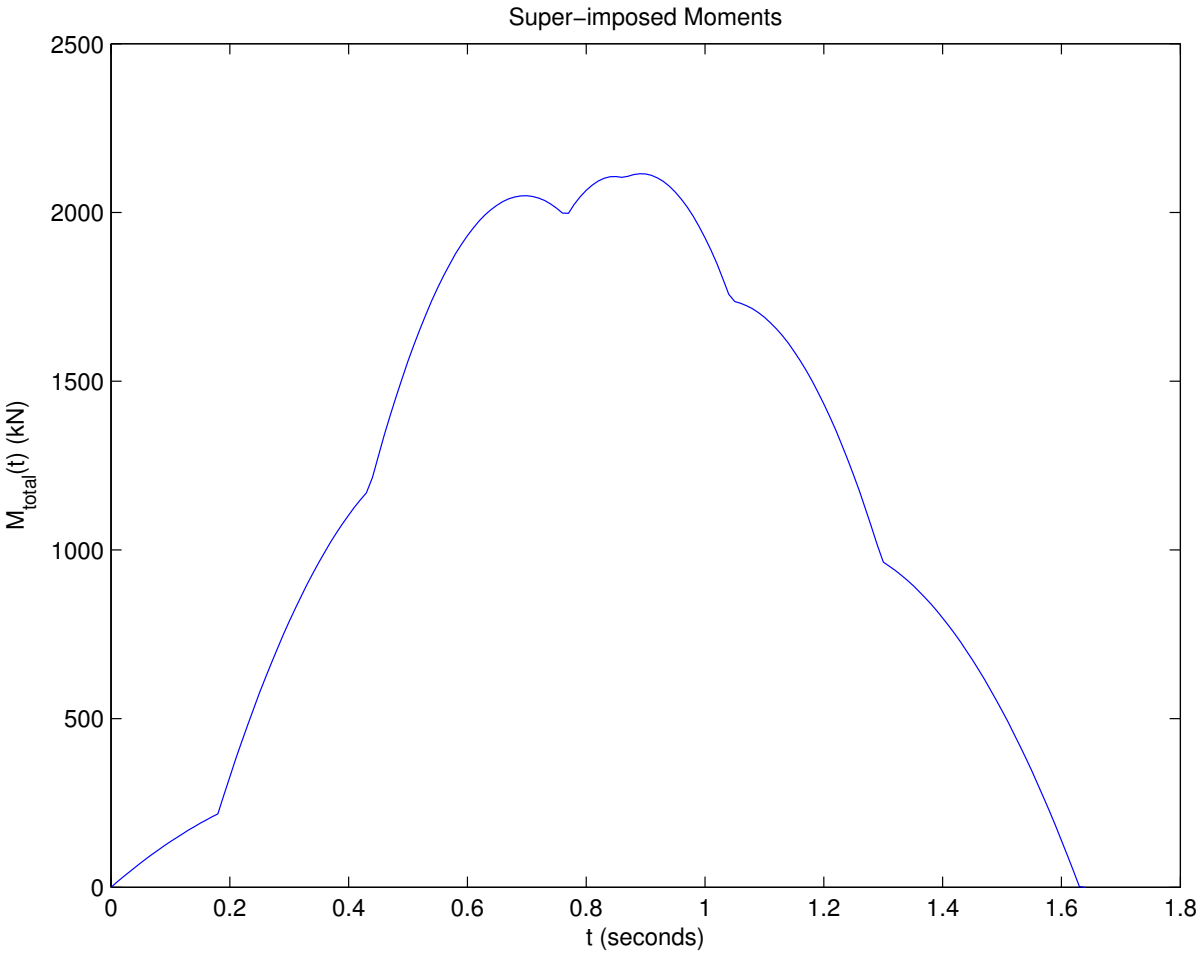

Figure 3.10: Moment of truck during traversal (superposition)

3.3.3 Combined Moment

The combined moment (computed by superposition) is plotted with respect to sample time, in Figure 3.10. The following is notable:

- Where the axle group (load) enters ($x = 0$) and leaves the test range ($x = L$), the transition is notably abrupt. In the real-life tests and subsequent plots, the transition is much smoother.
- The suspension is not modelled, even though it has noticable impacts on the signals due to its nature of operation. The suspension dampens the ride through spring mechanics. These spring mechanics are harmonic in nature, and manifest themselves in the strain measurements; it is especially noticeable at the vehicle's transition from the ramp onto the deck. Notwithstanding the additional realism that suspension modeling would provide, the variability of vehicle suspension systems makes suspension modeling an unsuitable form of simulation improvement.

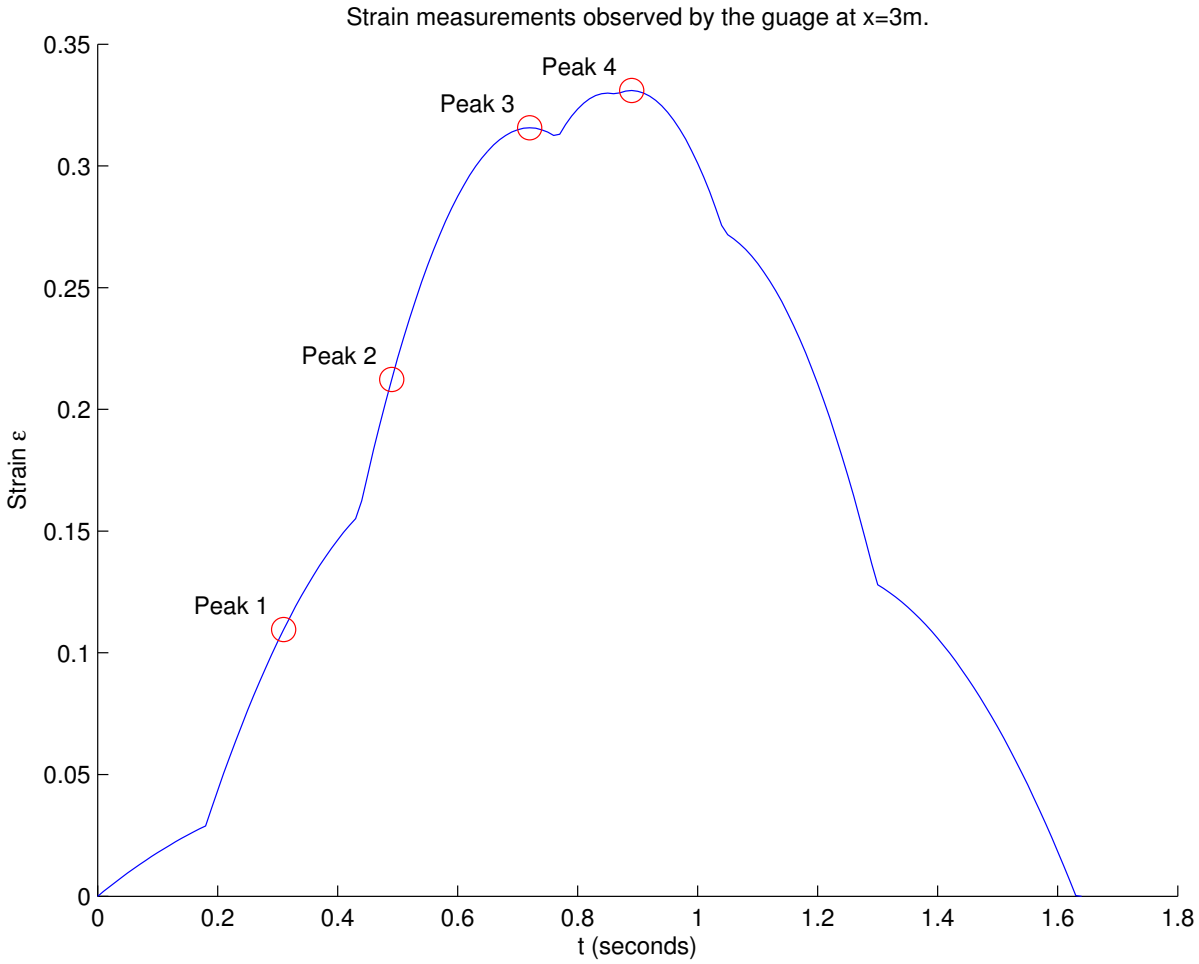

Figure 3.11: Strain Measurements of a Gauge at $x = 3$

3.3.4 Strain Measurements

The strain measurements of the gauge are plotted in Figure 3.11. The measurements differ from those presented in [1] – especially in the case of the first and second peak points. The difference is left as a point for further investigation and refinement (section 3.4 is dedicated to attempting to resolve discrepancies and flaws identified).

Peaks 3 and 4 in the simulated representations of the sampled strains ($f_s = 100Hz$) were measured, as shown in Figure 3.12 and Figure 3.13. The peak measurements are 316 and 331 microstrain, respectively. The third peak is detected at $t = 0.72$ seconds during the traversal, while the fourth peak is detected at $t = 0.89$ seconds. Peaks 1 and 2 are located approximately where the peaks would be if the signal was taken from actual strain gauge readings.

Offset/Non-Ideal Sampling

In order to simulate delayed/offset sampling, the samples were adjusted to represent them starting later than the truck's initial engagement with the test span. Specifically, a delay of half a sample period was incorporated (ie. starting at $t = 0.5Ts$), while maintaining the sampling rate of

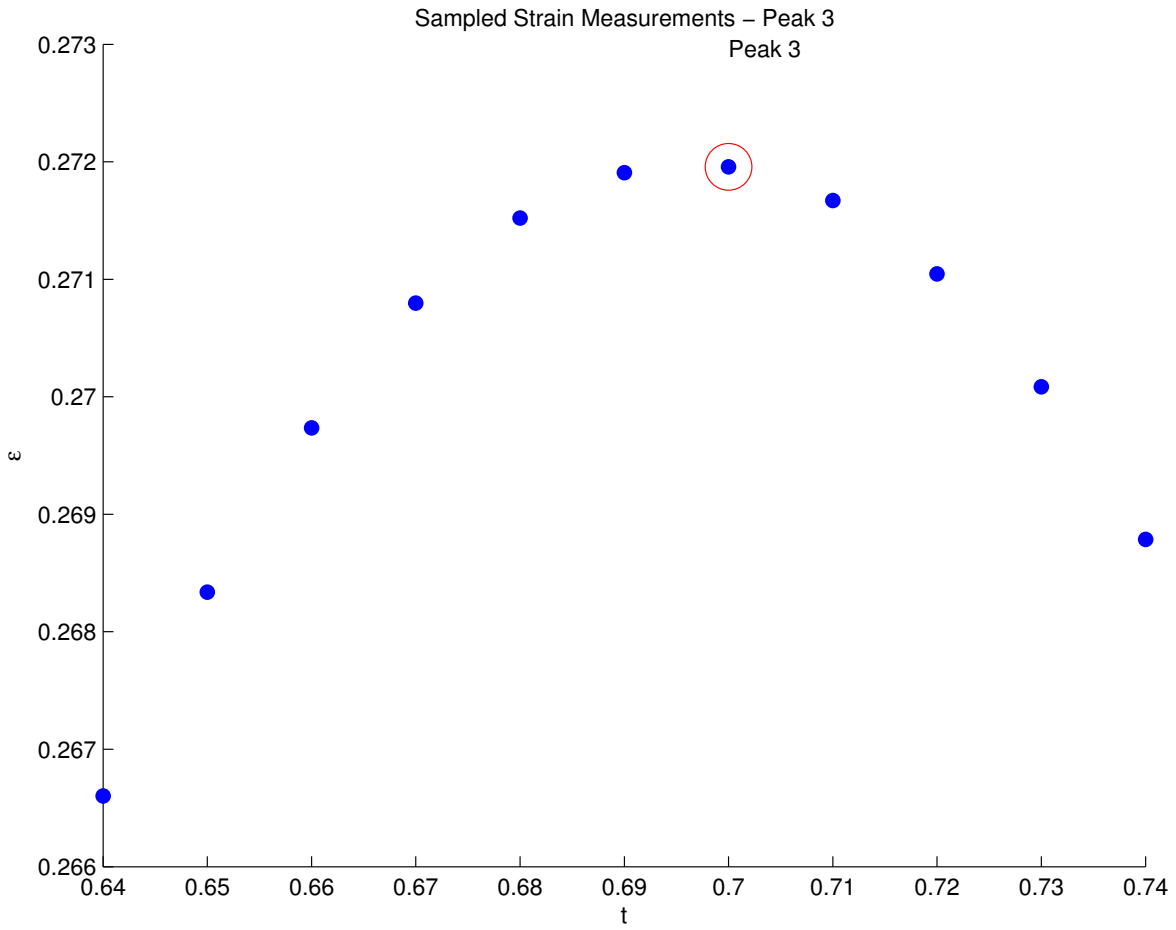

Figure 3.12: Strain Peak 3, Sampled at 100Hz

100Hz. The sampled strain under these conditions is shown in Figure 3.14. Peaks 3 and 4 were extracted as before, with peak 3 read at 316 microstrain and peak 4 as 331 microstrain. The relative errors are therefore notationally zero. However, to provide quantification, the relative error was calculated at 0.0153 % (peak 3) and 0.0150 (peak 4) %. To arrive at those values higher precision was allowed in the calculations.

The above results for relative error suggest that the sampling offset/missed peak does not have an impact as originally thought. These results are under scrutiny prior to conducting more investigation into the peak modelling accuracy. If the peaks are truly representative of the real-life behaviour, then the results are indeed acceptable. On the other hand, better modelling of peaks may make this simulation attempt and source of error more viable.

3.4 Improvements

3.4.1 Non-Truncated Moments

In order to refine the total vehicle load/moment representation (plotted in Figure 3.10), the measurements taken when an axle group is outside the test area ($x > L$), were included for a run.

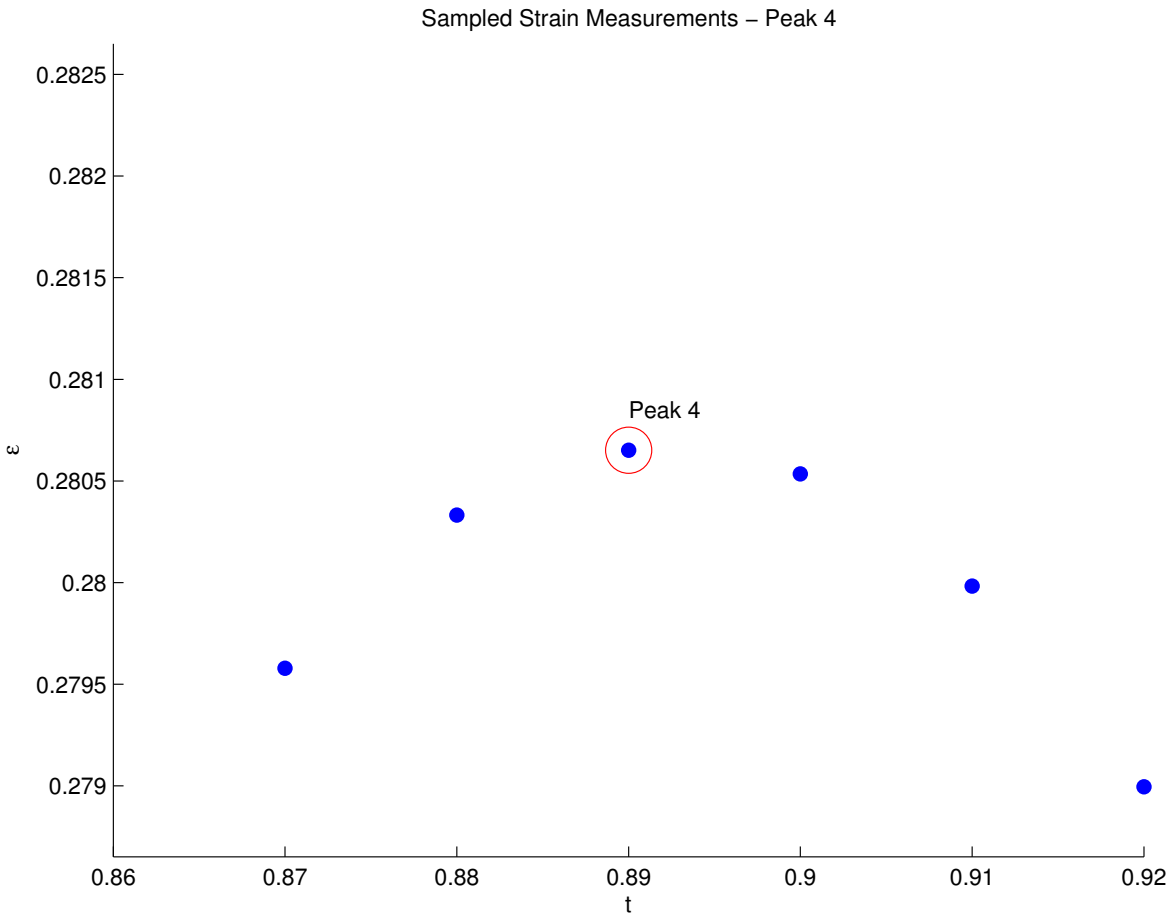

Figure 3.13: Strain Peak 4, Sampled at 100Hz

The objective was to smooth the curve, having noted the sharp transitions when the axle group enters/leaves the test range. The plots of the resulting individual group moments are shown in Figure 3.15, Figure 3.16, Figure 3.17 and Figure 3.18). As observed in the plots, there are significant negative components once the axle group has left the test range.

The moment plot for the run is provided in Figure 3.19. The large negative portions are caused by the large negative components in the individual moments.

Overall, better modeling of the "trailing off" of each load's moment after $x = L$ will likely aid in improving the accuracy of the analysis.

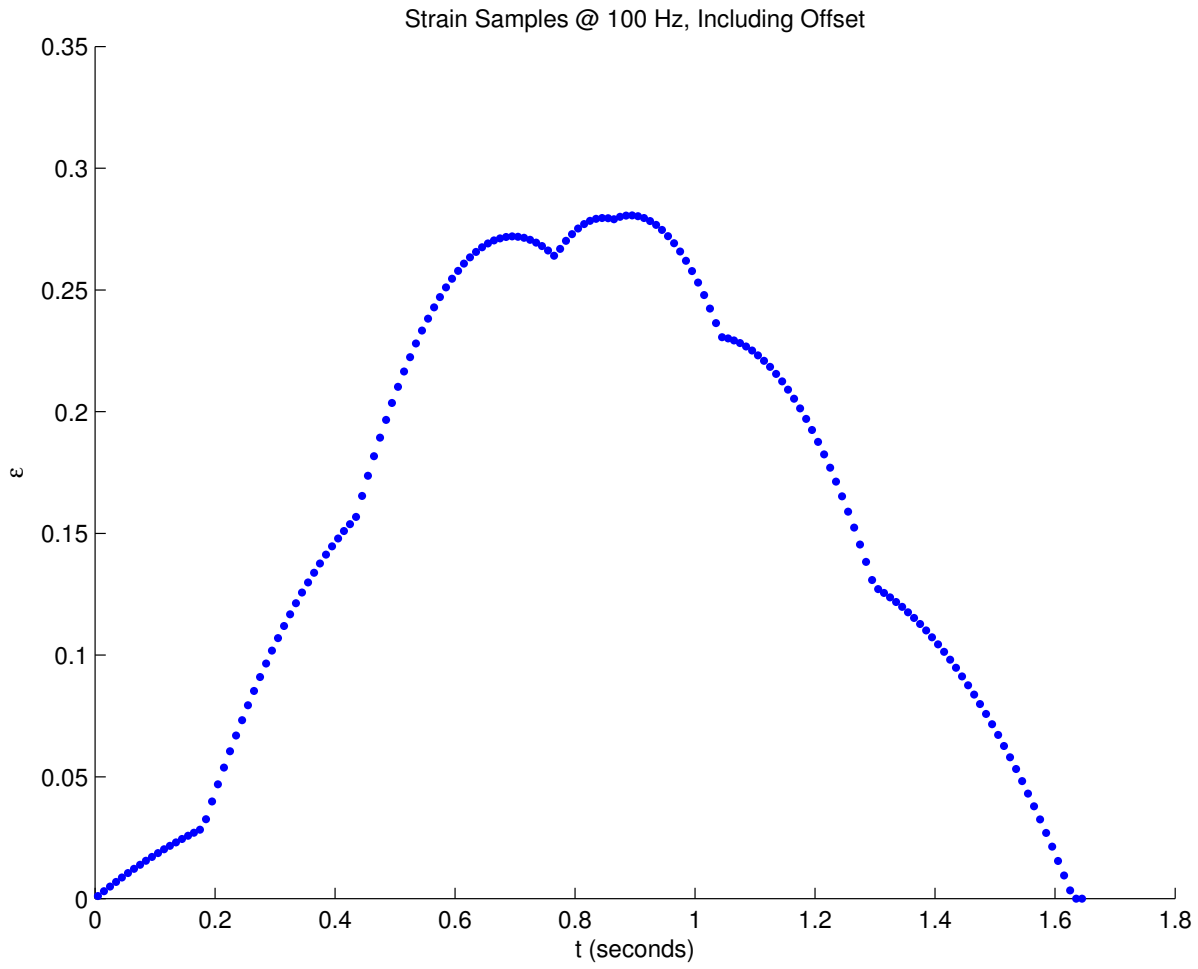

Figure 3.14: Sampled Strain with Sampling Offset

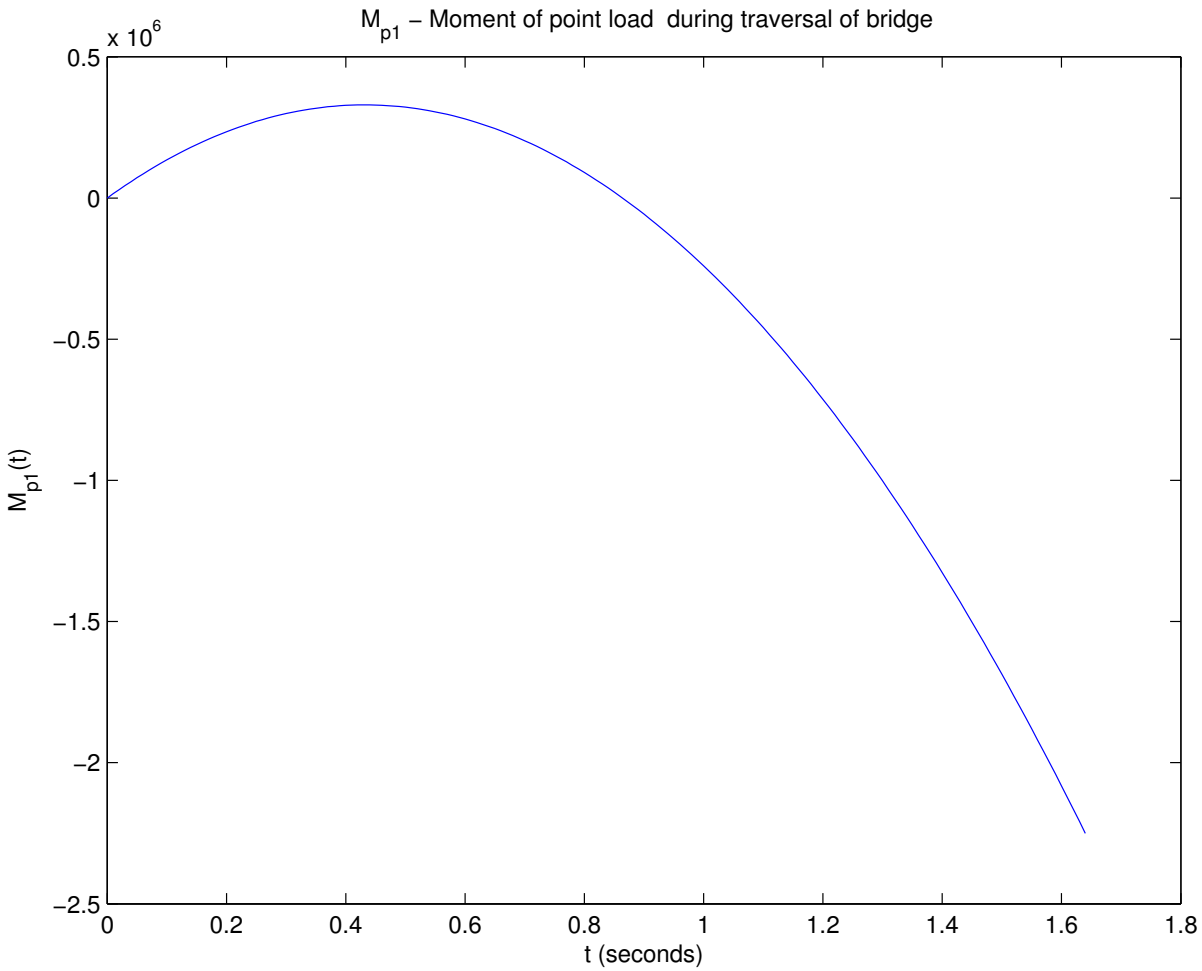

Figure 3.15: Moment of Axle Group (Point Load) 1 - Front Axle, no negative truncation for $x > L$

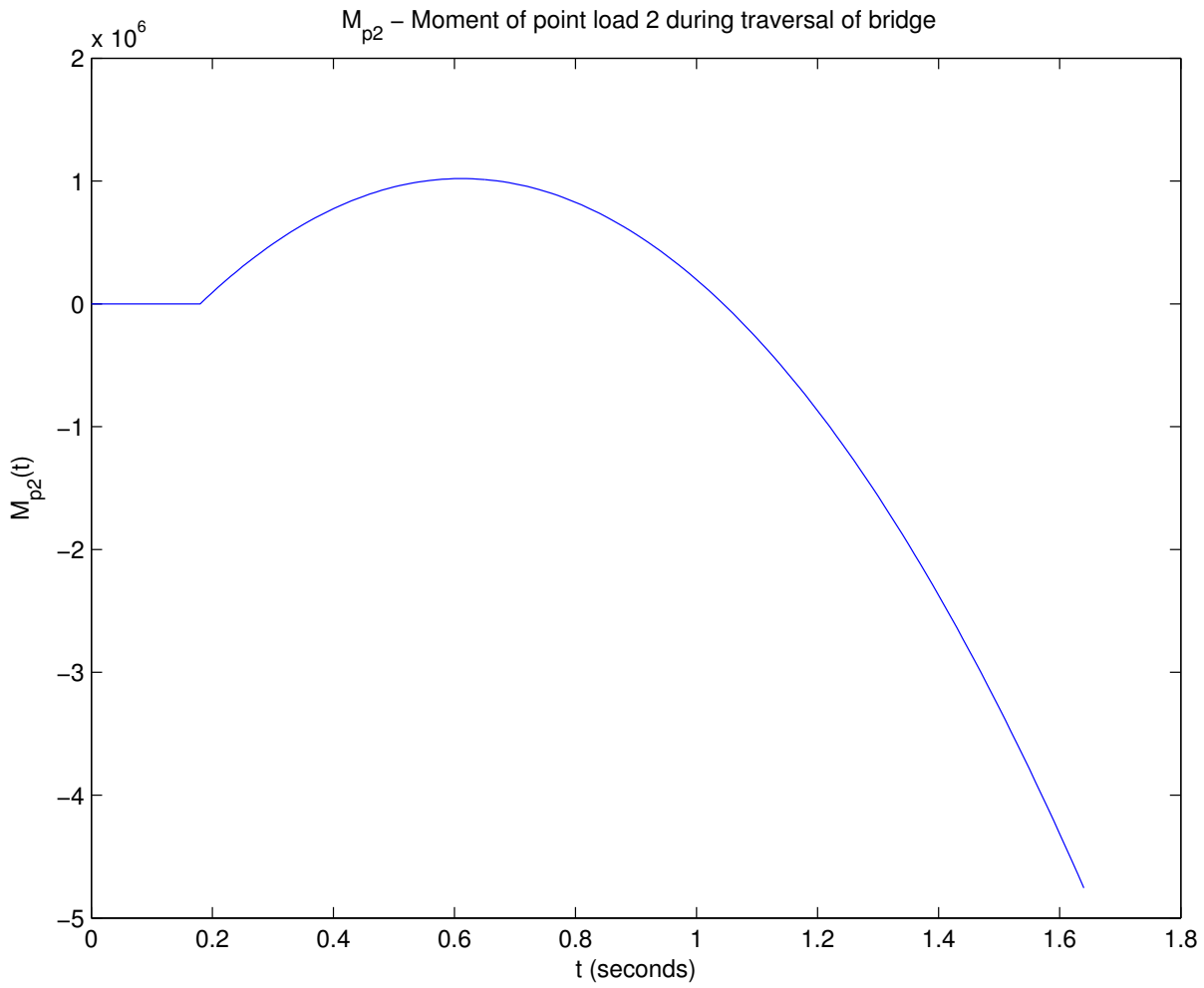

Figure 3.16: Moment of Axle Group (Point Load) 2 - no negative truncation for $x > L$

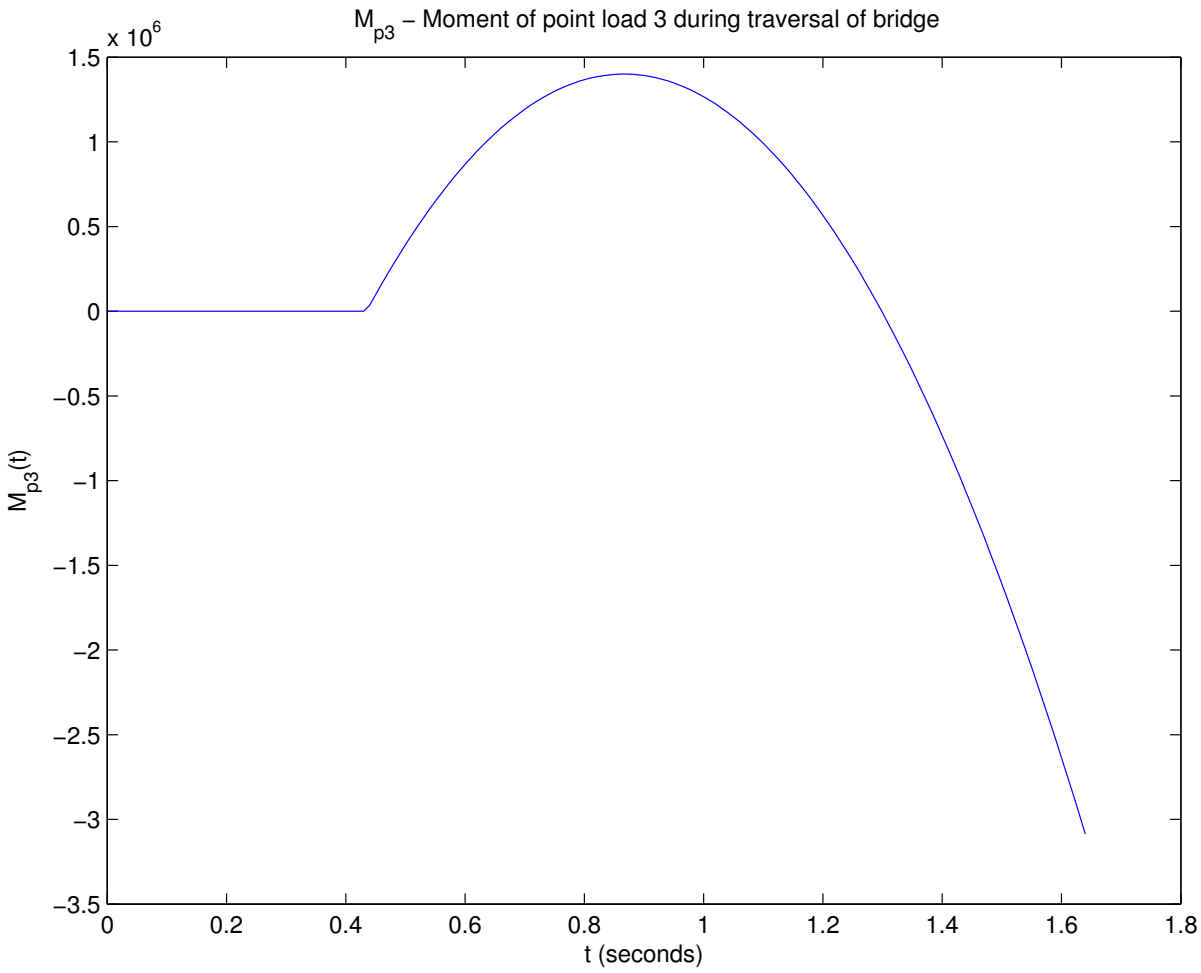

Figure 3.17: Moment of Axle Group (Point Load 3) - no negative truncation for $x > L$

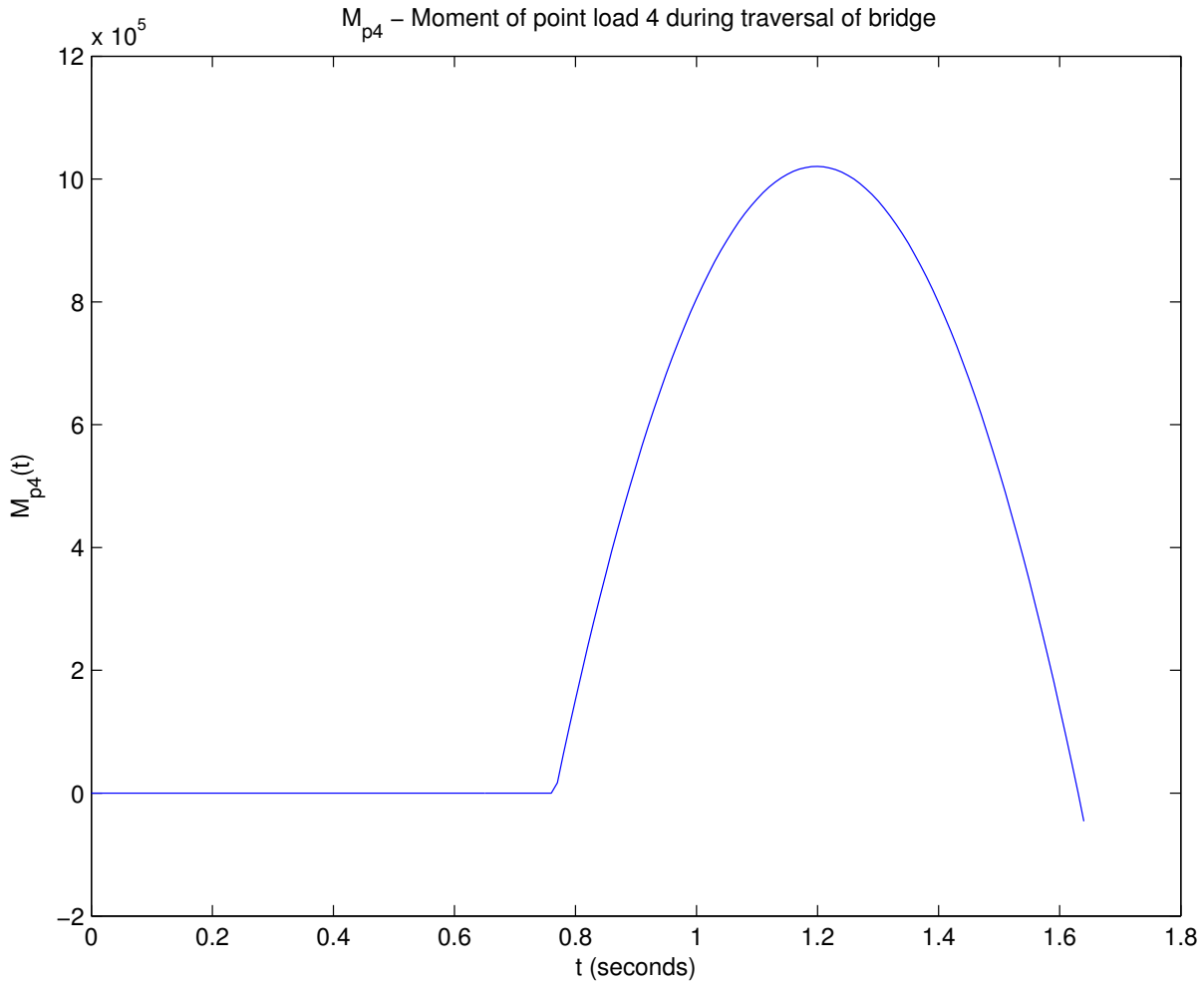

Figure 3.18: Moment of Axle Group (Point Load 4) - no negative truncation for $x > L$

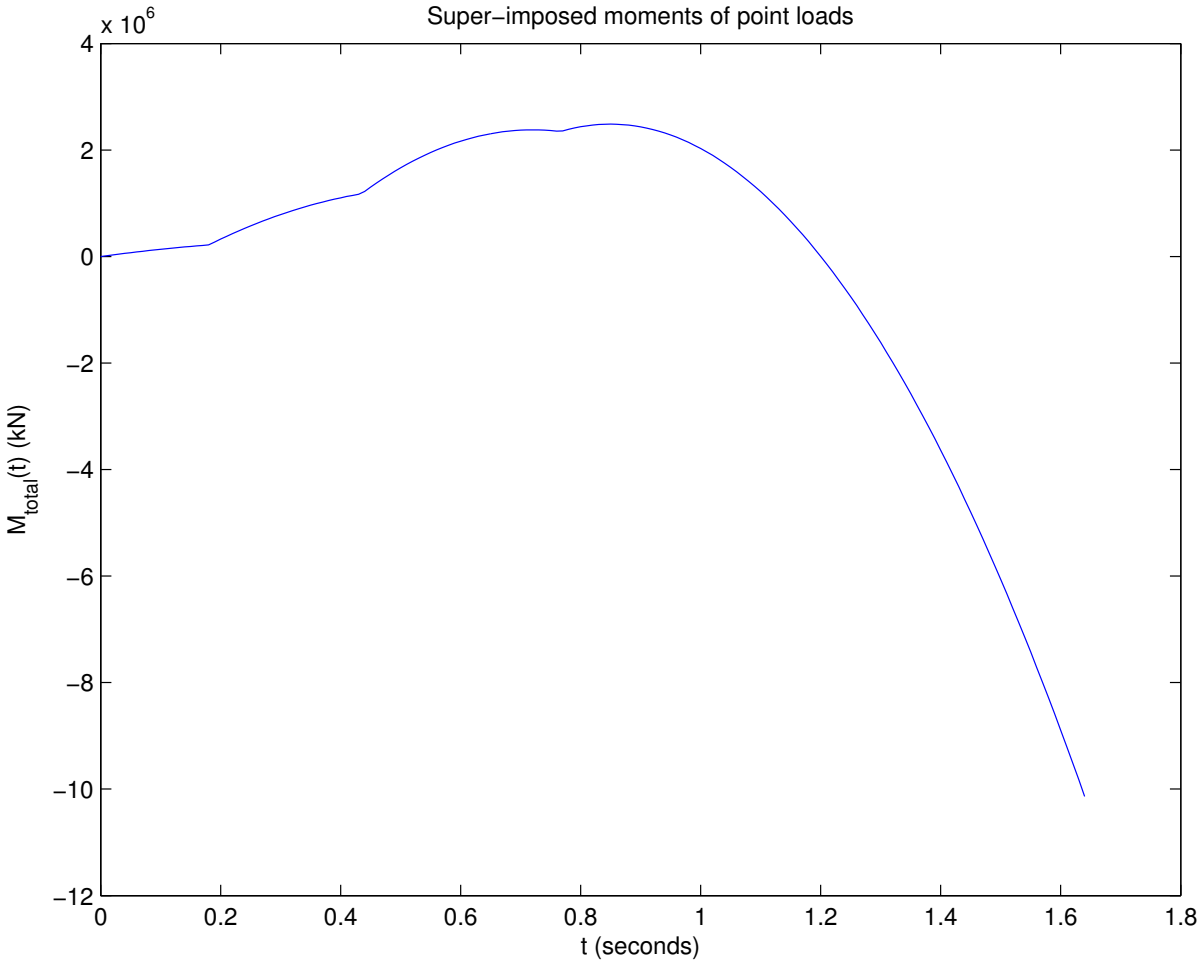

Figure 3.19: Moment, via superposition, as the truck travels across the bridge

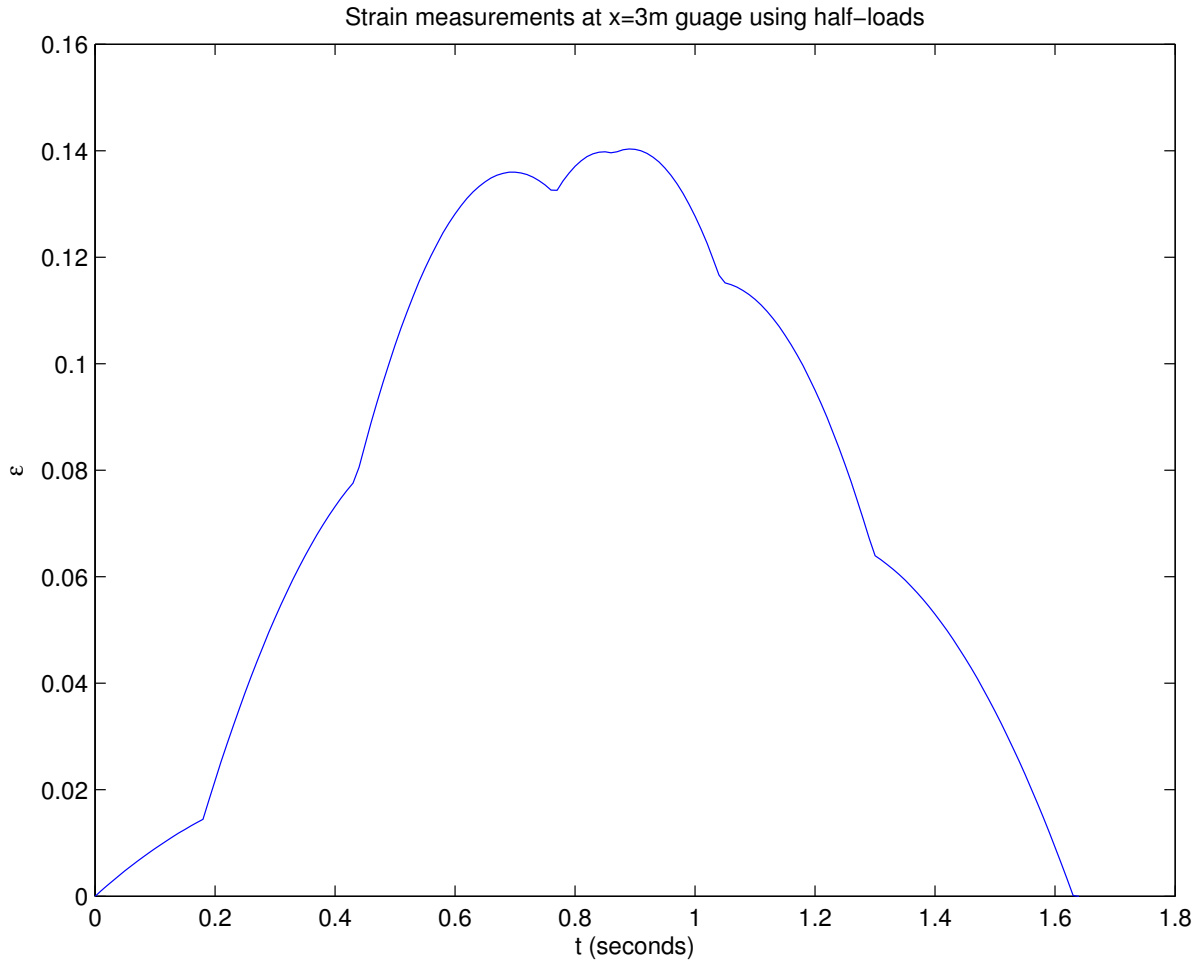

Figure 3.20: Strain Plot with Half Loading on the Girder

3.4.2 Load Sharing Across Girders

Based on the findings in [1], the load imposed on the first (leftmost) girder is approximately 50 percent of the total load for a truck traversing in the merging lane. The strain is plotted in Figure 3.20, showing an approximately 140 microstrain reading at the largest peak. [1] shows an upper reading of approximately 100 microstrain, leaving room for further improvement.

Chapter 4

Independent Component Analysis

Though accuracy has signfiicantly improved with respect to the straight-forward single vehicle events typically covered in literature [7, 1, 6]. On an open roadway, those conditions are not gauaranteed and BWIM systems such as the South Perimeter Bridge do capture multi-vehicle events. When trucks pass side-by-side, the signal is a mixture and not useable. In order to extract the weight of the trucks, each of the trucks' signals is required separately for processing.

4.1 ICA Background

Independent Component Analysis (ICA) is a method of Blind Source Separation (BSS) for extracting underlying components from data of varying sources such as stock prices [10] and health care [11]. The term "blind" implies that the process is applicable to scenarios where little is known about the original (source) signals. As identified later in this section, the latter scenario tends to fit with the SHM process —other than perhaps a picture taken, little is known about the trucks that are passing over a bridge aside from their strain measurements. [12]

The canonical scenario for ICA is the example of voices in a noisy room recorded by multiple microphones. The human brain is able to separate each voice into it's distinct components, otherwise conversing at a party would be a rather daunting challenge. Likewise, in certain applications, knowing the individual pieces (components) of each signal has practical value.

The inspiration for using ICA in BWIM came from reviewing other work based on ICA [13]. Subsequent literature searches and reviews yielded no obvious indication that others have attempted to use ICA in this fashion.

4.1.1 Signal Requirements

A set of required properties for source signals has been identified for the input signals in a mixture in order for them to be separable by this technique [12]. These properties are rooted in a number of observations about the effects of mixing signals.

When considering the signals, the signals must have non-Gaussian distributions [14]. The symmetrical distributions of Gaussian signal mixtures renders the data inoperable from the ICA perspective as the mixture contains insufficient directional information to orient the mixing matrix $\mathbf{A}$. A proof of that conjecture and further details of the non-Gaussian requirement is available in [14, pp. 5]. The resulting signal mixture adopts a Gaussian distribution, and therefore seeking a set of non-Gaussian signal components aids in extracting the signals.

Also, the signals must be "fundamentally unrelated" [12, pp. 7]. The example of voice signals meets this requirement because the voices are separate physical entities generating a signal. The concept is more formally classified under the umbrella of statistical independence —correlation. Simply knowing that the signals are unrelated is leveraged in recovery; the search entails then finding unrelated signals that vary in time. When mixing the signals, the independence is dissolved and a codependency is introduced. A part of the extraction process is then producing signals that are not dependent.

Finally, the increased complexity of a mixture is leveraged in the extraction by reducing the complexity of the extracted signals. In other words, the complexity of the source signals should be relatively low to make the extraction easier. [12]

4.1.2 Signal Mixtures

Clearly, the concept of signal mixtures is essential to explore the applicability of ICA to BWIM. The cornerstone presumption of ICA is that a mixed signal is inherently a combination of independent components that are non-Gaussian. The mixing of the signals produces a signal mixture that is more Gaussian. Therefore, in the separation procedure extracting the signals focuses on a return to independence and non-Gaussian signals. A bulk of the ICA literature reviewed [15, 16, 12, 14] leads the discussion with an explanation of signal mixtures. The remainder of this section is devoted to introducing the signal mixing process at a high level. Interested readers should consult [12, Ch 3,Ch 4] for a more in-depth treatment of the topic of signal mixtures. The final portion of this section briefly discusses the process of separation ("unmixing").

Mixing

The scenario for signal mixing can be demonstrated using the following example. Two recording stations, microphones in the case of a voice, are sampling and saving measurements from two independent sources. In a voice recording, the source signals are physically independent because they are generated by two individuals. In general terms, it is assumed that if the two sources are physically separate processes, they are classifiable as independent [12, 8]. A signal generated at a source is referred to by the vector $\mathbf{s_x}$ where the $\mathbf{x}$ subscript identifies which source generated the signal. Each entry in $\mathbf{s_x}$ has the form s_x^t where t denotes the time. Since all discussions deal with time, t is equivalent to the sample index.

At the recording location, for example microphone 1, the signal is captured (sampled) proportionally according to a mixture rule. For a microphone, the mixing rule is acceptably defined as the distance from the microphone, assuming that the voices are close in volume. Therefore, a sample x_1^t at $t = 1$ is a mixture of the two components:

$$x_1^1 = a_1^1 s_1^1 + a_1^2 s_2^1 \tag{4.1}$$

In Equation 4.1, a_1^1 denotes the relative amount of s_1^1 the mixture contains. Similarly, a_1^2 denotes the proportion of s_2^1 that the mixture contains. The same applies for x_2, but it is instead determined using the mixing coefficients a_2^1 and a_2^2 (the proportion of signal 1 and signal 2 taken for a sample at recorder 2). Across an entire sampling interval $[1, n]$, the mixtures $\mathbf{x_1}$ and $\mathbf{x_2}$ take the form elaborated in Equation 4.2 and Equation 4.3, respectively.

$$\begin{aligned}
\mathbf{x_1} = \left(x_1^1, x_1^2, \ldots, x_1^n\right) &= \left(a_1^1, a_2^1\right)^T \begin{bmatrix} s_1^1 \ldots s_1^n \\ s_2^1 \ldots s_2^n \end{bmatrix} \\
&= \begin{pmatrix} a_1^1 \\ a_2^1 \end{pmatrix} \begin{bmatrix} s_1^1 \ldots s_1^n \\ s_2^1 \ldots s_2^n \end{bmatrix} \\
&= \left((a_1^1 s_1^1 + a_2^1 s_2^1), (a_1^1 s_1^2 + a_2^1 s_2^2), \ldots, (a_1^1 s_1^n + a_2^1 s_2^n)\right)
\end{aligned} \tag{4.2}$$

$$\begin{aligned}
\mathbf{x_2} = \left(x_1^1, x_1^2, \ldots, x_1^n\right) &= \left(a_1^2, a_2^2\right)^T \begin{bmatrix} s_1^1 \ldots s_1^n \\ s_2^1 \ldots s_2^n \end{bmatrix} \\
&= \begin{pmatrix} a_1^2 \\ a_2^2 \end{pmatrix} \begin{bmatrix} s_1^1 \ldots s_1^n \\ s_2^1 \ldots s_2^n \end{bmatrix} \\
&= \left((a_1^2 s_1^1 + a_2^2 s_2^1), (a_1^2 s_1^2 + a_2^2 s_2^2), \ldots, (a_1^2 s_1^n + a_2^2 s_2^n)\right)
\end{aligned} \tag{4.3}$$

As shown in those equations, the same source values are used to generate $\mathbf{x_1}$ and $\mathbf{x_2}$; only the mixing parameters are varied to change the corresponding mixture value.

A much more convenient way of indicating the signal mixture is through a vector/matrix notation as shown in Equation 4.4. In this form, **A** contains the mixing coefficients and is referred to as the mixing matrix [12, 43]. The **s** matrix contains both source signals, and the result matrix **x** contains two mixtures as observed by each station.

$$\mathbf{x} = \mathbf{As} \tag{4.4}$$

Separation

While the above discussion lays the foundations of signal mixing, the more interesting process is obtaining the source components through separation.

$$\mathbf{s} = \mathbf{W}\mathbf{x} \tag{4.5}$$

Practically speaking, the separation matrix $\mathbf{W}$, an unknown due to lack of a priori knowledge of the mixing parameters ($\mathbf{A}$), is the solution of the problem that produces an estimator of the original signals. Therefore, the $\mathbf{s}$ signal in Equation 4.5 is more formally specified using estimator notation $\hat{\mathbf{s}}$. As observed during literature review [12], the $\mathbf{y}$ notation is more common in ICA discussions for identifying the extracted signals.

In ICA, the separation matrix is determined through various approaches [12]. The techniques centre around maximizing signal entropy in the extracted components, producing time or spatial separation, gradient ascent and using estimation theory to determine the maximum likelihood estimate of the separation matrix.

4.1.3 ICA Implementation

Implementing an ICA method was out of the scope of this thesis. Based on work performed in other research areas such as electrocardiogram separation [13], the FastICA [17] Matlab package was selected for performing the ICA tests. The initial iterations to experiment with the various parameters and methods were performed using the supplied functional GUI which is convenient for experimentation. The testing performed and documented below leveraged the more efficient function entry-point for the package.

FastICA itself is an implementation of the "fast fixed-point algorithm for independent component analysis" [17] that is suitable for use in an "exploratory fashion and for estimation of independent components (or sources)"[17]. The algorithm, authored by Hyvärinen [16] utilizes fixed-point iterations to improve on gradient descent methods, yielding 10-100 times better performance in third-party experiments. [17]

4.2 Applying ICA to BWIM

Extending the case of ICA to BWIM, the strain gauges are analogous to the recording microphones, with the voices equating to the vehicles traversing the instrumented sections. If the individual parts (truck signals) are recovered, then the BWIM analysis can be successfully performed on the separated components. As with the microphones, the "recorded" strain signals contain different mixtures of each signal ("voice"), akin to the conversation recorded at a party. The challenge arises in determining the way to separate the signals without prior knowledge, via an isolated measurement, of each truck's strain. Under those conditions, the magnitude of effort is reduced by a significant amount.

An important consideration of attempting to apply ICA to BWIM is whether the BWIM system meets the requirements established throughout the literature and discussed above. The source signals themselves meet the requirement of being from separate physical processes, or

independent. The signals may be from separate physical processes, but it is not enough of a guarantee owing to the simplicity in the assumption. While the trucks are likely different, if they are the same the process will not work.

There are also an adequate number of signal "recordings" available for performing the extraction. In each of the instrumented span sections (AA, CC, DD), there are a minimum of eight (8) strain gauges performing the measurement. Therefore, providing that at least two (2) strain gauge's measurements are used, the number of mixture samples exceeds the count of sources.

4.2.1 Signal Mixtures

Signal mixtures are evidently central to investigating ICA. Returning to the sound sampling domain aligns the forthcoming discussion with literature's seemingly canonical example, therefore the connection to SHM/BWIM is established after introducing the signal mixing process.

The microphone problem is structured around two spatially-separated microphones recording two people having a conversion in a party. Each microphone records both voices along with the residual noise of the party background. Assuming identical microphones, the mixture of the signals is dependent on the location of the microphone with respect to the source (voice). From a physical standpoint, if the two voices are equal in volume (signal amplitude), then the closer voice should prevail by some margin - the mixture contains a larger portion of the source closer to the microphone.

As the truck traverses the bridge, and particularly the instrumented span, its load is distributed across the eight (8) girders that support the deck. The expected distribution has the signal concentrated in the girders of the bridge surrounding the event. The assumption is taken from data obtained during controlled tests [6], specifically the distributions for Test 4 and Test 5, both of which captured single truck events ("Truck A followed by Truck B") in the east-bound direction with the vehicles traveling at a speed of 95 km/h. Crucially, the tests were performed in separate lanes, as evidenced by their distributions shown in Figure 4.1 and Figure 4.2, respectively. Therefore, these tests are an appropriate basis for the mixing parameters.

The test results for tests 6 and 12, "Truck A beside Truck B" [6], were not used as the data supplied contains no insight into the mixing proportions that would have resulted in the final distribution. The mixtures employed in the simulations would have been formulated based on estimated distributions and are unsuitable for making a determination of ICA's use and incorporation into the overall BWIM process.

$$\begin{aligned}\mathbf{A} &= \begin{bmatrix} a_1^1 & a_2^1 & a_3^1 & a_4^1 & a_5^1 & a_6^1 & a_7^1 & a_8^1 \\ a_1^2 & a_2^2 & a_3^2 & a_4^2 & a_5^2 & a_6^2 & a_7^2 & a_8^2 \end{bmatrix} \\ &= \begin{bmatrix} 0.258 & 0.2512 & 0.2202 & 0.1273 & 0.0781 & 0.0422 & 0.0231 & 0 \\ 0.1134 & 0.1562 & 0.2361 & 0.2192 & 0.1491 & 0.0749 & 0.0511 & 0 \end{bmatrix}\end{aligned} \tag{4.6}$$

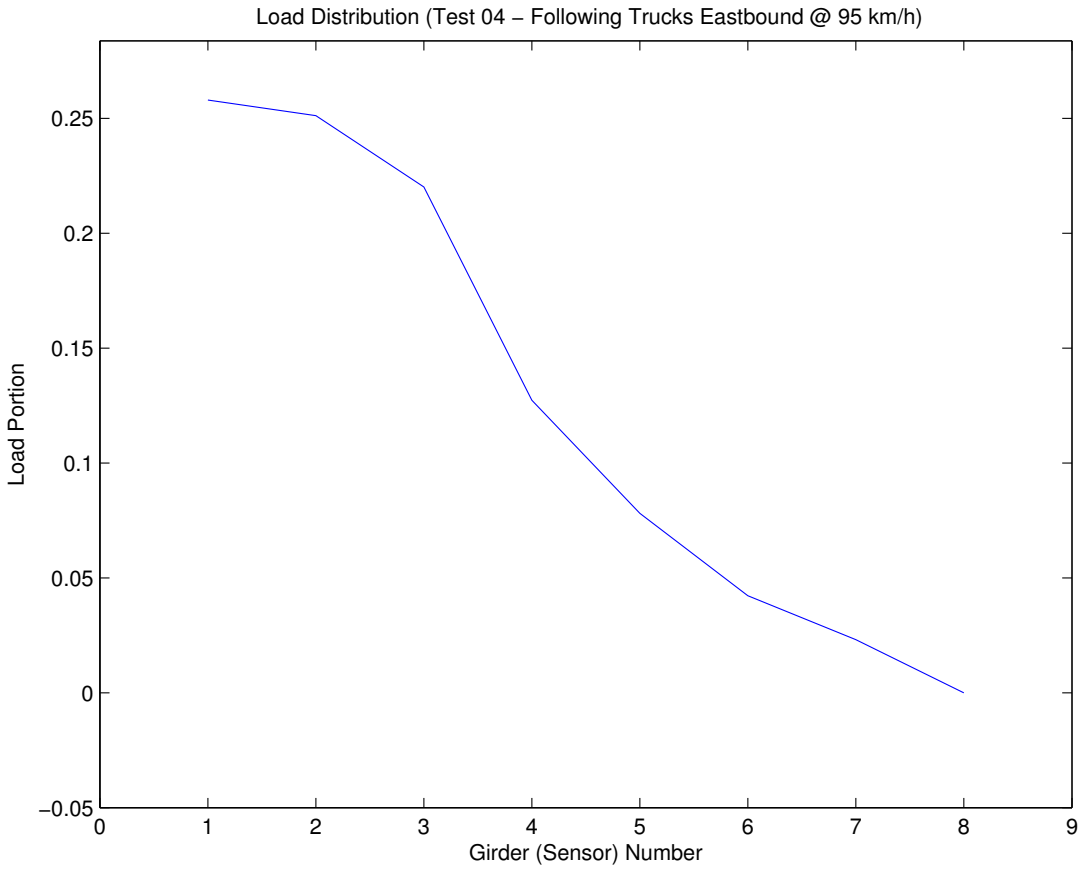

Figure 4.1: Test 4 Distribution

Based on the Test 4 and 5 data, the resulting mixture matrix **A** is shown in Equation 4.6. As an example, the strain on the southbound (passing) lane in the eastbound section is:

$$\begin{aligned} x = \epsilon_{mixed} &= A_{1,1}\epsilon_1 + A_{2,1}\epsilon_2 \\ &= 0.258\epsilon_1 + 0.1134\epsilon_2 \end{aligned} \tag{4.7}$$

Independently, the truck traversing the bridge generates a signal similar to what has been described, and simulated, in the earlier sections of this document. When more than one vehicle enters the section the load for both trucks is spread over the same eight (8) strain gauges, resulting in a mixed signal. Note that a multi-vehicle case is not the same as the event shown in Figure 4.3. In this case, the smaller vehicle, a passenger van, does not affect enough strain to appear in the measurements. Therefore, the event of Figure 4.3 is properly classified as single-vehicle event.

Furthermore, in selecting the multi-vehicle events, the simpler case of two trucks following each other (Figure 4.4) is not tested. For those cases, the existing procedures are capable of handling and processing those events. Some manipulation and pre-processing is required, but nonetheless it does not warrant additional attention. The interesting case, and the main target of the ICA work, is the "side-by-side" case where two vehicles are traveling through the instrumented section concurrently, with one, generally, in the passing lane and one in the driving

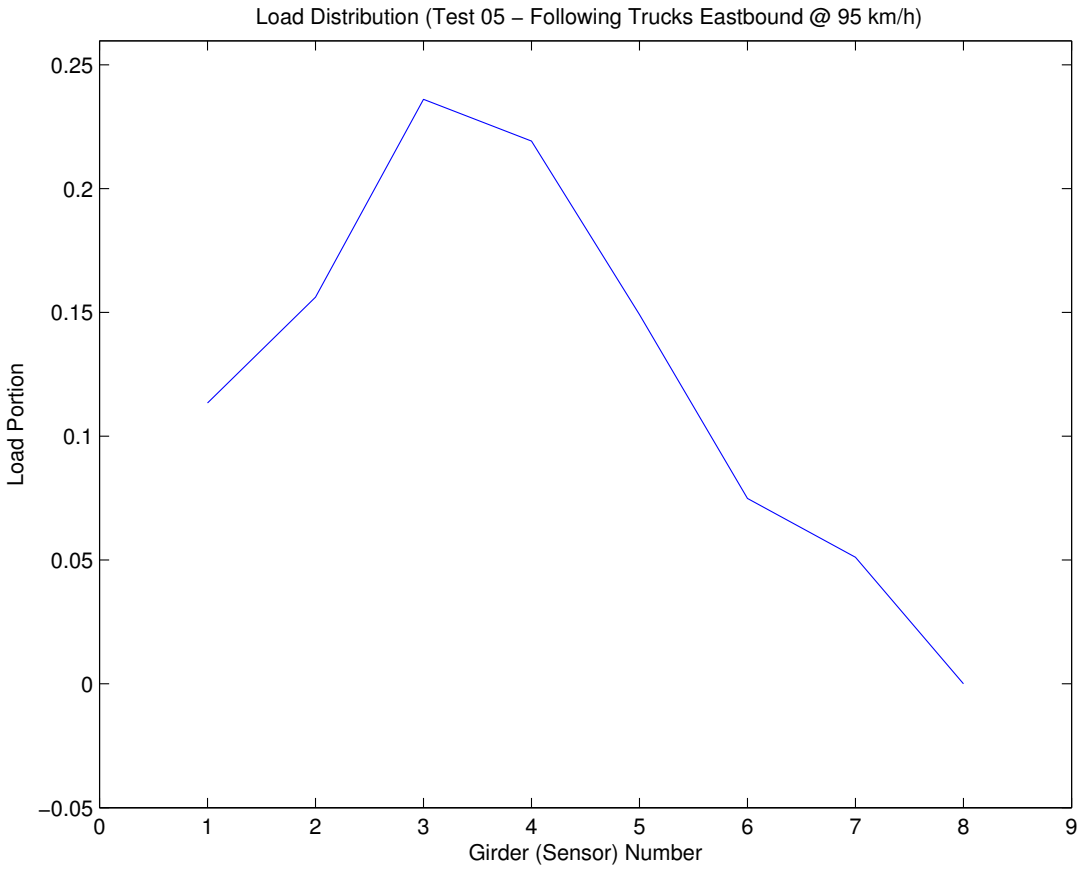

Figure 4.2: Test 5 Distribution

lane. Examples of the interesting cases are shown in Figure 4.5 and Figure 4.6.

4.2.2 Test Configurations

A multi-step assessment is used to determine the efficacy of ICA in the BWIM context:

- A set of signal mixtures approximating truck events is generated. The mixing parameters are derived from existing measurements performed during historical BWIM testing.
- The aforementioned generated signal mixtures are run through the FastICA processing suite to assess the validity of signal separation. A variant of parameters are used with the FastICA algorithm in order to propose a suitable set of parameters when applying ICA in the actual BWIM analysis.
- The experiment is repeated using more recent, live-collected results and compared against the results from the generated mixtures' testing. The same parameter variants from the previous steps are applied, against both the raw (unfiltered) data and data filtered using the existing BWIM Butterworth filter [6] to remove the signal harmonics and some bridge noise.

Figure 4.3: Example of a non-multiple vehicle event

Figure 4.4: Following Multi-Vehicle Event Example

Figure 4.5: Example of a multi-vehicle event (Garbage and Semi Truck)

Figure 4.6: Multi-vehicle event (Two Semi Trucks)

Table 4.1: FastICA Testing Permutations

Test Ordinal	Approach	Nonlinearity
1	defl	pow3
2	defl	tanh
3	defl	gauss
4	delf	skew
5	symm	pow3
6	symm	tanh
7	symm	gauss
8	symm	skew

The FastICA algorithm supports multiple parameter configurations. Each iteration assess eight permutations of the FastICA parameters in an attempt to recover the source signals. Table 4.1 lists the different combinations employed for each test iteration. The approach parameter refers to the decorrelation approach - "symm" implies the symmetric approach where parallel component estimation is employed, while "defl" implies using a method akin to projection pursuit and extracting parameters sequentially. The nonlinearity (g) parameter is for configuring the fixed point approach. The *g* parameter has the following options:

pow3 $g(u) = u^3$

tanh $g(u) = tanh(a1 * u)$

gauss $g(u) = u * e^{-a2frac2^22}$

skew $g(u) = u^2$

4.2.3 Assessment of Experimental Outcomes

A set of criteria is required to assess the fitness of ICA for application in BWIM. Any valid method for assessing the outputs must provide a measure of whether the signal is an adequate representation signal contained in the input measurements. For these experiments, two techniques are used to assess the outcomes of the outputs:

1. Visual Examination of output signals
2. Root Mean Square Error against the input signal mixture, or a comparison of the equivalence of $\mathbf{A} = \mathbf{A}^*$.

Visual Examination

Because the tests using the measured bridge data do not have the actual input (pre-mixture) signals available, Visual Examination is useful for at least determining the fitness of a recovered

signal —whether it appears to be a strain signal. The images captured on the bridge when an event occurs increases the efficacy and validity of the Visual Inspection technique since an experienced user can judge the extracted signals against expectations for a given vehicle type. For example, a double trailer is expected to have four (4) peaks in the signal.

Root Mean Square Error (RMSE - see below) is used for a mathematical comparison. In the trials using generated data, the recovered signals are compared against the source signals. The aforementioned lack of pre-mixture input signals make the RMSE technique inadequate for tests using the actual strain measurements. For the trials using the actual strain measurements, the RMSE between the original signal mixture and the estimated signal mixture is a suitable stand-in.

Root Mean Square Error

The Root Mean Square Error (RMSE - see Equation 4.8), also referred to as the Root Mean Square Deviation (RMSD), is selected for comparing the results of the signal extraction against the input signals. Where the source signals are known, post-processing of the recovered signals is required to adjust the scale and potentially direction of the separated signals. Without adjustment, the recovered signals are useless for BWIM - the BWIM process relies on accuracy in the strain values to detect traversal characteristics and determine the weight of the vehicle.

$$RMSE = \sqrt{\frac{\sum_{t=1}^{n}(\hat{y}_t - y_t)^2}{n}} \tag{4.8}$$

Since RMSE is taken relative to the estimator, a skew in the estimator's scale or lateral orientation will cause a discrepancy in the calculated value. To bring more meaning to the RMSE, an adjustment using simple rescaling is required. The techniques that were used for making the adjustment are discussed in the relevant section below.

4.3 ICA Using Generated Signals

The basic feasibility of ICA for separating BWIM signals is tested by using generating signals (using the same procedure as Chapter 3), which leaves the source signals available in their "raw" form and knowing the mixing matrix. As with Chapter 3, using a relative comparison of the source signal and extracted component's (estimator's) magnitudes negates concerns over the exact value of the weights. Likewise, the signal adjustments are also implemented using the relative measures, making them also transferable to scaling results from actual bridge data.

Two tests modeled on the scenario shown in Figure 4.5 (a garbage truck and semi-truck) are used to test ICA's extraction abilities:

- A garbage truck and semi-truck model constructed using idealized (noise-free signals).

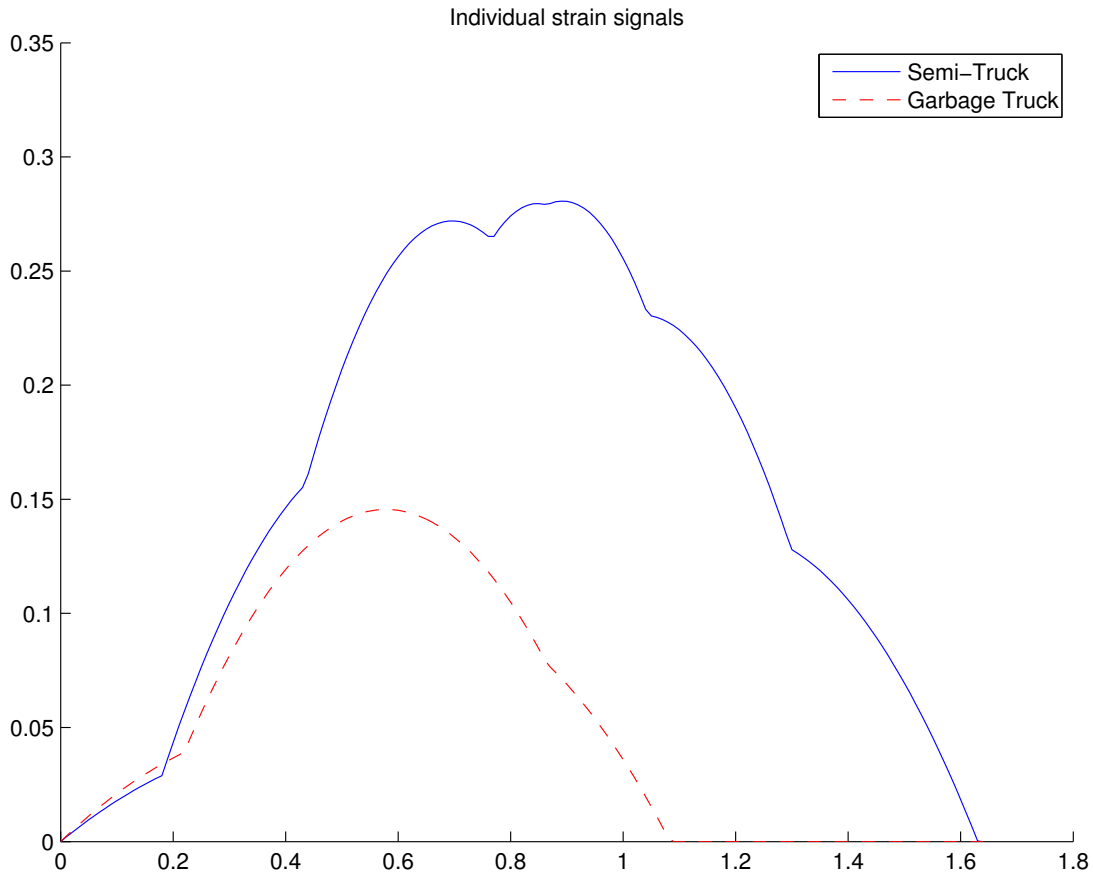

Figure 4.7: Individual Strain Curves - Semi and Garbage Truck

- The same trucks, garbage and semi, but including some additive noise.

In each test, the extracted signals are evaluated by comparing them against the source signals, as well as a reconstruction of the mixtures using the estimated mixing matrix $\hat{\mathbf{A}}$ inputs. The RMSE is calculated against the individual components as well as the original mixtures.

4.3.1 Test 1 - Garbage/Semi-Truck

The generated signals for the trucks are shown in Figure 4.7. In that figure, the shorter-length, smaller signal represents the garbage truck and the larger, longer signal is the semi-truck. The combined curve for the two profiles is shown in Figure 4.8. The $\mathbf{x}$ mixture is determined using the mixing matrix previously described.

When comparing the outputs of the function, an assumption is made that the range scales with the changes in the signals. The ratio of the original signal component i's range, R_{s_i}, to the estimated component's range, $R_{\hat{s}_i}$ is then computed and used as a means of rectifying the signal:

$$\alpha_i R_i^* = R_i \tag{4.9}$$

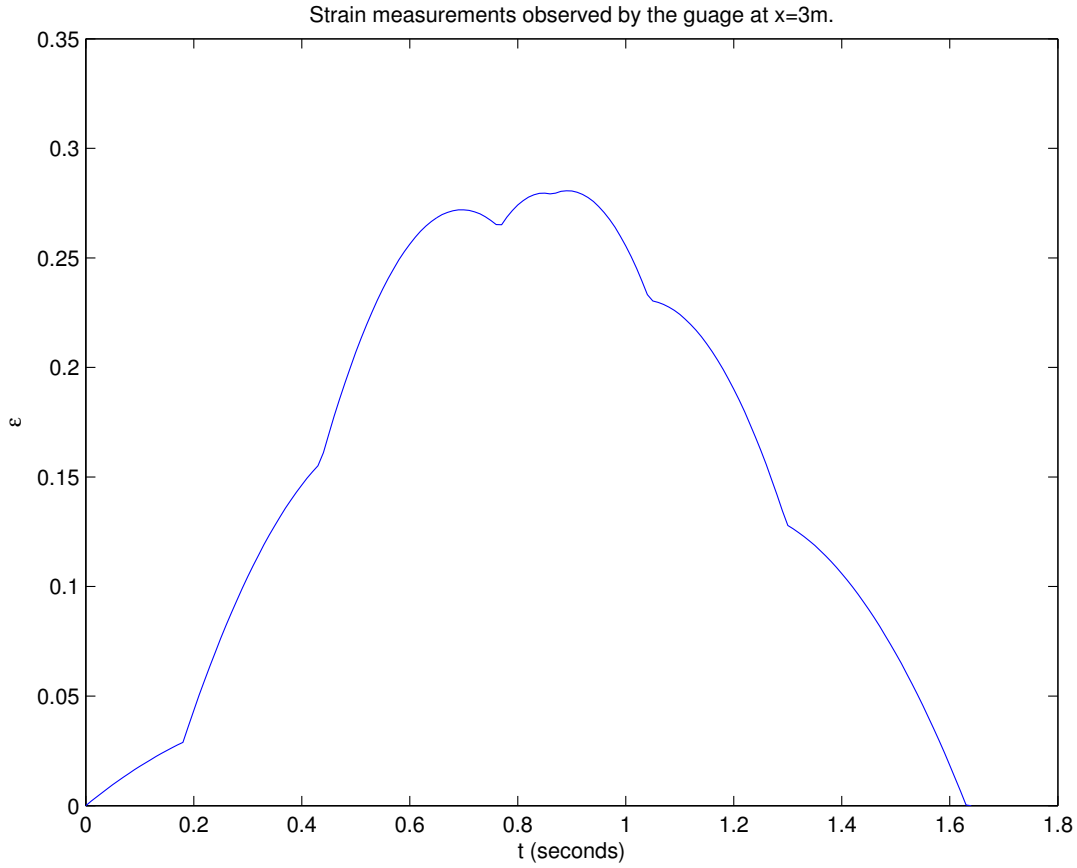

Figure 4.8: Combined Strain Curves - Semi and Garbage Truck

The estimated signal component is then scaled by α_i to return the estimator to the proper scale. A heuristic is applied to right inverted signals —when the maximum value of the signal component is lower in magnitude than the minimum value, the signal is inverted.

Results

All but one of the eight trials produced a set of source components. The successful trials were able to produce an estimate of the mixing matrix $\mathbf{A}$ that perfectly reconstructed the original mixture (see Figure 4.9). The results from Trial 2 are documented in this section, with the remaining trials' results cataloged in Appendix A.

In the case of unsuccessful trials, the recovered signals did not have a form that would have been generated from either of the vehicles that were simulated. In these instances the RMSE was not necessarily very different from the more successful trials. Since they lack the requisite form, the recovered signals are nonetheless insufficient for use in BWIM.

While the signal mixture was accurately reconstructed, the recovered signals are not sufficiently accurate. The source signals compared to the recovered signals are shown in Figure 4.10 and Figure 4.11. The RMSE in Trial 2 for each component is 0.02523 and 0.03582, respectively. The applied scale adjustments were 0.09309 and 0.04787, respectively.

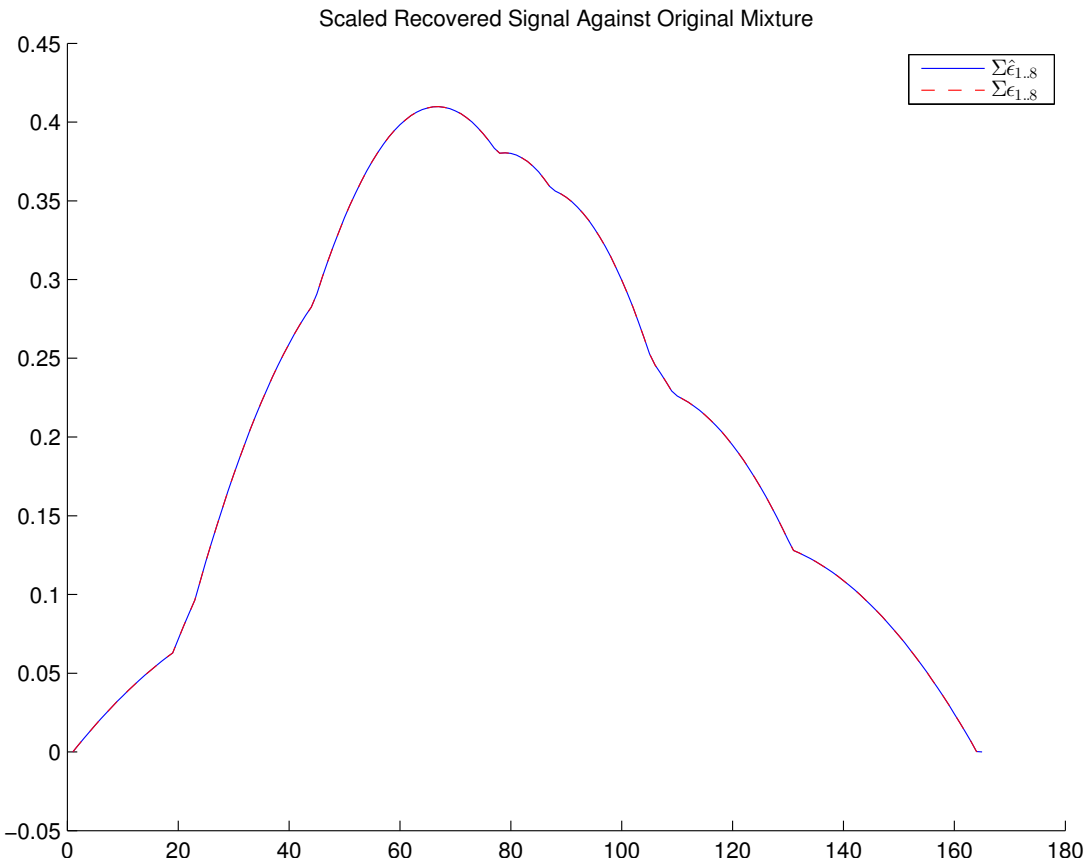

Figure 4.9: Original Signal Mixture Compared Against Estimated Mixture

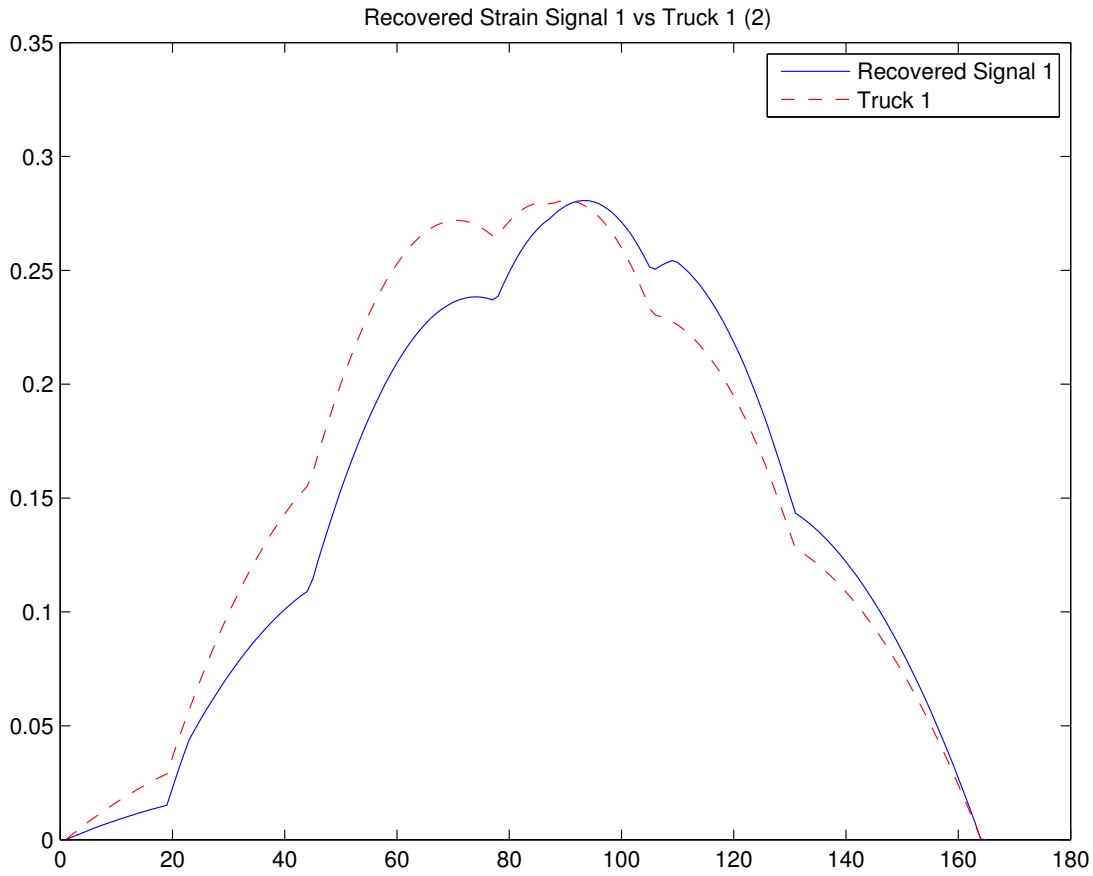

Figure 4.10: Recovered Signal 1 against Original Signal Mixture 1 (Trial 2)

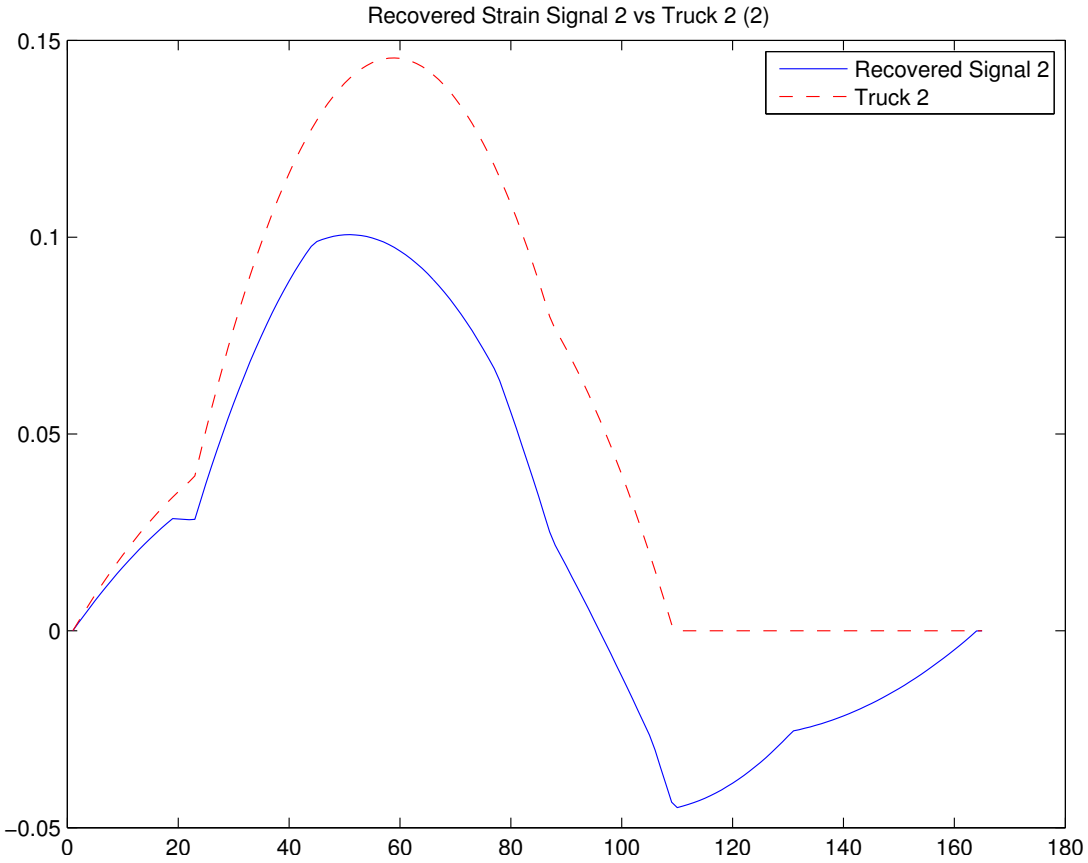

Figure 4.11: Recovered Signal 1 against Original Signal Mixture 1 (Trial 2)

4.3.2 Test 2 - Garbage/Semi-Truck with Noise

The method of executing the test is the same as above for the non-noise model of the garbage and semi-truck event. The difference is in producing the mixtures supplied to the algorithm. In this case, a noise model is applied by adding some Gaussian noise with a mean value of two (2) percent of the signal amplitude. The selected mean corresponds to the typical noise floor and event trigger point for the SHM data collection.

Results

The noise did not impact the ability to recover a highly accurate mixing matrix. In fact, the estimated mixing matrix $\hat{\mathbf{A}}$ perfectly reconstructs the original mixture (see Figure 4.12). The results from Trial 2 are documented in this section, with the remaining trials' results cataloged in Appendix B.

While the signal mixture was accurately reconstructed, the recovered signals are not sufficiently accurate. The source signals compared to the recovered signals are shown in Figure 4.13 and Figure 4.14. The RMSE in Trial 2 for each component is 0.08704 and 0.07968, respectively. The applied scale adjustments were 0.09941 and 0.04930, respectively. In comparison to the non-noisy model from the previous test, the RMSE was noticeably higher but the scaling adjustments were comparable. Overall, the noise modeling did not impact the results in a manner that discouraged further trials using actual data collected on the bridge.

4.4 ICA Using Actual Signals

While some potentially promising performance is evident in the simulated signals, those signals are obviously not entirely representative of the actual signals recorded on the bridge. A test against the actual bridge data (recorded samples) is required to make a final assessment of the ICA viability in BWIM.

Two tests were performed on the same data set that inspired the simulated signal tests - the garbage/semi-truck crossing. Each test was performed using the same eight (8) combinations of FastICA parameters previously identified in Table 4.1; the first extracted two (2) signal components and the second three (3) signal components. The reasoning behind using additional numbers of independent components is explained in subsection 4.4.2.

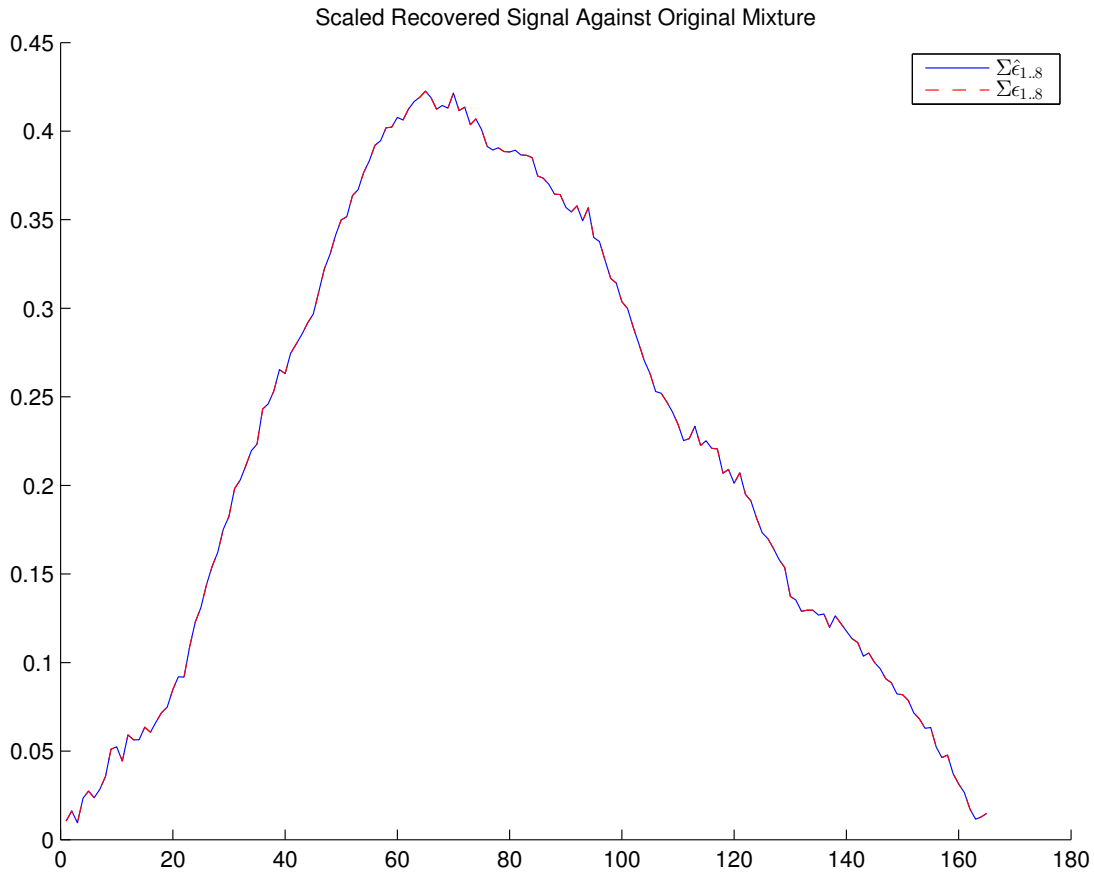

Figure 4.12: Original Signal Mixture Compared Against Estimated Mixture

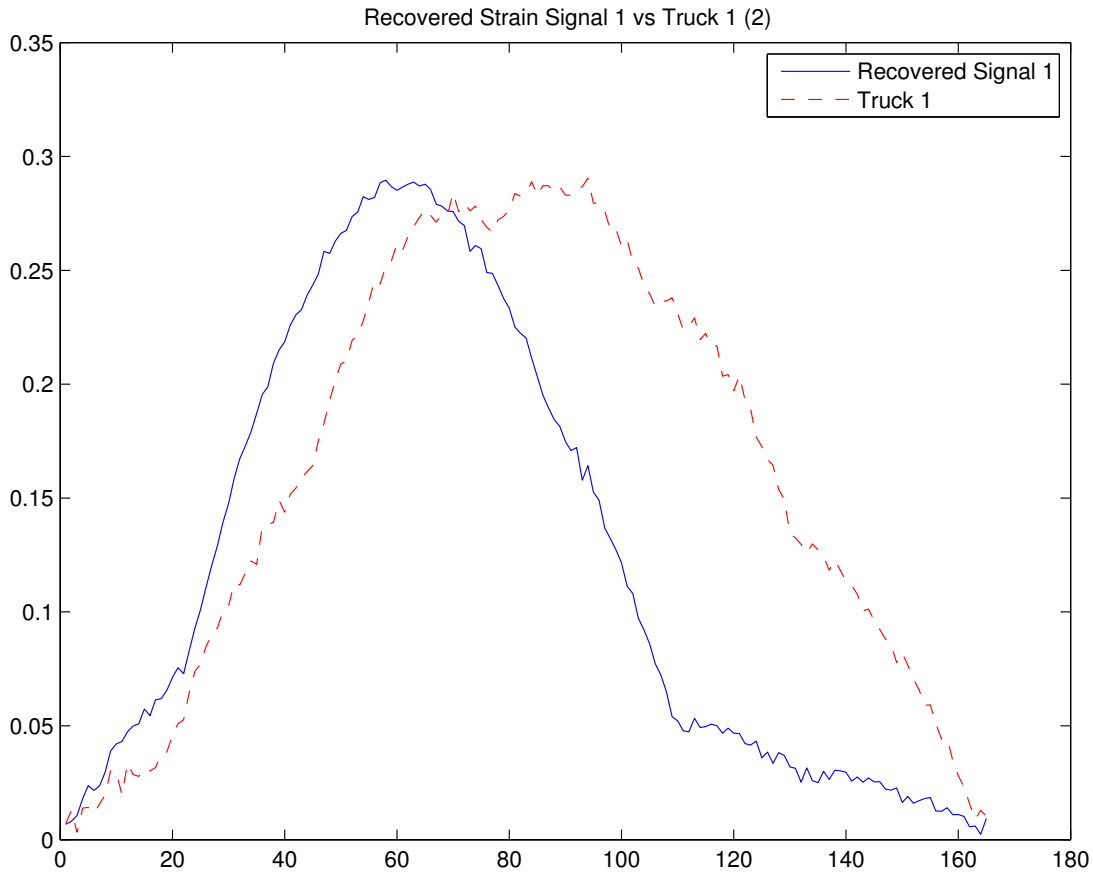

Figure 4.13: Recovered Signal 1 against Original Signal Mixture 1 (Trial 2)

Figure 4.14: Recovered Signal 1 against Original Signal Mixture 1 (Trial 2)

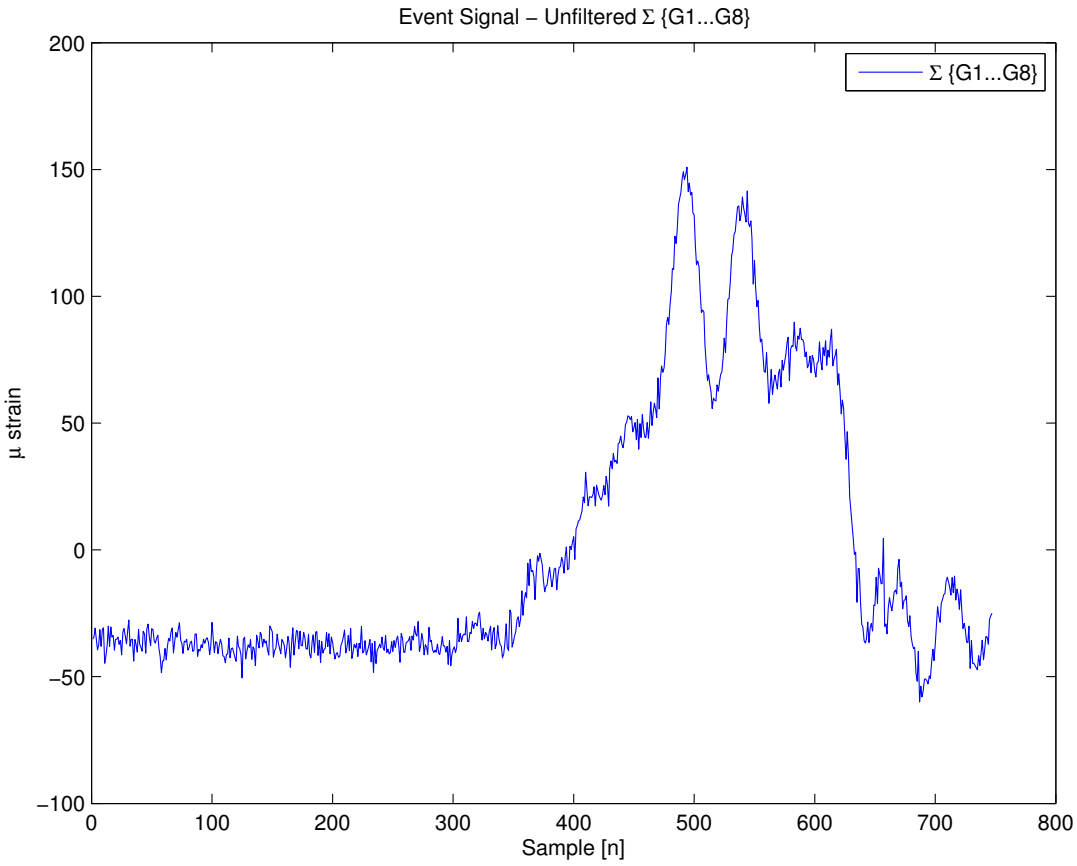

Figure 4.15: Truck Signal - Sum of Girders

4.4.1 Test 1 - Actual Garbage/Semi-Trick

Ideally, the signal that inspired the generated test should draw similar results. The signal is shown in the unfiltered and filtered (Butterworth) forms in Figure 4.15 and Figure 4.17, respectively. The filtered signals, if extracted, should be more useful in producing signals that, if properly recovered, may be directly supplied to the BWIM algorithms to derive the truck parameters (length, speed, weight).

Output comparison and assessment is more difficult owing to a lack of unmixed source signals. Although that would be the case in actual BWIM usage, it is also not ideal for evaluating the performance ICA against the actual bridge data. To facilitate assessment of the RMSE under these tests, the extracted components $\hat{\mathbf{s}}$ are remixed using the estimated mixing matrix $\hat{\mathbf{A}}$ to obtain the estimated original mixture $\hat{\mathbf{x}}$:

$$\hat{\mathbf{x}} = \hat{\mathbf{A}}\hat{\mathbf{s}} \tag{4.10}$$

The sum of the individual $\hat{\mathbf{x}}$ components, which are the girder readings, is the ϵ sum ordinarily used in BWIM and the RMSE calculation is as follows:

$$RMSE(\hat{\epsilon}) = \sqrt{\frac{\Sigma_{n=1}^{N}(\hat{\epsilon}_n - \epsilon_n)^2}{n}} \tag{4.11}$$

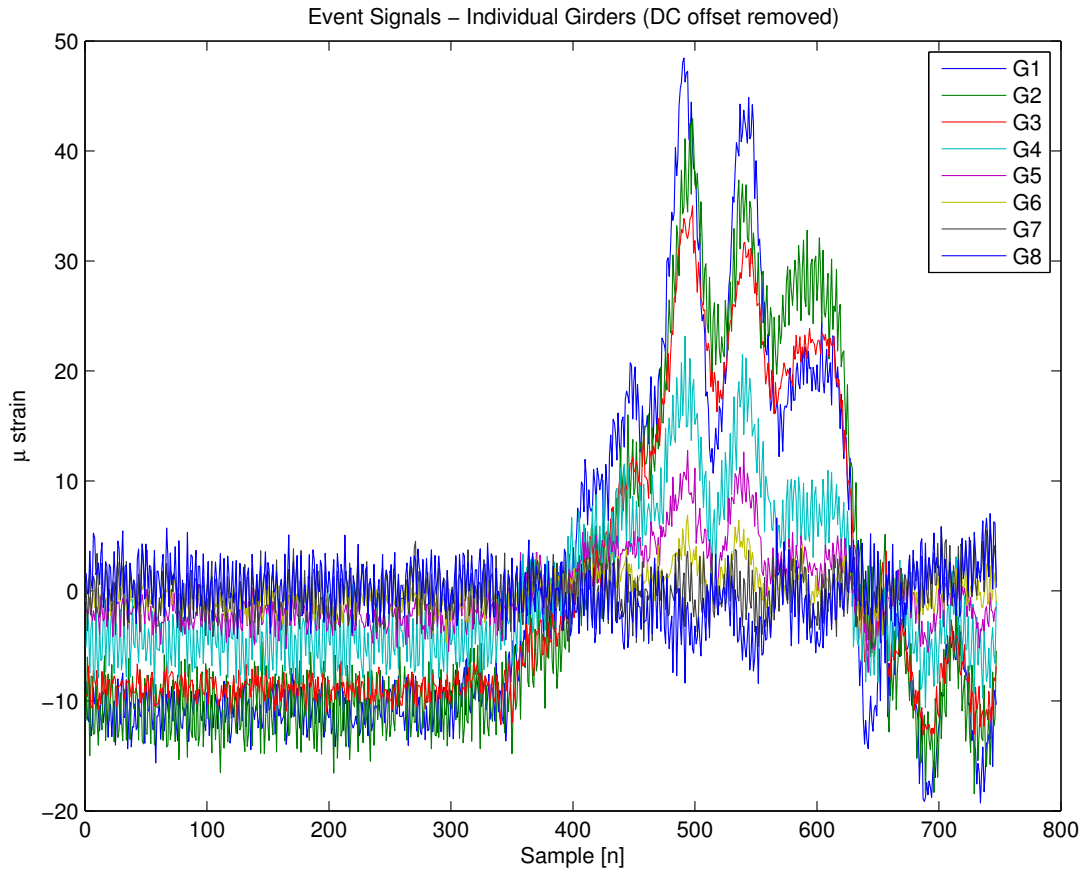

Figure 4.16: Truck Signal - Individual Girders

Where $\hat{\epsilon}$ represents the sum of each of the components in $\hat{\mathbf{x}}$; ϵ is used to denote the estimator of the strain. The downside of using this comparison is that it acknowledges ICA may be able to estimate the overall reproduction of the source signal, but not the quality of the components extracted. An alternative is performing the calculation against each of the estimated girder measures:

$$RMSE(\hat{\epsilon}_i) = \sqrt{\frac{\Sigma_{n=1}^{N}(\hat{\epsilon}_i, n - \epsilon_i, n)^2}{n}} \tag{4.12}$$

Where ϵ_i is the original sample from a girder. This methodology may produce more appropriate error measures as it determines the deviation in each component, therefore determining the ability to faithfully reproduce the eight (8) original signals. Since the eight (8) signals are available as the sampled data.

Results

Overall, the separation results showed limited potential for all eight (8) trials that were conducted. In each case, the previous observation that the unadjusted signals have carry less error held during these trials. To produce the error measurement, the RMSE was calculated by checking the filtered original mixture against the filtered remixed signal. The lowest RMSE was trial 8: 36.57

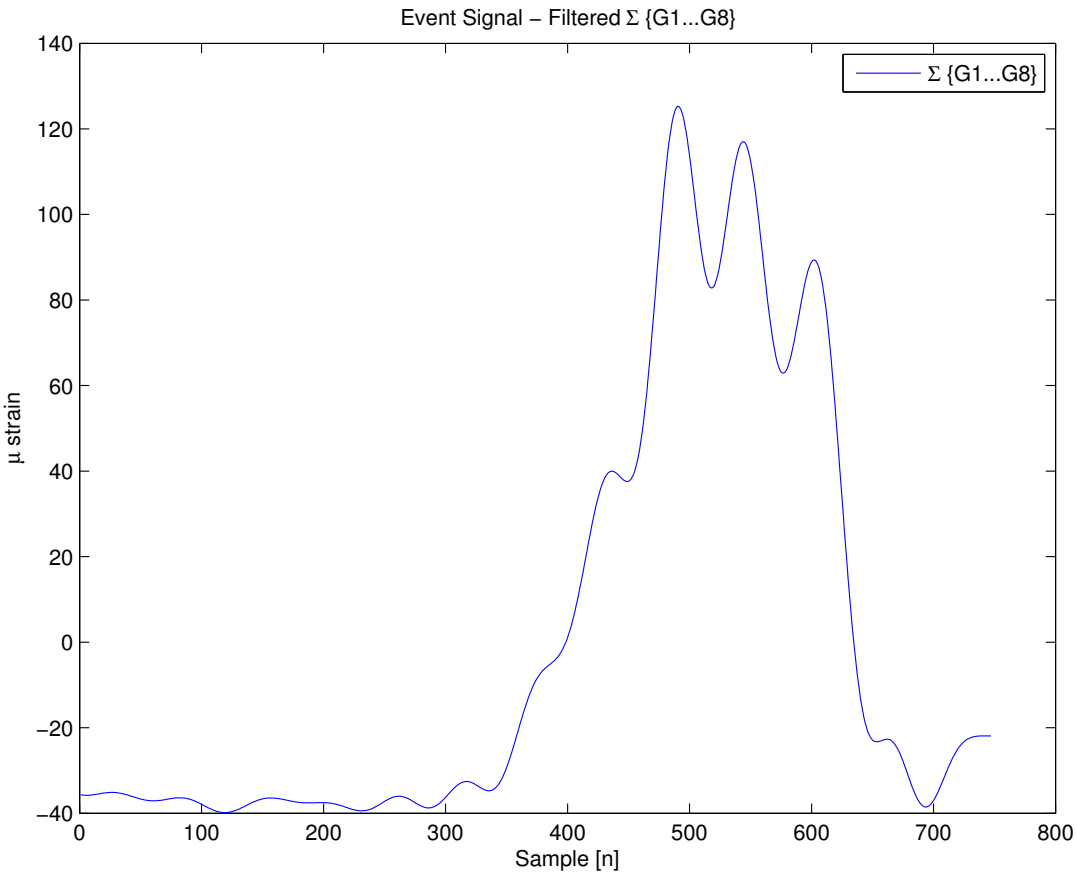

Figure 4.17: Truck Signal - Sum of Girders

(unadjusted) and 36.99 (adjusted by a factor of 0.8505). The extracted components from Trial 8 are shown in Figure 4.19 and Figure 4.20. The comparison of the original signal against the estimated mixture and recovered against the originals are shown in Figure 4.21 and Figure 4.22. This trial was also the only trial that required reduction (scale factor less than 1); the relevance of such a comparison is not clear, but noteworthy. On the other hand, the trial showing the largest RMSE was trial 5: 50.53 (unadjusted) and 51.30 (adjusted). The filtered and unfiltered extracted signals for that trial are shown in Figure 4.23 and Figure 4.24, respectively.

Appendix C contains the complete set of results for these trials.

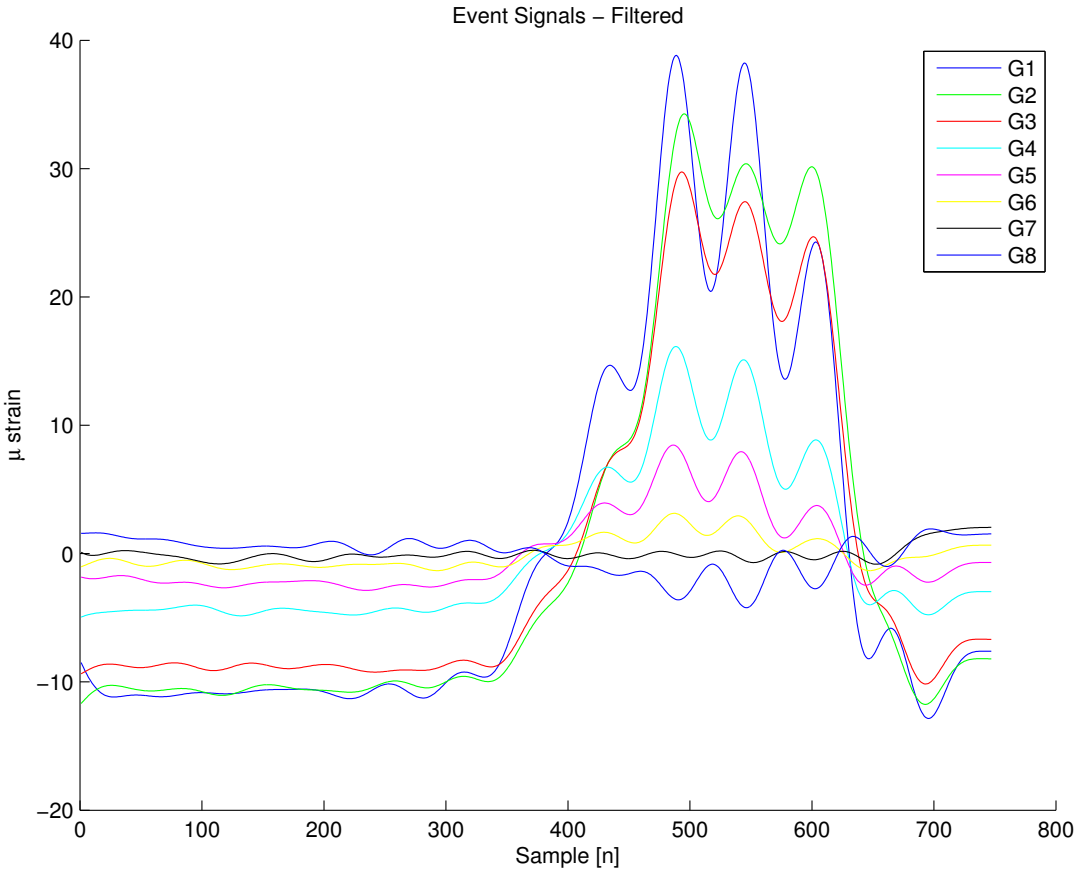

Figure 4.18: Truck Signal - Individual Girders

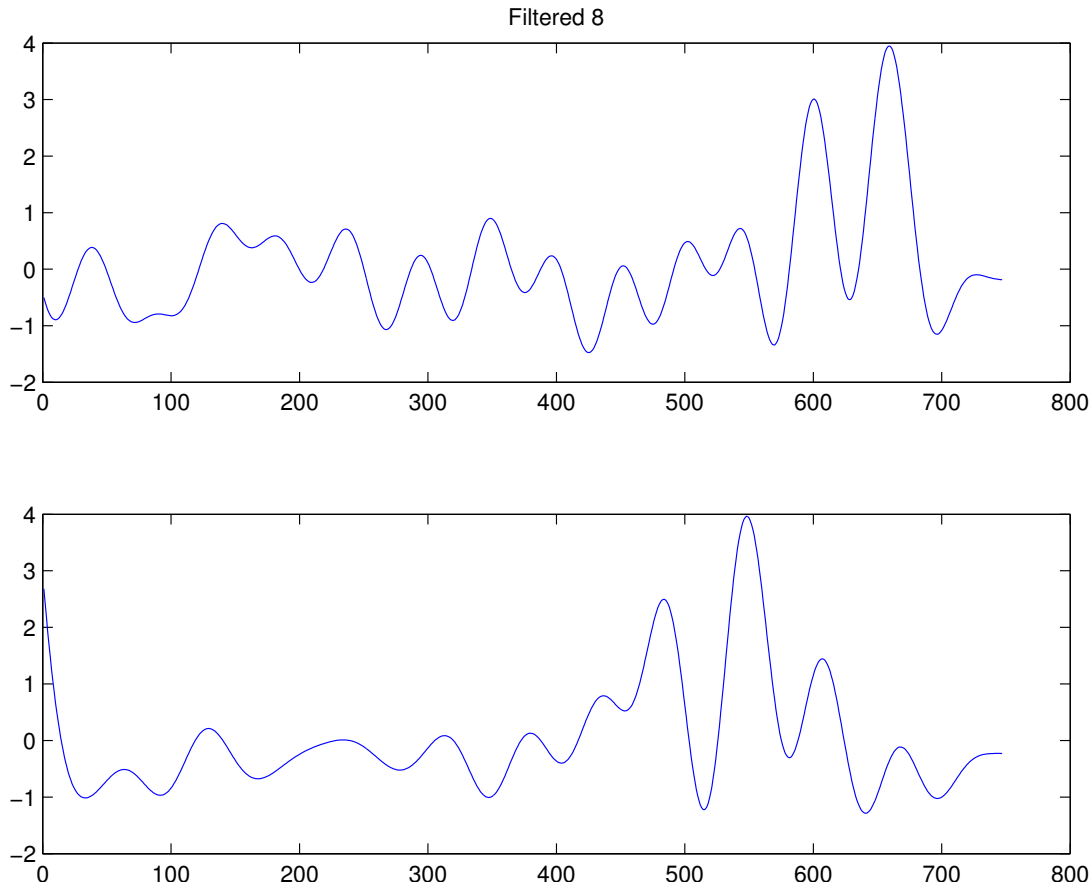

Figure 4.19: Extracted Signals (Trial 8 Filtered)

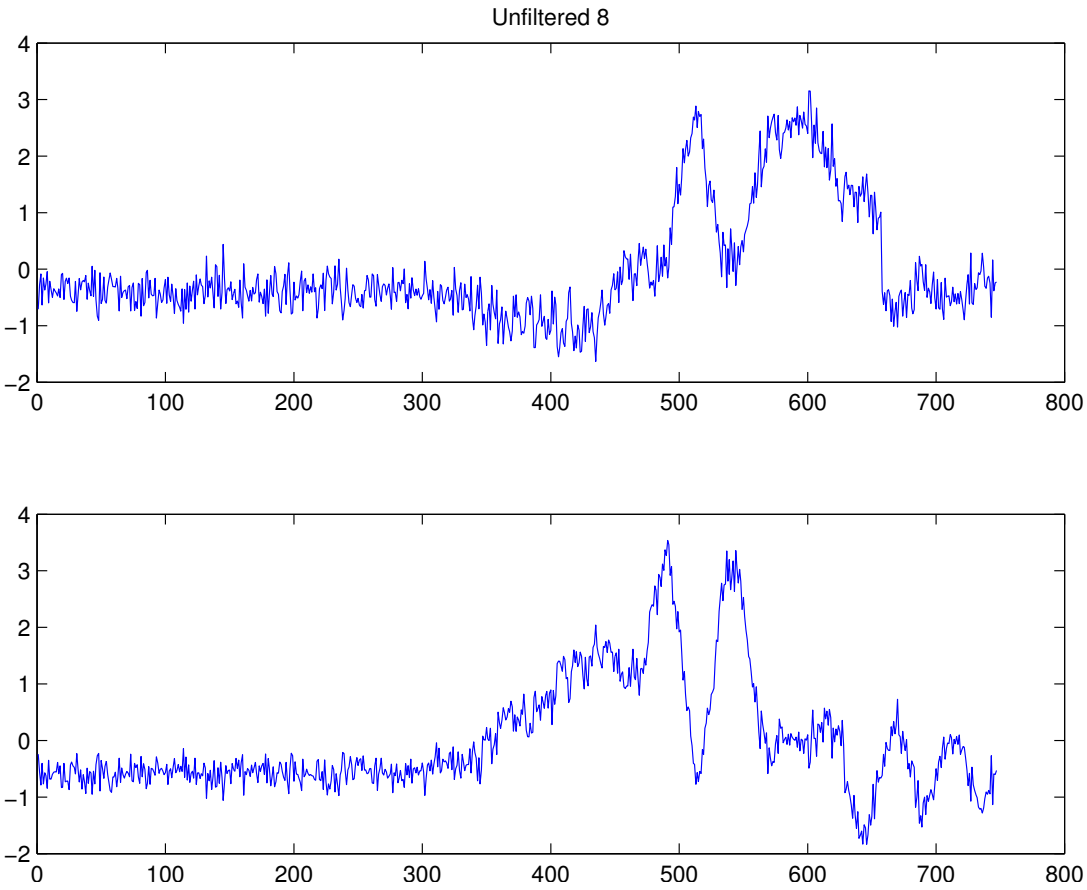

Figure 4.20: Extracted Signals (Trial 8 Unfiltered)

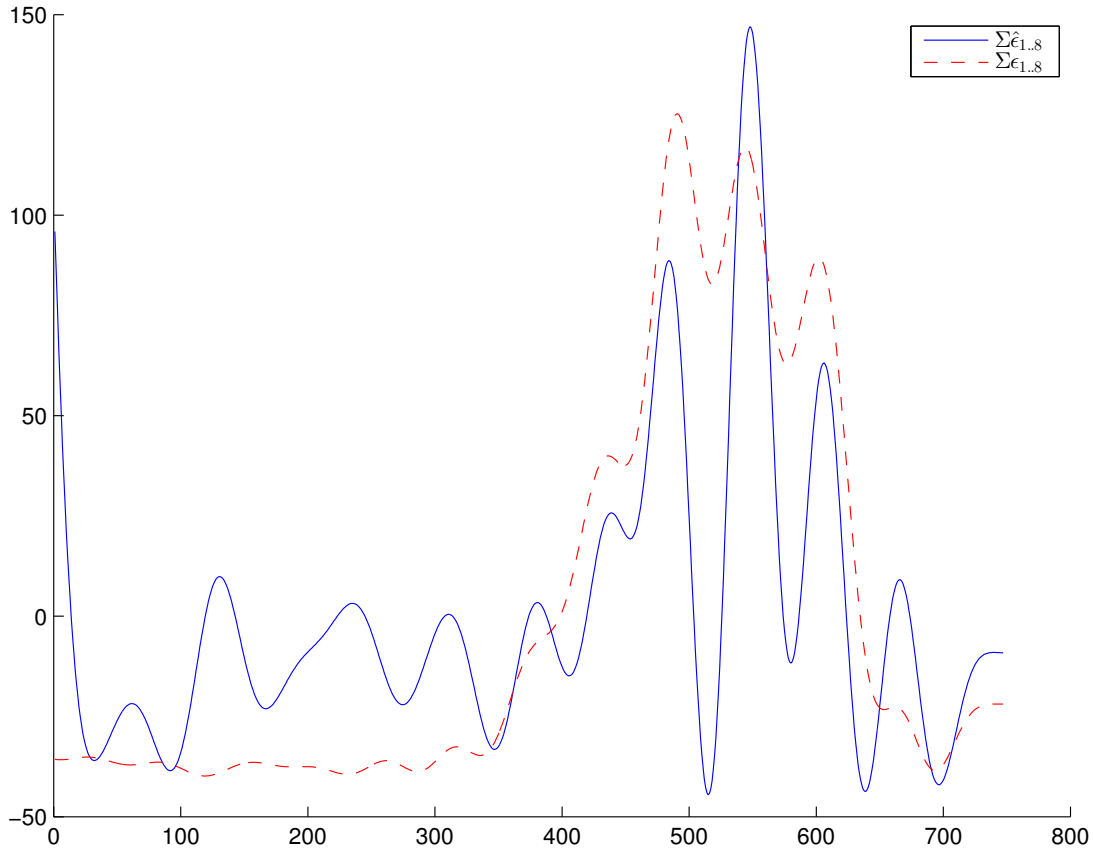

Figure 4.21: Original Mixture and Estimated Mixture Comparison (Trial 8 Filtered)

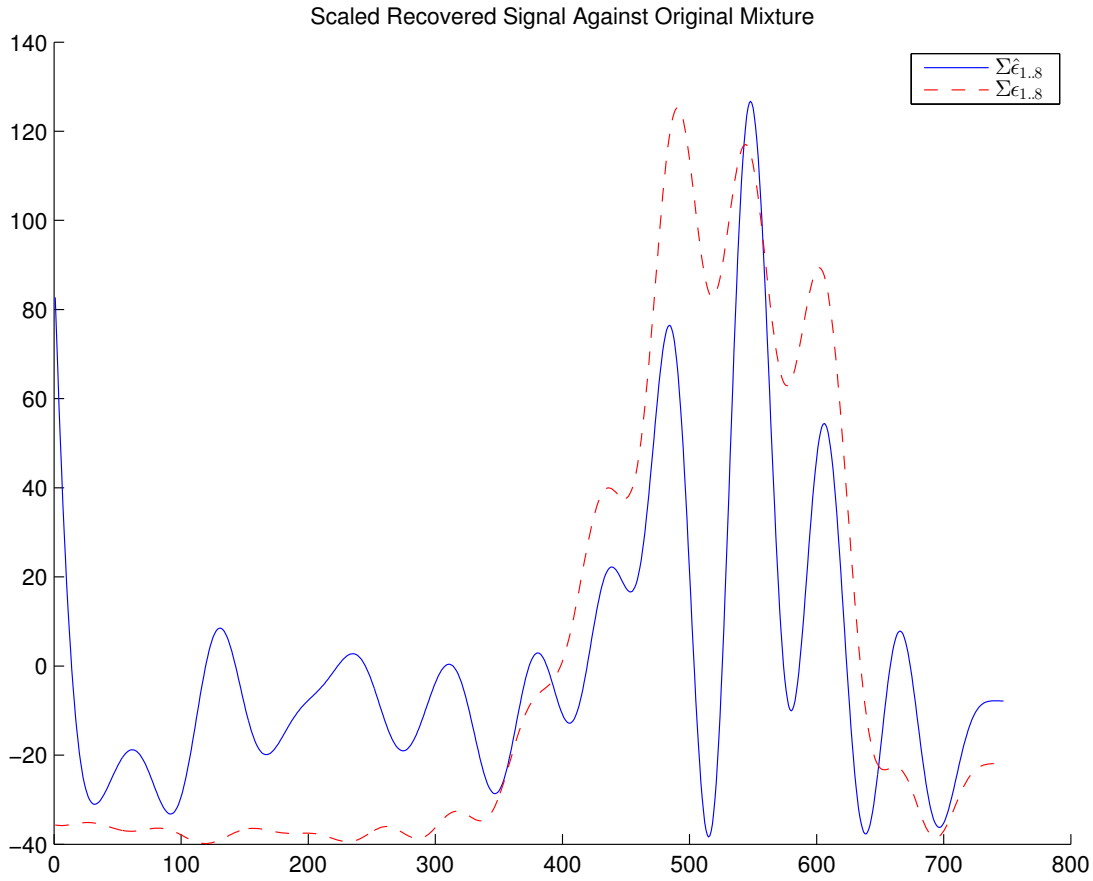

Figure 4.22: Original Mixture and Scaled Mixture Comparison (Trial 8 Filtered)

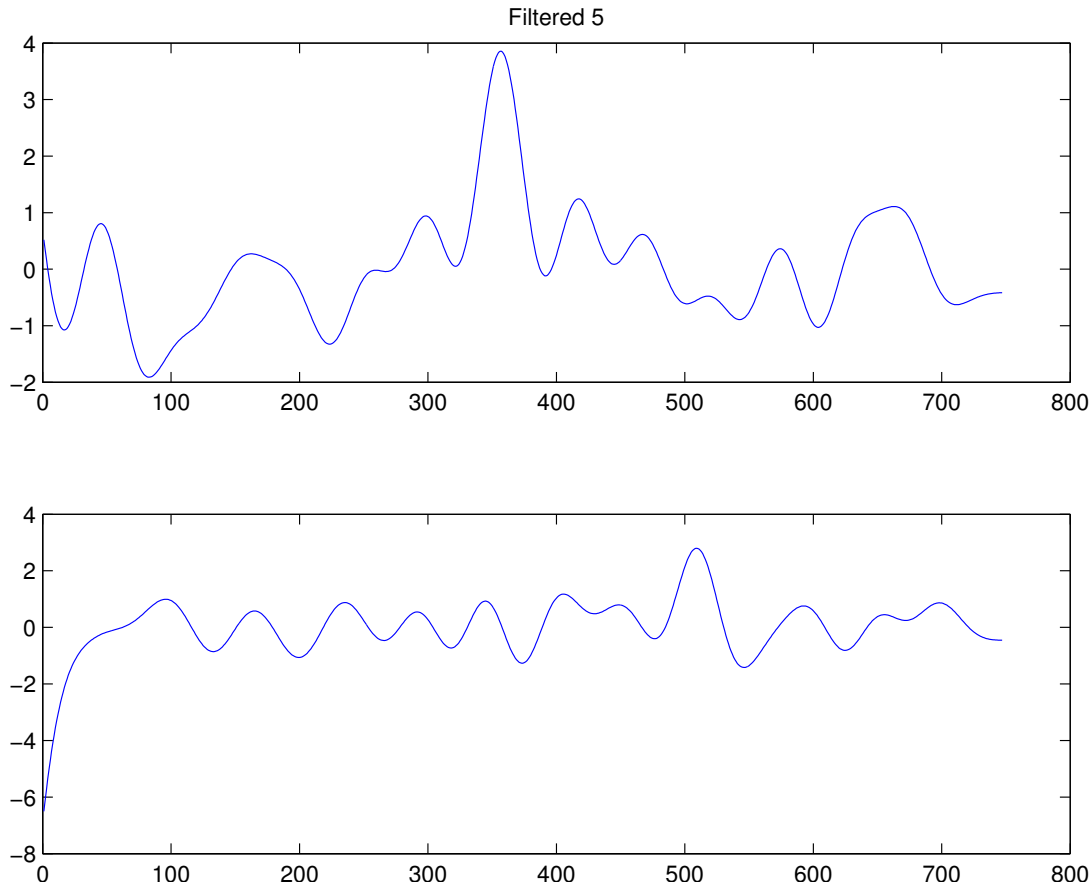

Figure 4.23: Extracted Signals (Trial 5 Filtered)

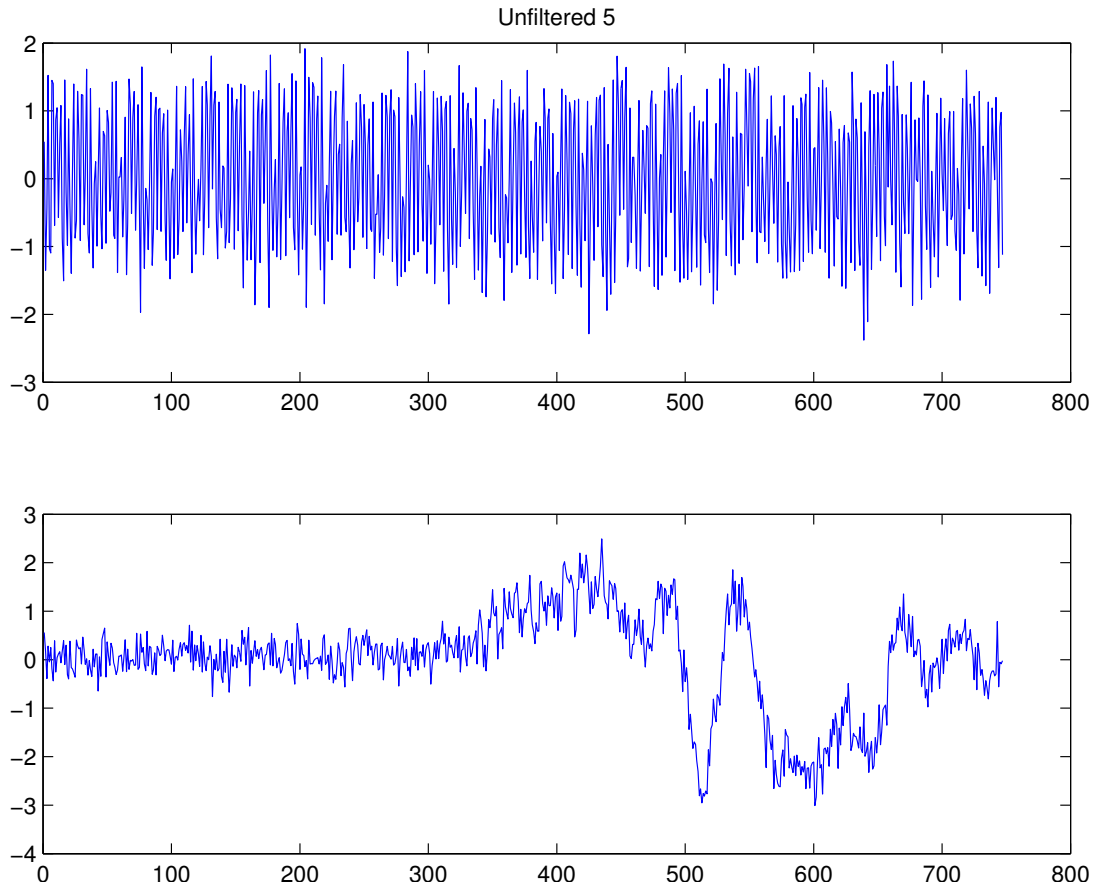

Figure 4.24: Extracted Signals (Trial 5 Unfiltered)

4.4.2 Test 2 - Actual Garbage/Semi-Truck, 3 Components

Based on the results of maternal-fetal electrocardiography separation [13], having additional trace sources, for example the nervous and other systems, may cause distortions in the extracted components. Attempting to remove a third component containing weaker signals caused by smaller traffic, weather, and bridge characteristics may help make the components more useful. To test the theory, the tests of the previous section are conducted again, but with FastICA being instructed to extract three (3) components.

The post-processing of the extracted data uses the same rescaling technique as the previous test; the inverting procedure was omitted. In practical terms, if extracted, the small noise component is discarded. However, when performing assessment against the original signal the extra component is included since removing it would increase the error measurement.

Results

The results of Trial 4 for both the filtered and unfiltered input mixtures are shown in Figure 4.25 and Figure 4.26. These signals were isolated as an example of the relatively more successful extractions, a selection justified by examining the RMSE of this trial. The RMSE in this case is 27.9302 (filtered input) and 28.2833 after the adjustment. However, the assessment of success must be taken in context. While the signals in the plots do bear some resemblance to valid truck measurements, there are spurious harmonics and other deviations that make the signals invalid for BWIM analysis.

For comparison, the worst performing RMSE value was Trial 5 with 47.2644 (unadjusted) and 47.6287 (after scaling by a factor of 1.2728). Those signals are shown in Figure 4.27 and Figure 4.28. A simple visual test confirms that the extracted signals do not match the expected patterns.

The harmonics that are present, especially in the filtered signal samples, bear some attention. Their source is unknown, but by visual inspection appears to be the remaining frequencies not removed via filtering/preprocessing, with some elements greatly exaggerated as witnessed by the magnitudes and volatility. On that basis, properly recovering the signal may instead require filtering to be done on the extracted components.

See Appendix D For the complete set of results from this series of trials.

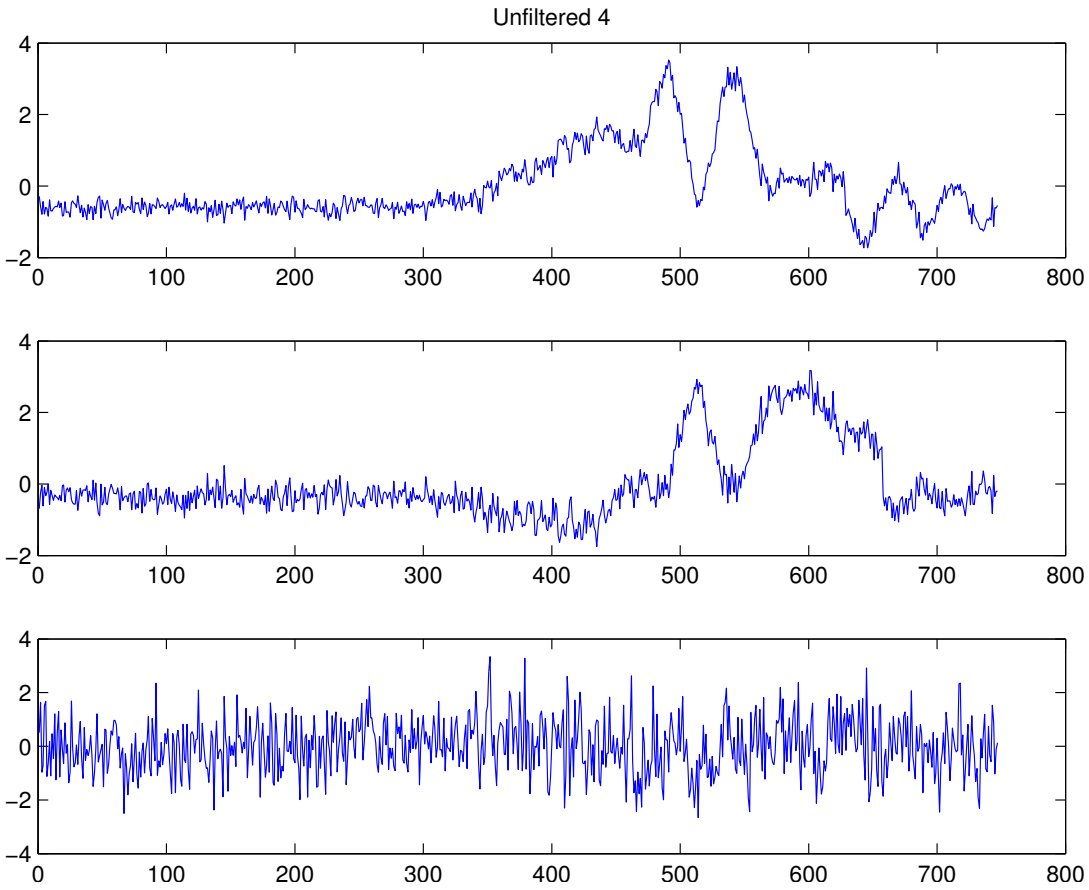

Figure 4.25: Trial 4 Extracted Components (Unfiltered Inputs)

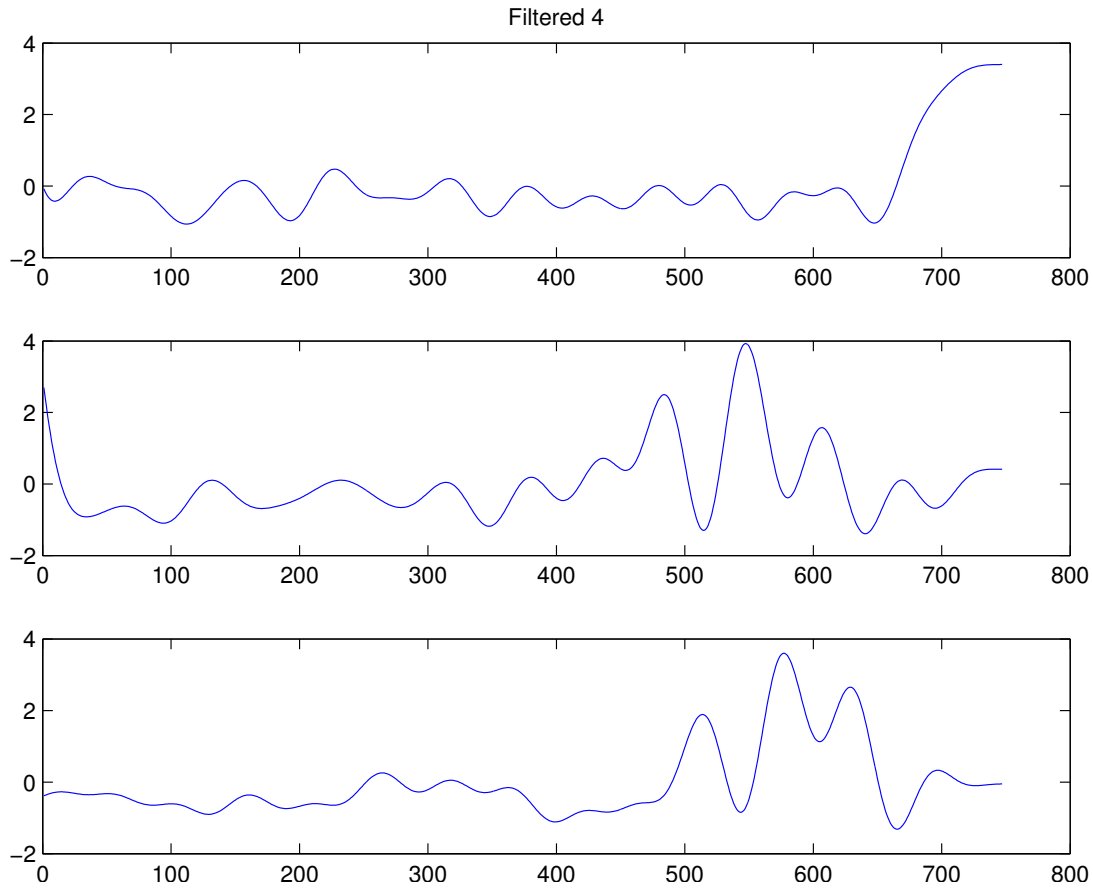

Figure 4.26: Trial 4 Extracted Components (Filtered Inputs)

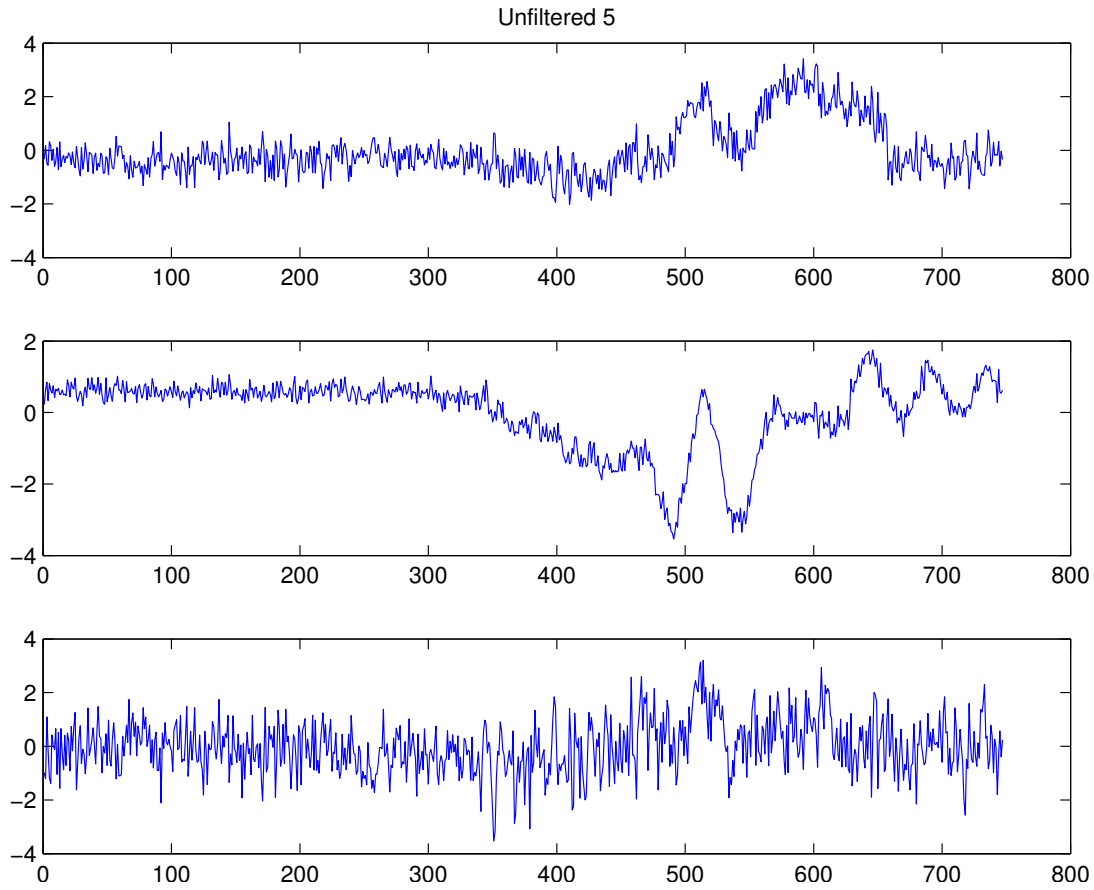

Figure 4.27: Trial 5 Extracted Components (Unfiltered Inputs)

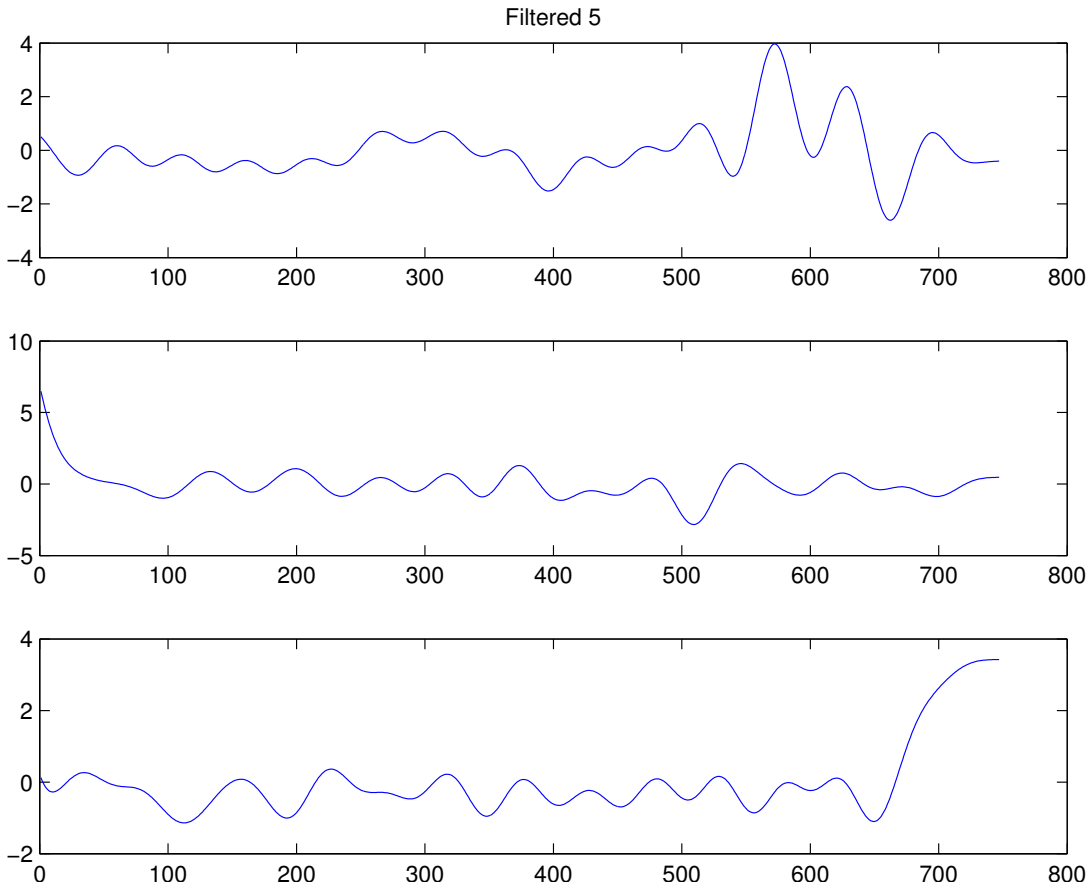

Figure 4.28: Trial 5 Extracted Components (Filtered Inputs)

Chapter 5

Conclusions and Recommendations

5.1 Conclusions

5.1.1 Sampling

Based on the examination of sample rate effects, doubling the sampling rate from 100 Hz to 200 Hz will not greatly improve the accuracy of the peaks in the strain measurements. A corollary of that observation is that the sampling can be safely performed at 100 Hz to produce signals that are useful for BWIM.

5.1.2 ICA

From the previously provided data and results, ICA may be a viable option for handling multiple vehicle events in the Manitoba BWIM system. However, as evidenced in the experiments described above, the ability for ICA to extract meaningful results from actual bridge measurements is disappointing. A large problem is that ICA was overwhelmingly unable to separate the proper nature of both source signals without inducing undesirable harmonics. Obviously, there is low probability of any source signal information or characteristics being available, making adjustments such as the ones performed during the generated signal extraction tests virtually impossible to transfer to the actual cases. The alternative of comparing against the original signal has merits, but a problem in that the original signal seems to be fairly well recovered through the estimated mixing matrix while the individual components are wildly inaccurate.

5.2 Recommendations

5.2.1 Sampling

Future work on the sampling rate is not recommended. Chapter 3 demonstrates that there is likely no further improvement to be made. In fact, in the case of an environment with storage

constraints, implementers can attain sufficient accuracy for BWIM without high sampling rates.

5.2.2 ICA

The above is not to say that ICA has no future with BWIM. Additional research into both signal characteristics and more sophisticated post-processing may result in a useful source extraction capability. The recommendation for any further work in this area is to establish whether a sufficient post-processing model exists, and furthermore how such a model manifests itself. Developing heuristic models for comparison may aid in coaxing the proper source signals from the mixture. Such a model may include human intervention in the form of reviewing captured event pictures, a task that may very well be automated through machine learning.

Fundamentally, the visual examination lacks robust qualities. Depending on the signal charactersitics uncovered, a more sound and deterministic method of confirming signal accuracy is available. Comparing a given set of characteristics such as frequency spectra and distribution may be the key to better recovery.

The results of the ICA clearly indicate that the assumptions on signal independence based on separate physical sources is questionable. An assessment of the signal correlation and its use on removing dependent components of the signals before any further processing is performed is warranted. From all the recommendations put forth, the correlation is favoured as the starting point for future work on BWIM and ICA.

Another suggestion for future investigation is to attempt extracting the components using unfiltered signals and then apply the standard bridge noise filter. Doing so may stand a better chance of producing useful signals for BWIM analysis, as the signals appeared closer to the expected form in some of the trial using unfiltered signals. Coupled with the attempts to perform signal characterization and reduce correlation, ICA may be made acceptable to BWIM systems.

References

[1] *SHM of bridges using weigh-in-motion*, Vancouver, Canada, November 2007. Paper 118.

[2] K. Helmi. Bridge weigh in motion (bwim) using shm data.

[3] Fred Moses. Weigh-in-motion system using instrumented bridges. *Transportation Engineering Journal*, 105(3):233–249, 1979.

[4] Satish C Sharma, George Stamatinos, and John Wyatt. Evaluation of ird-wim-5000-a canadian weigh-in-motion system. *Canadian journal of civil engineering*, 17(4):514–520, 1990.

[5] Teerachai Deesomsuk and Tospol Pinkaew. Evaluation of effectiveness of vehicle weight estimations using bridge weigh-in-motion. *The IES Journal Part A: Civil & Structural Engineering*, 3(2):96–110, 2010.

[6] Baidar Bakht, Aftab Mufti, Leslie Jaeger, and Karim Hemli. Determining gross vehicle weights by bwim. Technical report, ISIS Canada Resource Centre, July 2013.

[7] C. et al Wall. A non-intrusive bridge weigh-in-motion system for a single span steel girder bridge using only strain measurements.

[8] Debra Whistler. Oklahoma opens first of 9 high-tech weight stations. *Fleet Owner*, April 2012. Accessed: 2015-06-09.

[9] Marc A. Soiferman. Data fusion for detection of faults in slab-on-girder bridges. Master's thesis, University of Manitoba, 2009.

[10] Andrew D. Back and Andreas S. Weigend. A first application of independent component analysis to extracting structure from stock returns. *International Journal of Neural Systems*, 08(04):473–484, 1997.

[11] C.F. Beckmann and S.M. Smith. Probabilistic independent component analysis for functional magnetic resonance imaging. *Medical Imaging, IEEE Transactions on*, 23(2):137–152, Feb 2004.

[12] James V. Stone. *Independent Component Analysis : A Tutorial Introduction*. MIT Press, 2004.

[13] Kathryn Marcynuk. Independent component analysis for maternal-fetal electrocardiography. Master's thesis.

[14] Aapo Hyvärinen and Erkki Oja. Independent component analysis: algorithms and applications. *Neural networks*, 13(4):411–430, 2000.

[15] *Blind Signal Separation: Statistical Principles*, volume 86. IEEE, October 1999.

[16] Aapo Hyvärinen. Fast and robust fixed-point algorithms for independent component analysis. *Neural Networks, IEEE Transactions on*, 10(3):626–634, 1999.

[17] Josh Karhunen. The fastica package for matlab. `http://research.ics.aalto.fi/ica/fastica/index.shtml`, 2013. Accessed: 2015-06-01.

Appendix A

Independent Component Analysis Results - Simulated Data

The following material is the exhaustive collection of the simulation results from the garbage truck/semi-truck simulations that were performed. As mentioned in chapter 4, several combinations of the event parameters were tried. See the applicable section of the document for the description.

In each of the sections below, $\hat{\mathbf{A}}$ is used to denote that the matrix in question is the estimated mixing matrix.

A.1 Trial 1

Estimated mixing matrix:

$$\hat{\mathbf{A}} = \begin{bmatrix} 0.02438 & 0.02617 & 0.02821 & 0.02070 & 0.01348 & 0.0069804 & 0.004358 & 0 \\ 0.01427 & 0.01323 & 0.01014 & 0.004647 & 0.002636 & 0.001508 & 0.0006771 & 0 \end{bmatrix} \tag{A.1}$$

Estimated separation matrix:

$$\mathbf{W} = \begin{bmatrix} -24.54 & -10.10 & 21.05 & 37.10 & 27.17 & 12.97 & 10.15 & 0 \\ 81.71 & 47.95 & -26.42 & -72.35 & -54.48 & -25.53 & -20.94 & 0 \end{bmatrix} \tag{A.2}$$

Table A.1 provides the RMSE values of each component's estimate $\hat{s}$ against the actual mixture component s.

Table A.1: RMSE of Source Signal Estimates —Trial 1

Estimated Component ($\hat{s_i}$)	Actual Component (s_j)	RMSE
$\hat{s_1}$	s_1	0.07407
$\hat{s_1}$	s_2	0.08311
$\hat{s_2}$	s_1	0.1284
$\hat{s_2}$	s_2	0.08286

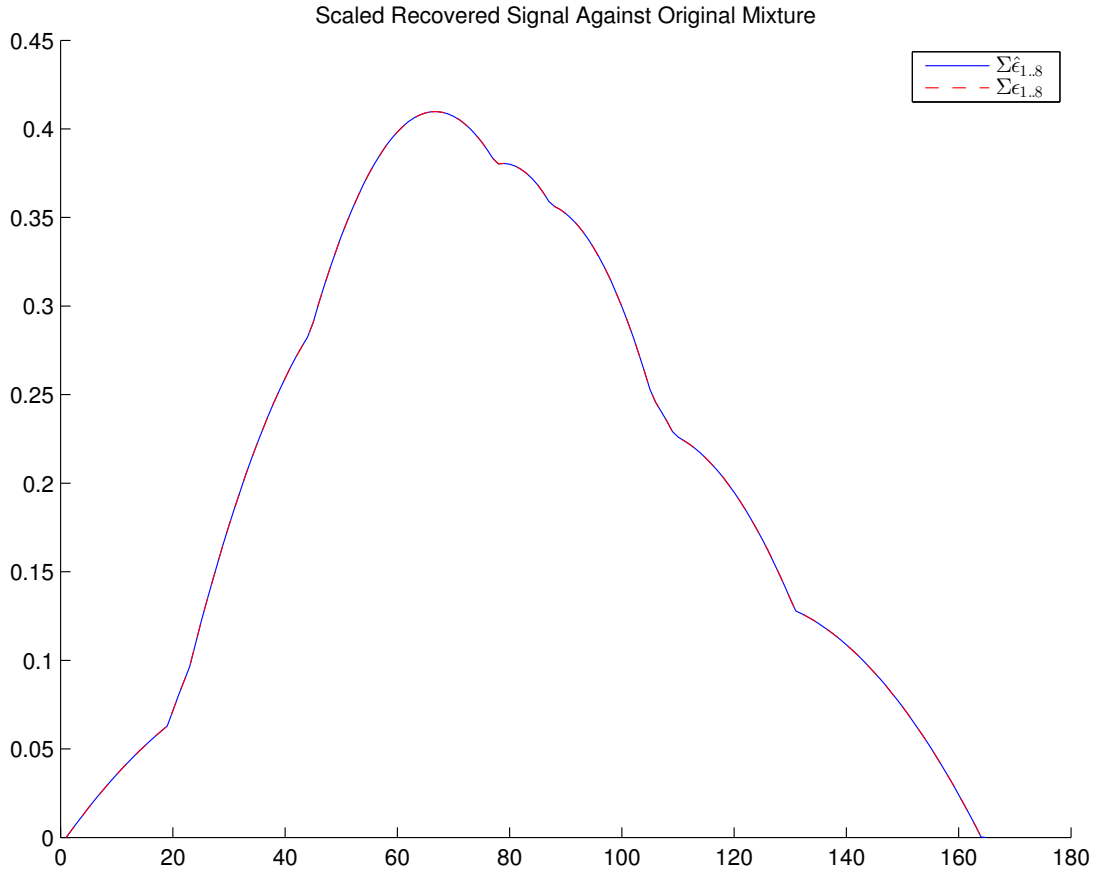

Figure A.1: Original Signal Mixture Compared Against Estimated Mixture

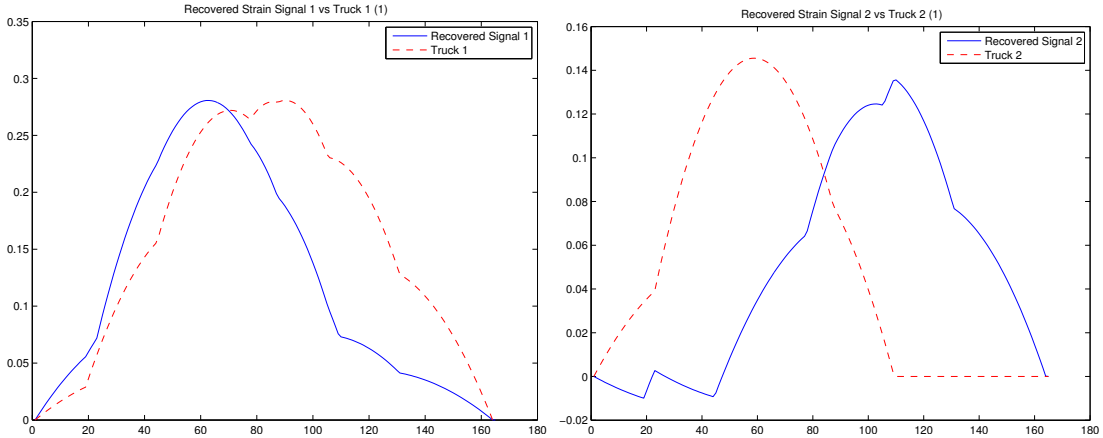

(a) Recovered 1 vs Original 1

(b) Recovered 2 vs Original 2

(c) Recovered 1 vs Original 2

(d) Recovered 2 vs Original 1

Figure A.2: Trial 1 Original vs Recovered Signals

Table A.2: RMSE of Source Signal Estimates —Trial 2

Estimated Component ($\hat{s_i}$)	Actual Component (s_j)	RMSE
$\hat{s_1}$	s_1	0.02523
$\hat{s_1}$	s_2	0.1317
$\hat{s_2}$	s_1	0.1638
$\hat{s_2}$	s_2	0.03583

A.2 Trial 2

Estimated mixing matrix:

$$\hat{\mathbf{A}} = \begin{bmatrix} 0.02556 & 0.02571 & 0.02432 & 0.01554 & 0.009798 & 0.005192 & 0.003024 & 0 \\ 0.01203 & 0.01409 & 0.01752 & 0.01444 & 0.009620 & 0.004903 & 0.003210 & 0 \end{bmatrix} \tag{A.3}$$

Estimated separation matrix:

$$\mathbf{W} = \begin{bmatrix} 53.49 & 33.83 & -9.874 & -38.67 & -29.55 & -13.71 & -11.53 & 0 \\ -66.46 & -35.45 & 32.30 & 71.52 & 53.22 & 25.14 & 20.22 & 0 \end{bmatrix} \tag{A.4}$$

Table A.2 provides the RMSE values of each component's estimate $\hat{s}$ against the actual mixture component s.

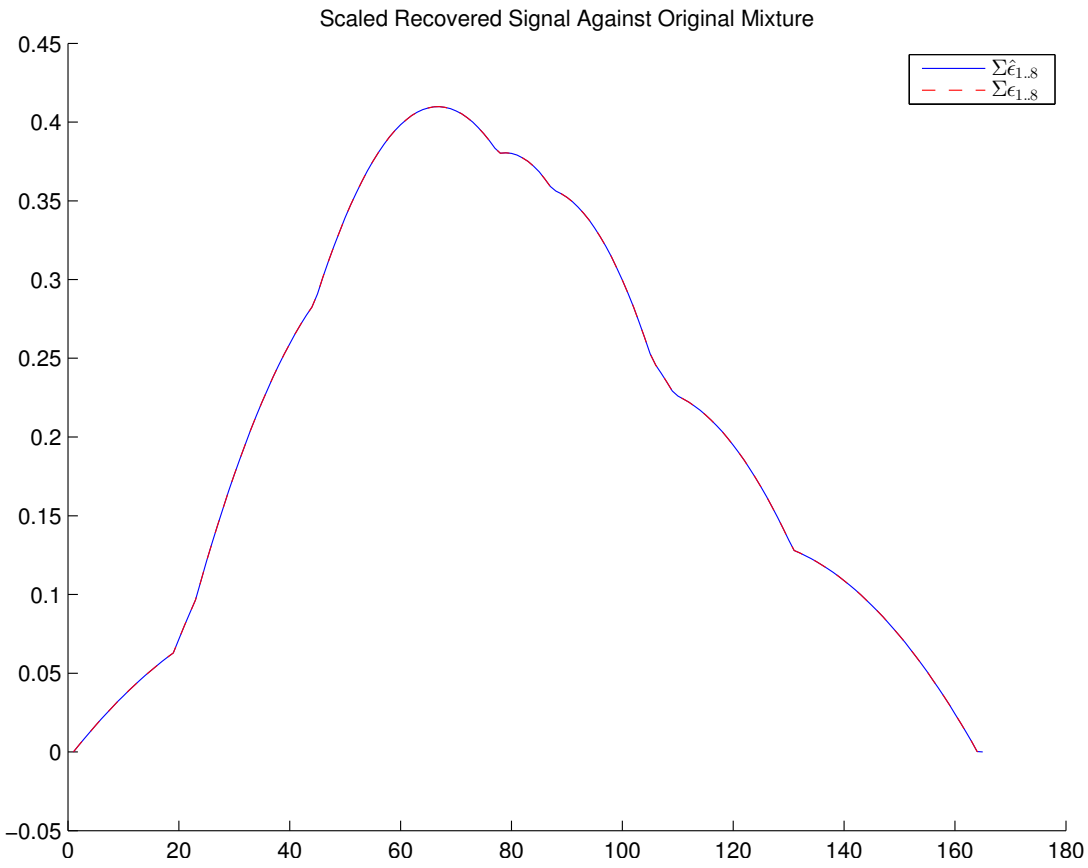

Figure A.3: Original Signal Mixture Compared Against Estimated Mixture

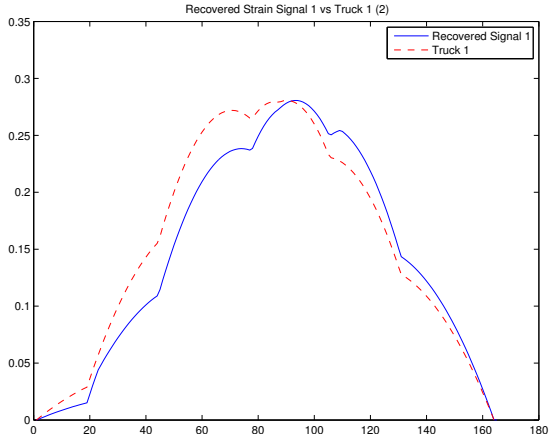

(a) Recovered 1 vs Original 1

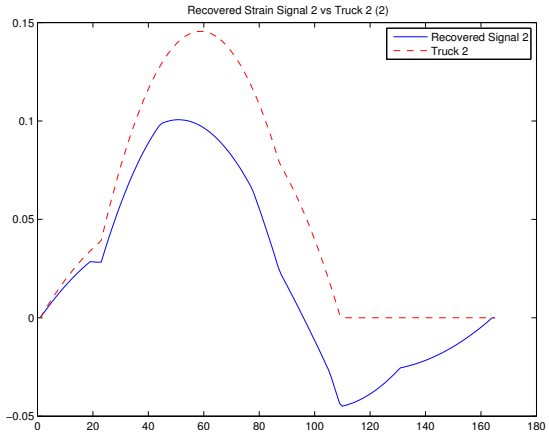

(b) Recovered 2 vs Original 2

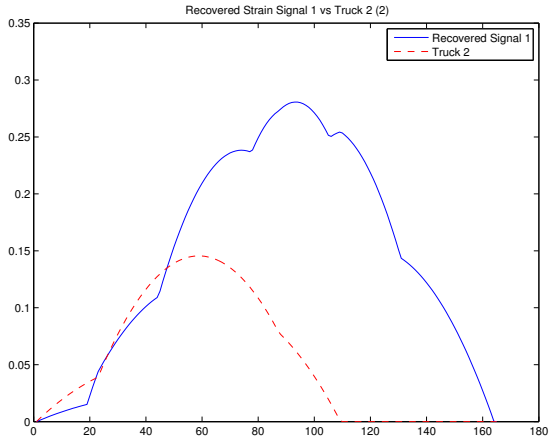

(c) Recovered 1 vs Original 2

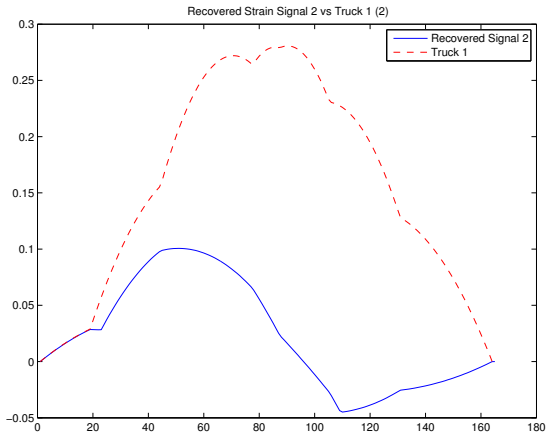

(d) Recovered 2 vs Original 1

Figure A.4: Trial 2 Original vs Recovered Signals

Table A.3: RMSE of Source Signal Estimates —Trial 3

Estimated Component ($\hat{s_i}$)	Actual Component (s_j)	RMSE
$\hat{s_1}$	s_1	0.08547
$\hat{s_1}$	s_2	0.07806
$\hat{s_2}$	s_1	0.12118
$\hat{s_2}$	s_2	0.07976

A.3 Trial 3

Estimated mixing matrix:

$$\hat{\mathbf{A}} = \begin{bmatrix} 0.02292 & 0.02480 & 0.02712 & 0.020168 & 0.01317 & 0.006807 & 0.004274 & 0 \\ 0.01651 & 0.01563 & 0.01275 & 0.006579 & 0.003896 & 0.002159 & 0.001085 & 0 \end{bmatrix} \quad \text{(A.5)}$$

Estimated separation matrix:

$$\mathbf{W} = \begin{bmatrix} -32.14 & -14.57 & 23.45 & 43.76 & 32.19 & 15.322 & 12.08 & 0 \\ 79.03 & 46.78 & -24.31 & -68.53 & -51.67 & -24.19 & -19.89 & 0 \end{bmatrix} \quad \text{(A.6)}$$

Table A.3 provides the RMSE values of each component's estimate $\hat{s}$ against the actual mixture component s.

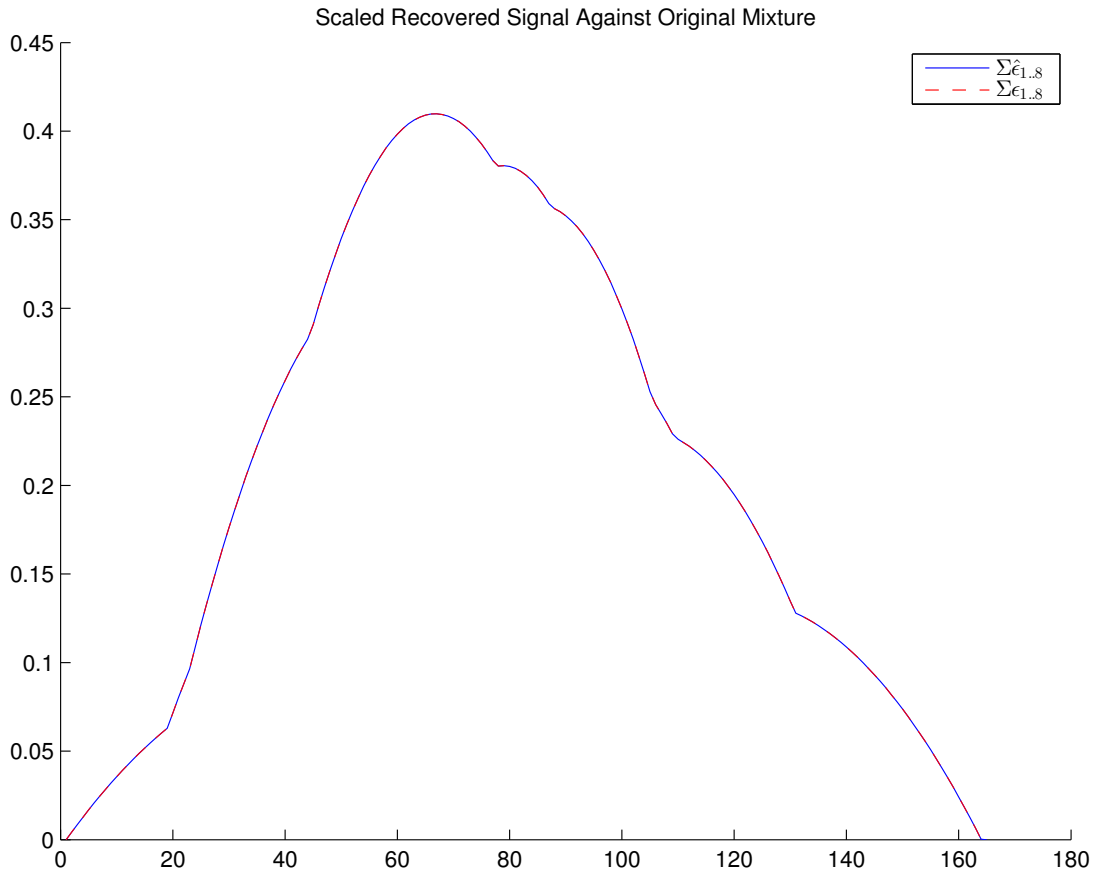

Figure A.5: Original Signal Mixture Compared Against Estimated Mixture (Trial 3)

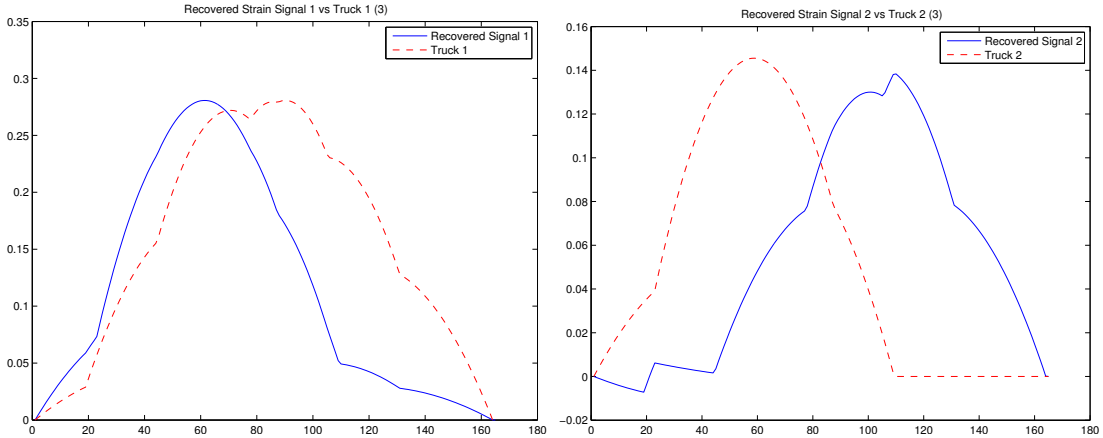

(a) Recovered 1 vs Original 1

(b) Recovered 2 vs Original 2

(c) Recovered 1 vs Original 2

(d) Recovered 2 vs Original 1

Figure A.6: Trial 3 Original vs Recovered Signals

Table A.4: RMSE of Source Signal Estimates —Trial 5

Estimated Component ($\hat{s_i}$)	Actual Component (s_j)	RMSE
$\hat{s_1}$	s_1	0.2011
$\hat{s_1}$	s_2	0.1444
$\hat{s_2}$	s_1	0.08764
$\hat{s_2}$	s_2	0.05556

A.4 Trial 4

This run of the simulation did not successfully extract the signal components.

A.5 Trial 5

Estimated mixing matrix:

$$\hat{\mathbf{A}} = \begin{bmatrix} 0.004240 & 0.006181 & 0.009864 & 0.009410 & 0.006428 & 0.003220 & 0.002215 & 0 \\ -0.02793 & -0.02866 & -0.02830 & -0.01901 & -0.01213 & -0.006375 & -0.003813 & 0 \end{bmatrix} \tag{A.7}$$

Estimated separation matrix:

$$\mathbf{W} = \begin{bmatrix} -78.95 & -43.62 & 33.77 & 79.58 & 59.44 & 28.00 & 22.66 & 0 \\ -32.32 & -22.32 & 0.2575 & 16.68 & 13.16 & 5.976 & 5.290 & 0 \end{bmatrix} \tag{A.8}$$

Table A.4 provides the RMSE values of each component's estimate $\hat{s}$ against the actual mixture component s.

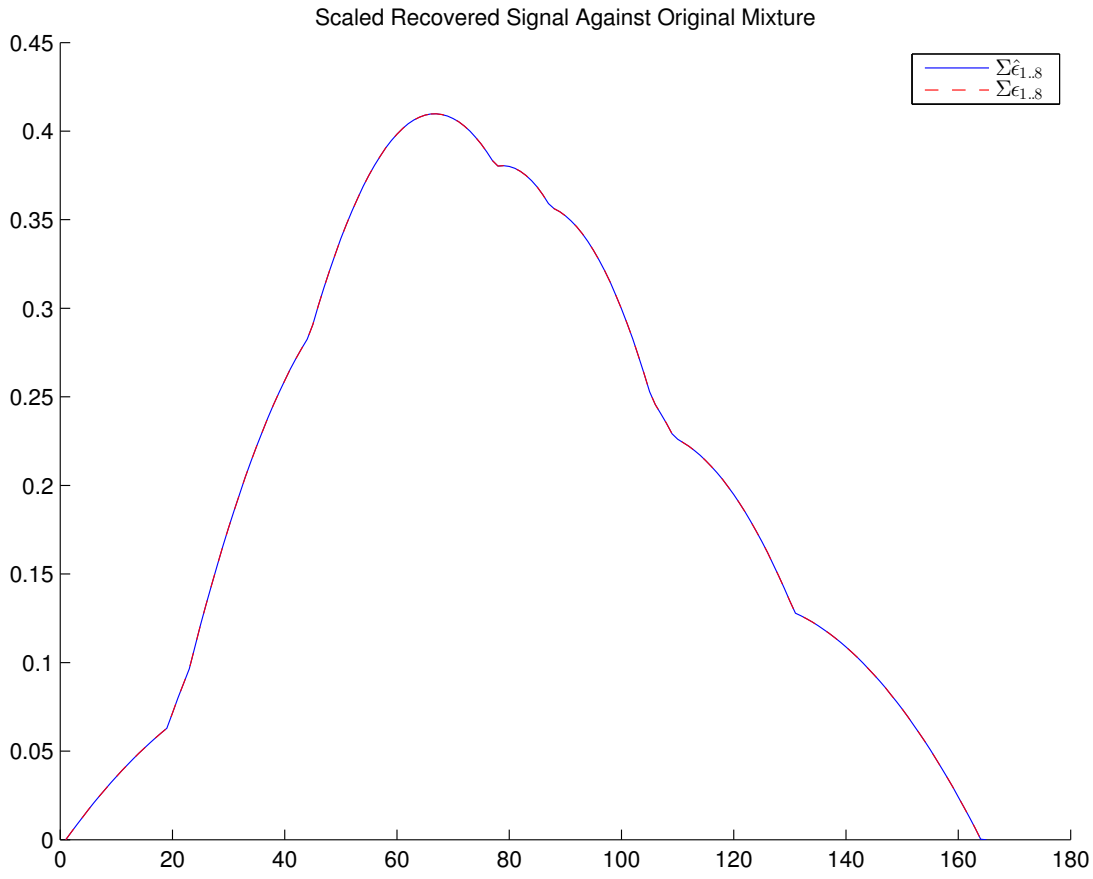

Figure A.7: Original Signal Mixture Compared Against Estimated Mixture (Trial 5)

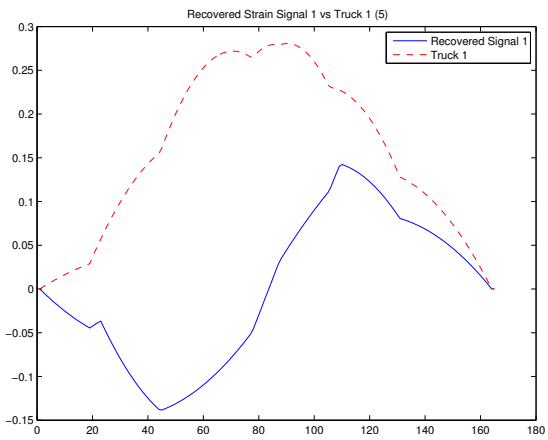

(a) Recovered 1 vs Original 1

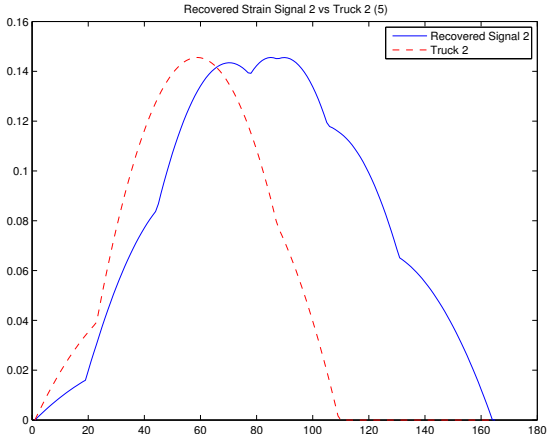

(b) Recovered 2 vs Original 2

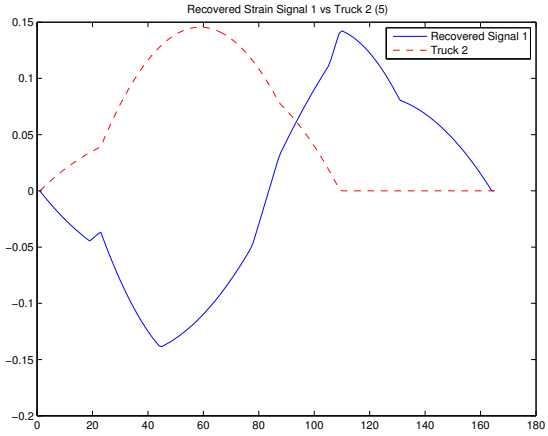

(c) Recovered 1 vs Original 2

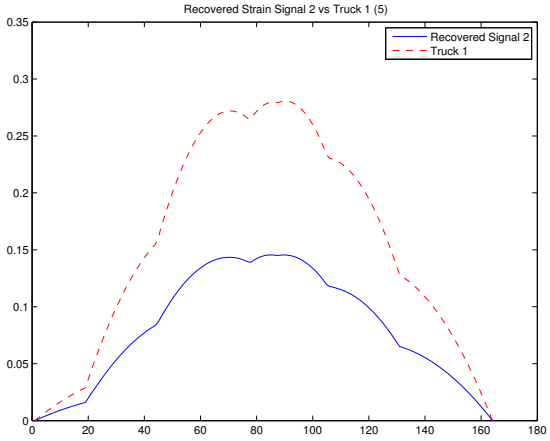

(d) Recovered 2 vs Original 1

Figure A.8: Trial 5 Original vs Recovered Signals

Table A.5: RMSE of Source Signal Estimates —Trial 6

Estimated Component ($\hat{s_i}$)	Actual Component (s_j)	RMSE
$\hat{s_1}$	s_1	0.06265
$\hat{s_1}$	s_2	0.1339
$\hat{s_2}$	s_1	0.1290
$\hat{s_2}$	s_2	0.0007700

A.6 Trial 6

Estimated mixing matrix:

$$\hat{\mathbf{A}} = \begin{bmatrix} 0.02005 & 0.01950 & 0.01704 & 0.009803 & 0.006006 & 0.003248 & 0.001773 & 0 \\ 0.019897 & 0.02190 & 0.02466 & 0.01881 & 0.01235 & 0.006360 & 0.004038 & 0 \end{bmatrix} \quad \text{(A.9)}$$

Estimated separation matrix:

$$\mathbf{W} = \begin{bmatrix} 72.67 & 43.75 & -20.13 & -60.41 & -45.68 & -21.34 & -17.64 & 0 \\ -44.69 & -22.06 & 27.12 & 54.42 & 40.24 & 19.09 & 15.18 & 0 \end{bmatrix} \quad \text{(A.10)}$$

Table A.5 provides the RMSE values of each component's estimate $\hat{s}$ against the actual mixture component s.

A.7 Trial 7

Estimated mixing matrix:

$$\hat{\mathbf{A}} = \begin{bmatrix} 0.02272 & 0.02461 & 0.02697 & 0.02009 & 0.01312 & 0.006781 & 0.004261 & 0 \\ -0.01678 & -0.01593 & -0.01308 & -0.006819 & -0.004053 & -0.002241 & -0.001136 & 0 \end{bmatrix} \quad \text{(A.11)}$$

Estimated separation matrix:

$$\mathbf{W} = \begin{bmatrix} -33.08 & -15.13 & 23.73 & 44.57 & 32.80 & 15.61 & 12.31 & 0 \\ -78.64 & -46.61 & 24.03 & 68.00 & 51.25 & 24.01 & 19.75 & 0 \end{bmatrix} \quad \text{(A.12)}$$

Table A.6 provides the RMSE values of each component's estimate $\hat{s}$ against the actual mixture component s.

A.8 Trial 8

Estimated mixing matrix:

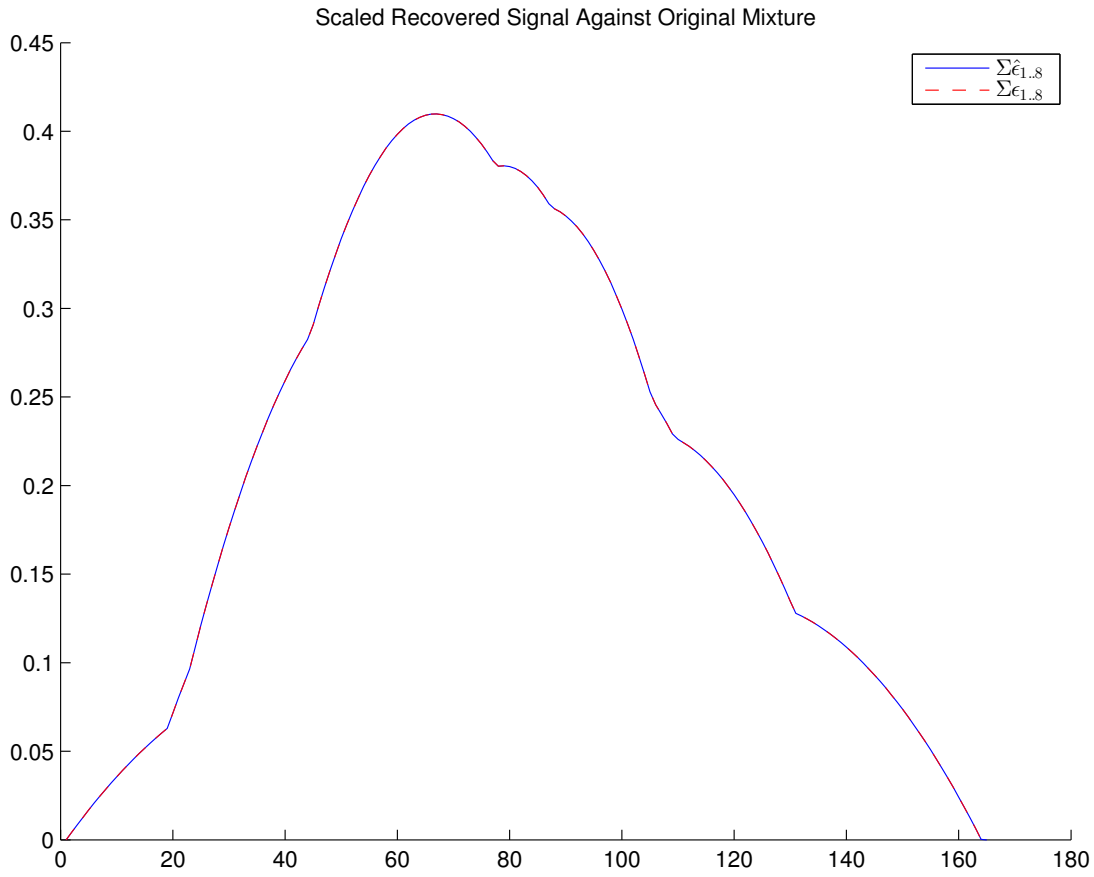

Figure A.9: Original Signal Mixture Compared Against Estimated Mixture (Trial 6)

Table A.6: RMSE of Source Signal Estimates —Trial 7

Estimated Component ($\hat{s}_i$)	Actual Component (s_j)	RMSE
$\hat{s_1}$	s_1	0.08697
$\hat{s_1}$	s_2	0.07747
$\hat{s_2}$	s_1	0.1203
$\hat{s_2}$	s_2	0.07940

$$\hat{\mathbf{A}} = \begin{bmatrix} 0.01609 & 0.01518 & 0.01226 & 0.006211 & 0.003656 & 0.002035 & 0.001007 & 0 \\ 0.02322 & 0.02508 & 0.02735 & 0.02029 & 0.01324 & 0.006845 & 0.004293 & 0 \end{bmatrix} \quad \text{(A.13)}$$

Estimated separation matrix:

$$\mathbf{W} = \begin{bmatrix} 79.60 & 47.04 & -24.73 & -69.31 & -52.25 & -24.47 & -20.11 & 0 \\ -30.70 & -13.72 & 23.00 & 42.51 & 31.24 & 14.88 & 11.71 & 0 \end{bmatrix} \quad \text{(A.14)}$$

Table A.7 provides the RMSE values of each component's estimate $\hat{s}$ against the actual mixture component s.

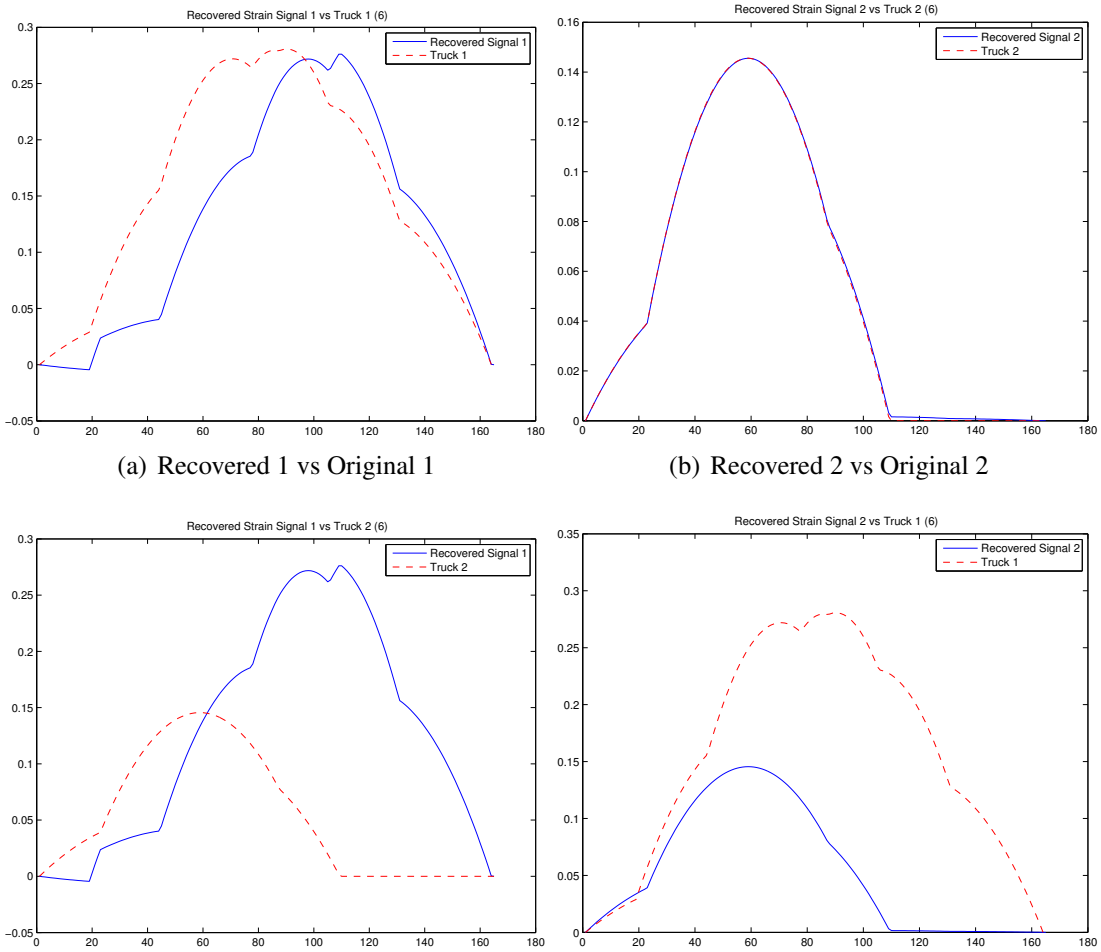

(a) Recovered 1 vs Original 1

(b) Recovered 2 vs Original 2

(c) Recovered 1 vs Original 2

(d) Recovered 2 vs Original 1

Figure A.10: Trial 6 Original vs Recovered Signals

Table A.7: RMSE of Source Signal Estimates —Trial 8

Estimated Component ($\hat{s_i}$)	Actual Component (s_j)	RMSE
$\hat{s_1}$	s_1	0.087238
$\hat{s_1}$	s_2	0.129233
$\hat{s_2}$	s_1	0.117603
$\hat{s_2}$	s_2	0.013598

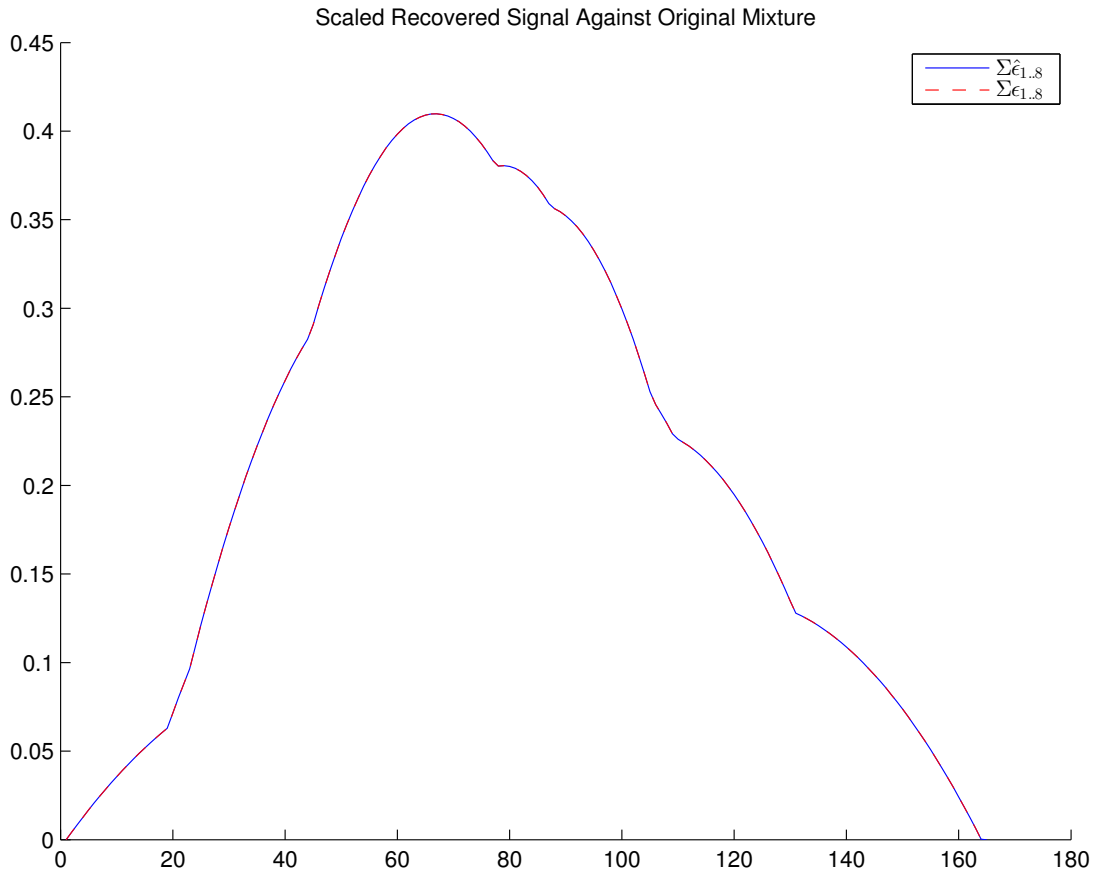

Figure A.11: Original Signal Mixture Compared Against Estimated Mixture (Trial 7)

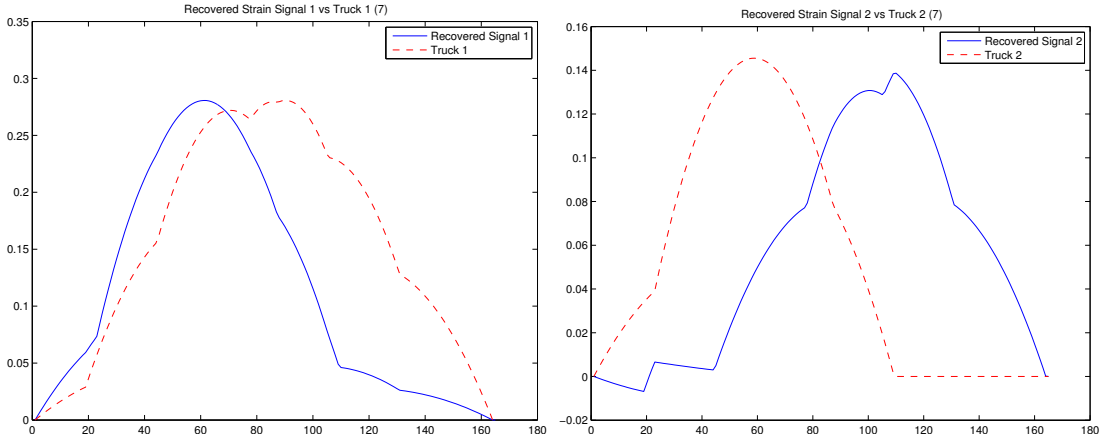

(a) Recovered 1 vs Original 1

(b) Recovered 2 vs Original 2

(c) Recovered 1 vs Original 2

(d) Recovered 2 vs Original 1

Figure A.12: Trial 7 Original vs Recovered Signals

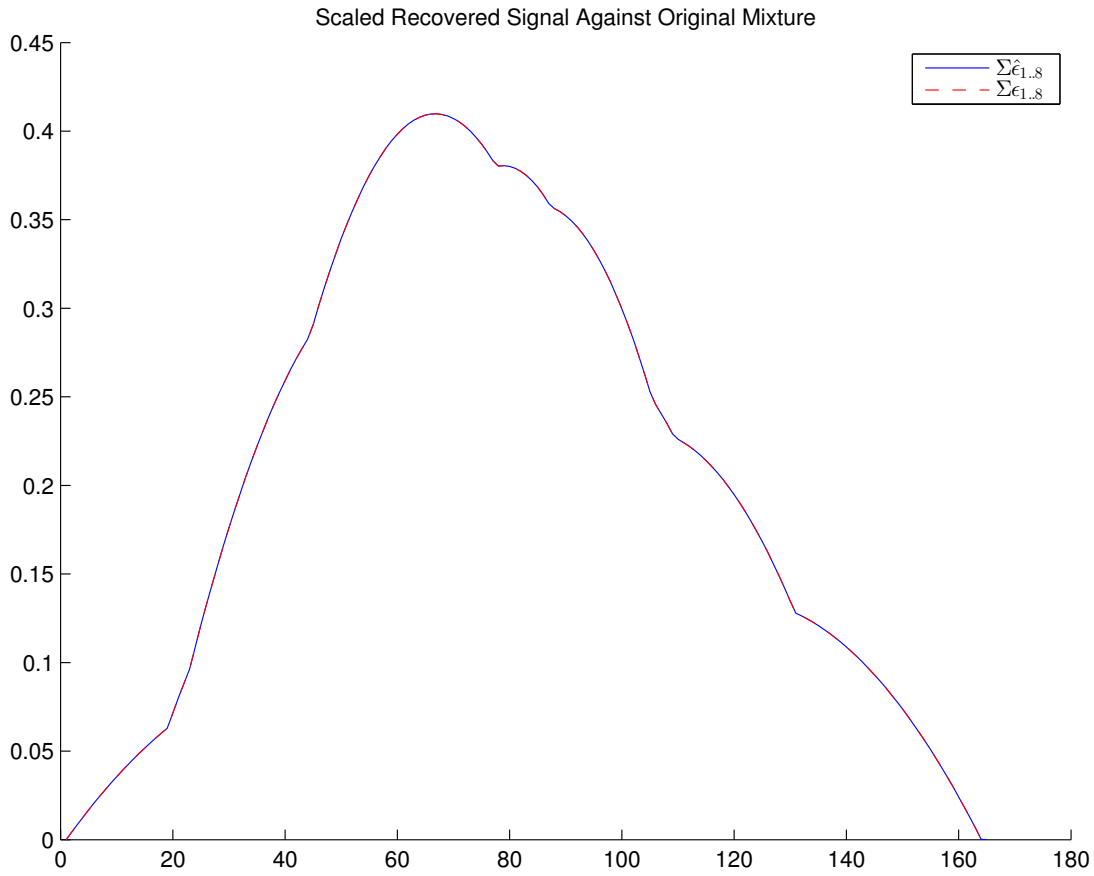

Figure A.13: Original Signal Mixture Compared Against Estimated Mixture (Trial 8)

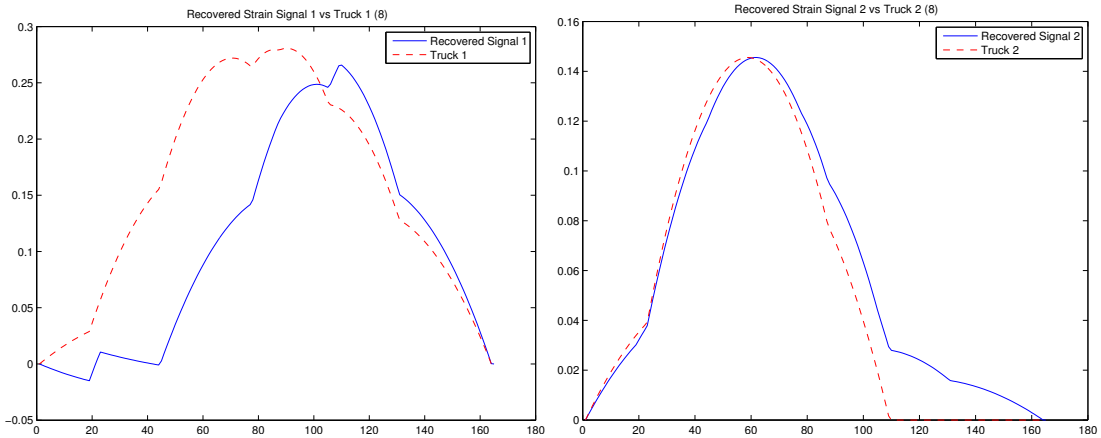

(a) Recovered 1 vs Original 1

(b) Recovered 2 vs Original 2

(c) Recovered 1 vs Original 2

(d) Recovered 2 vs Original 1

Figure A.14: Trial 8 Original vs Recovered Signals

Appendix B

Independent Component Analysis Results - Simulated Data with Noise

This appendix contains the results of attempting to recover the simulated source signals that incoporate a noise model (subsection 4.3.2).

B.1 Trial 1

$$\hat{\mathbf{A}} = \begin{bmatrix} -0.02393 & -0.02575 & -0.02789 & -0.02055 & -0.01339 & -0.006933 & -0.004336 & 0 \\ 0.01492 & 0.01393 & 0.01091 & 0.005227 & 0.003016 & 0.001704 & 0.0008005 & 0 \end{bmatrix} \tag{B.1}$$

$$\mathbf{W} = \begin{bmatrix} 26.90 & 11.48 & -21.80 & -39.17 & -28.73 & -13.70 & -10.75 & 0 \\ 81.20 & 47.79 & -25.84 & -71.43 & -53.81 & -25.21 & -20.70 & 0 \end{bmatrix} \tag{B.2}$$

Table B.1 provides the RMSE values of each component's estimate $\hat{s}$ against the actual mixture component s.

Table B.1: RMSE of Source Signal Estimates —Trial 1

Estimated Component ($\hat{s_i}$)	Actual Component (s_j)	RMSE
$\hat{s_1}$	s_1	0.07715
$\hat{s_1}$	s_2	0.08568
$\hat{s_2}$	s_1	0.12887
$\hat{s_2}$	s_2	0.08231

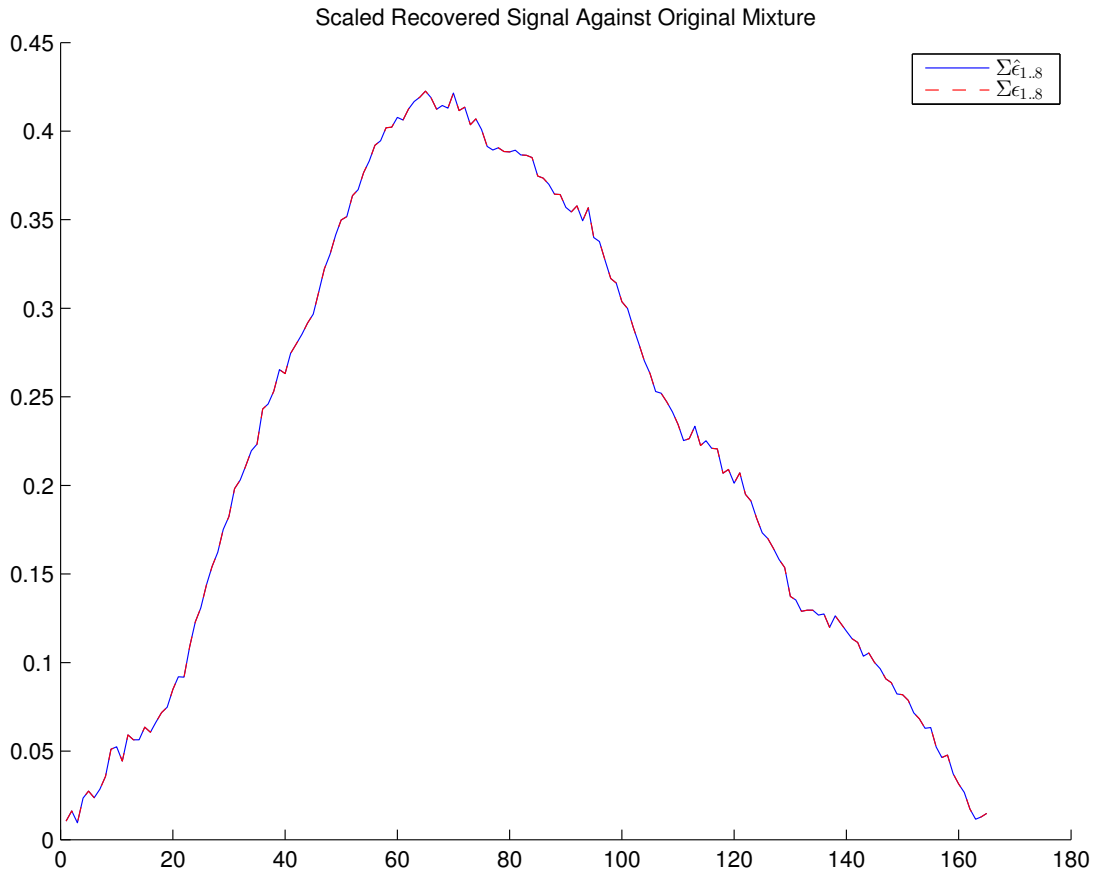

Figure B.1: Original Signal Mixture Compared Against Estimated Mixture

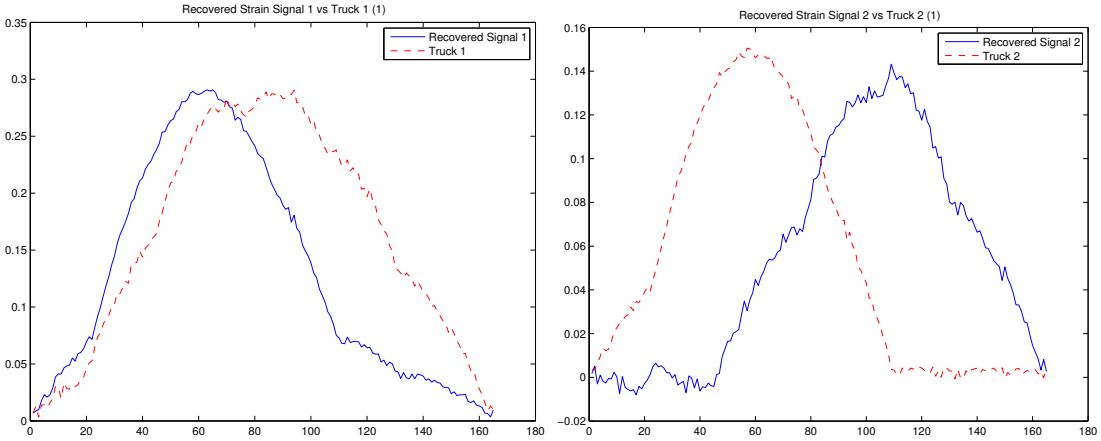

(a) Recovered 1 vs Original 1

(b) Recovered 2 vs Original 2

(c) Recovered 1 vs Original 2

(d) Recovered 2 vs Original 1

Figure B.2: Recovered Signals Versus Original Components —ICA Simulation with Noise, Trial 1

Table B.2: RMSE of Source Signal Estimates —Trial 2

Estimated Component ($\hat{s_i}$)	Actual Component (s_j)	RMSE
$\hat{s_1}$	s_1	0.08704
$\hat{s_1}$	s_2	0.08064
$\hat{s_2}$	s_1	0.1227
$\hat{s_2}$	s_2	0.07968

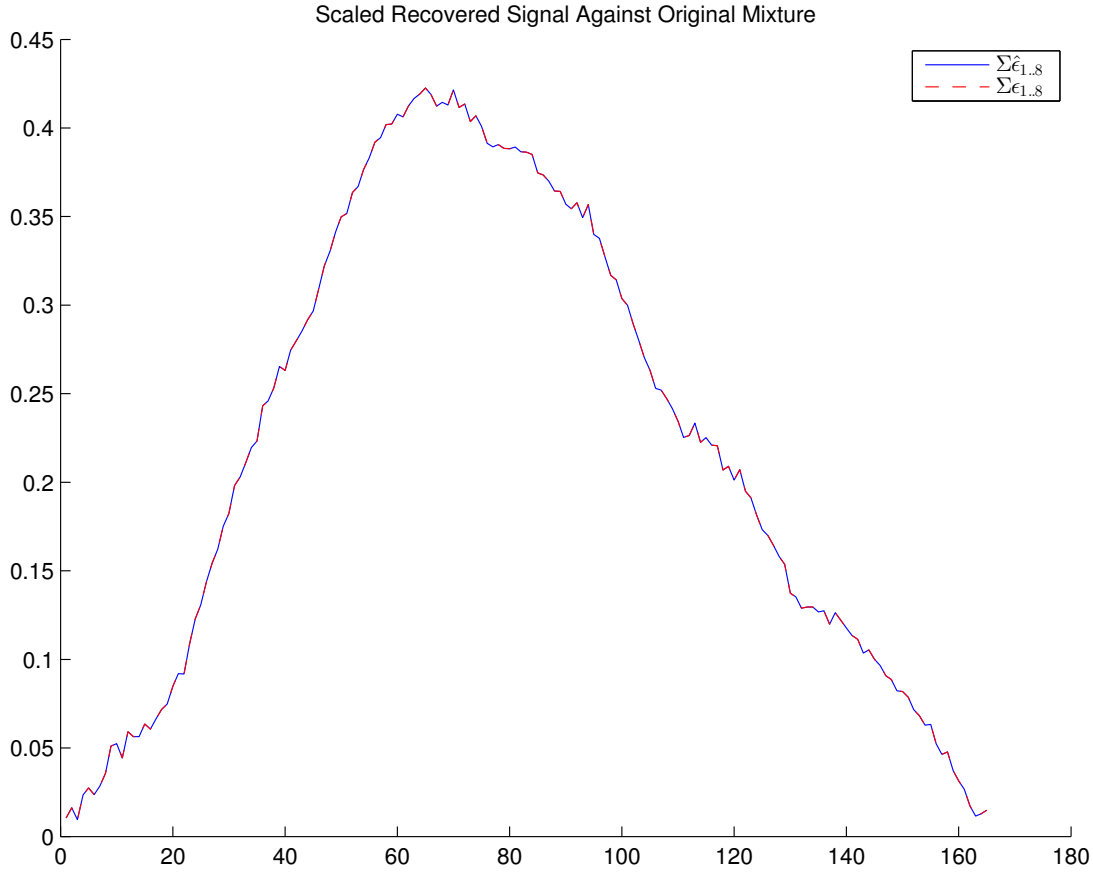

Figure B.3: Original Signal Mixture Compared Against Estimated Mixture

B.2 Trial 2

$$\hat{\mathbf{A}} = \begin{bmatrix} -0.02268 & -0.02457 & -0.02694 & -0.02008 & -0.01311 & -0.006777 & -0.004259 & 0 \\ -0.01676 & -0.01592 & -0.01308 & -0.006830 & -0.004063 & -0.002245 & -0.001140 & 0 \end{bmatrix} \tag{B.3}$$

$$\mathbf{W} = \begin{bmatrix} 33.23 & 15.22 & -23.77 & -44.69 & -32.89 & -15.65 & -12.35 & 0 \\ -78.83 & -46.74 & 24.04 & 68.1741 & 51.37 & 24.05 & 19.78 & 0 \end{bmatrix} \tag{B.4}$$

Table B.2 provides the RMSE values of each component's estimate $\hat{s}$ against the actual mixture component s.

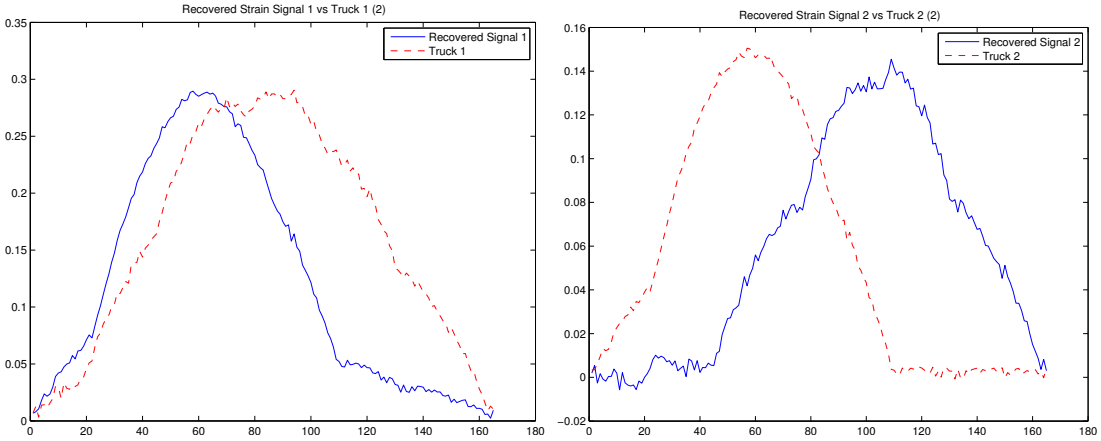

(a) Recovered 1 vs Original 1

(b) Recovered 2 vs Original 2

(c) Recovered 1 vs Original 2

(d) Recovered 2 vs Original 1

Figure B.4: Recovered Signals Versus Original Components —ICA Simulation with Noise, Trial 2

Table B.3: RMSE of Source Signal Estimates —Trial 3

Estimated Component ($\hat{s_i}$)	Actual Component (s_j)	RMSE
$\hat{s_1}$	s_1	0.02746
$\hat{s_1}$	s_2	0.1307
$\hat{s_2}$	s_1	0.1658
$\hat{s_2}$	s_2	0.03545

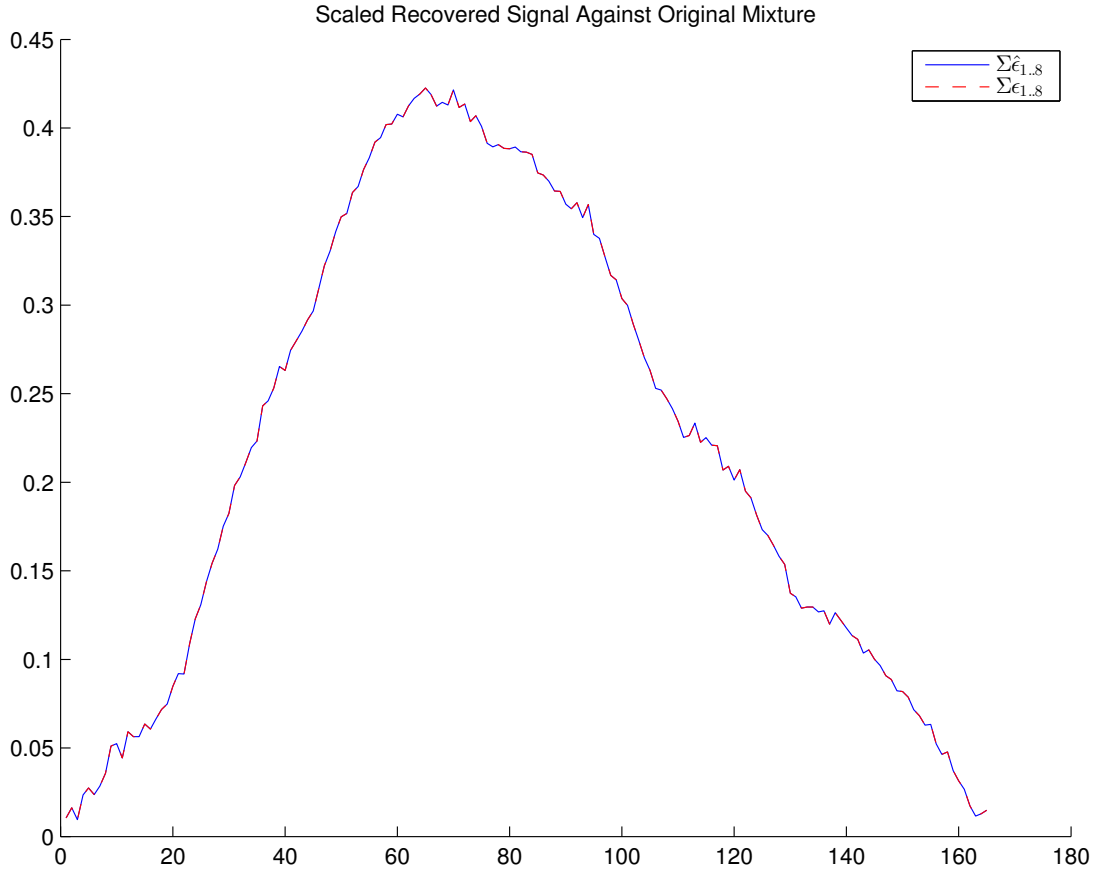

Figure B.5: Original Signal Mixture Compared Against Estimated Mixture (Trial 3)

B.3 Trial 3

$$\hat{\mathbf{A}} = \begin{bmatrix} 0.02537 & 0.02550 & 0.02408 & 0.01536 & 0.0096813 & 0.005132 & 0.002986 & 0 \\ -0.01232 & -0.014390 & -0.01780 & -0.01462 & -0.009732 & -0.004962 & -0.003245 & 0 \end{bmatrix} \tag{B.5}$$

$$\mathbf{W} = \begin{bmatrix} 54.43 & 34.35 & -10.28 & -39.62 & -30.26 & -14.04 & -11.80 & 0 \\ 66.00 & 35.16 & -32.21 & -71.18 & -52.96 & -25.02 & -20.11 & 0 \end{bmatrix} \tag{B.6}$$

Table B.3 provides the RMSE values of each component's estimate $\hat{s}$ against the actual mixture component s.

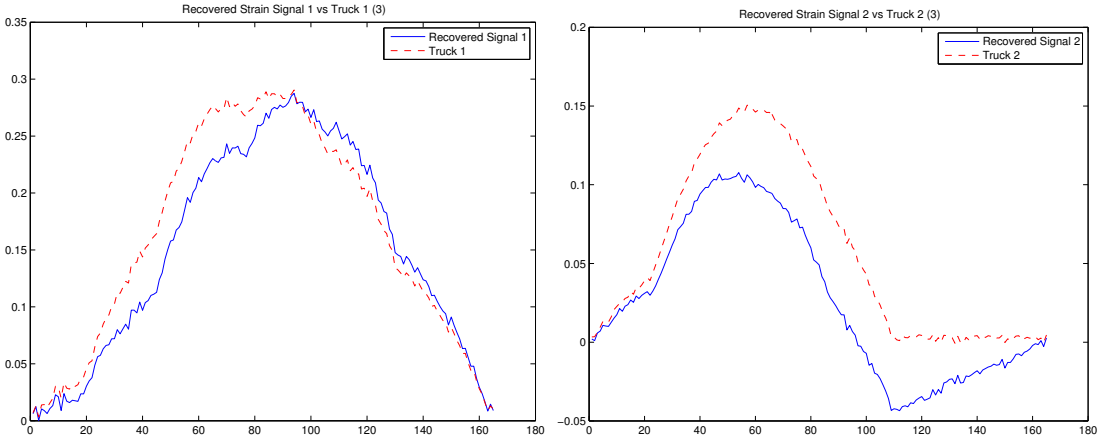

(a) Recovered 1 vs Original 1

(b) Recovered 2 vs Original 2

(c) Recovered 1 vs Original 2

(d) Recovered 2 vs Original 1

Figure B.6: Recovered Signals Versus Original Components —ICA Simulation with Noise, Trial 3

Table B.4: RMSE of Source Signal Estimates —Trial 5

Estimated Component ($\hat{s_i}$)	Actual Component (s_j)	RMSE
$\hat{s_1}$	s_1	0.07663
$\hat{s_1}$	s_2	0.1300
$\hat{s_2}$	s_1	0.1241
$\hat{s_2}$	s_2	0.008057

B.4 Trial 4

No result for test 4 - the extraction failed to converge.

B.5 Trial 5

$$\hat{\mathbf{A}} = \begin{bmatrix} 0.01802 & 0.01728 & 0.01458 & 0.007958 & 0.004799 & 0.002625 & 0.001379 & 0 \\ 0.02169 & 0.02363 & 0.026154 & 0.01966 & 0.01286 & 0.006639 & 0.004188 & 0 \end{bmatrix} \quad \text{(B.7)}$$

$$\mathbf{W} = \begin{bmatrix} 76.82 & 45.80 & -22.66 & -65.48 & -49.43 & -23.12 & -19.05 & 0 \\ -37.63 & -17.84 & 25.09 & 48.47 & 35.74 & 16.99 & 13.45 & 0 \end{bmatrix} \quad \text{(B.8)}$$

Table B.4 provides the RMSE values of each component's estimate $\hat{s}$ against the actual mixture component s.

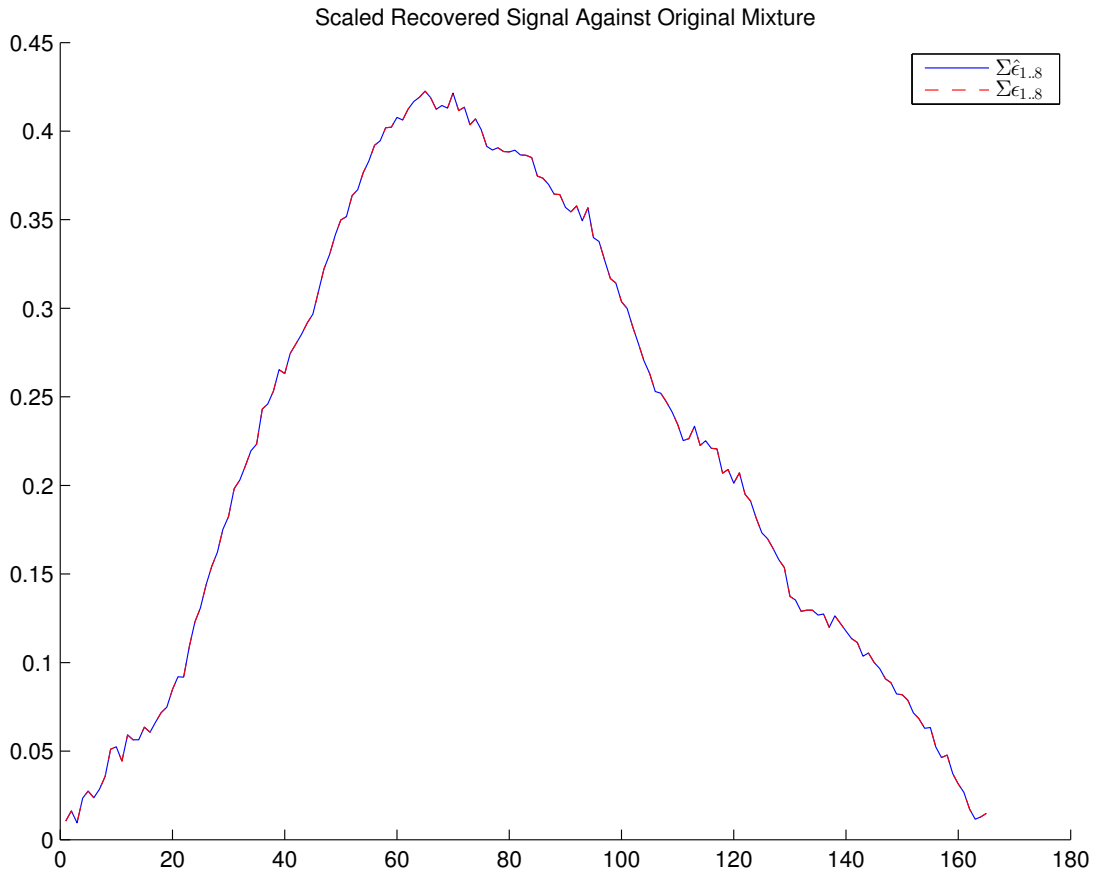

Figure B.7: Original Signal Mixture Compared Against Estimated Mixture (Trial 5)

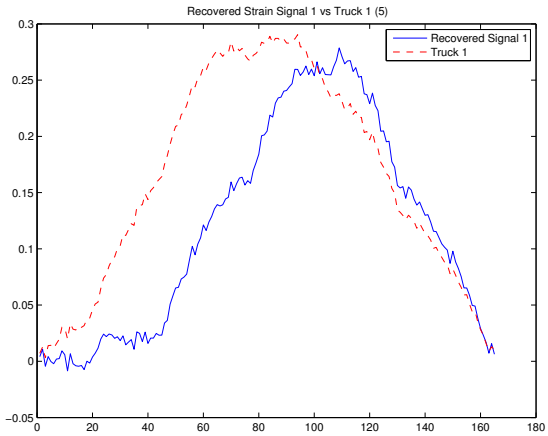

(a) Recovered 1 Against Original 1

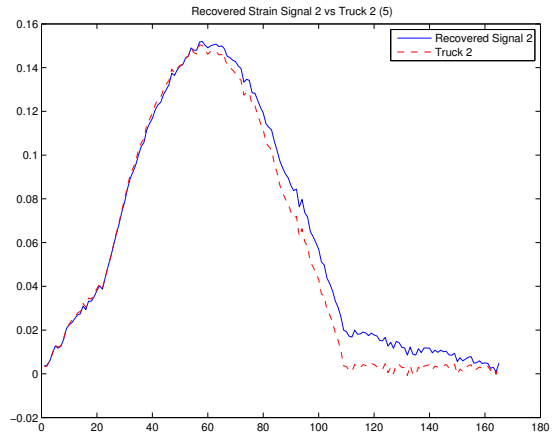

(b) Recovered 2 Against Original 2

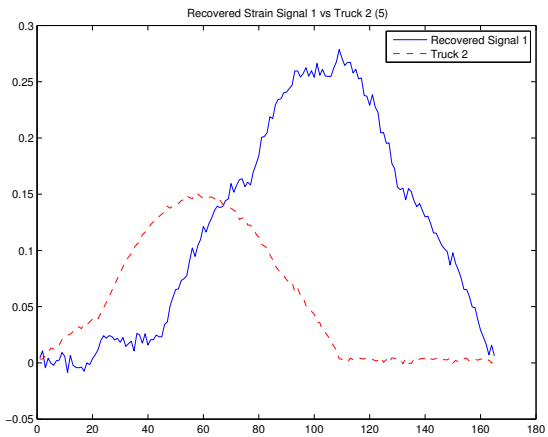

(c) Recovered 1 Against Original 2

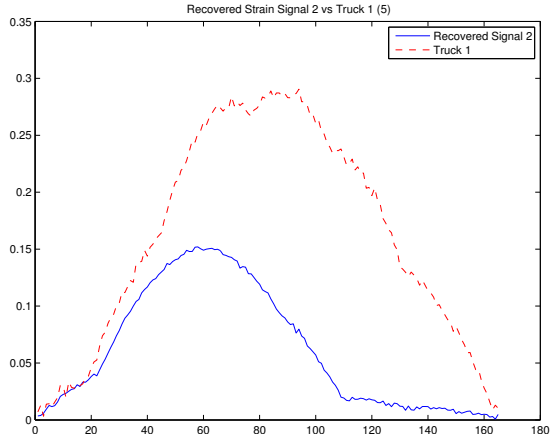

(d) Recovered 2 Against Original 1

Figure B.8: Recovered Signals Versus Original Components —ICA Simulation with Noise, Trial 5

Table B.5: RMSE of Source Signal Estimates —Trial 6

Estimated Component ($\hat{s_i}$)	Actual Component (s_j)	RMSE
$\hat{s_1}$	s_1	0.09333
$\hat{s_1}$	s_2	0.07757
$\hat{s_2}$	s_1	0.1192
$\hat{s_2}$	s_2	0.07820

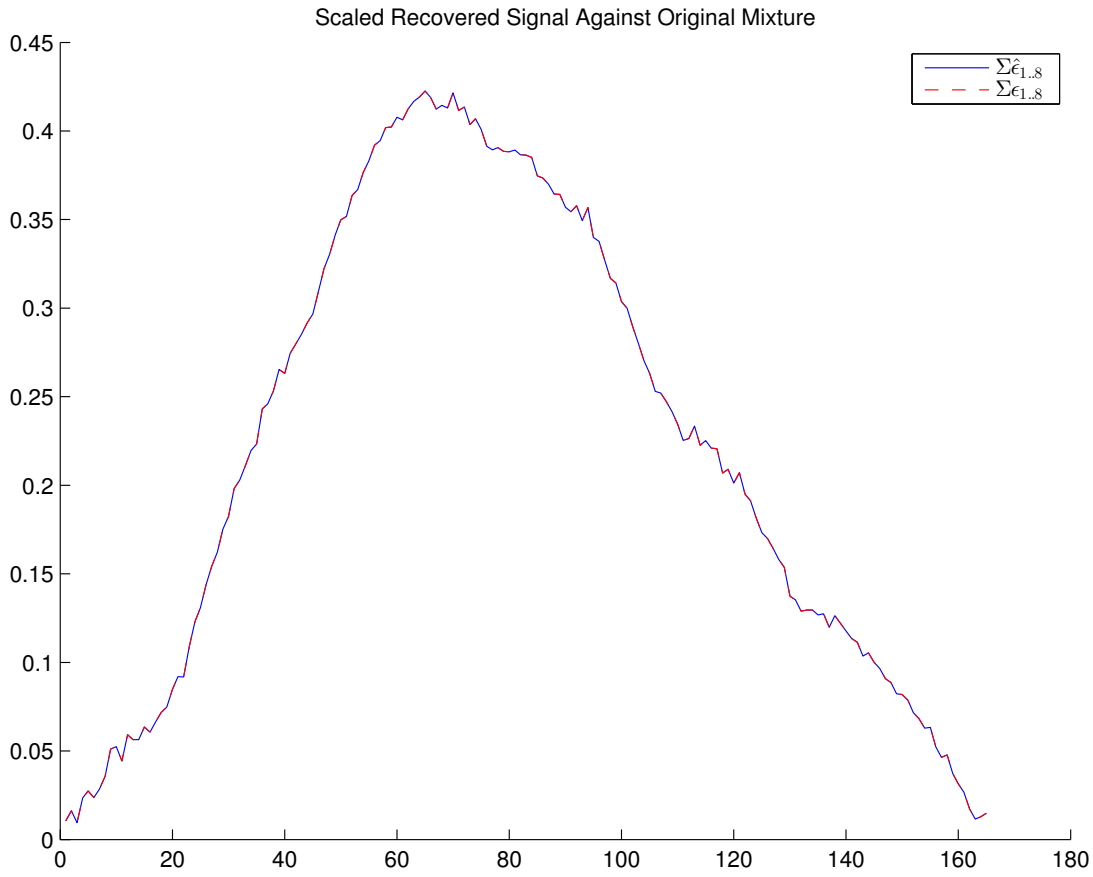

Figure B.9: Original Signal Mixture Compared Against Estimated Mixture (Trial 6)

B.6 Trial 6

$$\hat{\mathbf{A}} = \begin{bmatrix} 0.02185 & 0.02378 & 0.02628 & 0.01973 & 0.01290 & 0.006662 & 0.004200 & 0 \\ -0.01783 & -0.01707 & -0.01435 & -0.007784 & -0.004685 & -0.002567 & -0.001342 & 0 \end{bmatrix} \tag{B.9}$$

$$\mathbf{W} = \begin{bmatrix} -36.95 & -17.40 & 24.89 & 47.89 & 35.30 & 16.78 & 13.28 & 0 \\ -77.15 & -45.96 & 22.88 & 65.90 & 49.74 & 23.27 & 19.17 & 0 \end{bmatrix} \tag{B.10}$$

Table B.5 provides the RMSE values of each component's estimate $\hat{s}$ against the actual mixture component s.

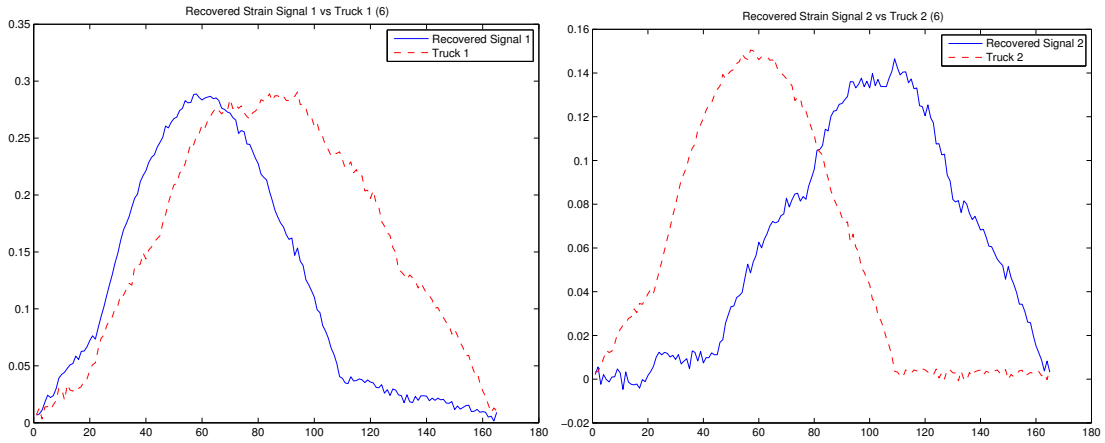

(a) Recovered 1 vs Original 1

(b) Recovered 2 vs Original 2

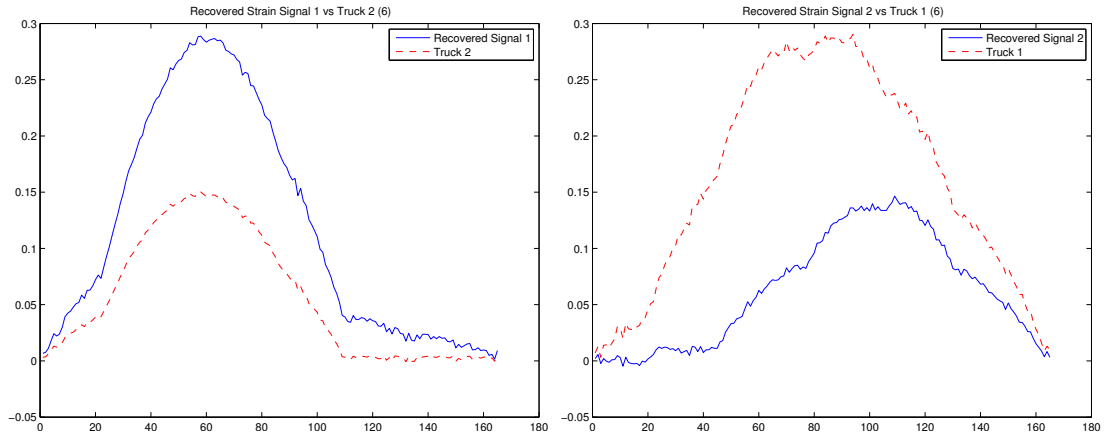

(c) Recovered 1 vs Original 2

(d) Recovered 2 vs Original 1

Figure B.10: Recovered Signals Versus Original Components —ICA Simulation with Noise, Trial 6

Table B.6: RMSE of Source Signal Estimates —Trial 7

Estimated Component ($\hat{s_i}$)	Actual Component (s_j)	RMSE
$\hat{s_1}$	s_1	0.076812
$\hat{s_1}$	s_2	0.129933
$\hat{s_2}$	s_1	0.124051
$\hat{s_2}$	s_2	0.008158

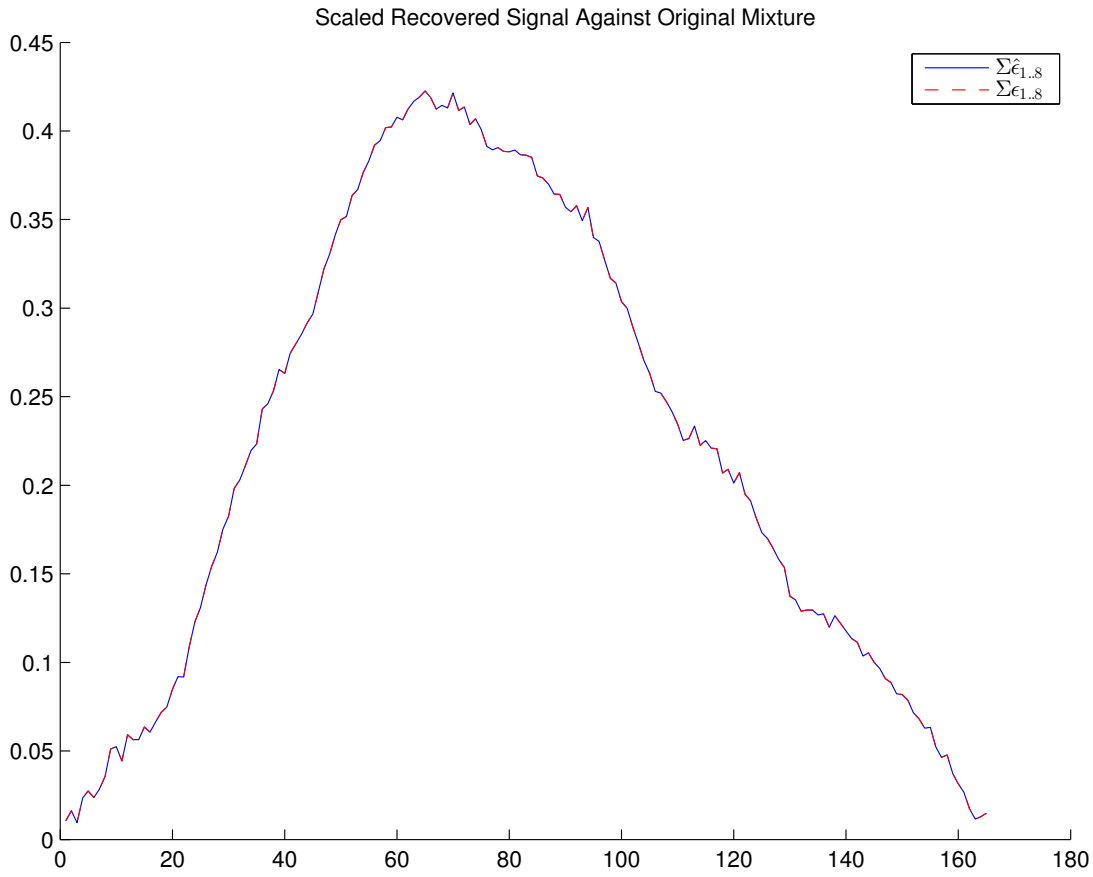

Figure B.11: Original Signal Mixture Compared Against Estimated Mixture (Trial 7)

B.7 Trial 7

$$\hat{\mathbf{A}} = \begin{bmatrix} 0.01799 & 0.01725 & 0.01455 & 0.007931 & 0.004781 & 0.002616 & 0.001374 & 0 \\ 0.02172 & 0.02365 & 0.02617 & 0.01967 & 0.01287 & 0.006642 & 0.004190 & 0 \end{bmatrix} \quad \text{(B.11)}$$

$$\mathbf{W} = \begin{bmatrix} 76.874 & 45.825 & -22.693 & -65.543 & -49.477 & -23.144 & -19.071 & 0 \\ -37.525 & -17.773 & 25.06 & 48.379 & 35.671 & 16.954 & 13.419 & 0 \end{bmatrix} \quad \text{(B.12)}$$

Table B.6 provides the RMSE values of each component's estimate $\hat{s}$ against the actual mixture component s.

Figure B.12 shows each of the original components against the recovered compoennts.

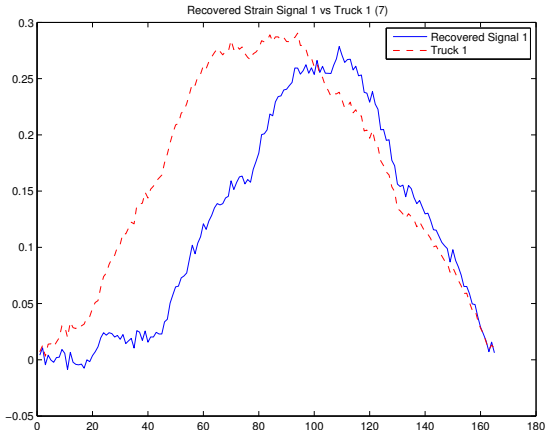

(a) Recovered 1 vs Original 1

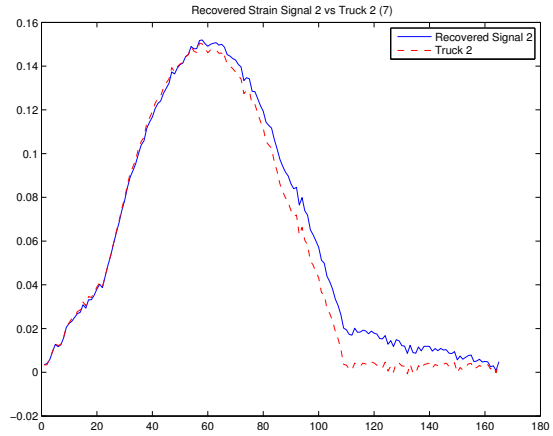

(b) Recovered 2 vs Original 2

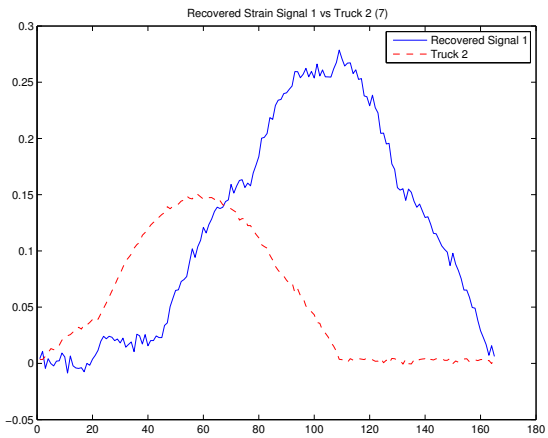

(c) Recovered 1 vs 2

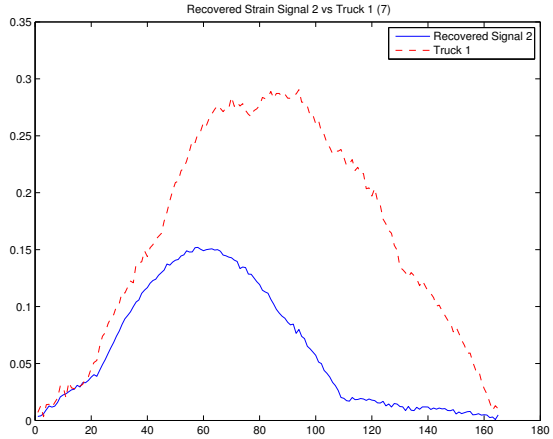

(d) Recovered 2 vs 1

Figure B.12: Recovered Signals Versus Original Components —ICA Simulation with Noise, Trial 7

Table B.7: RMSE of Source Signal Estimates —Trial 8

Estimated Component ($\hat{s_i}$)	Actual Component (s_j)	RMSE
$\hat{s_1}$	s_1	0.08941
$\hat{s_1}$	s_2	0.1290
$\hat{s_2}$	s_1	0.1180
$\hat{s_2}$	s_2	0.01470

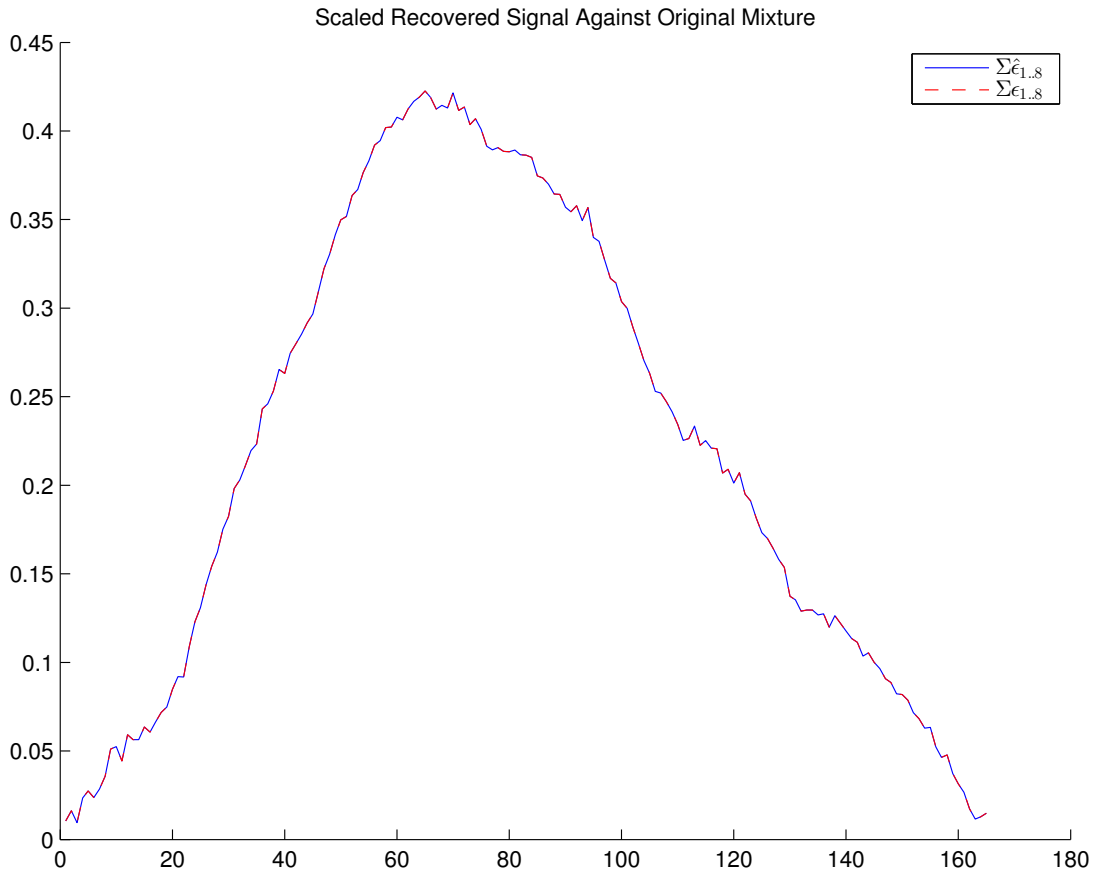

Figure B.13: Original Signal Mixture Compared Against Estimated Mixture (Trial 8)

B.8 Trial 8

$$\hat{\mathbf{A}} = \begin{bmatrix} 0.01592 & 0.01501 & 0.01209 & 0.006095 & 0.003582 & 0.001997 & 0.0009839 & 0 \\ 0.02327 & 0.02514 & 0.02740 & 0.02031 & 0.01325 & 0.006854 & 0.004298 & 0 \end{bmatrix} \tag{B.13}$$

$$\mathbf{W} = \begin{bmatrix} 79.99 & 47.26 & -24.89 & -69.70 & -52.54 & -24.60 & -20.22 & 0 \\ -30.32 & -13.50 & 22.88 & 42.17 & 30.99 & 14.76 & 11.62 & 0 \end{bmatrix} \tag{B.14}$$

Table B.7 provides the RMSE values of each component's estimate $\hat{s}$ against the actual mixture component s.

Figure B.14 shows each of the original signal components against the recovered components.

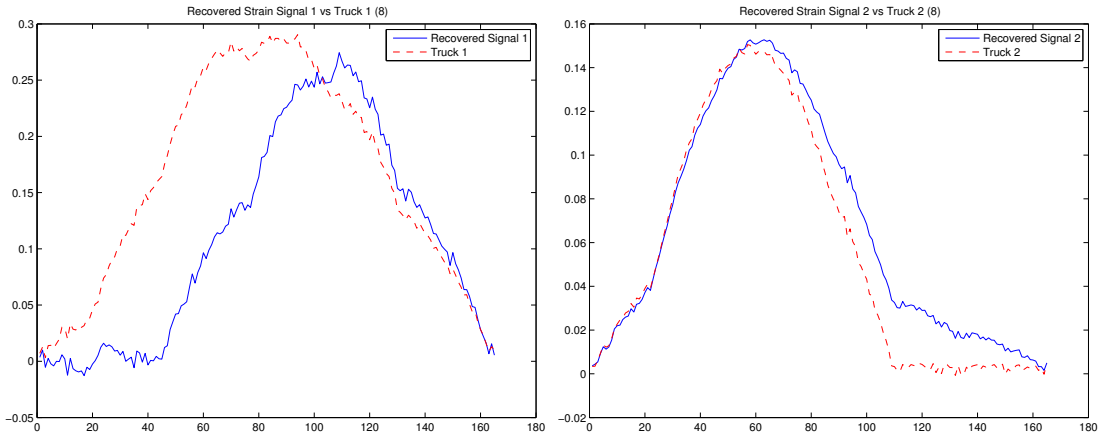

(a) Recovered 1 vs Original 1

(b) Recovered 2 vs Original 2

(c) Recovered 1 vs Original 2

(d) Recovered 2 vs Original 1

Figure B.14: Recovered Signals Versus Original Components —ICA Simulation with Noise, Trial 8

Appendix C

Independent Component Analysis Results - Actual Data, 2 Component Separation

This appendix presents the results for the first trial conducted using an event sample from the South Perimeter Bridge. The event is the semi-truck and garbage truck mixture that is used throughout the discussions on ICA. The separation attempts to recover two independent components using the recurring eight (8) combinations of FastICA parameters.

C.1 Trial 1

Estimated mixing matrix:

$$\hat{\mathbf{A}} = \begin{bmatrix} -2.480 & -3.047 & -2.488 & -1.217 & -0.4998 & -0.2132 & 0.001404 & 0.3365 \\ -8.818 & -8.539 & -7.210 & -3.587 & -1.899 & -0.6231 & 0.1373 & 0.7683 \end{bmatrix} \quad \text{(C.1)}$$

Estimated separation matrix:

$$\mathbf{W} = \begin{bmatrix} 1.463 & -0.2039 & -0.07393 & -2.915 & 0.3962 & 0.3721 & -0.8377 & 1.650 \\ 0.002520 & -1.257 & 1.395 & 1.702 & -2.930 & -0.8775 & 1.405 & 0.1874 \end{bmatrix} \quad \text{(C.2)}$$

RMSE (unadjusted) = 41.42

RMSE (scaled) = 43.35

Scale factor = 1.408

Figure C.1 and Figure C.2 show the extracted components. Figure C.3 show the recovered signal mixture against, both with and without scaling.

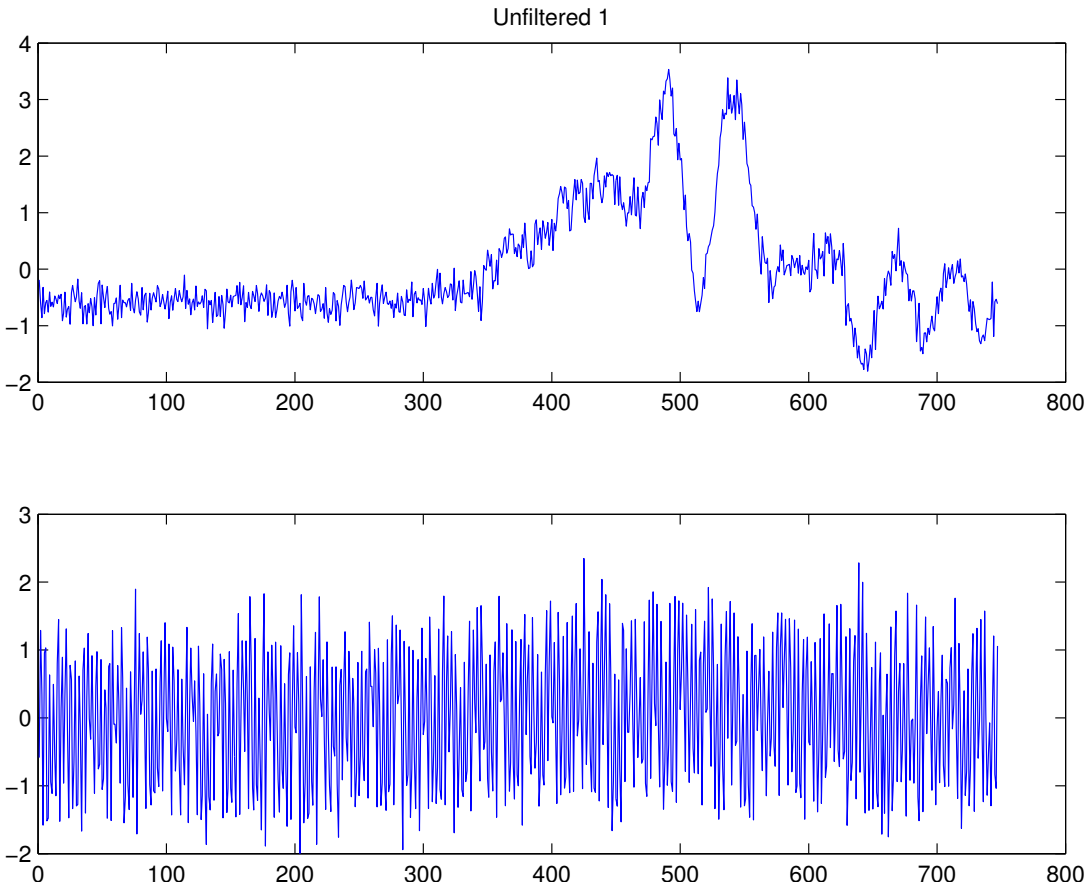

Figure C.1: Recovered Signals from Trial 1, Unfiltered Data

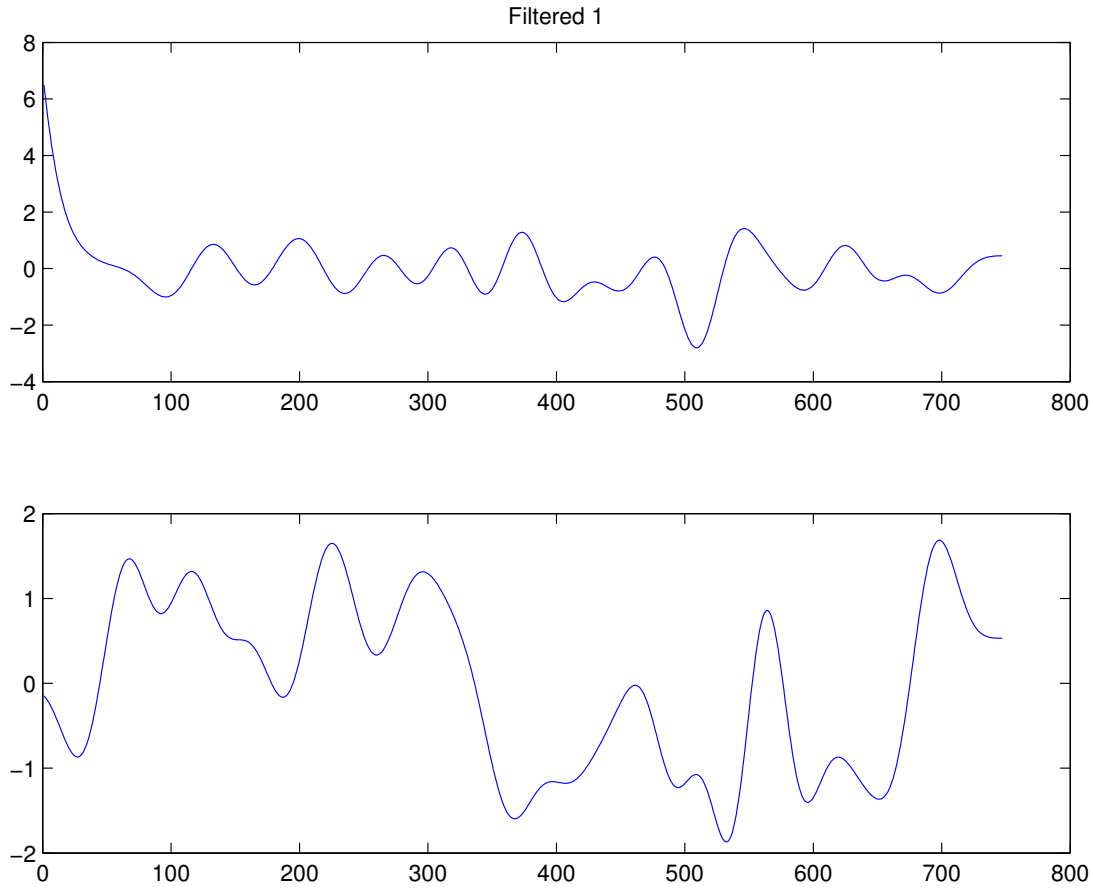

Figure C.2: Recovered Signals from Trial 1, Filtered Data

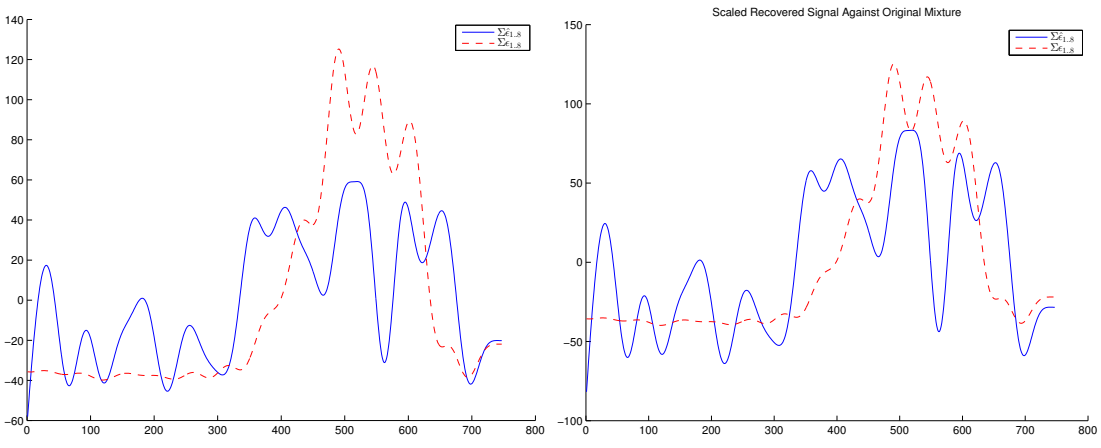

(a) Filtered, Unscaled (b) Filtered, Scaled

Figure C.3: Original/Estimated Mixture Comparisons —Actual Signals 2 Components, Trial 1

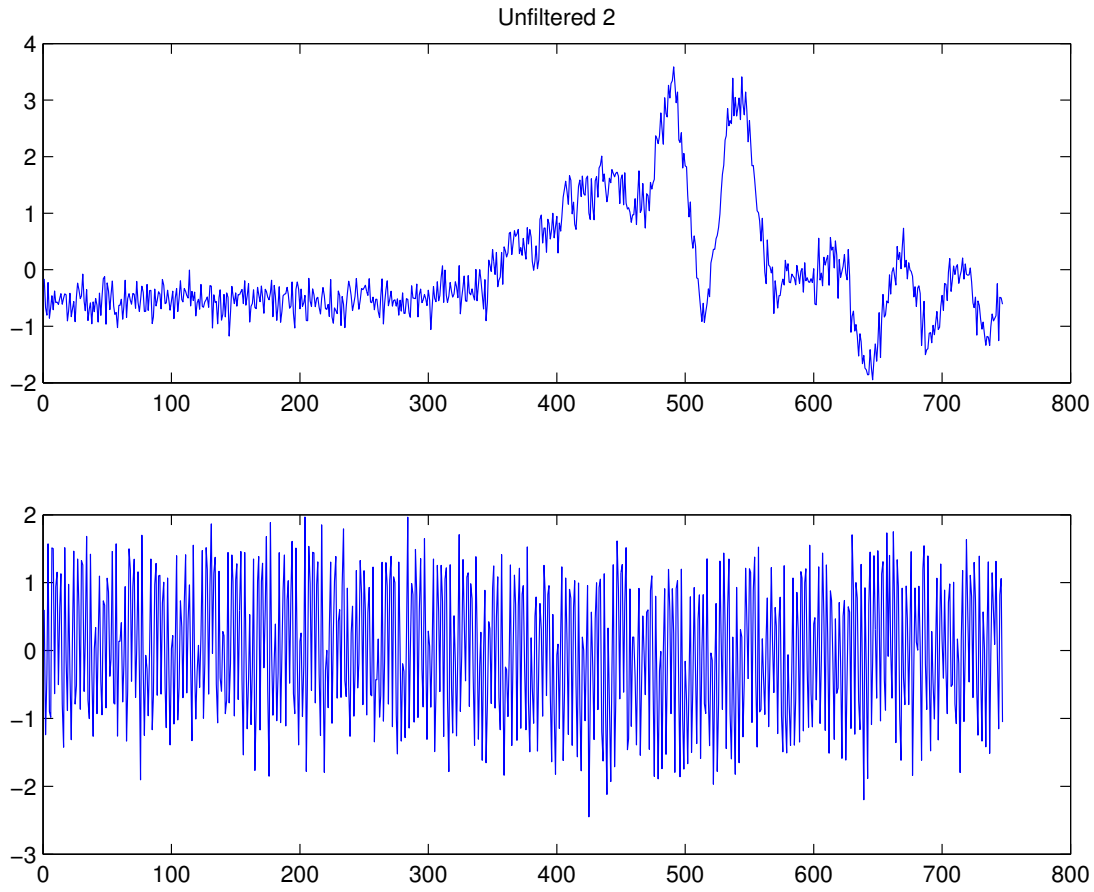

Figure C.4: Recovered Signals from Trial 2, Unfiltered Data

C.2 Trial 2

Estimated mixing matrix:

$$\hat{\mathbf{A}} = \begin{bmatrix} 8.276 & 8.540 & 7.101 & 3.415 & 1.634 & 0.7680 & 0.2167 & -0.5423 \\ -7.138W & -7.010 & -5.902 & -2.808 & -1.184 & -0.2058 & 0.5580 & 0.8422 \end{bmatrix} \tag{C.3}$$

Estimated separation matrix:

$$\mathbf{W} = \begin{bmatrix} 0.2929 & 0.7383 & -1.092 & 0.1575 & -1.709 & 2.916 & -0.1120 & -0.1152 \\ -0.2719 & -0.2664 & 0.4975 & -0.04846 & 0.5544 & -0.3987 & 1.603 & -0.3893 \end{bmatrix} \tag{C.4}$$

RMSE (unadjusted) = 36.16

RMSE (scaled) = 37.05

Scale factor = 1.216

Figure C.4 and Figure C.5 show the extracted components. Figure C.6 shows the recovered signal mixture against the original mixtures, both with and without scaling.

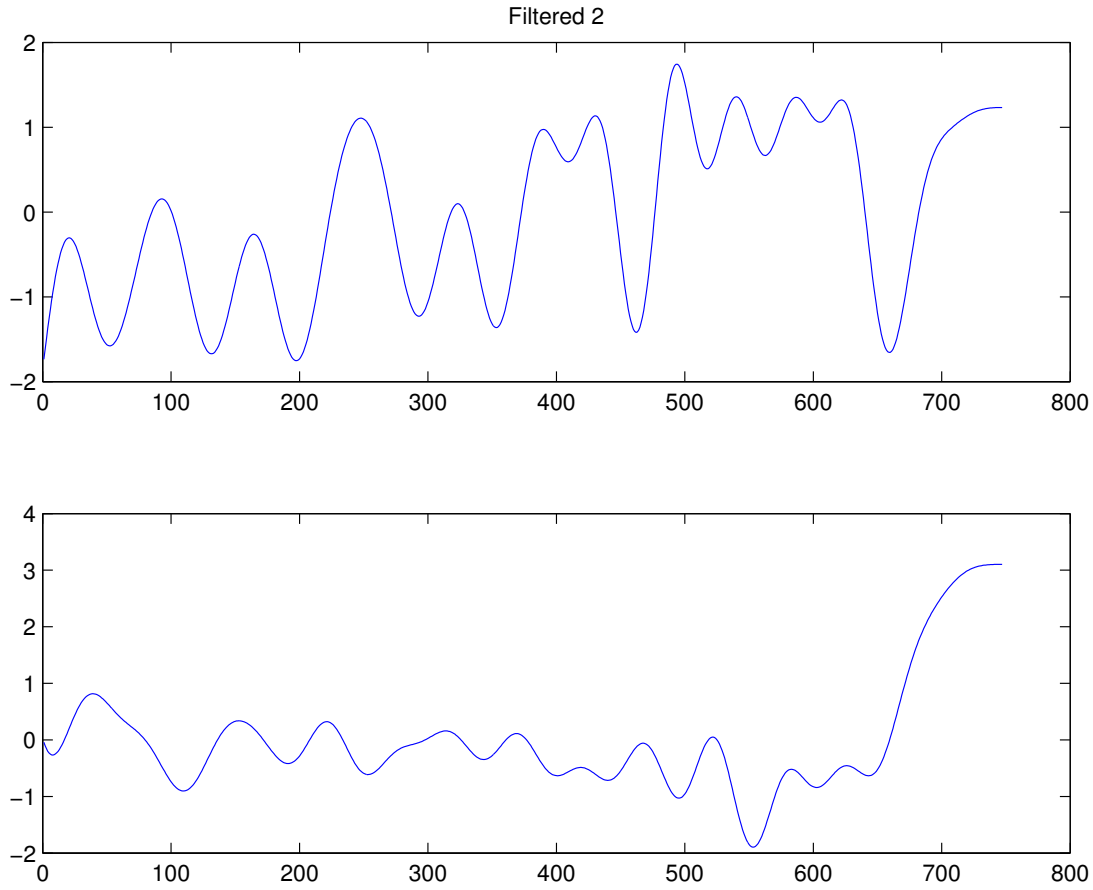

Figure C.5: Recovered Signals from Trial 2, Filtered Data

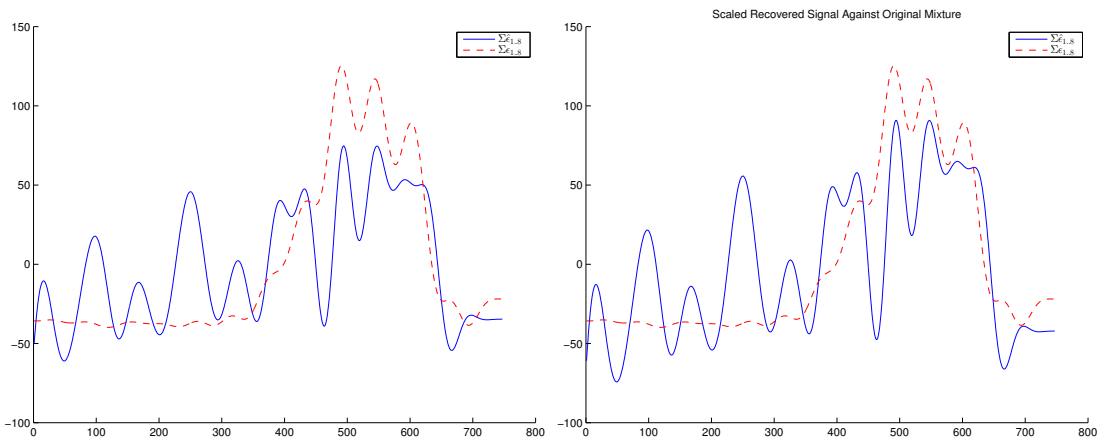

(a) Filtered, Unscaled (b) Filtered, Scaled

Figure C.6: Original/Estimated Mixture Comparisons —Actual Signals 2 Components, Trial 2

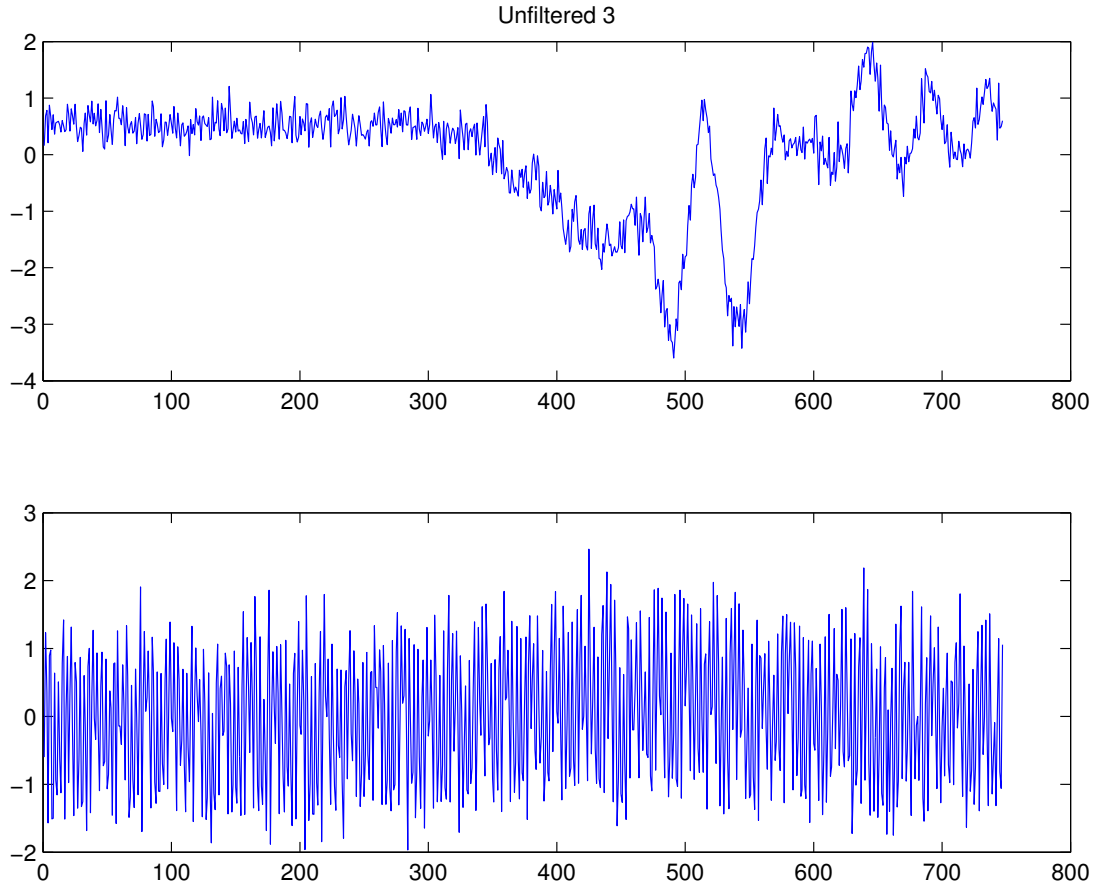

Figure C.7: Recovered Signals from Trial 3, Unfiltered Data

C.3 Trial 3

Estimated mixing matrix:

$$\hat{\mathbf{A}} = \begin{bmatrix} -1.832 & -3.323 & -2.591 & -0.9353 & -0.3569 & -0.1591 & -0.04026 & 0.08228 \\ 2.806 & 2.877 & 2.386 & 1.062 & 0.3494 & -0.1350 & -0.6015 & -0.5086 \end{bmatrix} \tag{C.5}$$

Estimated separation matrix:

$$\mathbf{W} = \begin{bmatrix} 1.596 & -0.1410 & -0.3403 & -2.507 & -0.5597 & 0.3378 & -0.1863 & 0.9182 \\ -0.0805 & 0.1879 & -0.2355 & 0.1334 & 0.4487 & -0.3732 & -1.729 & 0.2785 \end{bmatrix} \tag{C.6}$$

RMSE (unadjusted) = 50.42

RMSE (scaled) = 51.36

Scale factor = 1.794

Figure C.7 and Figure C.8 show the extracted components. Figure C.9 shows the recovered signal mixture against the original scaling, both with and without scaling.

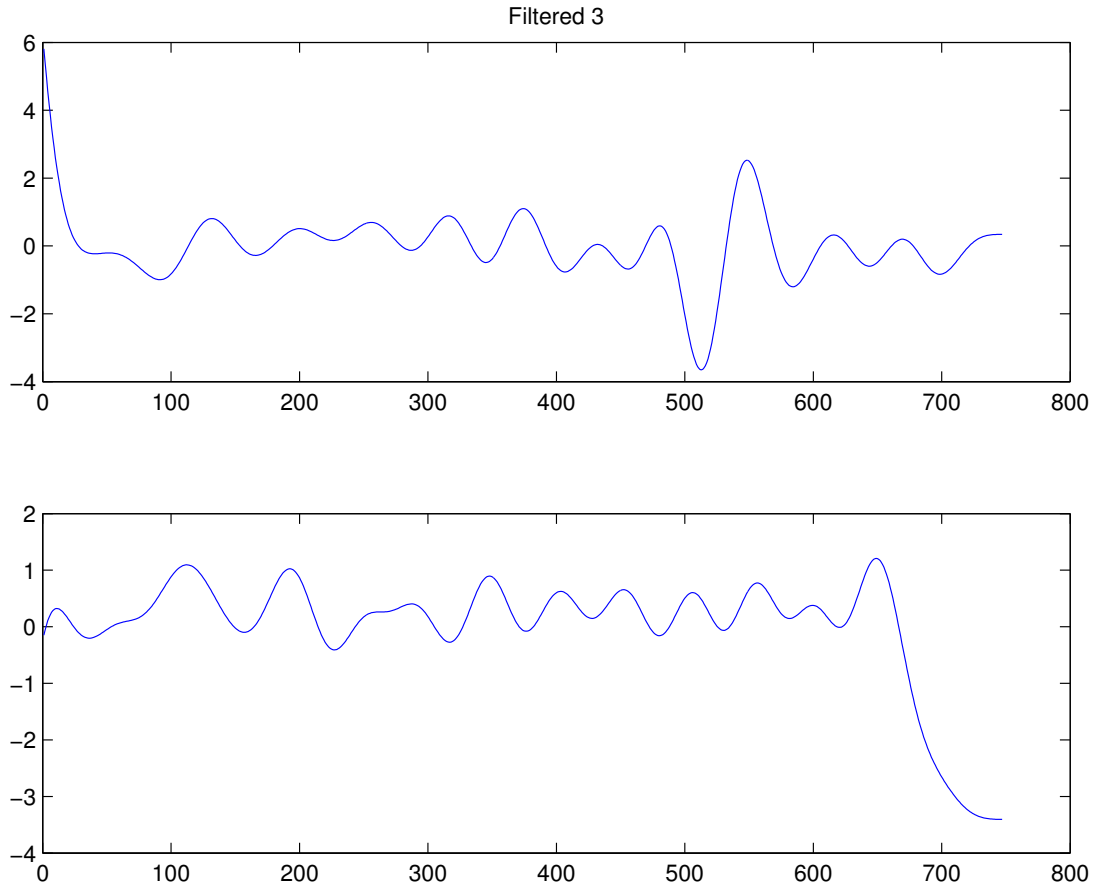

Figure C.8: Recovered Signals from Trial 3, Filtered Data

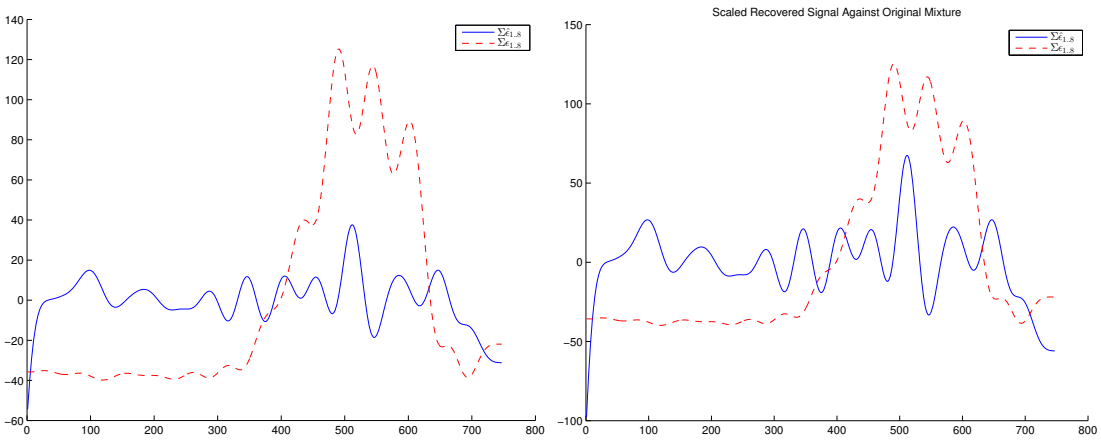

(a) Filtered, Unscaled (b) Filtered, Scaled

Figure C.9: Original/Estimated Mixture Comparisons —Actual Signals 2 Components, Trial 3

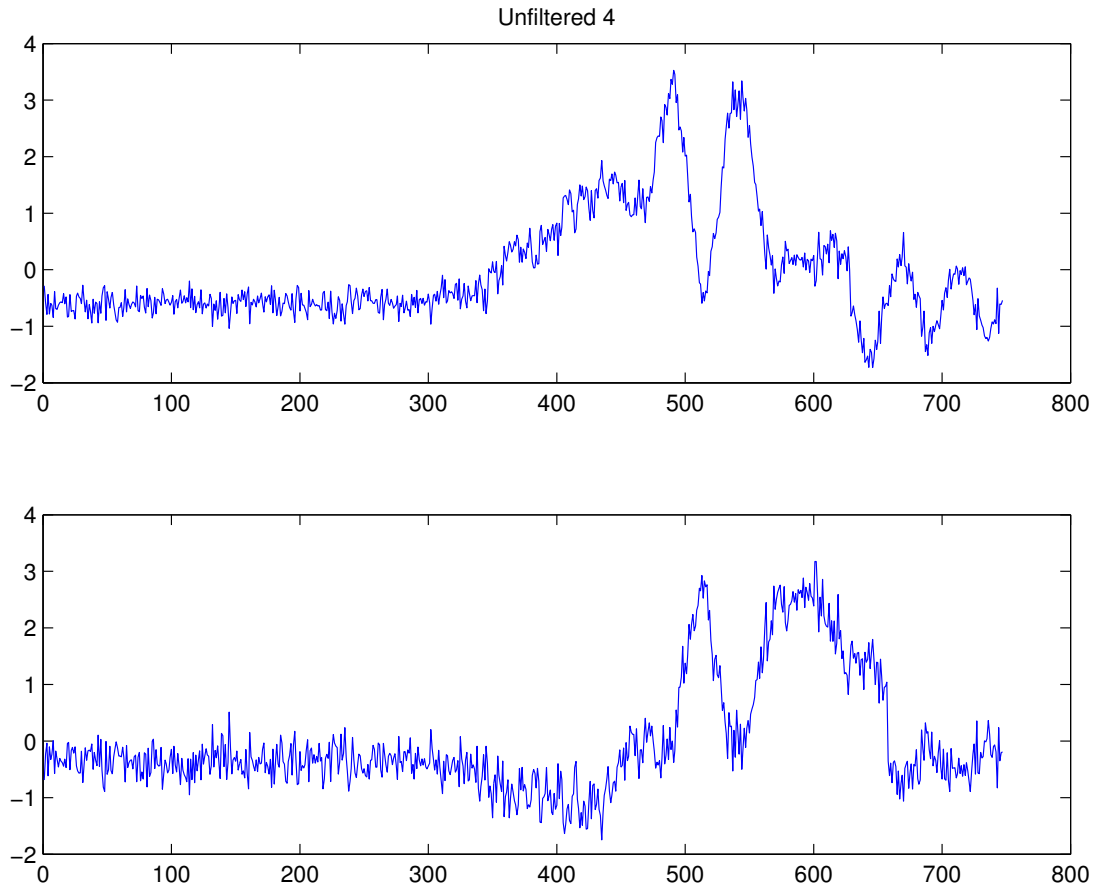

Figure C.10: Recovered Signals from Trial 4, Unfiltered Data

C.4 Trial 4

Estimated mixing matrix:

$$\hat{\mathbf{A}} = \begin{bmatrix} 5.591 & 8.679 & 6.678 & 2.096 & 0.6931 & 0.1642 & -0.02287 & -0.1635 \\ 11.40 & 9.791 & 8.658 & 4.529 & 2.286 & 0.7729 & -0.1182 & -1.082 \end{bmatrix} \tag{C.7}$$

Estimated separation matrix:

$$\mathbf{W} = \begin{bmatrix} 0.0504 & 0.6241 & -0.7293 & 0.2322 & -0.2459 & -0.2992 & -0.05462 & 0.5871 \\ 0.9613 & -0.5056 & 0.3284 & -1.170 & -0.9916 & 0.08702 & 0.2409 & 0.2984 \end{bmatrix} \tag{C.8}$$

RMSE (unadjusted) = 28.62

RMSE (scaled) = 28.97

Scale factor = 0.8954

Figure C.10 and Figure C.11 show the extracted components. Figure C.12 shows the recovered signal mixture against, both with and without scaling.

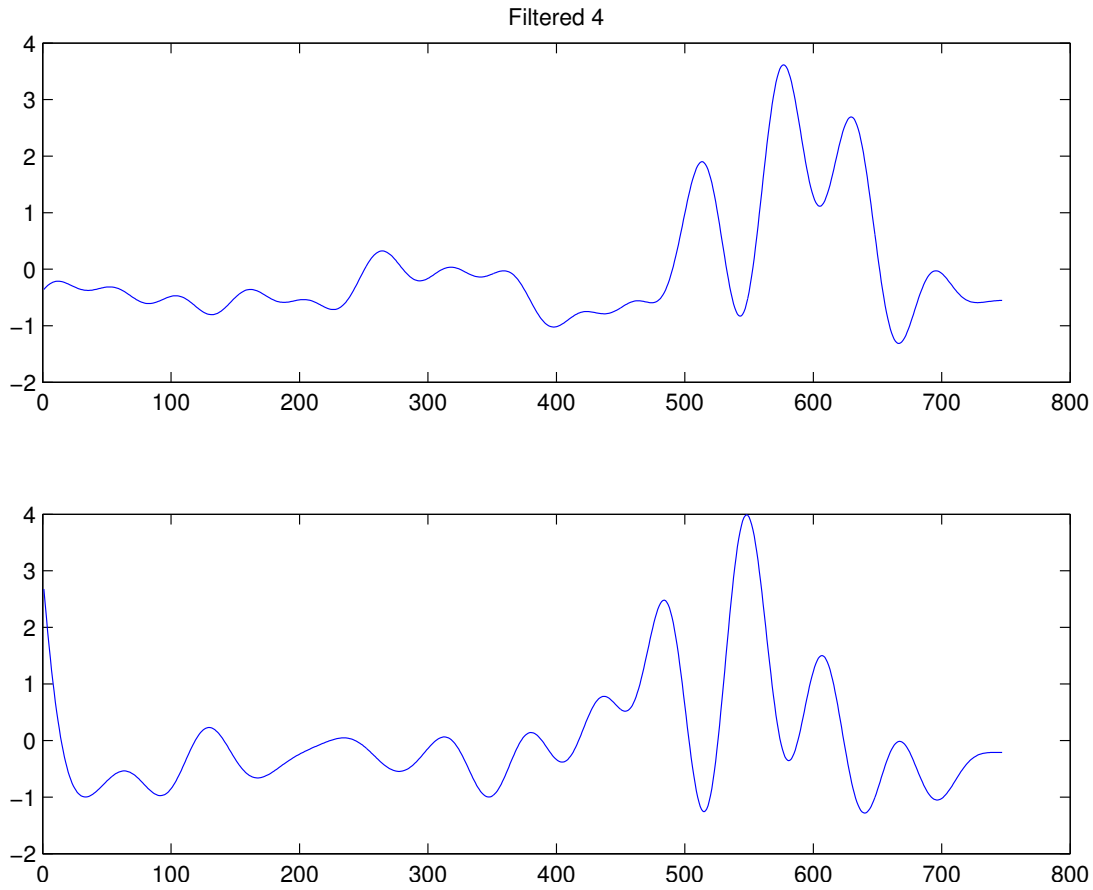

Figure C.11: Recovered Signals from Trial 4, Filtered Data

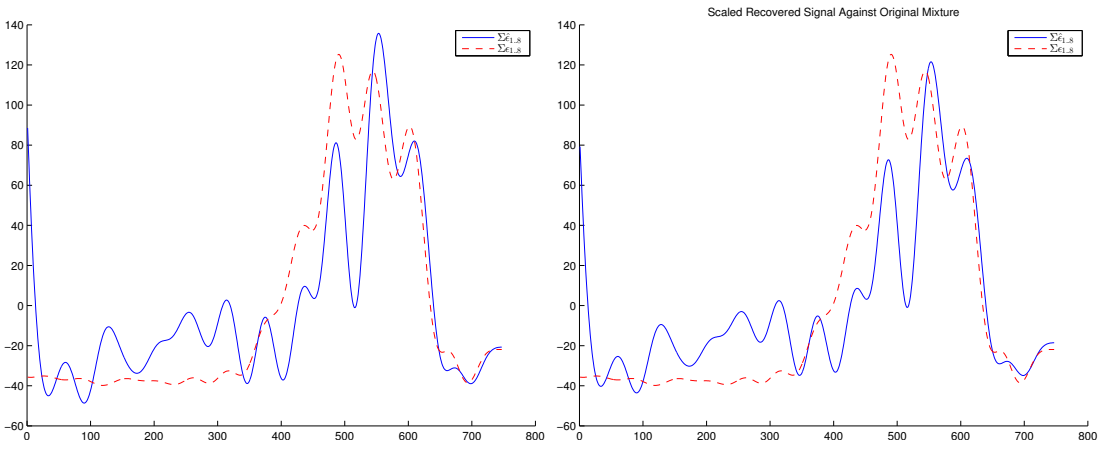

(a) Filtered, Unscaled (b) Filtered, Scaled

Figure C.12: Original/Estimated Mixture Comparisons —Actual Signals 2 Components, Trial 4

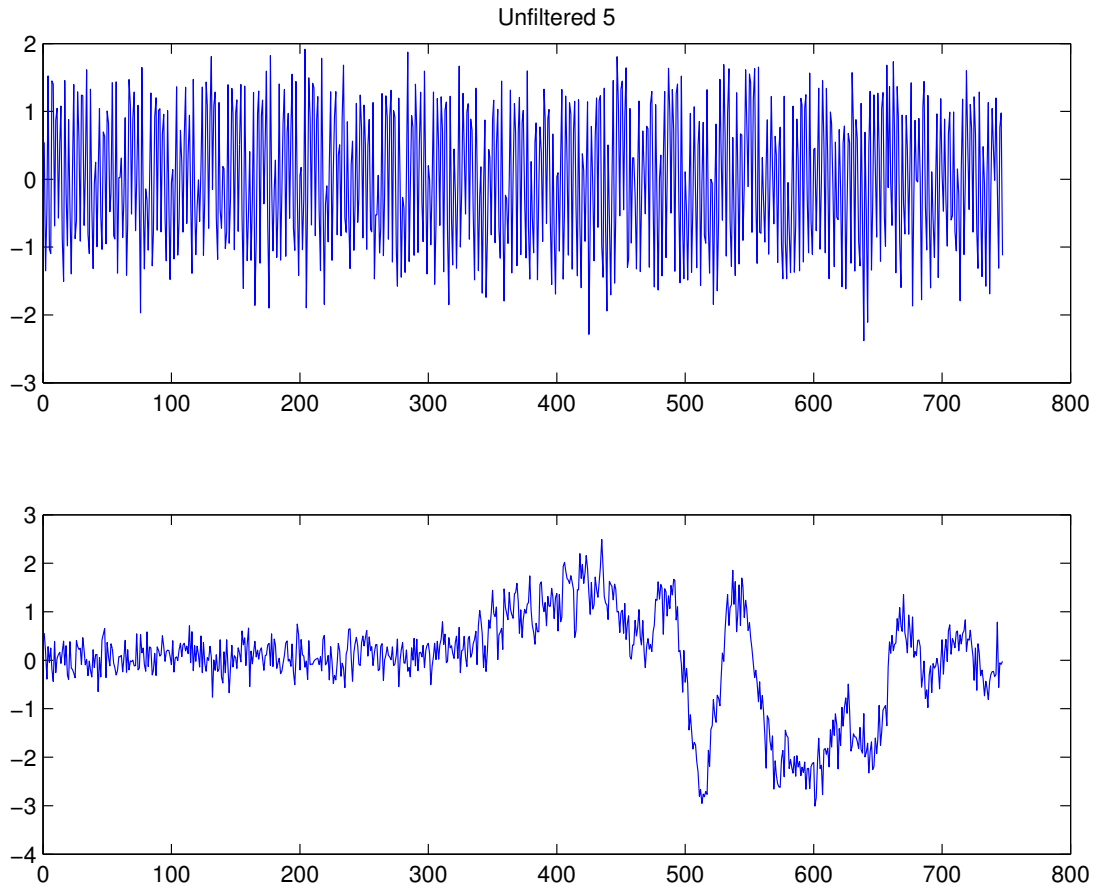

Figure C.13: Recovered Signals from Trial 5, Unfiltered Data

C.5 Trial 5

Estimated mixing matrix:

$$\hat{\mathbf{A}} = \begin{bmatrix} -0.9440 & -1.664 & -1.509 & -0.3203 & -0.01884 & -0.1371 & -0.006544 & 0.03456 \\ 2.468 & 3.027 & 2.470 & 1.212 & 0.4985 & 0.2118 & -0.001279 & -0.3362 \end{bmatrix} \tag{C.9}$$

Estimated separation matrix:

$$\mathbf{W} = \begin{bmatrix} -0.09554 & 1.288 & -1.772 & -0.08697 & 2.634 & -3.101 & 0.9381 & -0.4862 \\ -1.463 & 0.2134 & 0.06022 & 2.915 & -0.3795 & -0.3967 & 0.8479 & -1.655 \end{bmatrix} \tag{C.10}$$

RMSE (unadjusted) = 50.81

RMSE (scaled) = 51.45

Scale factor = 1.762

Figure C.13 and Figure C.14 show the extracted components. Figure C.15 shows the recovered signal mixture against, both with and without scaling.

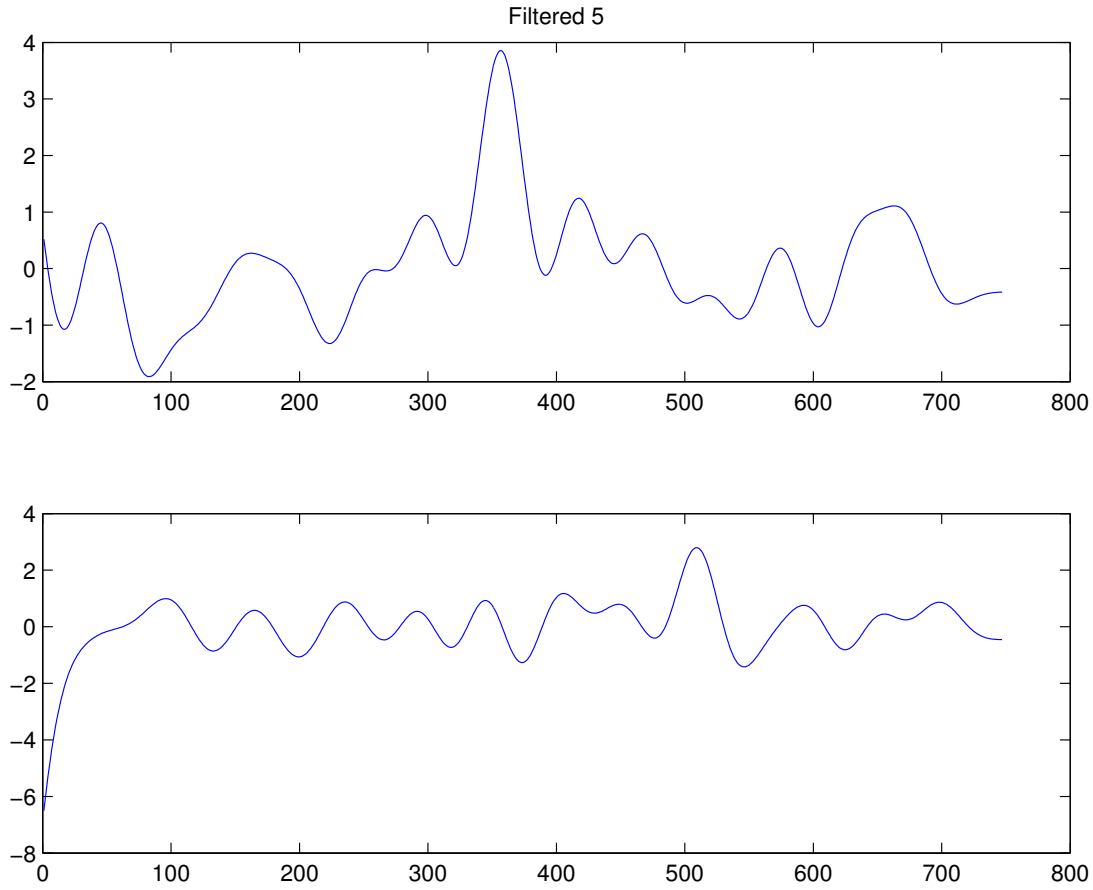

Figure C.14: Recovered Signals from Trial 5, Filtered Data

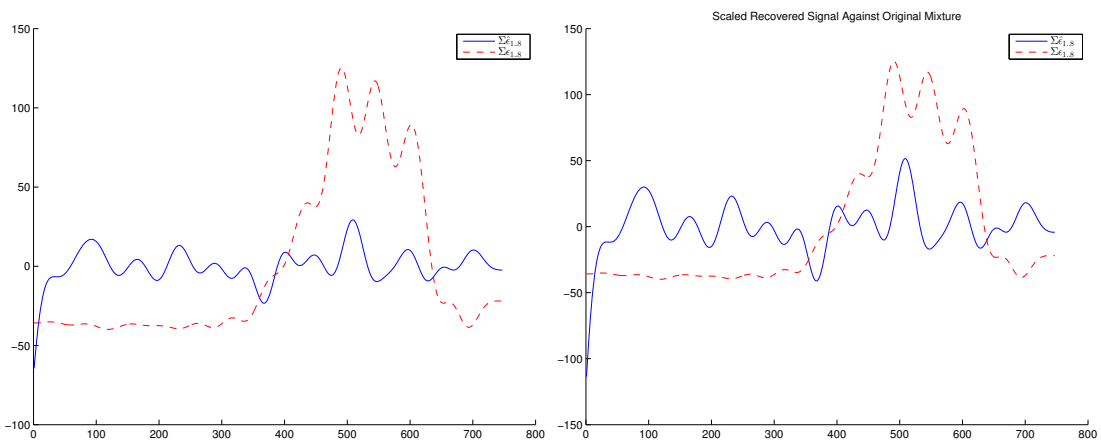

(a) Filtered, Unscaled (b) Filtered, Scaled

Figure C.15: Original/Estimated Mixture Comparisons —Actual Signals 2 Components, Trial 5

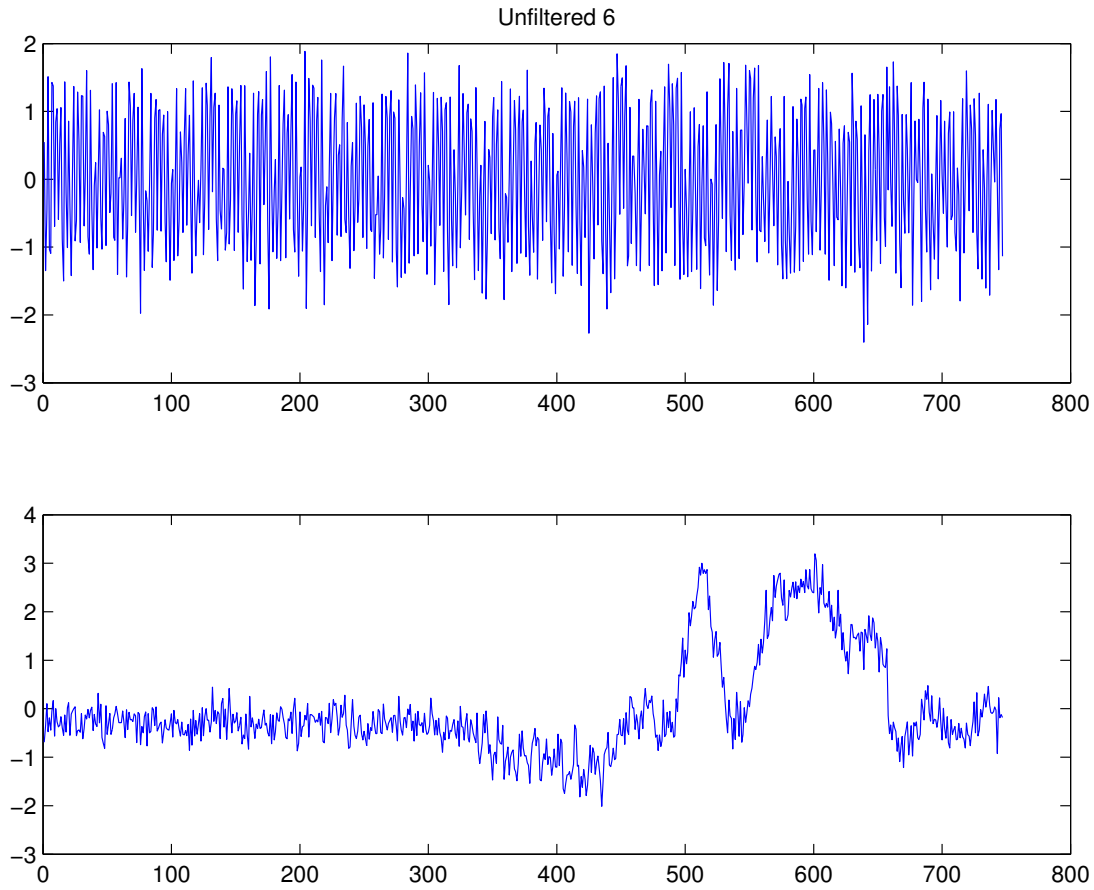

Figure C.16: Recovered Signals from Trial 6, Unfiltered Data

C.6 Trial 6

Estimated mixing matrix:

$$\hat{\mathbf{A}} = \begin{bmatrix} -2.725 & -2.683 & -2.242 & -1.023 & -0.3380 & 0.1409 & 0.6035 & 0.5107 \\ -3.716 & -5.479 & -4.195 & -1.443 & -0.4398 & -0.1298 & -0.05667 & -0.08097 \end{bmatrix} \tag{C.11}$$

Estimated unmixing matrix:

$$\mathbf{W} = \begin{bmatrix} 0.009363 & -0.1662 & 0.2351 & -0.03688 & -0.4116 & 0.3992 & 1.704 & -0.3031 \\ -0.4597 & -0.1360 & 0.4965 & -0.9794 & 1.993 & 0.3421 & -0.07160 & -1.641 \end{bmatrix} \tag{C.12}$$

RMSE (unadjusted) = 48.92

RMSE (scaled) = 49.83

Scale factor = 1.541

Figure C.16 and Figure C.17 show the extracted components. Figure C.18 shows the recovered signal mixture against, both with and without scaling.

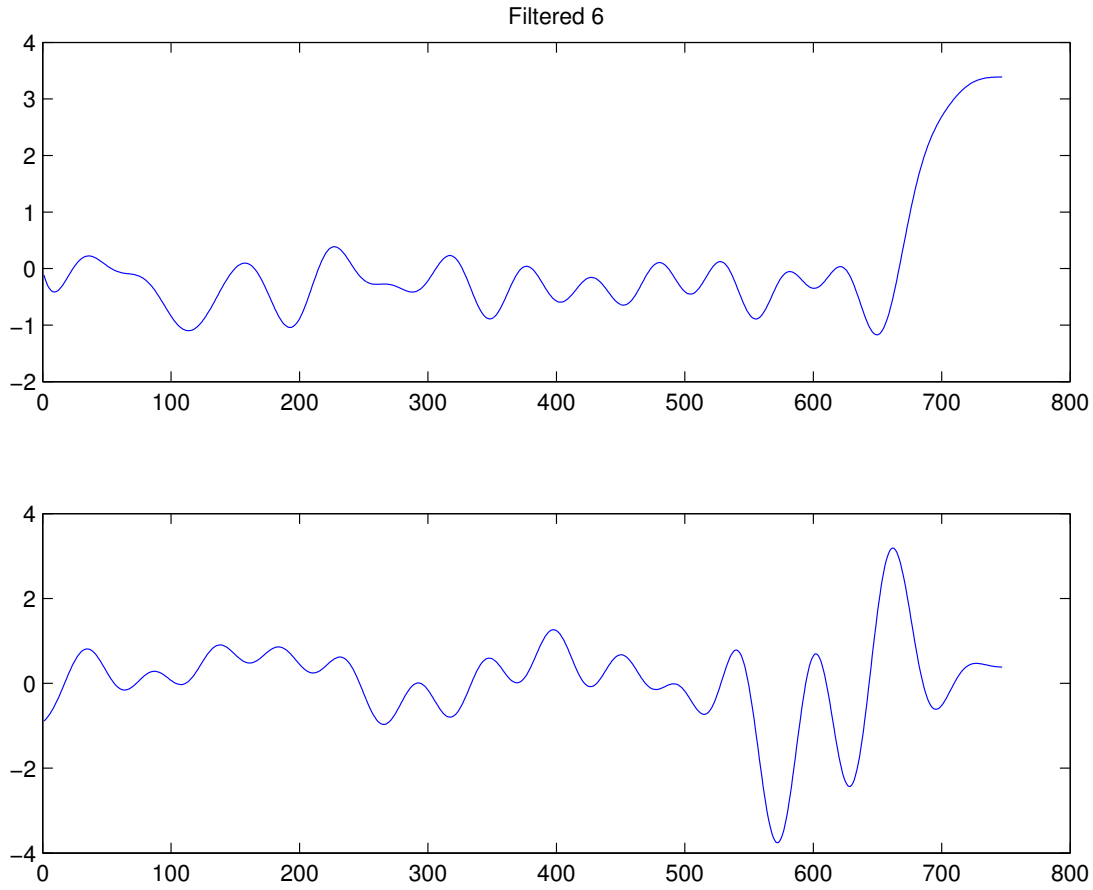

Figure C.17: Recovered Signals from Trial 6, Filtered Data

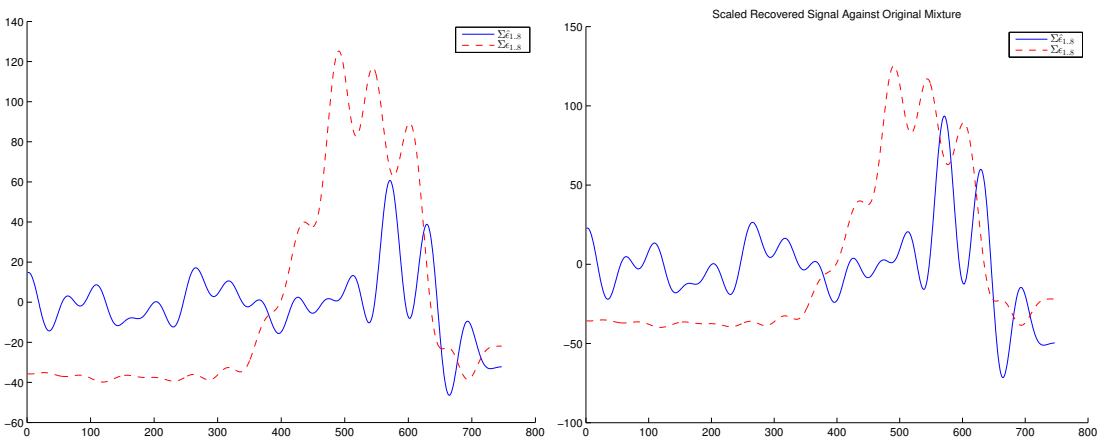

(a) Filtered, Unscaled (b) Filtered, Scaled

Figure C.18: Original/Estimated Mixture Comparisons —Actual Signals 2 Components, Trial 6

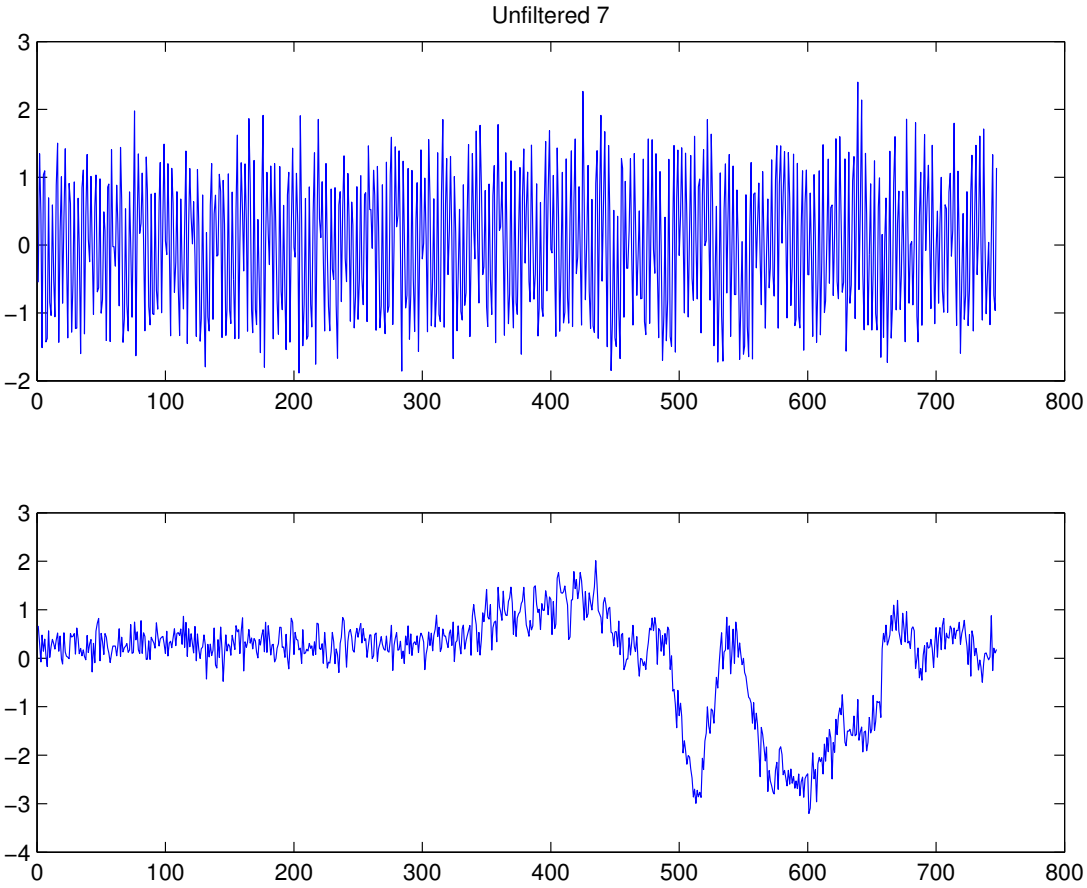

Figure C.19: Recovered Signals from Trial 7, Unfiltered Data

C.7 Trial 7

Estimated mixing matrix:

$$\hat{\mathbf{A}} = \begin{bmatrix} 3.695 & 5.437 & 4.160 & 1.433 & 0.4387 & 0.1316 & 0.05400 & 0.08470 \\ -2.720 & -2.688 & -2.245 & -1.016 & -0.3352 & 0.1416 & 0.6041 & 0.5112 \end{bmatrix} \quad \text{(C.13)}$$

Estimated separation matrix:

$$\mathbf{W} = \begin{bmatrix} 0.4918 & 0.1655 & -0.5395 & 0.8932 & -1.972 & -0.2179 & -0.01876 & 1.681 \\ -0.007942 & -0.1695 & 0.2363 & 0.03167 & -0.4374 & 0.3538 & 1.728 & -0.3035 \end{bmatrix} \quad \text{(C.14)}$$

RMSE (unadjusted) = 48.96

RMSE (scaled) = 49.93

Scale factor = 1.562

Figure C.19 and Figure C.20 show the extracted components. Figure C.21 shows the recovered signal mixture against, both with and without scaling.

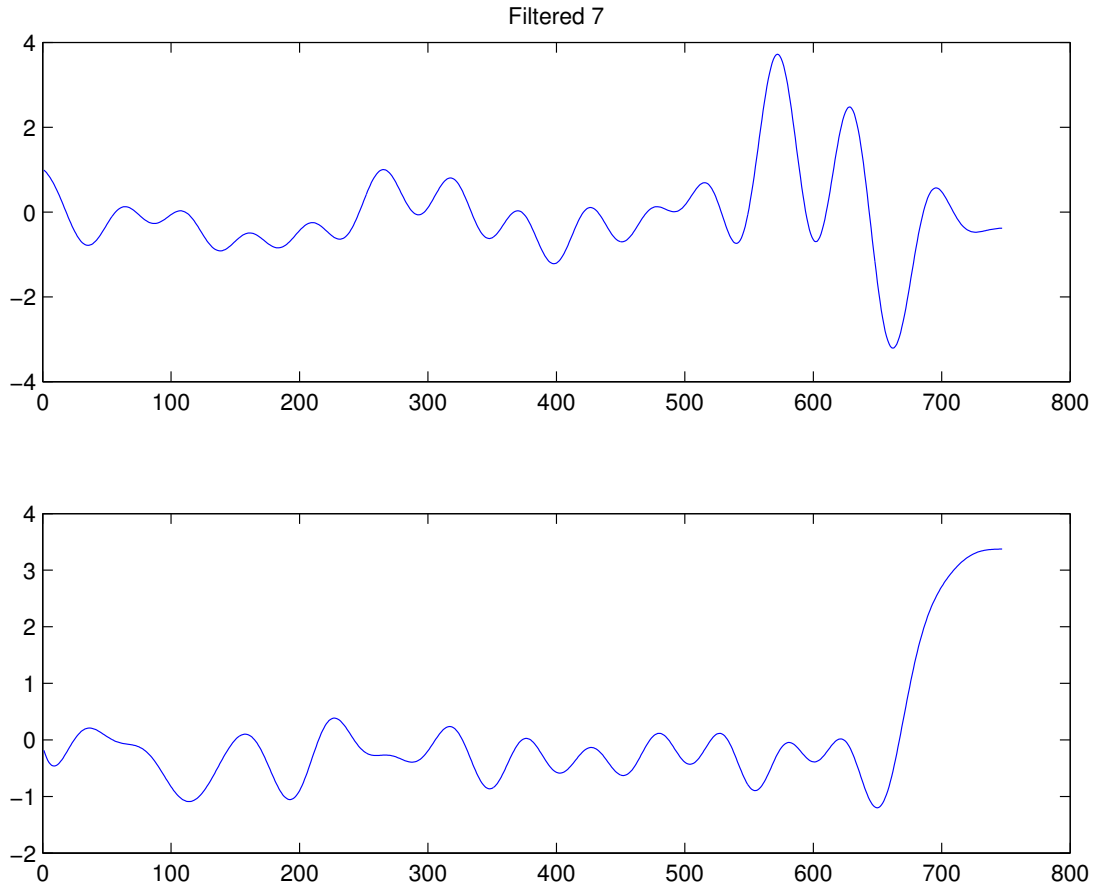

Figure C.20: Recovered Signals from Trial 7, Filtered Data

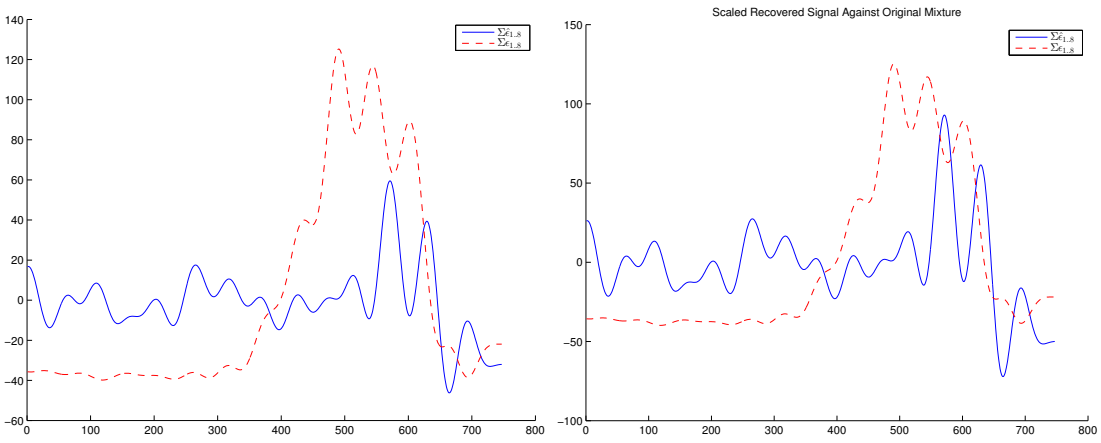

(a) Filtered, Unscaled (b) Filtered, Scaled

Figure C.21: Original/Estimated Mixture Comparisons —Actual Signals 2 Components, Trial 7

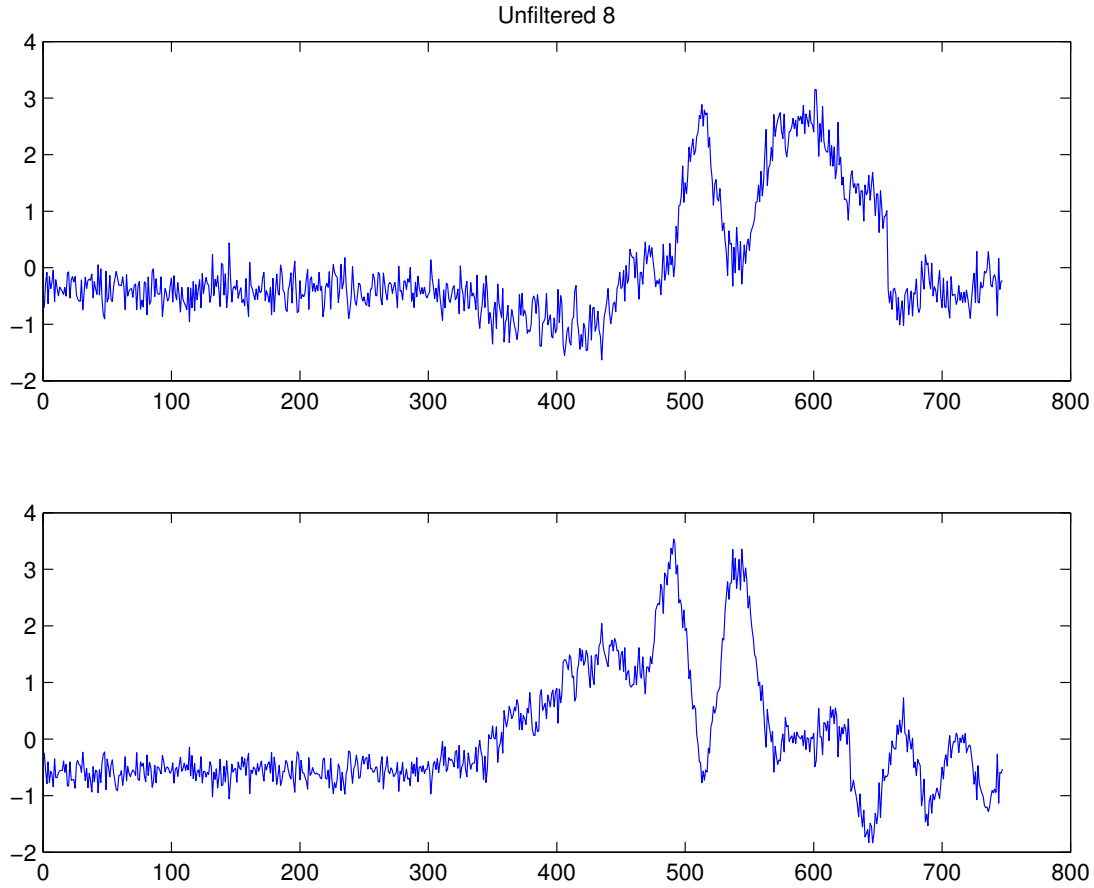

Figure C.22: Recovered Signals from Trial 8, Unfiltered Data

C.8 Trial 8

Estimated mixing matrix:

$$\hat{\mathbf{A}} = \begin{bmatrix} 0.9067 & 2.041 & 1.556 & 0.1363 & 0.002987 & -0.1100 & -0.1616 & -0.3813 \\ 11.47 & 9.871 & 8.722 & 4.561 & 2.298 & 0.7770 & -0.1161 & -1.076 \end{bmatrix} \quad \text{(C.15)}$$

Estimated separation matrix:

$$\mathbf{W} = \begin{bmatrix} -0.2055 & 0.4636 & -0.1706 & -1.666 & 2.231 & -0.4033 & 0.3768 & -1.947 \\ 0.9616 & -0.5145 & 0.3299 & -1.107 & -1.046 & 0.0506 & 0.2430 & 0.3570 \end{bmatrix} \quad \text{(C.16)}$$

RMSE (unadjusted) = 36.68

RMSE (scaled) = 37.03

Scale factor = 0.8622

The extracted signals are shown in Figure C.22 and Figure C.23. Figure C.24 shows the recovered signal mixture against, both with and without scaling.

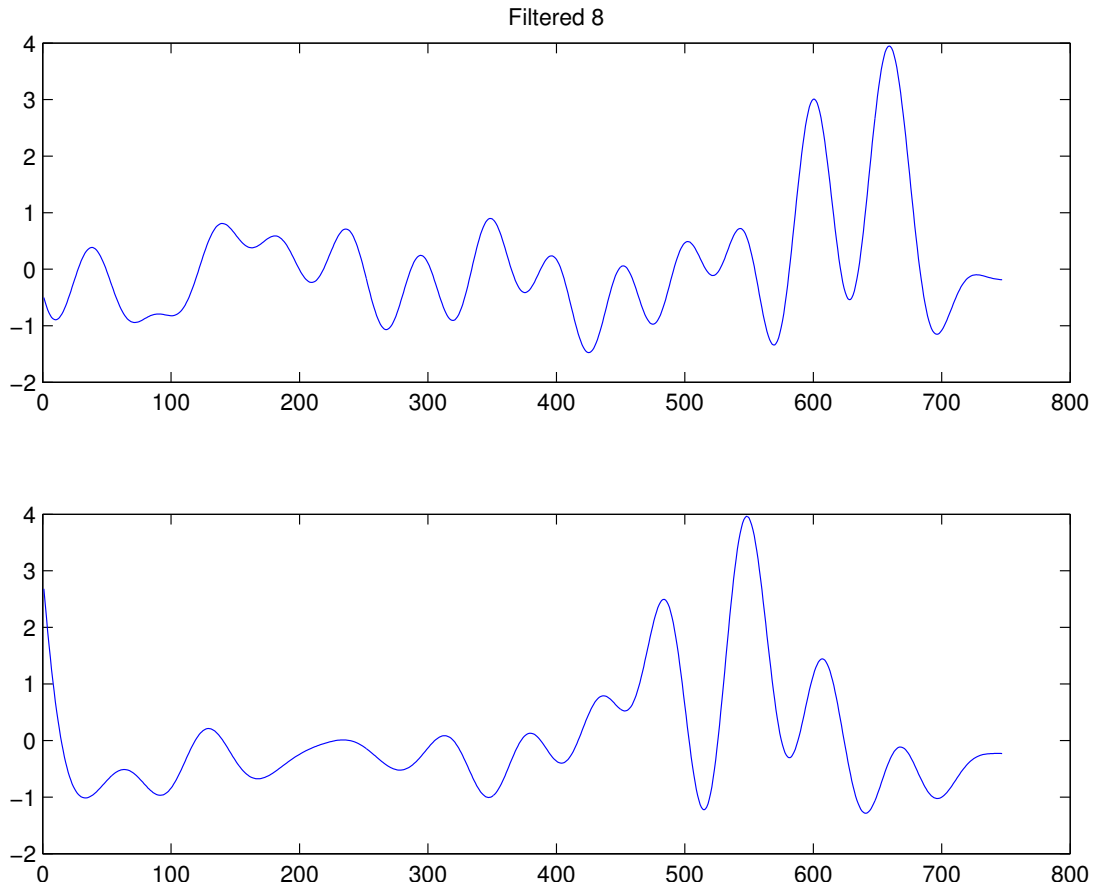

Figure C.23: Recovered Signals from Trial 8, Filtered Data

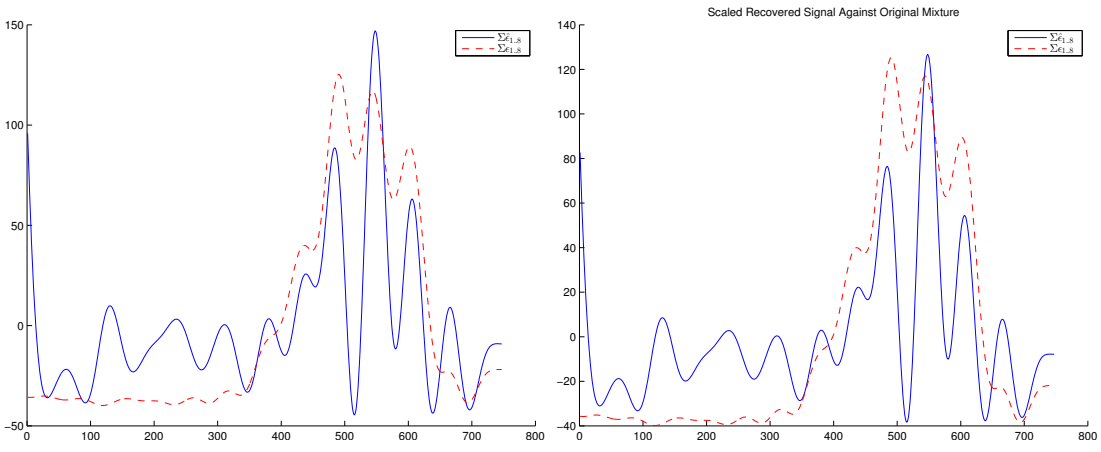

(a) Filtered, Unscaled (b) Filtered, Scaled

Figure C.24: Original/Estimated Mixture Comparisons —Actual Signals 2 Components, Trial 8

Appendix D

Independent Component Analysis Results - Actual Data, 3 Component Separation

D.1 Trial 1

Estimated mixing mtarix:

$$\hat{\mathbf{A}} = \begin{bmatrix} -2.815 & -2.813 & -2.336 & -1.073 & -0.3485 & 0.1380 & 0.5980 & 0.502 \\ 2.483 & 3.050 & 2.490 & 1.218 & 0.5002 & 0.2131 & -0.001921 & -0.3370 \\ 2.368 & 2.391 & 1.948 & 1.112 & 0.4397 & 0.2226 & 0.08989 & 0.1377 \end{bmatrix} \tag{D.1}$$

Estimated separation matrix:

$$\mathbf{W} = \begin{bmatrix} 0.04949 & -0.1612 & 0.2497 & -0.2988 & -0.2366 & 0.5420 & 1.614 & -0.3463 \\ -1.463 & 0.2040 & 0.07374 & 2.915 & -0.3961 & -0.3725 & 0.8363 & -1.650 \\ 0.2001 & -0.2361 & -0.1017 & 1.937 & -2.714 & 0.4650 & -0.3344 & 1.852 \end{bmatrix} \tag{D.2}$$

RMSE (unadjusted) = 34.34

RMSE (scaled) = 34.89

Scale factor = 0.8412

Figure D.1 and Figure D.2 show the extracted components. Figure D.3 shows the recovered signal mixture against, both with and without scaling.

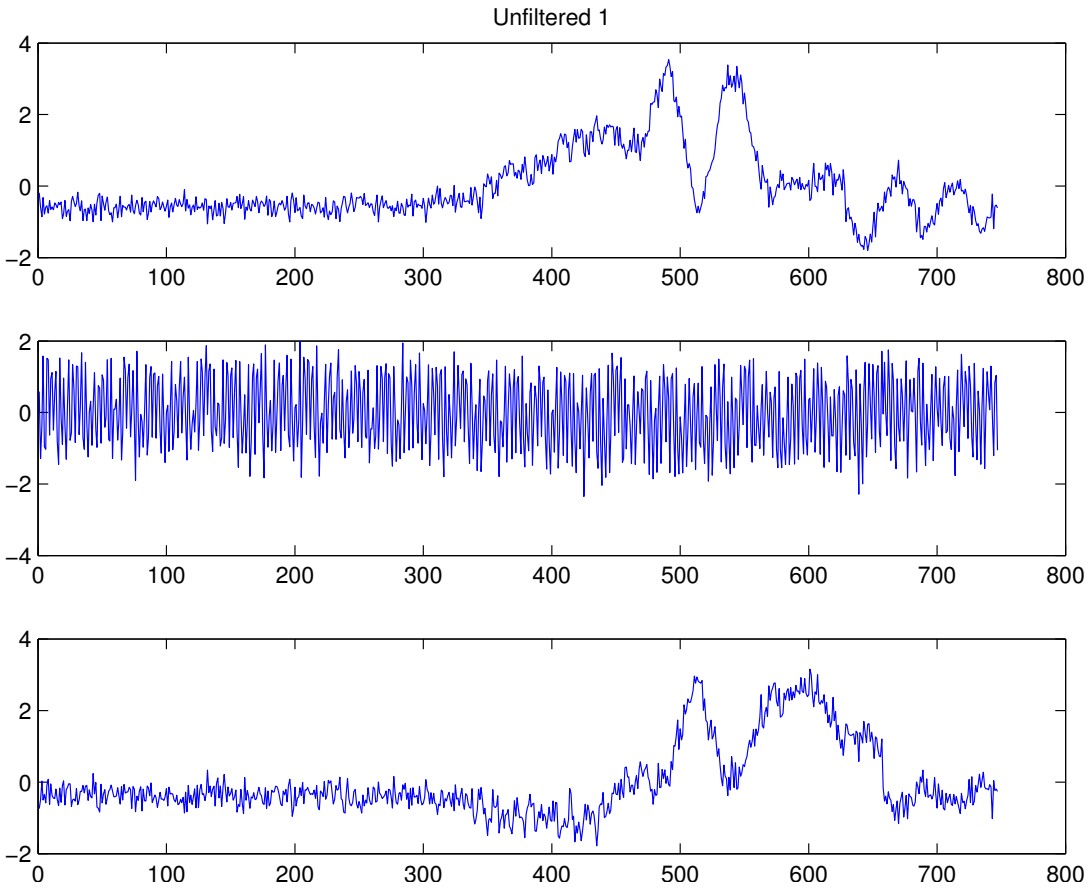

Figure D.1: Recovered Signals from Trial 1, Unfiltered Data

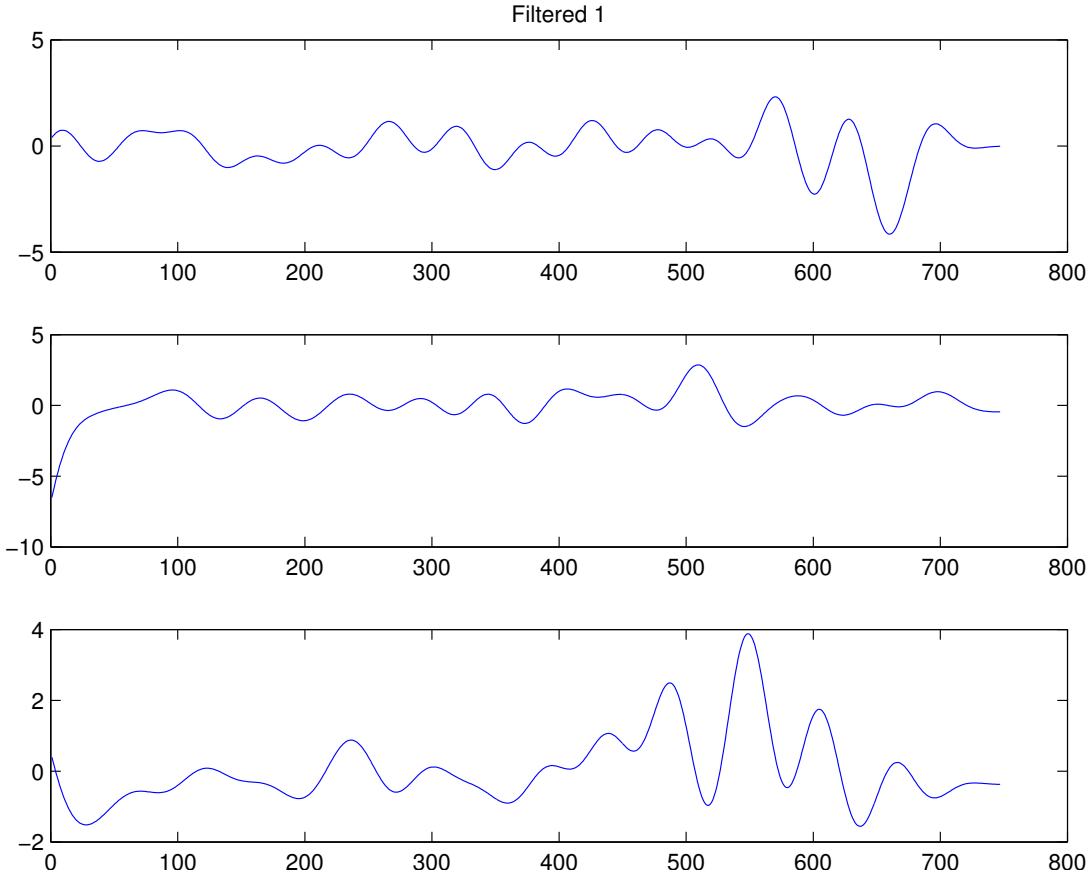

Figure D.2: Recovered Signals from Trial 1, Filtered Data

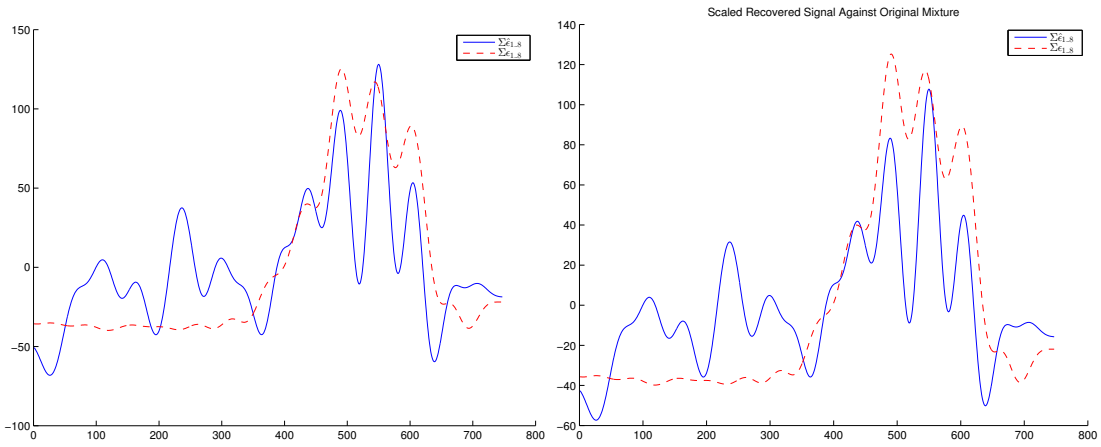

(a) Filtered, Unscaled (b) Filtered, Scaled

Figure D.3: Original/Estimated Mixture Comparisons —Actual Signals 3 Components, Trial 1

D.2 Trial 2

Estimated mixing matrix:

$$\hat{\mathbf{A}} = \begin{bmatrix} -3.283 & -4.574 & -3.689 & -1.524 & -0.6383 & -0.2539 & -0.01778 & 0.2534 \\ 3.787 & 5.523 & 4.235 & 1.466 & 0.4500 & 0.1262 & 0.04297 & 0.06775 \\ 2.671 & 2.639 & 2.205 & 1.007 & 0.3327 & -0.1420 & -0.6039 & -0.5136 \end{bmatrix} \tag{D.3}$$

Estimated separation matrix:

$$\mathbf{W} = \begin{bmatrix} 1.570 & -0.1070 & -0.3483 & -2.633 & -0.2843 & 0.3890 & -0.3707 & 1.102 \\ 0.4884 & 0.1401 & -0.5109 & 0.9289 & -1.976 & -0.3672 & 0.04036 & 1.661 \\ -0.06453 & 0.1782 & -0.2283 & 0.07982 & 0.4858 & -0.4080 & -1.697 & 0.2323 \end{bmatrix} \tag{D.4}$$

RMSE (unadjusted) = 35.01

RMSE (scaled) = 35.10

Scale factor = 0.9349

Figure D.4 and Figure D.5 show the extracted components. Figure D.6 shows the recovered signal mixture against, both with and without scaling.

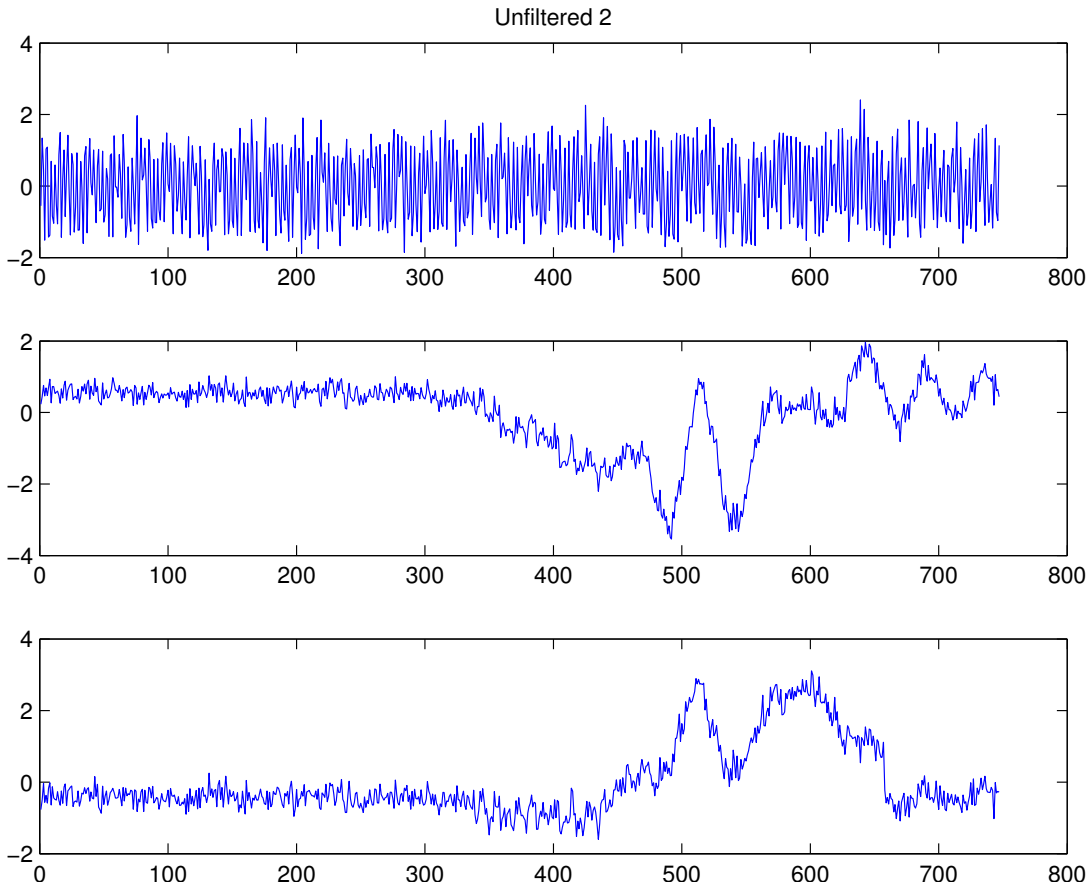

Figure D.4: Recovered Signals from Trial 2, Unfiltered Data

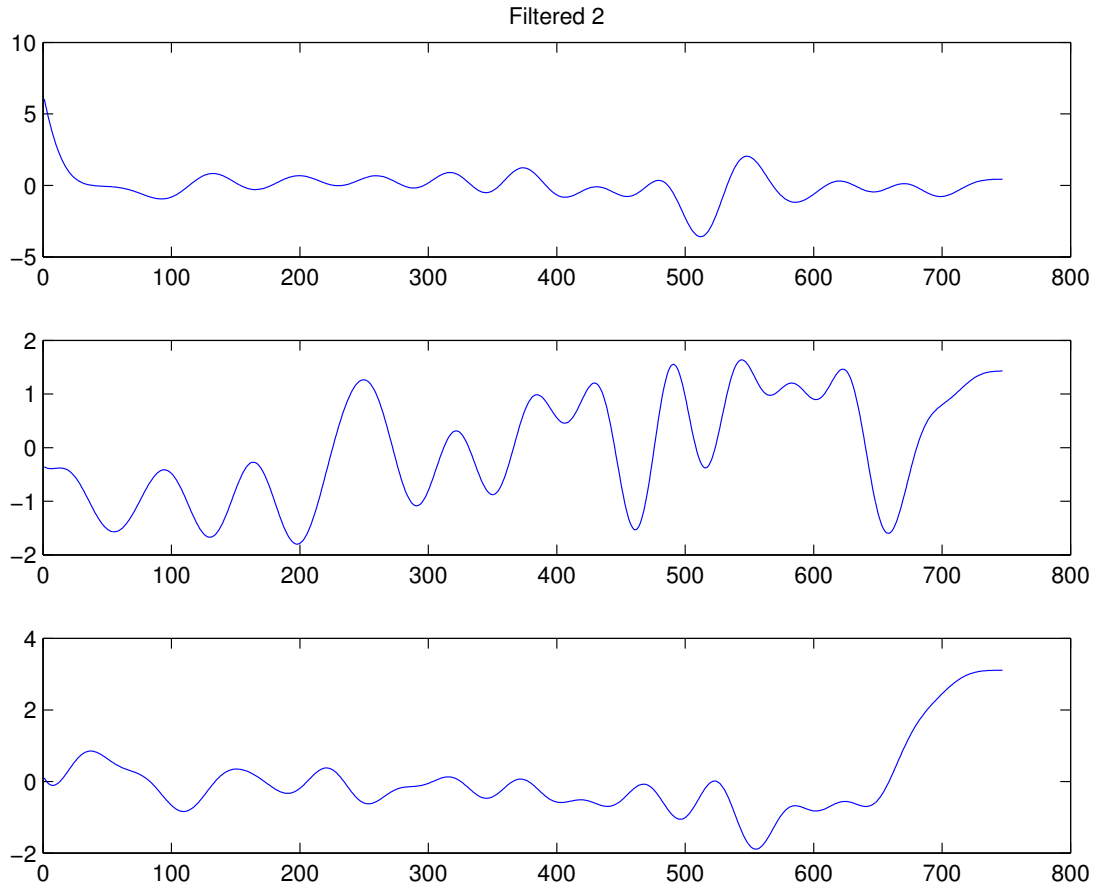

Figure D.5: Recovered Signals from Trial 2, Filtered Data

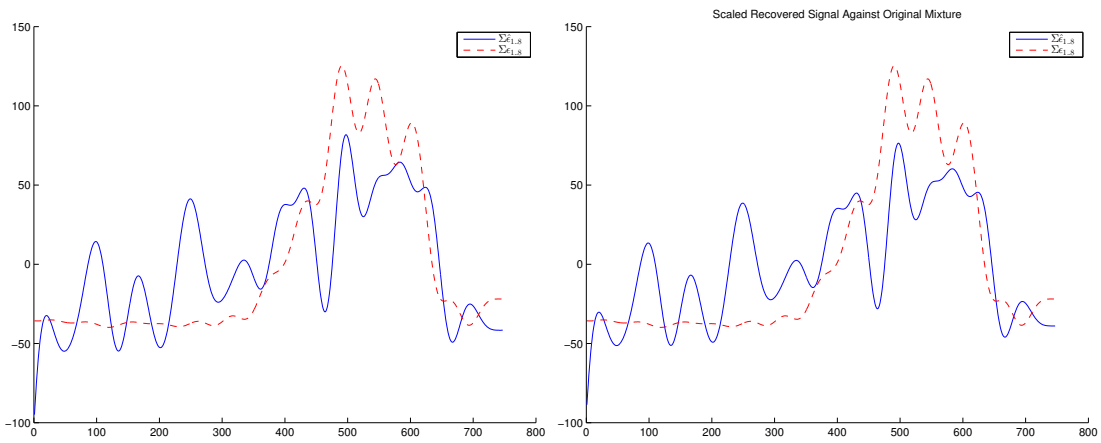

(a) Filtered, Unscaled (b) Filtered, Scaled

Figure D.6: Original/Estimated Mixture Comparisons —Actual Signals 3 Components, Trial 2

D.3 Trial 3

Estimated mixing matrix:

$$\hat{\mathbf{A}} = \begin{bmatrix} -1.832 & -3.322 & -2.590 & -0.9352 & -0.3568 & -0.1590 & -0.04026 & 0.0823 \\ -7.937 & -7.963 & -6.617 & -3.246 & -1.571 & -0.7342 & -0.2352 & 0.5195 \\ 1.024 & 4.139 & 2.899 & 0.1334 & -0.2818 & -0.2386 & -0.003697 & 0.2103 \end{bmatrix} \tag{D.5}$$

Estimated separation matrix:

$$\mathbf{W} = \begin{bmatrix} 1.596 & -0.1410 & -0.3403 & -2.507 & -0.5597 & 0.3378 & -0.1862 & 0.9182 \\ -0.5642 & -0.8542 & 1.354 & 0.2041 & 1.670 & -2.589 & -0.1351 & 0.06625 \\ 0.3305 & -0.1613 & 0.2055 & -0.1147 & -0.4247 & -1.932 & 0.7828 & 0.8155 \end{bmatrix} \tag{D.6}$$

RMSE (unadjusted) = 31.74

RMSE (scaled) = 32.43

Scale factor = 0.8382

Figure D.7 and Figure D.8 show the extracted components. Figure D.9 shows the recovered signal mixture against, both with and without scaling.

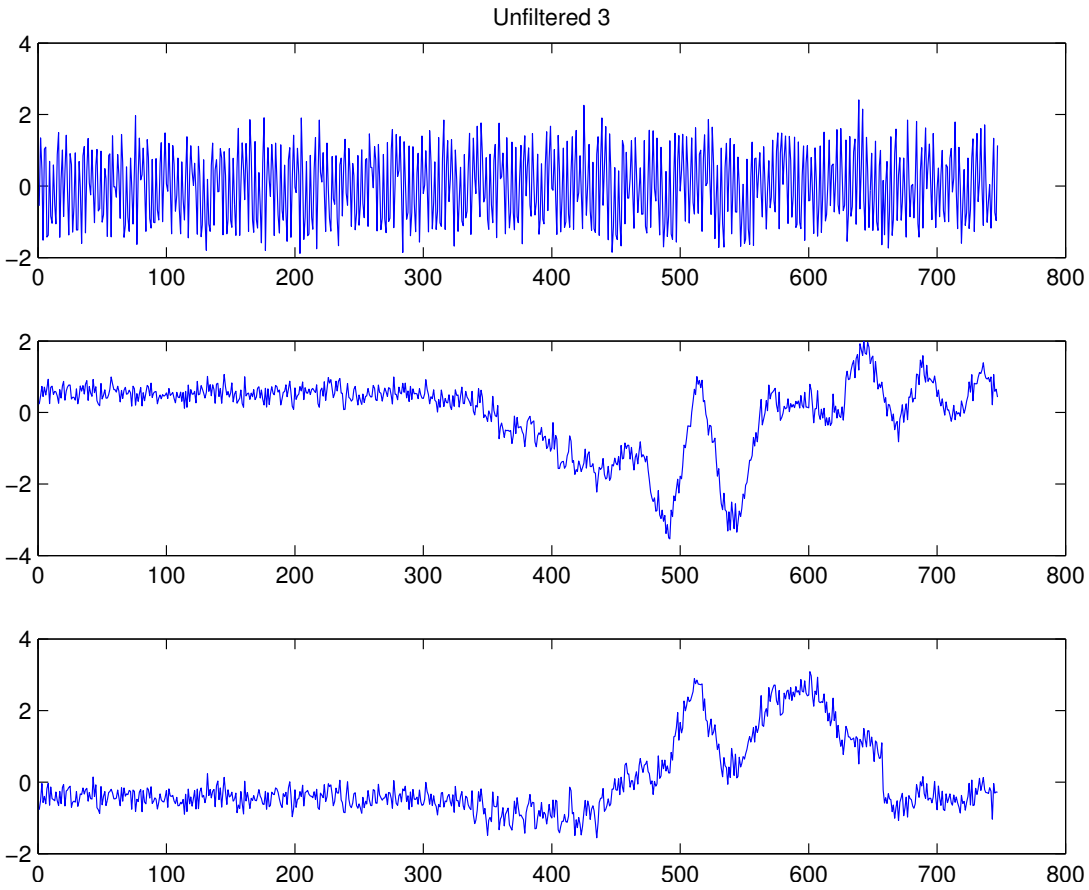

Figure D.7: Recovered Signals from Trial 3, Unfiltered Data

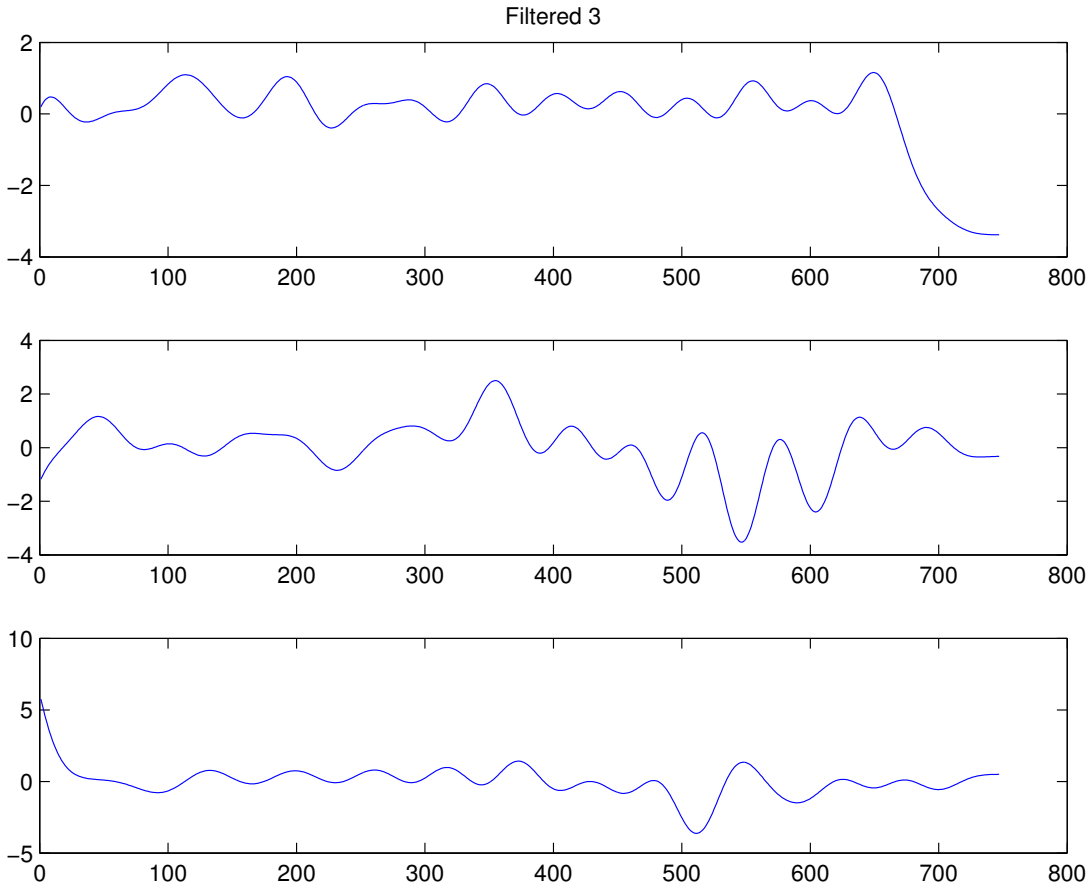

Figure D.8: Recovered Signals from Trial 3, Filtered Data

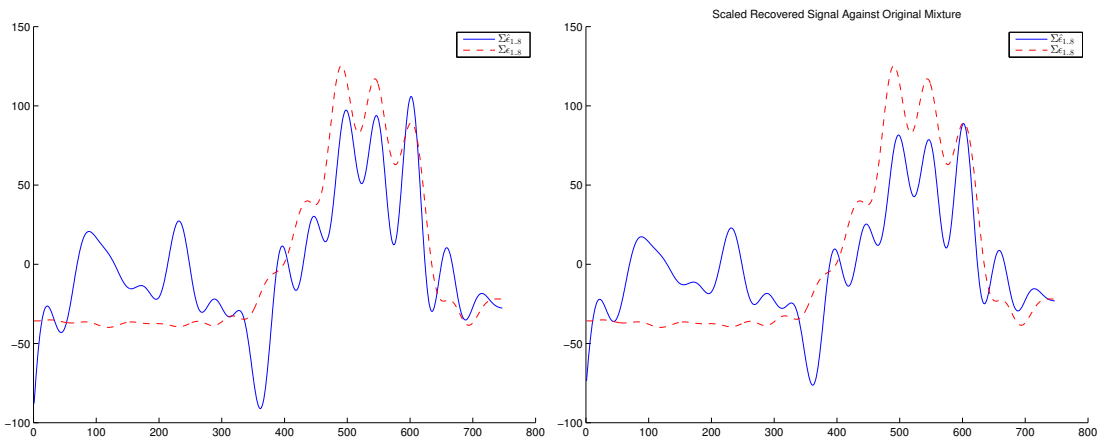

(a) Filtered, Unscaled (b) Filtered, Scaled

Figure D.9: Original/Estimated Mixture Comparisons —Actual Signals 3 Components, Trial 3

D.4 Trial 4

Estimated mixing matrix:

$$\hat{\mathbf{A}} = \begin{bmatrix} 11.45 & 9.917 & 8.750 & 4.546 & 2.286 & 0.7709 & -0.1191 & -1.082 \\ -1.286 & -1.526 & -1.189 & -0.4684 & -0.04537 & 0.2380 & 0.5842 & 0.3457 \\ 0.3647 & 1.505 & 1.106 & -0.07618 & -0.08137 & -0.1114 & -0.09506 & -0.3108 \end{bmatrix} \tag{D.7}$$

Estimated separation matrix:

$$\mathbf{W} = \begin{bmatrix} 0.9659 & -0.4971 & 0.3176 & -1.166 & -1.013 & 0.07921 & 0.2491 & 0.3034 \\ 0.1723 & -0.2698 & 0.3408 & -0.4001 & -0.4280 & 0.4190 & 1.777 & -0.3750 \\ -0.2121 & 0.4447 & -0.1371 & -1.692 & 2.222 & -0.3638 & 0.5715 & -2.013 \end{bmatrix} \tag{D.8}$$

RMSE (unadjusted) = 27.93

RMSE (scaled) = 28.28

Scale factor = 0.8981

Figure D.10 and Figure D.11 show the extracted components. Figure D.12 shows the recovered signal mixture against, both with and without scaling.

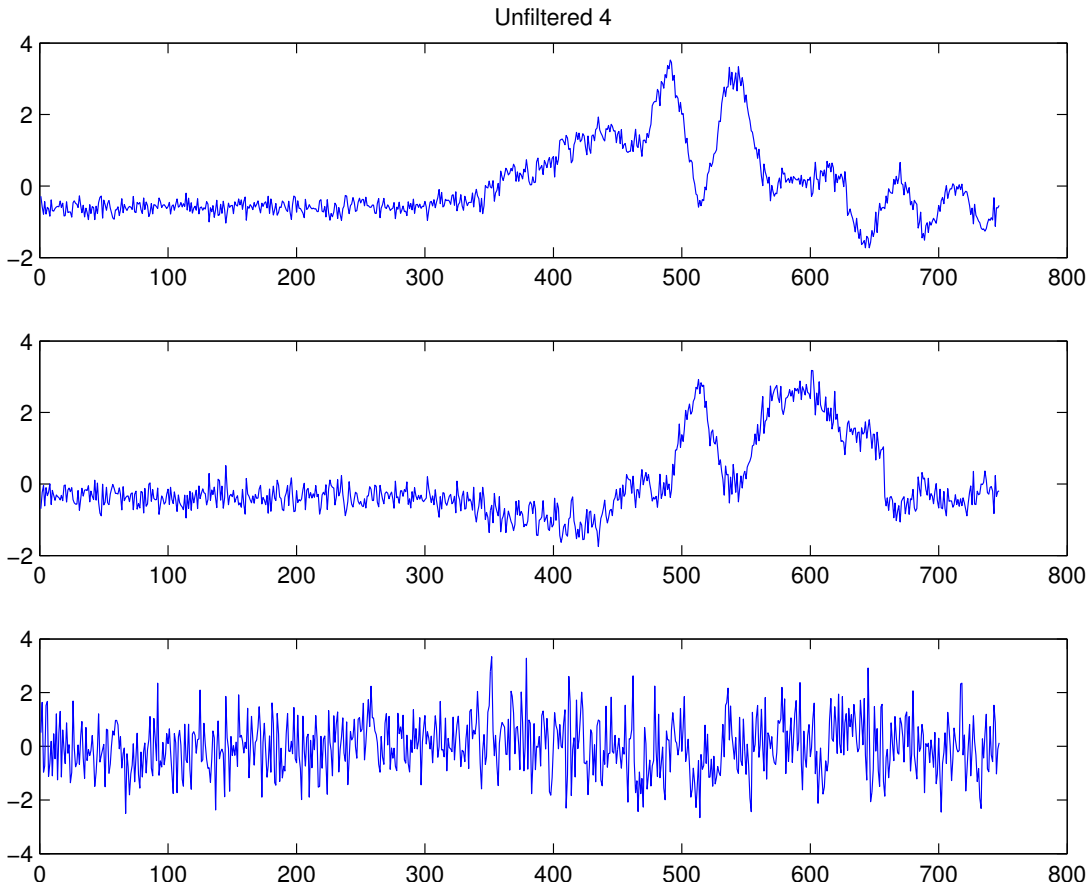

Figure D.10: Recovered Signals from Trial 4, Unfiltered Data

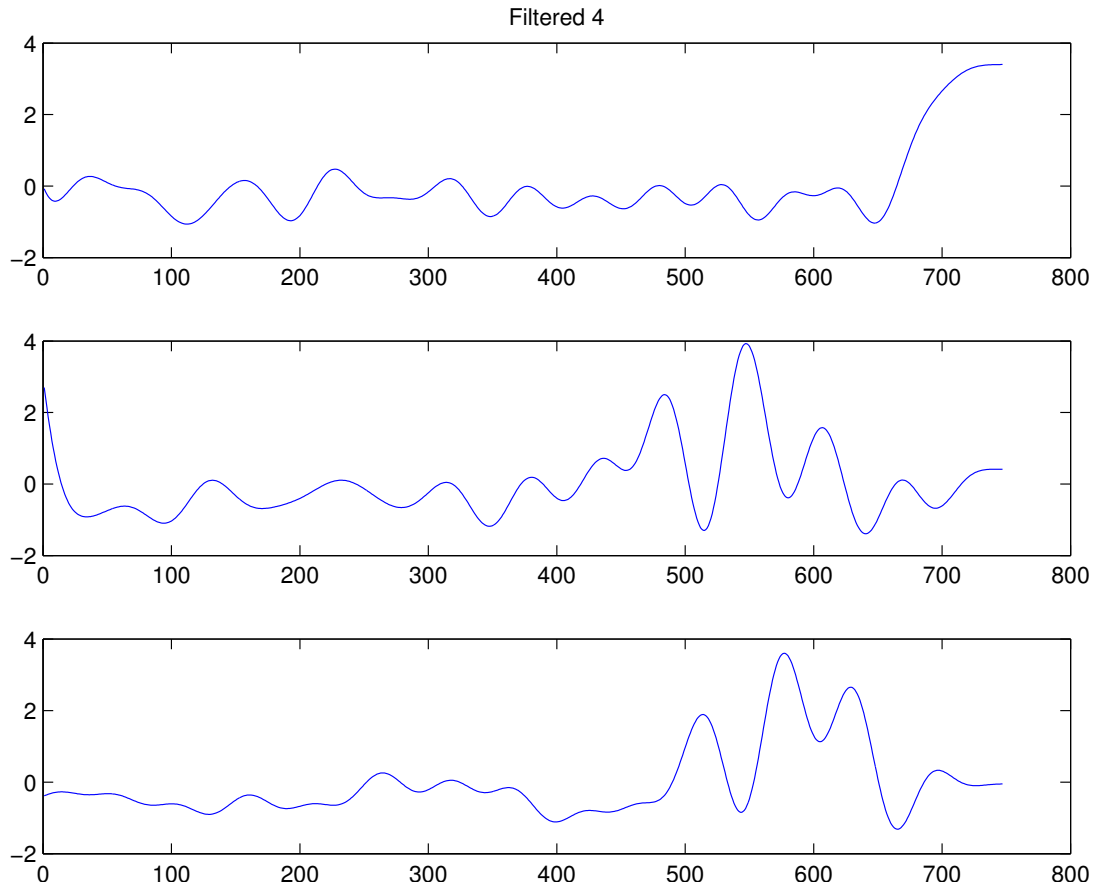

Figure D.11: Recovered Signals from Trial 4, Filtered Data

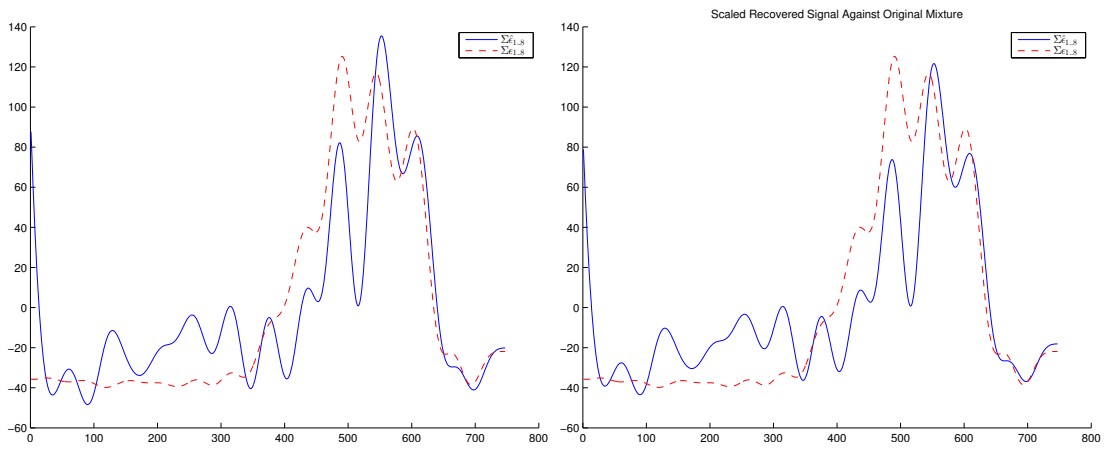

(a) Filtered, Unscaled (b) Filtered, Scaled

Figure D.12: Original/Estimated Mixture Comparisons —Actual Signals 3 Components, Trial 4

D.5 Trial 5

Estimated mixing matrix:

$$\hat{\mathbf{A}} = \begin{bmatrix} -2.587 & -3.203 & -2.609 & -1.258 & -0.5137 & -0.2165 & 0.0008638 & 0.3374 \\ 2.632 & 2.524 & 2.116 & 1.003 & 0.3299 & -0.1421 & -0.6017 & -0.5062 \\ 4.098 & 6.275 & 4.795 & 1.563 & 0.4619 & 0.1053 & 0.05389 & 0.02453 \end{bmatrix} \tag{D.9}$$

Estimated separation matrix:

$$\mathbf{W} = \begin{bmatrix} 1.459 & -0.2055 & -0.06875 & -2.936 & 0.4228 & 0.3960 & -0.8448 & 1.622 \\ -0.064236 & 0.1583 & -0.2315 & 0.2276 & 0.3401 & -0.4820 & -1.650 & 0.2810 \\ 0.3111 & 0.1555 & -0.4442 & 1.091 & -1.672 & -1.084 & 0.5569 & 1.250 \end{bmatrix} \tag{D.10}$$

RMSE (unadjusted) = 47.26

RMSE (scaled) = 47.63

Scale factor = 1.273

Figure D.13 and Figure D.14 show the extracted components. Figure D.15 shows the recovered signal mixture against, both with and without scaling.

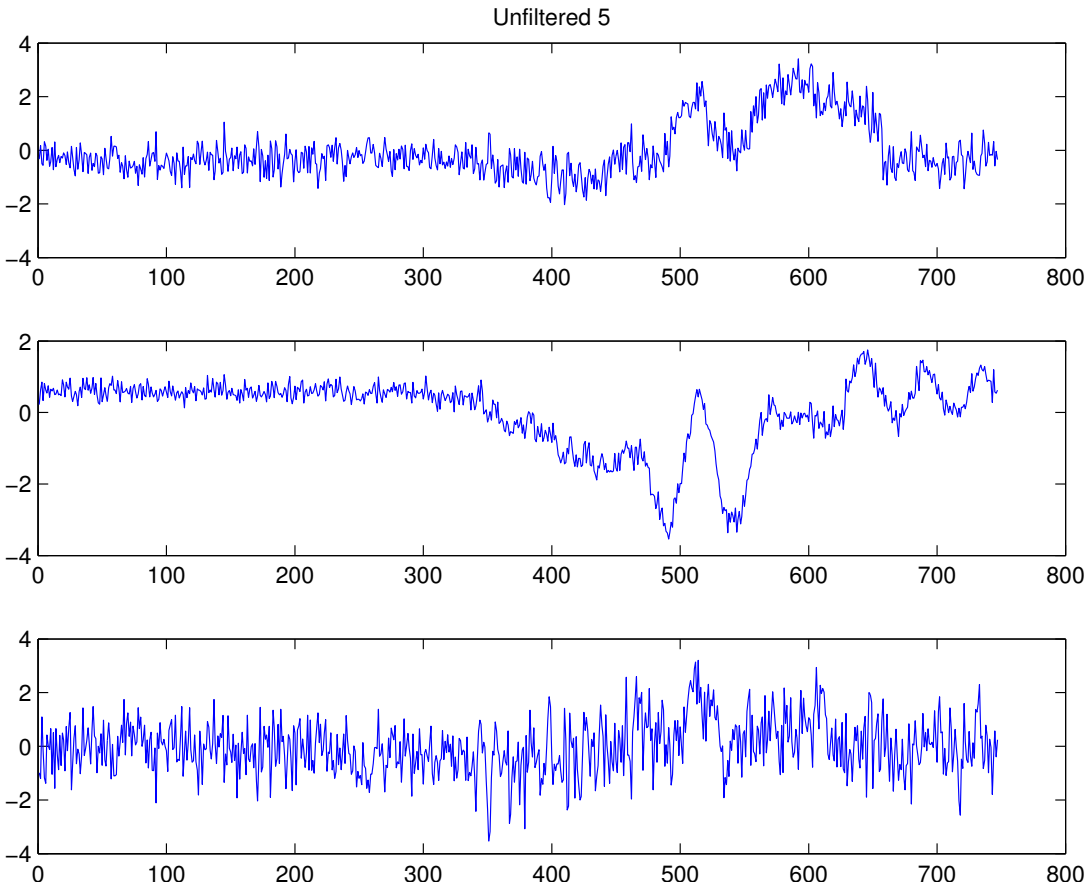

Figure D.13: Recovered Signals from Trial 5, Unfiltered Data

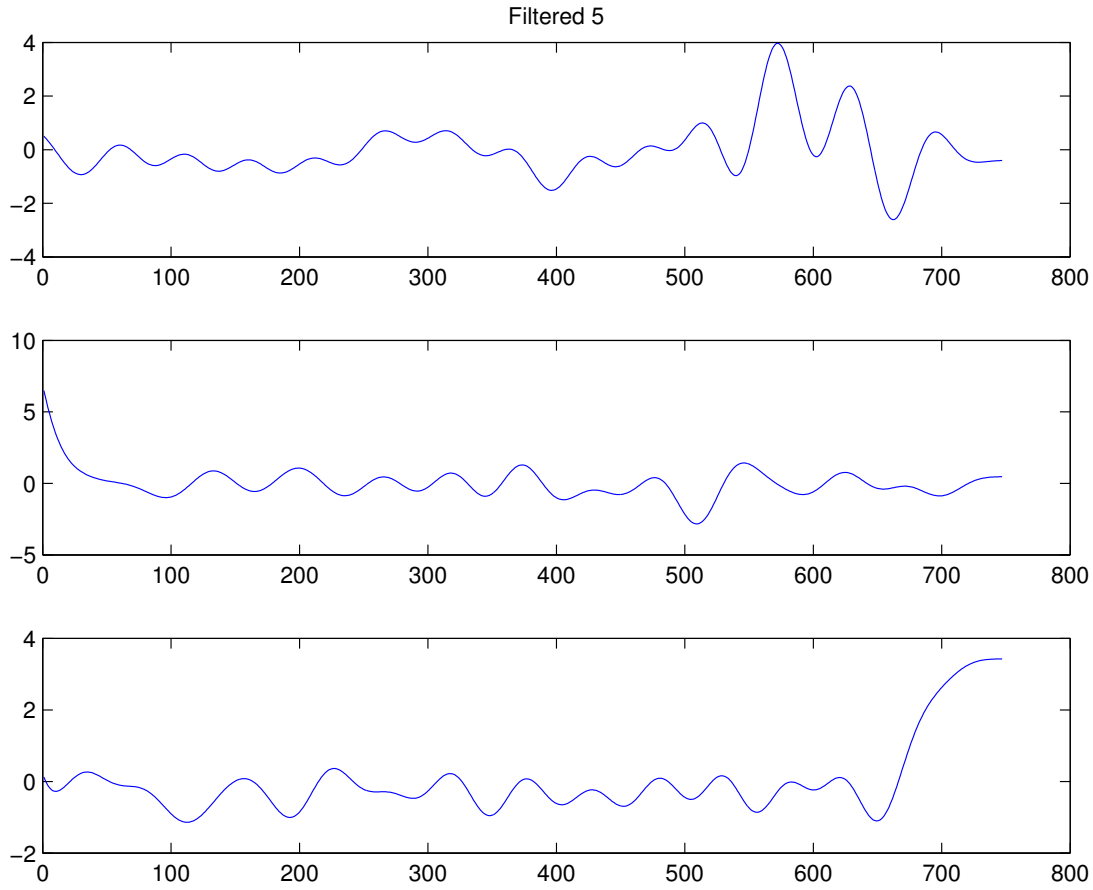

Figure D.14: Recovered Signals from Trial 5, Filtered Data

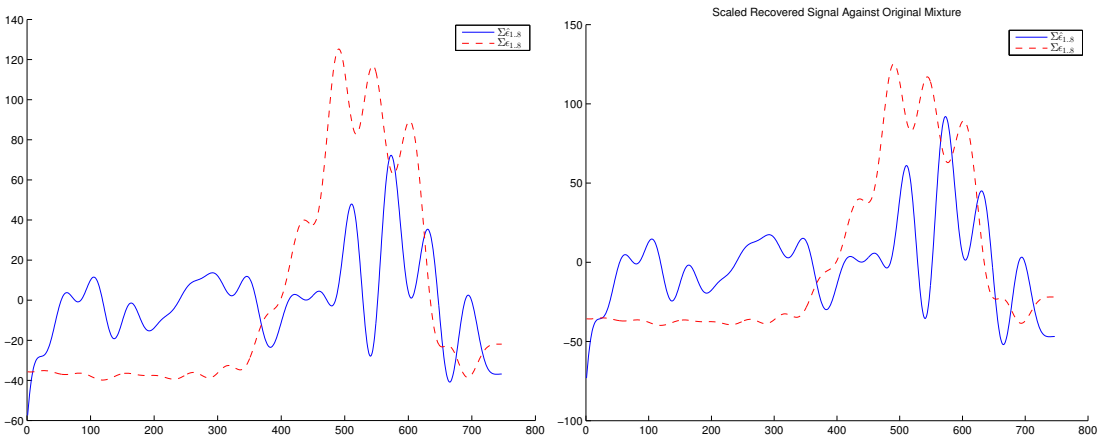

(a) Filtered, Unscaled (b) Filtered, Scaled

Figure D.15: Original/Estimated Mixture Comparisons —Actual Signals 3 Components, Trial 5

D.6 Trial 6

Estimated mixing matrix:

$$\hat{\mathbf{A}} = \begin{bmatrix} 5.678 & 6.657 & 5.522 & 2.485 & 1.109 & 0.4112 & -0.008387 & -0.5099 \\ 2.369 & 2.437 & 2.006 & 0.8767 & 0.2571 & -0.1702 & -0.6010 & -0.4691 \\ 11.37 & 9.110 & 8.240 & 4.658 & 2.415 & 0.8577 & -0.04421 & -1.095 \end{bmatrix} \quad \text{(D.11)}$$

Estimated unmixing matrix:

$$\mathbf{W} = \begin{bmatrix} -1.4680.012180.41302.651 - 0.03841 - 0.51420.6258 - 1.265 \\ -0.022730.2011 - 0.27480.059240.4266 - 0.3871 - 1.7340.3286 \\ 0.4963 - 0.81090.74730.06126 - 1.288 - 0.60370.85070.02815 \end{bmatrix} \quad \text{(D.12)}$$

RMSE (unadjusted) = 46.70

RMSE (scaled) = 47.05

Scale factor = 1.252

Figure D.16 and Figure D.17 show the extracted components. Figure D.18 shows the recovered signal mixture against, both with and without scaling.

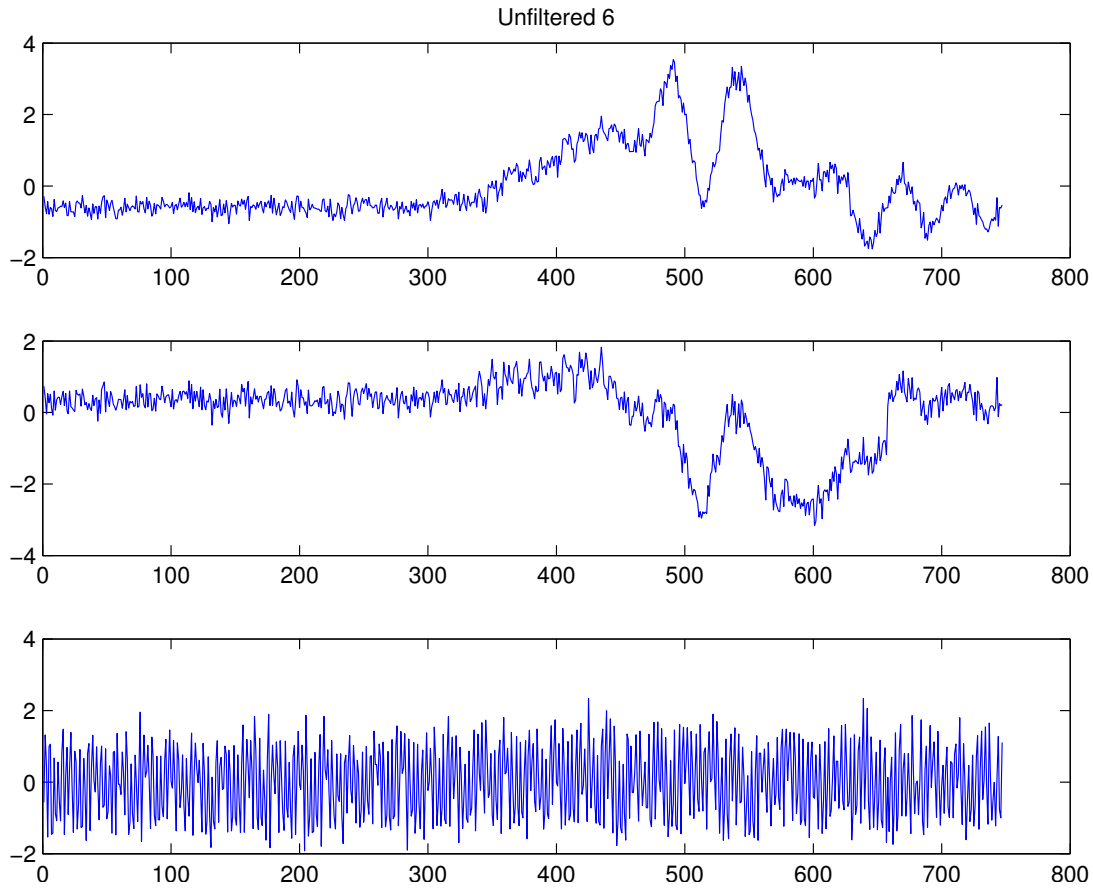

Figure D.16: Recovered Signals from Trial 6, Unfiltered Data

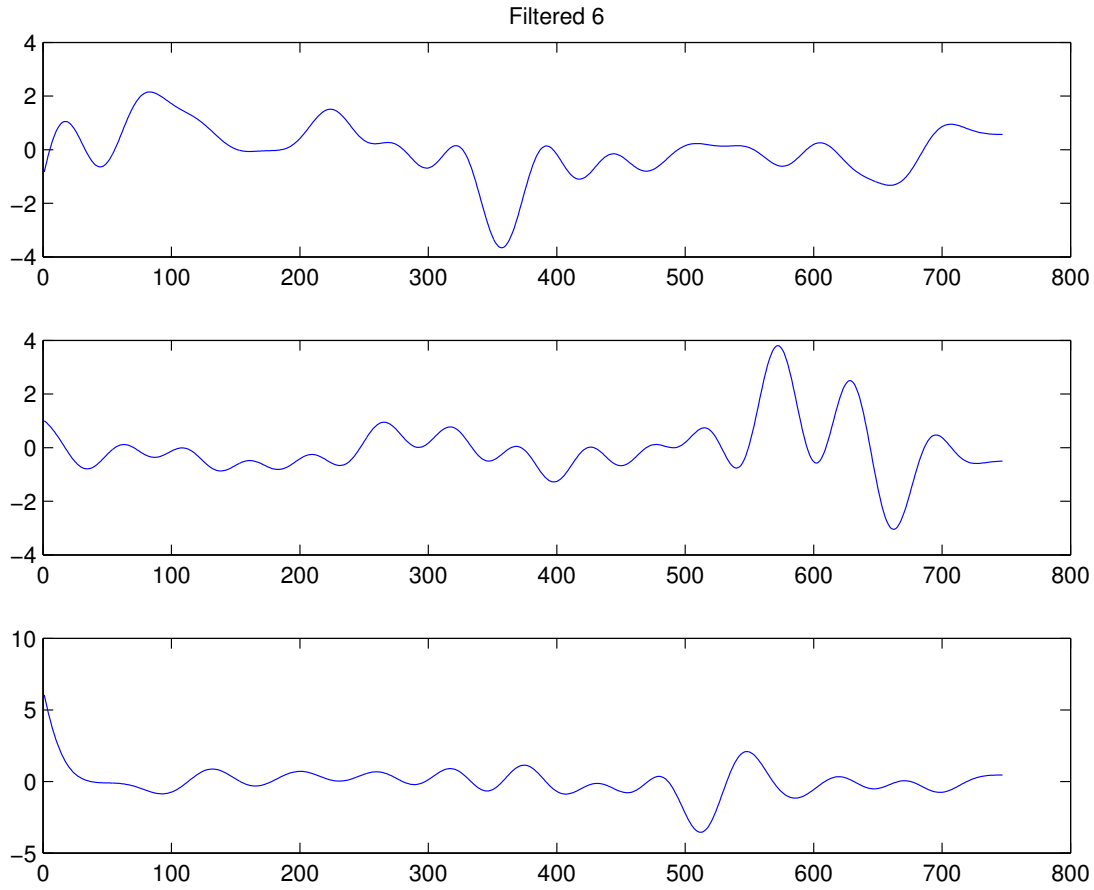

Figure D.17: Recovered Signals from Trial 6, Filtered Data

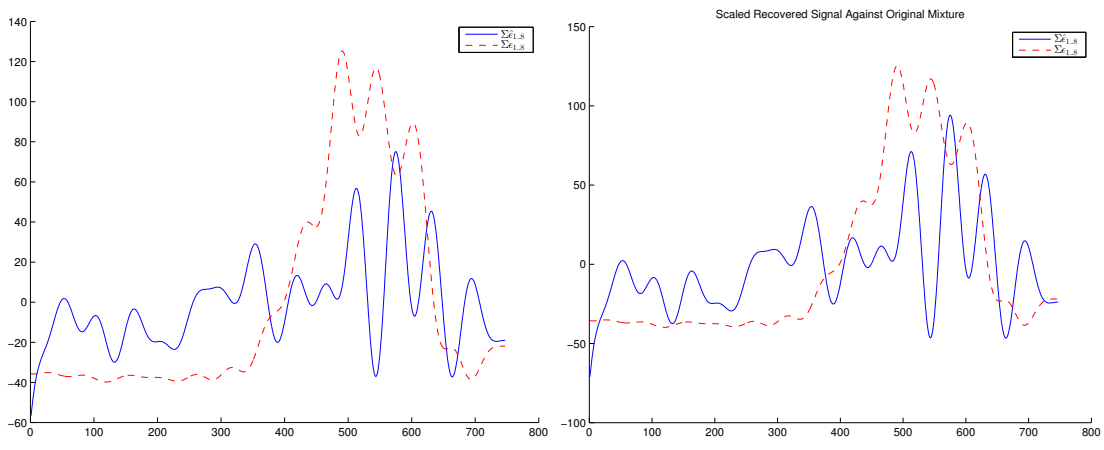

(a) Filtered, Unscaled (b) Filtered, Scaled

Figure D.18: Original/Estimated Mixture Comparisons —Actual Signals 3 Components, Trial 6

D.7 Trial 7

Estimated mixing matrix:

$$\hat{\mathbf{A}} = \begin{bmatrix} -3.994 & -3.898 & -3.617 & -1.538 & -0.7792 & -0.1821 & 0.2899 & 0.4822 \\ 1.545 & 3.045 & 2.346 & 0.8209 & 0.3001 & 0.1408 & 0.04784 & -0.05460 \\ -11.78 & -11.52 & -9.685 & -4.7954 & -2.381 & -0.7911 & 0.1478 & 0.8974 \end{bmatrix} \tag{D.13}$$

Estimated unmixing matrix:

$$\mathbf{W} = \begin{bmatrix} 0.2886 & 1.300 & -2.085 & 0.9200 & -1.010 & -0.2401 & 1.247 & -0.2128 \\ -1.594 & 0.1712 & 0.2929 & 2.534 & 0.5462 & -0.3591 & 0.2182 & -0.9238 \\ -0.3710 & -1.063 & 1.462 & 0.8609 & -1.018 & -0.8561 & 1.282 & -0.6907 \end{bmatrix} \tag{D.14}$$

RMSE (unadjusted) = 35.13

RMSE (scaled) = 35.65

Scale factor = 0.8424

Figure D.19 and Figure D.20 show the extracted components. Figure D.21 shows the recovered signal mixture against, both with and without scaling.

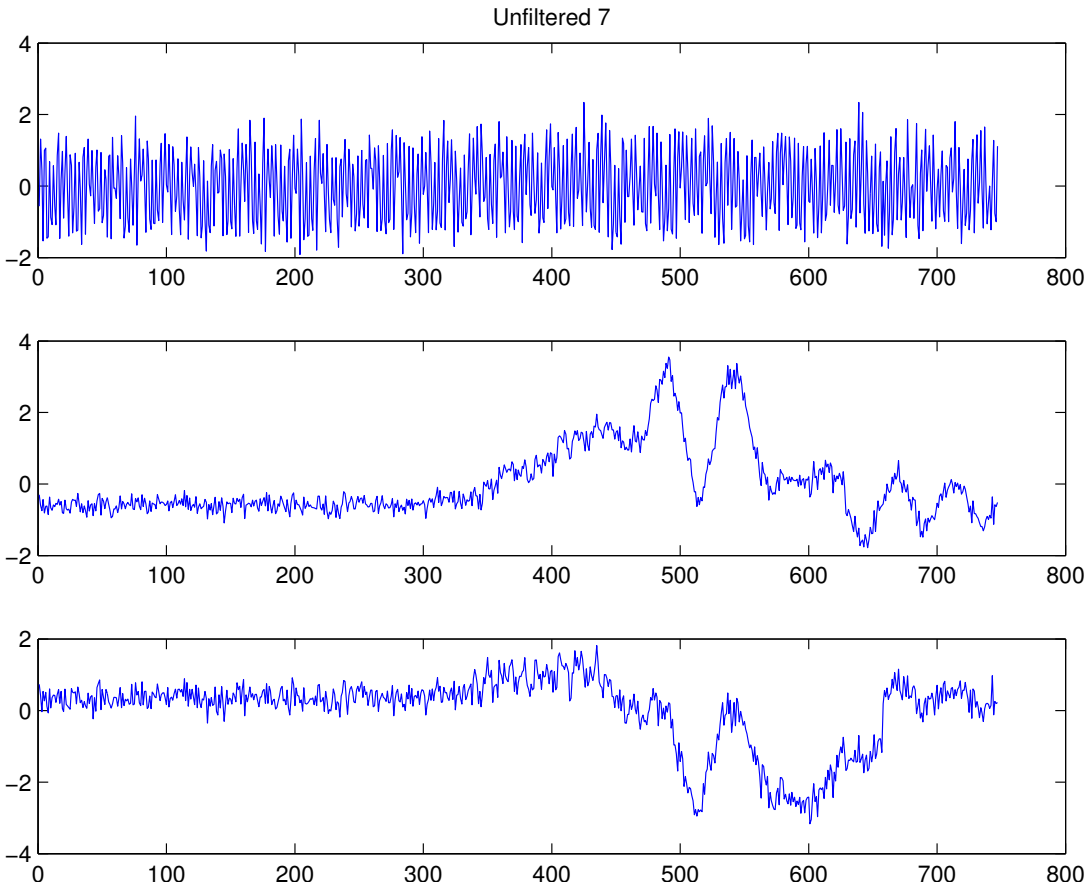

Figure D.19: Recovered Signals from Trial 7, Unfiltered Data

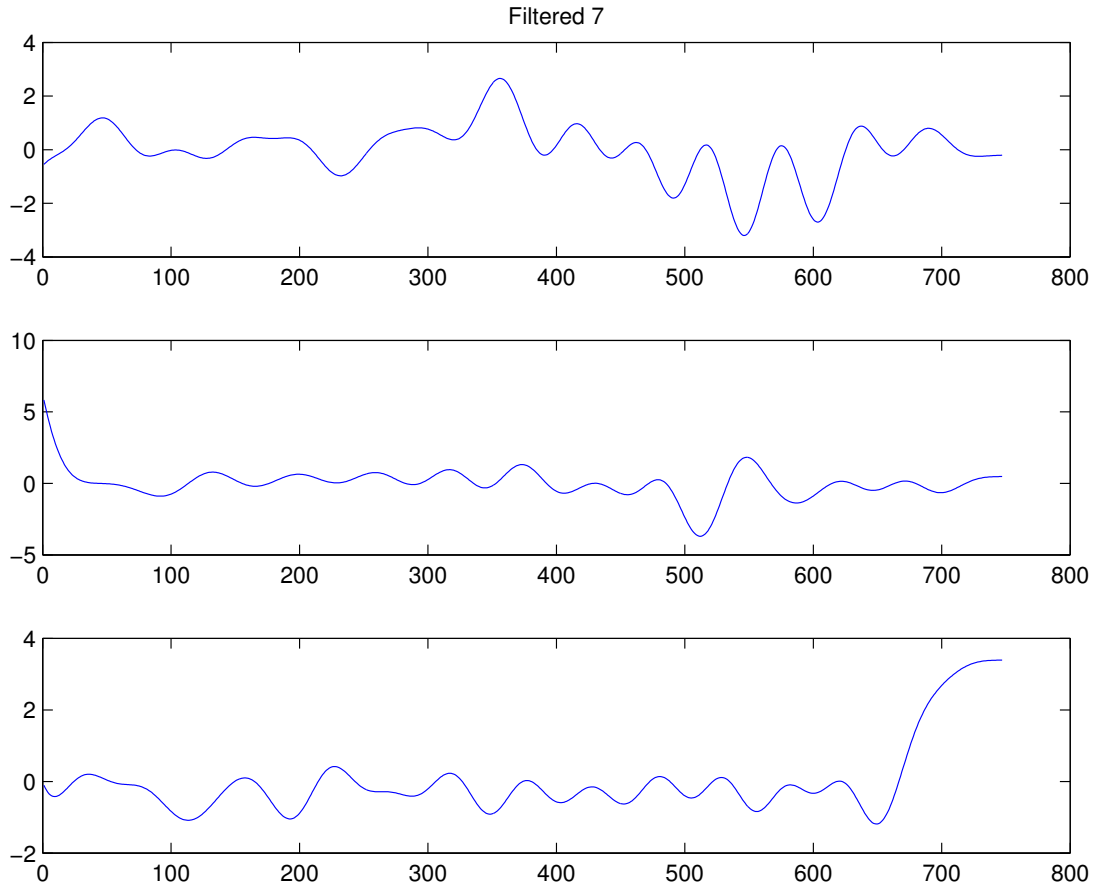

Figure D.20: Recovered Signals from Trial 7, Filtered Data

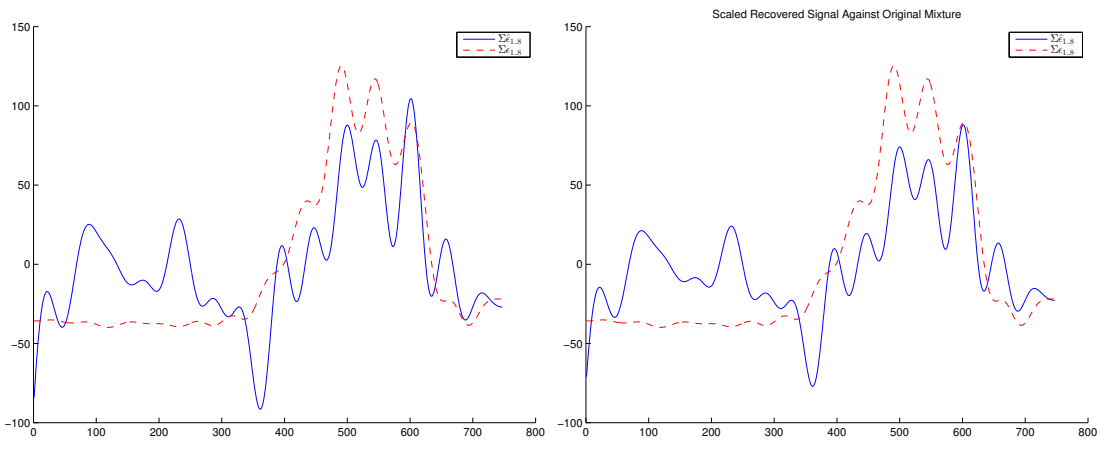

(a) Filtered, Unscaled (b) Filtered, Scaled

Figure D.21: Original/Estimated Mixture Comparisons —Actual Signals 3 Components, Trial 7

D.8 Trial 8

Estimated mixing matrix:

$$\hat{\mathbf{A}} = \begin{bmatrix} -1.747 & -1.774 & -1.460 & -0.6414 & -0.1358 & 0.2003 & 0.5991 & 0.4055 \\ 12.03 & 10.32 & 9.125 & 4.821 & 2.471 & 0.8651 & -0.05049 & -1.081 \\ 3.326 & 2.987 & 2.383 & 1.409 & 0.8117 & 0.1838 & 0.0288 & -0.3082 \end{bmatrix} \tag{D.15}$$

Estimated unmixing matrix:

$$\mathbf{W} = \begin{bmatrix} 0.03686 & -0.1101 & 0.1759 & -0.2374 & -0.1283 & 0.1710 & 1.849 & -0.4577 \\ 0.8942 & -0.4693 & 0.3000 & -1.102 & -0.7835 & 0.001937 & 0.3511 & 0.3554 \\ -0.2529 & 1.423 & -1.820 & -0.09325 & 2.787 & -2.714 & 1.066 & -0.8678 \end{bmatrix} \tag{D.16}$$

RMSE (unadjusted) = 28.29

RMSE (scaled) = 28.70

Scale factor = 0.8886

The extracted signals are shown in Figure D.22 and Figure D.23.

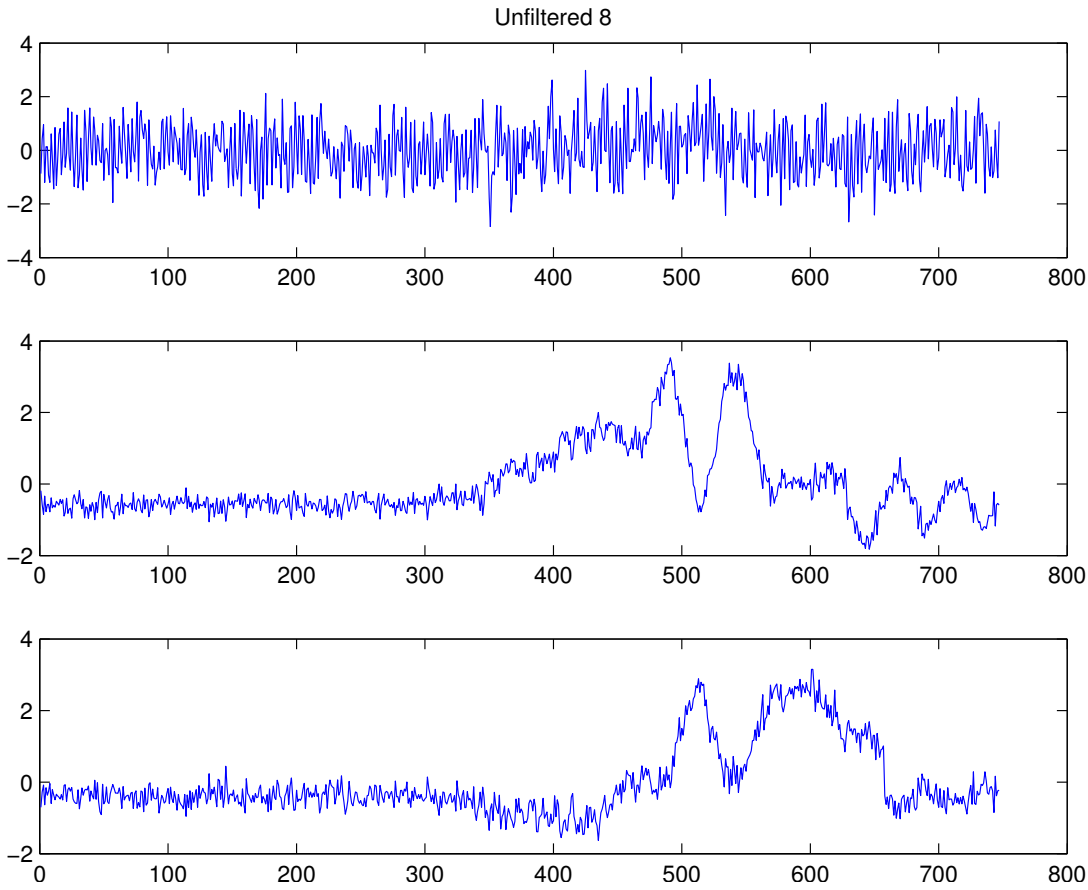

Figure D.22: Recovered Signals from Trial 8, Unfiltered Data

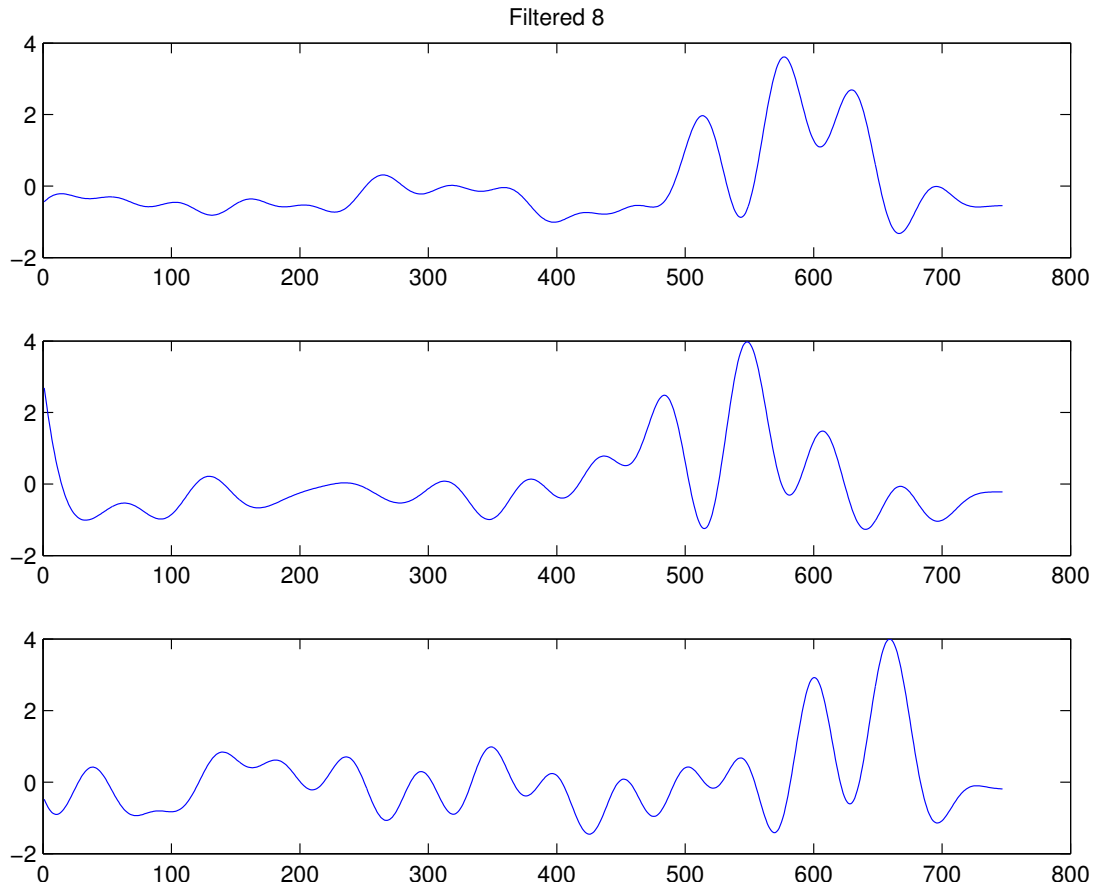

Figure D.23: Recovered Signals from Trial 8, Filtered Data

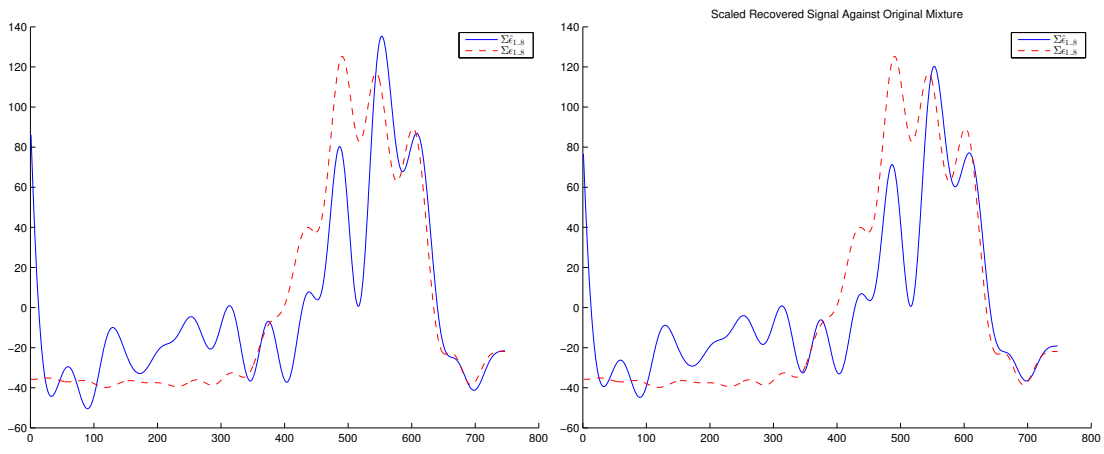

(a) Filtered, Unscaled (b) Filtered, Scaled

Figure D.24: Original/Estimated Mixture Comparisons —Actual Signals 3 Components, Trial 8